



<https://theses.gla.ac.uk/>

Theses Digitisation:

<https://www.gla.ac.uk/myglasgow/research/enlighten/theses/digitisation/>

This is a digitised version of the original print thesis.

Copyright and moral rights for this work are retained by the author

A copy can be downloaded for personal non-commercial research or study,
without prior permission or charge

This work cannot be reproduced or quoted extensively from without first
obtaining permission in writing from the author

The content must not be changed in any way or sold commercially in any
format or medium without the formal permission of the author

When referring to this work, full bibliographic details including the author,
title, awarding institution and date of the thesis must be given

Enlighten: Theses

<https://theses.gla.ac.uk/>
research-enlighten@glasgow.ac.uk

ADSORPTION STUDIES ON CLEAN AND
SULPHUR-POISONED SUPPORTED COPPER
CATALYSTS

A Thesis Submitted for the Degree of Doctor of
Philosophy of the University of Glasgow

BY

SAMIR MOHSON BEDN AL-SARAY

Department of Chemistry, August 1990

© S. M. B. Al-Saray, 1990

ProQuest Number: 11007362

All rights reserved

INFORMATION TO ALL USERS

The quality of this reproduction is dependent upon the quality of the copy submitted.

In the unlikely event that the author did not send a complete manuscript and there are missing pages, these will be noted. Also, if material had to be removed, a note will indicate the deletion.



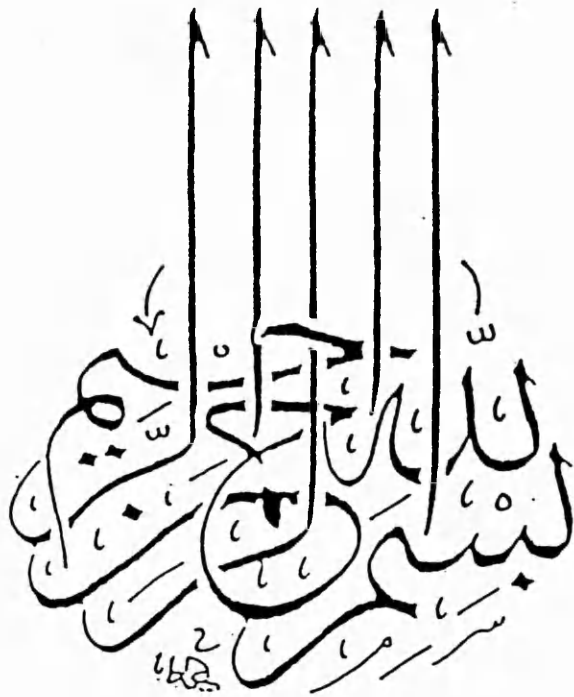
ProQuest 11007362

Published by ProQuest LLC (2018). Copyright of the Dissertation is held by the Author.

All rights reserved.

This work is protected against unauthorized copying under Title 17, United States Code
Microform Edition © ProQuest LLC.

ProQuest LLC.
789 East Eisenhower Parkway
P.O. Box 1346
Ann Arbor, MI 48106 – 1346



ACKNOWLEDGEMENTS

I would like to thank my supervisor Professor G. Webb for his unfailing help, advice and encouragement throughout the course of this study, and Dr. K. C. Campbell for his help and assessment during the period of this research and the completion of this thesis.

As with any piece of research, I have been dependent on the technical assistance of many of the technical staff of the chemistry department. In particular Mr. K. Shepherd and T. Boyle.

Throughout the period of this research, I have been fortunate in having received encouragement and help from my colleagues in surface chemistry. They contributed many constructive suggestions and comments to shape the material of this thesis, particularly, Drs. G. D. McLellan and M. Keane for their valuable criticism and help.

My sincere gratitude to the Iraqi government for giving me the opportunity to continue my postgraduate study in spite of all difficulties during the years of the war.

Ultimately, I am indebted to my family and friends whose patience, love and support enabled me to complete this study.

SUMMARY

The adsorption of methanol, carbon monoxide, and carbon dioxide has been studied in a pulse flow system on "clean" and hydrogen sulphide poisoned alumina-supported copper, a commercial copper/zinc oxide/alumina catalyst, zinc oxide, and alumina surfaces. Adsorption of hydrogen sulphide was also studied, while the interaction of methanol and carbon monoxide with "clean" surfaces of the above catalysts was investigated by FTIR.

The catalytic decomposition of methanol on copper-based catalysts resulted in the formation of carbon monoxide, carbon dioxide and hydrogen. The formation of carbon dioxide was attributed to the interaction of the product carbon monoxide with the unreduced oxide on the catalyst surface. Use of a carbon monoxide flow as a reducing agent to ensure the complete reduction of copper-based catalysts surfaces, showed that carbon monoxide and hydrogen are the major products of the decomposition reaction. The reaction of methanol on zinc oxide also resulted in the formation of carbon monoxide, carbon dioxide and hydrogen. Interaction of carbon monoxide with the oxide surface was responsible for the formation of carbon dioxide, as was evident from the change in the oxide colour from grey to blue during methanol interaction, suggesting a conversion of the oxide to a metallic zinc. At higher reaction temperatures and increased methanol exposure, trace amounts of methane were formed. On an alumina surface, methanol interacts

dissociatively to form carbon monoxide and methane as major products, together with small amounts of, carbon dioxide and water.

Sulphur was found to have a great influence on the catalytic activity. The presence of small concentrations of H₂S on the catalyst surface greatly reduced the catalytic activity towards methanol decomposition, but no change in the catalyst selectivity was observed due to this poisoning effect.

¹⁴C-labelled carbon monoxide and carbon dioxide were used to study the extent of the adsorption and the effect of sulphur poisoning on copper-based catalysts.

The results showed that carbon monoxide interacts with copper-based catalysts forming a strongly held carbonate species, due to the presence of unreduced oxide. Desorption experiments show two adsorption peaks corresponding to a relatively weakly adsorbed and strongly held species. No significant carbon monoxide adsorption was observed on the oxide surfaces.

¹⁴C-carbon dioxide interacts with the catalyst surfaces in a similar way to that of carbon monoxide; significant adsorption occurs on the oxide surfaces. Preadsorbed sulphur reduces the extent of the adsorption of both carbon monoxide and carbon dioxide, by weakening the adsorbate-metal bond, as indicated by the shift of the desorption peaks to lower temperatures.

³⁵S-H₂S strongly adsorbs on all surfaces. The adsorption is irreversible on Cu/Al₂O₃, Cu-ZnO/Al₂O₃ and

ZnO, with zinc oxide bulk zinc sulphide is formed. Trace amounts of water are found to increase the ability of the oxide to adsorb H₂S.

FTIR investigations of the interaction of methanol shows that, on copper catalysts, methoxy species are formed, while on zinc oxide the methoxy species decompose to form a carbonato species as well as carbon monoxide and carbon dioxide. On alumina bands due to methoxy, formate, CO, CO₂ and water are observed. The methoxy species decomposes to a formate species upon being heated.

Contents

Acknowledgements

Summary

1.	Chapter One : Introduction	1
1.1	General Introduction.....	1
1.2	The Catalytic properties of Copper-Based Catalysts	3
1.2.1	Activity of Copper-Based Catalysts	3
1.2.2	Catalysis by Zinc Oxide	9
1.3	The Adsorption of Hydrogen	14
1.3.1	The Adsorption of Hydrogen on a Copper Surface	14
1.3.2	The Adsorption of Hydrogen on Zinc Oxide surfaces	16
1.4	The Adsorption of Water	19
1.4.1	The Adsorption of Water on Copper Surfaces ..	19
1.4.2	Water Adsorption on Zinc Oxide	21
1.5	The Adsorption of Carbon Monoxide	23
1.5.1	The Adsorbed State of Carbon Monoxide on Metal Surfaces	23
1.5.2	Chemisorption State of Carbon Monoxide on Copper Surfaces	27
1.5.3	The Adsorption of Carbon Monoxide on Copper Catalysts.....	29
1.5.4	Carbon Monoxide Chemisorption State on Zinc Oxide	33

1.6	The Adsorption of Carbon Dioxide	34
1.6.1	The Adsorption of Carbon Dioxide on Copper Surfaces.....	34
1.6.2	The Adsorption of Carbon Dioxide on Zinc Oxide Surfaces.....	38
1.7	Reactions on Copper Catalysts	40
1.7.1	Methanol Synthesis	40
1.7.1.1	The Role of Carbon Dioxide in Methanol Synthesis	45
1.7.2	Water-Gas Shift Reaction (WGS)	48
1.7.3	Methanol Decomposition on Copper-Based Catalysts	51
1.7.3.1	Methanol Decomposition on Copper Surfaces ...	51
1.7.3.2	The Effect of Oxygen on the Decomposition of Methanol on Copper Catalysts	54
1.7.3.3	Mechanism of Methanol Decomposition on Copper Surfaces	57
1.7.3.4	Methanol Decomposition on Zinc Oxide Surfaces.....	59
1.7.3.5	Mechanism of Methanol Decomposition on Zinc oxide surfaces	62
1.8	Poisoning of Methanol Catalysts	65
1.8.1	Introduction	65
1.8.2	Poisoning of Copper Catalysts	67
1.8.2.1	The Sulphur-Copper Bond	69
1.8.3	The Adsorption of Hydrogen Sulphide On Copper-Based catalysts	70

1.8.3.1	The Adsorption of Hydrogen Sulphide On Copper Surfaces	70
1.8.3.2	The Reaction Between Hydrogen Sulphide and Zinc Oxide	72
1.8.4	The Effect of Sulphur on the Adsorption of Other molecules	74
1.8.4.1	The Effect of Sulphur on the Adsorption of Carbon Monoxide and Carbon Dioxide.....	74
1.8.4.2	The Effect of Sulphur on the Catalytic Decomposition of Methanol	76
1.8.4.3	Sulphur Poisoning of Methanol Synthesis Catalysts	78
1.8.4.4	Sulphur Poisoning the Water-Gas Shift Reaction.....	79
2.	Chapter Two : The Objectives of this Work...	81
3.	Chapter Three : Experimental	83
3.1	Materials and Gases	83
3.1.1	Materials	83
3.1.2	Gases	85
3.2	The Apparatus	86
3.2.1	The Vacuum System	87
3.2.2	The Flow System (Sampling System)	88
3.2.3	The Analytical System	89
3.3	The Experimental Procedure	91
3.3.1	Catalysts Treatment and Activation	91
3.3.2	Experimental Procedure	93
3.3.3	Analysis of Reactant and Products	94
3.4	³⁵ S-H ₂ S Pulse System	95

3.4.1	The Flow System	95
3.4.2	The Reaction Vessel	96
3.4.3	The Geiger-Muller Counter	97
3.5	¹⁴ C-Experimental	99
3.5.1	Isoflo Scintillation Counting.....	99
3.6	Preparation of Labelled Gases	102
3.6.1	{ ³⁵ S-}Hydrogen Sulphide Preparation	102
3.6.2	The Preparation of ¹⁴ C-Carbon Monoxide and Carbon Dioxide	103
3.6.2.1	The Preparation of ¹⁴ C-Carbon Monoxide	103
3.6.2.2	The Preparation of ¹⁴ C-Carbon Dioxide	105
3.7	<i>In Situ</i> FTIR Spectroscopy, Experimental Procedures	105
3.8	Treatment of the results.....	108
4.	Chapter Four : Methanol Decomposition on Clean and Hydrogen Sulphide Poisoned Copper-Based Catalyst Surfaces	110
4.1	Decomposition of Methanol on Clean and Poisoned surfaces	110
4.2	Methanol Decomposition on Clean surfaces ...	110
4.2.1	The Decomposition of Methanol on Clean Cu/Al ₂ O ₃ Surface	110
4.2.2	Methanol Decomposition on Cu-ZnO/Al ₂ O ₃ Surface.....	116
4.2.3	Methanol Decomposition on ZnO Surface	120
4.2.4	Methanol Decomposition on Al ₂ O ₃ Surface	124

4.3	Methanol Decomposition on H ₂ S Poisoned Surface.....	125
4.3.1	Effect of H ₂ S poisoning on the Catalytic Decomposition of Methanol on a Cu/Al ₂ O ₃ Surface.....	125
4.3.2	Effect of H ₂ S Poisoning on Methanol Decomposition on Cu-ZnO/Al ₂ O ₃	127
4.3.3	Methanol Decomposition on ZnO Surface Poisoned with Hydrogen Sulphide	129
4.3.4	The Decomposition of Methanol on Al ₂ O ₃ Surface Poisoned with Hydrogen Sulphide	130
5.	Chapter Five : The Adsorption of Carbon Monoxide and Carbon Dioxide on Clean and Poisoned Copper-Based Catalyst Surfaces	133
5.1	Carbon Monoxide Adsorption on Clean and Poisoned Copper-Based Catalysts	133
5.1.1	The Adsorption of Carbon Monoxide on Clean and Poisoned Cu/Al ₂ O ₃ Surfaces	133
5.1.2	The Adsorption of Carbon Monoxide on Clean and Poisoned Cu-ZnO/Al ₂ O ₃ Surfaces	138
5.1.3	The Adsorption of Carbon Monoxide on Unreduced Cu/Al ₂ O ₃ and Cu-ZnO/Al ₂ O ₃ Surfaces	141
5.2	The Adsorption of Carbon Monoxide on Oxide Surfaces	142
5.2.1	Carbon Monoxide Adsorption on Zinc Oxide Surfaces	142

5.2.2	^{14}C -Carbon Monoxide Adsorption on an Alumina Surface	143
5.3	^{14}C -Carbon Dioxide Adsorption on Copper-Based and Related Catalysts	143
5.3.1	The Adsorption of ^{14}C -Carbon Dioxide on a $\text{Cu}/\text{Al}_2\text{O}_3$ Surface	144
5.3.2	^{14}C -Carbon Dioxide Adsorption on H_2S Poisoned $\text{Cu}/\text{Al}_2\text{O}_3$ Surface	148
5.3.3	Adsorption Isotherms of ^{14}C -Carbon Dioxide on Clean and Poisoned $\text{Cu-ZnO}/\text{Al}_2\text{O}_3$ Surfaces	149
5.3.4	^{14}C -Carbon Dioxide Desorption from Clean and H_2S Poisoned $\text{Cu-ZnO}/\text{Al}_2\text{O}_3$ Catalyst Surfaces	151
5.3.5	The Adsorption of ^{14}C -Carbon Dioxide on Clean and H_2S Poisoned ZnO Catalyst	153
5.3.6	The Adsorption of ^{14}C -Carbon Dioxide on Clean and H_2S Poisoned Alumina Surfaces	156
6.	Chapter Six : Radiotracer Study of the Adsorption of ^{35}S - H_2S on Copper-Based Catalyst Surfaces	159
6.1	The Adsorption of ^{35}S - H_2S on Copper-Based Catalysts	159
6.1.1	Adsorption of ^{35}S - H_2S on $\text{Cu}/\text{Al}_2\text{O}_3$ Surfaces	159

6.1.2	The Adsorption Isotherm of $^{35}\text{S-H}_2\text{S}$ on Cu-ZnO/Al ₂ O ₃	161
6.2	The Adsorption of $^{35}\text{S-H}_2\text{S}$ on an Alumina Surface.....	163
6.3	The Adsorption of $^{35}\text{S-H}_2\text{S}$ on a ZnO Surface ..	164
6.3.1	$^{35}\text{S-H}_2\text{S}$ Adsorption Isotherm on Untreated ZnO Surface	164
6.3.2	The Effect of Carbon Dioxide on the Adsorption Isotherm of $^{35}\text{S-H}_2\text{S}$ on ZnO	167
6.3.3	The Exchange of $^{35}\text{S-H}_2\text{S}$ with Unlabelled H ₂ S on ZnO Surface	167
6.3.4	Effect of Water on $^{35}\text{S-H}_2\text{S}$ Adsorption Isotherm on ZnO Surface	168
7.	Chapter Seven : The Spectroscopic Study of the Interaction of Methanol and Carbon Monoxide on Copper-Based Catalyst Surfaces	172
7.1	The Interaction of Methanol with Copper-Based Catalysts	172
7.1.1	FTIR Spectra of Methanol Adsorbed on Cu/Al ₂ O ₃	172
7.1.2	The Interaction of Methanol with Cu-ZnO/Al ₂ O ₃ Catalyst	174
7.1.3	The Interaction of Methanol with a ZnO Catalyst	175
7.1.4	Methanol Interaction with Alumina	178
7.2	FTIR Spectroscopic Study of the Interaction of Carbon Monoxide with Copper-Based Catalyst Surfaces	183

7.2.1	Carbon Monoxide Adsorption on Cu/Al ₂ O ₃	183
7.2.2	FTIR study of the Interaction of Carbon Monoxide with Cu-ZnO/Al ₂ O ₃	184
8.	Chapter Eight : Discussion	186
8.1	Introduction	186
8.2	Methanol Decomposition on Cu/Al ₂ O ₃ and Cu/ZnO/Al ₂ O ₃ Catalysts	186
8.3	Methanol Decomposition on Zinc Oxide	196
8.4	Methanol Decomposition on Al ₂ O ₃	200
8.5	The Adsorption of Carbon Monoxide on copper-based catalysts	203
8.6	The Adsorption of Carbon Dioxide on Copper-based catalysts	210
8.7	The Adsorption of ¹⁴ C-Carbon Dioxide on ZnO Surfaces	215
8.8	Heats of Adsorption of Carbon Monoxide and Carbon Dioxide on Copper-Based Catalysts ...	216
8.9	The Adsorption of ¹⁴ C-Carbon Dioxide on Alumina Surfaces	219
8.10	The Adsorption of ³⁵ S-H ₂ S on Copper-Based Catalysts	220
8.11	The Adsorption of ³⁵ S-H ₂ S on Alumina Surfaces.....	224
8.12	The Adsorption of ³⁵ S-H ₂ S on ZnO Surfaces ...	226
8.13	The Effect of Water on ³⁵ S-H ₂ S Adsorption on zinc oxide.....	228
	References	230

CHAPTER ONE

INTRODUCTION

1.1 GENERAL INTRODUCTION

The objective of catalysis is to increase the rate of a specific reaction. In heterogeneous catalysis the catalyst provides active sites ^[1] at the surface on to which reactants are adsorbed. These active sites are located on the surface where bonding sites are provided or charge exchange is possible, thus forming reactive intermediates. Good catalysts are expected to achieve high rates and have high selectivity.

Extensive efforts have been made to understand the area of heterogeneous catalyst in both its industrial and fundamental fields. In industry the main interest is the development of a practical catalyst which possesses high activity and selectivity for the reaction concerned and which operates efficiently under the industrial conditions ^[2]. These catalyst developments have been dominated by trial and error procedures. On the other hand the theme of the fundamental studies is to understand, at the atomic level, the nature of the catalytic process. The characterisation of the catalyst surface has been improved with the use of physical and chemical techniques to study processes at the gas-solid interface. However, there is a large difference in the pressure at which industrial

processes are carried out; 1 atm and higher, and those at which fundamental studies are done, often less than 10^{-9} atm, and therein lies the main difficulty in discussing heterogeneous catalysis mechanisms. Also, in fundamental catalytic studies difficulties arise from the use of many different techniques, which result in the emission of electrons or other charged particles, for which low pressure is essential to avoid scattering. This is the principal difficulty in connection with the use of fundamental techniques such as LEED to monitor surfaces involved in industrial reactions. There are also difficulties in making comparisons between carefully cleaned and well characterised surfaces reacting with pure gases, and catalysts used under industrial conditions. Some of these fundamental studies have been described by Somorjai [3]. Despite these differences between fundamental laboratory work and industrial research and development, workers in the two areas have made a considerable effort to understand the catalytic activity of metal catalysts. However, the long known definition of a catalyst as a *"substance which increases the rate of a chemical reaction without itself being consumed"* has not been improved upon. The question which then has to be asked is by what mechanism catalysts work. Furthermore, no general theory of catalysis is in sight.

The main understanding of heterogeneous catalysis came from the correlation of the catalytic properties with other properties of metals. Two of these properties, which

attracted the attention of investigators, were the electronic and the geometric properties of metals [4]. The transition group metals represent the most catalytically active metals, and their activity had been associated with d-electrons. The method used to assess the importance of metallic d-band structure to catalytic activity was to change the electronic occupancy of the d-band by alloying it with a metal of similar atomic size. This avoided change in surface geometry, while a change in the electronic properties could be obtained. However, it was subsequently found that the surface properties of metal alloys were different from those of the bulk as also was their composition.

The surface geometry factor, on the other hand, has been investigated using metals in various state of dispersion, or investigating reactivities of different single-crystal surfaces. Results here showed that broad classes of behaviour can be observed and each reaction system has to be considered individually.

1.2 THE CATALYTIC PROPERTIES OF COPPER-BASED CATALYSTS

1.2.1 Activity of Copper-Based Catalysts

The conversion of carbon monoxide and carbon dioxide into methanol on copper-based catalysts has attracted considerable attention owing to the industrial and economic importance of the process. However, the nature of the

active sites on these catalysts and the role of each of their components, with particular reference to copper-zinc oxide type catalysts, are still the subject of much debate.

Herman *et al.* [5] studied a wide variety of catalyst compositions, with catalysts consisting of hexagonal zinc oxide and tetragonal copper oxide after calcination. The active sites in these catalysts after use or reduction, was made up essentially of metallic copper and zinc oxide. Nevertheless, there was evidence for the presence of a copper ion [Cu (I)] species which is dissolved in zinc oxide, with compensating oxide ion deficiencies.

Klier *et al.* [6] concluded that in the activated catalyst, up to 50% of the copper is dissolved in zinc oxide. A highly dispersed phase containing copper ions [Cu (I)] substituted for the zinc ion (Zn^{2+}) in the tetrahedral sites of the wurtzite lattice was related to a characteristic near-infrared absorption feature, observed in diffuse reflectance spectra of these activated catalysts. The copper ion [Cu (I)] was considered to activate the carbon monoxide with hydrogen being activated by the zinc oxide.

In another study, two dimensional metallic copper and monovalent copper species were found to be responsible for the catalytic activity of copper-zinc oxide [7]. The monovalent copper species were also considered to be responsible for the methanol synthesis reaction [8]. This species is stable under synthesis reaction conditions and may exist as a crystalline copper phase, whilst the

concentration of these species depends on the metal-support ratio and on the calcination temperature of about 350°C. Heating copper-containing evaporated film catalysts, deposited on Cr_2O_3 , in vacuum produces the surface stabilised copper ion [Cu (I)] whose concentration depends on the treatment temperature ^[9]. The low temperature vacuum heating of calcined Cu/ Cr_2O_3 evaporated layers to $\geq 375^\circ\text{C}$ forms a surface copper ion [Cu (I)] phase which is stable for reduction with hydrogen at 270°C, and cuprous chromite, which is responsible for the surface-stabilised copper ion.

The above authors related the use of vacuum heating to the controlled production of copper ion species. However, Rao *et al.* ^[10] showed that there is more than one copper species in copper-containing catalysts, and they suggested a copper ion dissolved in a unique site in zinc oxide together with metallic copper. The methanol synthesis reaction is believed to proceed through the formation of a methoxy species on a copper ion, this methoxide species is stabilised as an anion with an electron being donated from zinc oxide. The impurity states, as induced by the presence of copper ions, are thought to have a smaller ionisation potential than that of an intrinsic zinc oxide surface and thus promote methoxide stabilisation ^[11]. To summarise, the above studies indicate that methanol is produced from the hydrogenation of carbon monoxide on copper-based catalysts, and that in the composition range of 15 to 85% copper oxide, up to 15% of the copper becomes dissolved in

the zinc oxide ^[5] as [Cu (I)] ions.

In contrast, a number of authors have proposed that metallic copper is the active component in copper-containing catalysts. Raney copper-based catalysts have been used for methanol synthesis with different loading of copper in the catalysts composition. In this case it is thought that copper is likely to be present as metallic copper (Cu^0) under methanol synthesis conditions ^[12]. A series of Raney copper-containing catalysts prepared by leaching a series of copper-zinc-alumina alloys, containing about 50 wt% alumina and differing copper/zinc ratios, with aqueous sodium hydroxide until complete reaction had taken place, have been used for methanol synthesis. The activity of these catalysts showed that Raney catalysts prepared from alloys containing approximately 50 wt% alumina, 30-36 wt% copper and 14-20 wt% zinc had the highest activity for methanol synthesis ^[13]. The active component for these Raney catalysts was found to be metallic copper. An X-ray photoelectron spectroscopic (XPS) ^[14] study of a synthesis catalyst consisting of 43% copper, 47% zinc oxide and 10% alumina, showed that under a reaction condition of a gas feed consisted of 73% hydrogen, 25% carbon monoxide and 2% carbon dioxide at 250°C, the active components of the catalyst consisted of metallic copper and zinc oxide, and that only very small amounts of the catalyst, <2% of the copper in active copper-zinc oxide catalysts, was non-metallic.

A model single-crystal surface structure of copper-zinc

oxide catalysts has been prepared and characterised for the methanol synthesis reaction [15]. Under reaction conditions of a carbon monoxide and hydrogen pressure of 1500 torr in a temperature range of 230-330°C, the copper which is in direct contact with zinc oxide "may be slightly oxidised". However, all of the remaining copper is completely metallic. Baussart et al. [16] studied the selective hydrogenation of carbon dioxide to methanol on the low-pressure synthesis catalyst using X-ray powder diffraction (XRD), diffuse reflectance (DRIFT) and gas chromatography. These authors concluded that the presence of Cu₂O correlates with higher selectivity of the catalyst. In contrast, no indication was found for Cu₂O in a carbon monoxide shift catalyst investigated by X-ray absorption near edge spectroscopy (XANES) [17].

Recently, extended X-ray absorption fine structure (EXAFS) studies have been used to investigate the active copper sites in reduced copper-zinc oxide catalysts with a copper content of about 30 wt%, activated by reduction in a 0.5-3% hydrogen in nitrogen gas flow, at 250°C. Highly dispersed copper clusters have been observed [18]. The synergistic relationship between copper and zinc oxide was related to a simple copper dispersion effect [19], and the synthesis rate correlated with effective surface area measured by the adsorption of carbon monoxide. However, Waugh et al. [20] showed that copper activity correlates well with copper surface area, independent of whether the catalyst includes zinc oxide or not. They see no important

role for zinc oxide in determining methanol synthesis activity.

Klier and co-workers [21, 22] presented a much different picture from that of the Waugh model. The presence of zinc oxide was found to be essential for catalytic activity, and the catalysts containing the zinc oxide (1010) and the hexagonal platelets with (0001) orientation are active and selective for methanol synthesis. Also, zinc oxide is considered to act as a catalyst promoter, and the common feature of zinc oxide in all methanol synthesis catalysts (e.g. Cu/ZnO and Cu/ZnO/Al₂O₃) is the high content of copper dissolved in zinc oxide. This represents the major difference from the chemical properties of the individual components. Frost [23], recently, proposed that the reality of the synergy and its origin lies in the perturbation of the oxide defect equilibria by metal/oxide junctions in the catalyst raising the ionised oxygen vacancies concentrations in the surface. He suggested that, when copper is brought into contact with the oxide, an equilibrium is established in which electrons are produced by ionising the oxygen vacancies, and a net transfer of charge from the oxide to the metal occurs. However, the electron transfer between copper metal and zinc oxide may play a contributory but not an essential role in the synthesis [22].

Clearly, there is still a great deal of confusion regarding the nature of the active sites responsible for the activity in methanol synthesis catalysts, The complex

and heterogeneous nature of the catalysts subjected to experimental investigation form one of the reasons behind this confusion. Also, the confusion is due to the difficulties in separating effects due to various moieties which appear on the catalyst surface. Despite all this confusion, the activated copper/zinc oxide-alumina catalysts appear to contain two forms of copper, copper with strong interaction with the zinc oxide phase [22], and finely dispersed copper metal supported on zinc oxide. The structure of the zinc oxide phase is identified as a solution of copper ions [Cu (I)] dissolved in zinc oxide. This consideration was based on the facts that, copper ions activate chemisorbed carbon monoxide while hydrogen is activated by the zinc oxide surface. This proposal agreed with methanol synthesis mechanism [6, 22]. Also, zinc oxide acts as stabiliser for the active sites of copper ions [24].

1.2.2 Catalysis by Zinc Oxide

Zinc oxide crystals are formed [25-28] from alternate layers of zinc and oxygen atoms (ions), as shown in figure [1.1], disposed in a wurtzite hexagonal close-packed structure with elongated axis. The zinc atoms partially fill the empty space among the oxygen atoms, and this is possible because of the difference in size between the zinc and oxygen atoms. Though many of the zinc oxide properties are dependent on the crystal structure and the arrangement

of the zinc and oxygen atoms, the thermal properties are influenced by the bond strength of the atoms.

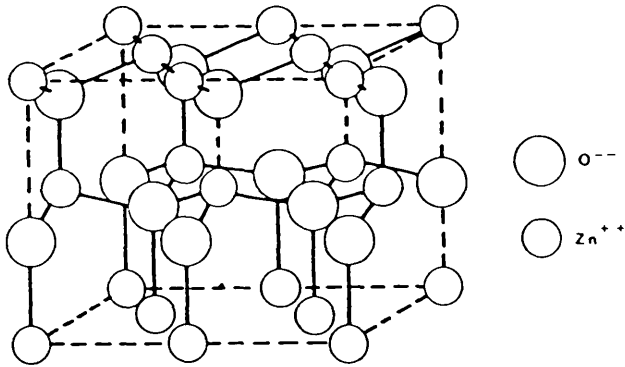


Figure 1.1 Zinc Oxide Crystal Structure

The lattice of pure zinc oxide consists of a periodic arrangement of zinc and oxygen ions (Zn^{2+} , O^{2-}) as shown in figure [1.2 A]

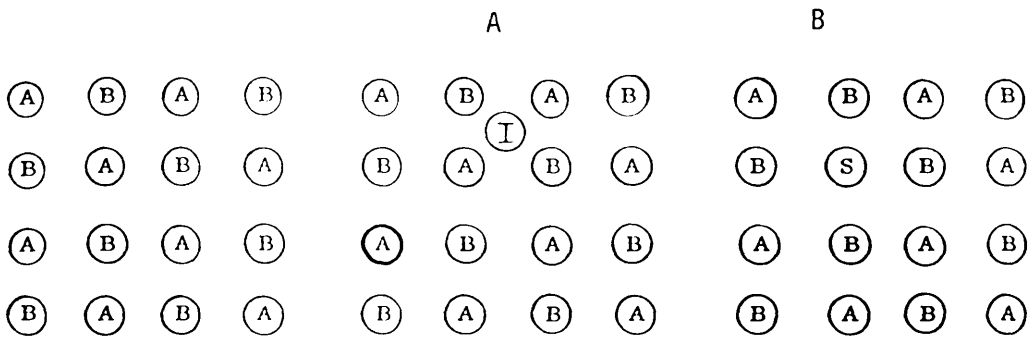
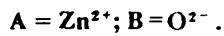


Fig.1.2 Modification of the crystal structure of ZnO . Interstitial atom I (in A), substitute, S (in B)



At higher temperature (approximately 400-900°C) in the presence of hydrogen or carbon monoxide [29, 30], a partial reduction of the oxide will occur. Each oxygen atom on removal releases an atom of zinc and two electrons, and the zinc atom moves to the unoccupied space between oxygen atoms, thus, this additional zinc may be termed an "interstitial" atom. The charge on that atom and the electron deposition are subject of controversy and it appears that interstitial atoms (usually termed *excess zinc*) may carry variable amounts of charge (Zn , Zn^+ , and Zn^{2+}), which depend mainly on temperature. Accordingly, the number of free electrons varies. However, zinc atoms in zinc oxide crystals could be replaced by selected foreign metallic atoms at elevated temperatures [figure 1.2 B]. This substitution process can markedly alter the crystal properties, depending upon the nature, concentration and valency of the foreign atom [30, 31]. For example, monovalent atoms such as lithium, potassium and sodium decrease the oxide conductivity, whereas, trivalent atoms, typified by gallium, aluminium and indium, raise that property. Thus the catalytic activity of the oxide could be altered. In the decomposition of methanol, the activation energy for the reaction on zinc oxide [32] decreases in the presence of lithium (Li^+), while there is a slight increase when aluminum ions (Al^{3+}) are present in the oxide. Small amounts of lithium ions have a relatively large effect on the zinc oxide surface area [33].

Zinc oxide has been used for a long time [1] as a favourite solid for investigation of the chemisorption mechanism. Early investigators of catalytic processes, noticed that the adsorption of gases on zinc oxide, particularly at elevated temperatures, is mainly chemisorption. This was the first insight into the catalytic properties of zinc oxide. Many papers have been published concerning the mechanism of the chemisorption of gases, principally, hydrogen (see section 1.3.2) and oxygen.

The chemisorption of oxygen on zinc oxide was extensively studied by Nelson and Duck [34]. They modified the chemisorption properties in zinc oxide powder by subjecting their samples to high-temperature evacuation treatment, which removed some oxygen and developed an excess of zinc in the lattice (as mentioned earlier). The evacuation temperature was in the range 300-500°C and the adsorption of oxygen was carried out at room temperature on a sample evacuated at 480°C. This procedure was found to initiate the adsorption process. The samples then had a high adsorption activity for both oxygen and hydrogen when exposed to these gases. The adsorption of oxygen which occurred rapidly in the initial stages, took place by the release of an electron from the excess zinc atoms (Zn^+ ions) forming Zn^{2+} ions. Then the liberated electrons diffused to the surface and combined with the oxygen atoms to form adsorbed oxygen ions (O^{2-}), until the surface was saturated. In the same manner the adsorption of hydrogen

occurred. Miller and Morrison [35] found that the adsorption and desorption of oxygen by zinc oxide influences its catalytic activity and they explained the mechanism of this effect by considering that the desorption of oxygen from zinc oxide above 500°C in air leaves adsorption sites on the surface of the sample. These available sites are considered to be excess zinc atoms near the surface. At lower temperature, the chemisorption of oxygen then occurred on the oxide surface. The mechanism is a charge transfer process, in which an electron from the excess zinc atom becomes trapped on the oxygen, setting up a barrier layer of singly charged oxygen (O^-) ions, and this explains why zinc oxide has a high affinity for hydrogen, which is readily chemisorbed when admitted to the catalyst surface.

Hydrogen is chemisorbed on zinc oxide by conversion to hydroxyl ions (OH^-). In this process it returns an electron to the zinc oxide, thereby increasing its conductance. Infrared spectra showed three hydroxyl bands due to chemisorbed hydrogen [36]. This finding confirmed the expected location of hydroxylated ZnO ion pairs on the (1010) face of the crystal. On polycrystalline ZnO, it has been suggested that the surface was made up of (1010) and (0001) surface in equal quantities [37]. Each hydroxyl group is bonded to a zinc ion. Evacuation of zinc oxide at 600°C for 30 hours causes a reduction in the hydroxyl surface density. However, the hydroxyl groups remaining after evacuation were considered to be bound to Zn-O pairs,

which occur in line on the (1010) surfaces [36, 37].

1.3 THE ADSORPTION OF HYDROGEN

1.3.1 The Adsorption of Hydrogen on a Copper Surface

The adsorption of hydrogen on metal catalysts has an important influential effect in a number of industrial catalytic reactions.

Many studies have shown that, at low temperature, the dissociative adsorption of hydrogen occurs by a non-activated process [38] with respect to surface impurities and the catalyst reduction regime. Furthermore, Alexander and Pritchard [39] used the surface potential of atomic hydrogen, by assuming a dissociative chemisorption, to monitor the spontaneous chemisorption process, and the isosteric heat of adsorption was found to be typically between 40 and 50 kJ mol⁻¹ and dependent on the coverage of their copper film. However, studies of the adsorption and desorption of hydrogen on low index single crystals and a stepped copper surface showed that adsorption was an activated process involving energy barriers which depended on the crystallographic orientations of the catalyst surface [40]. Moreover, Taylor et al. [41] have shown that a significant exchange on copper foil did occur at higher temperature, with catalyst activity enhanced owing to the surface bond formation with vacant d-orbitals in the copper which were created through a d-s electron promotion. In

contrast, Shield and Russell [42] observed the adsorption of molecular hydrogen on granular copper at room temperature, and they concluded that traces of impurities in the copper were responsible for the adsorption. Also Takenchi et al. [43] found that 0.1 monolayer was adsorbed at 100°C on reduced copper oxide samples prepared by a fast reduction technique at 200°C.

Sinfelt et al. [44] found that copper is less active than nickel or cobalt toward the adsorption of hydrogen and the copper activity for the adsorption process was decreased at above 365°C. The same observation was noticed for supported copper in 1927 by Regerson and Swearingen [45]. In their study they proposed that hydrogen was adsorbed strongly on copper and a rapid loss in the adsorption capacity was observed with increasing temperature.

Most of the above studies show the ability of copper samples to adsorb hydrogen dissociatively, and this has been explained in terms of trace transition metal impurities [38-42]. These suggestions were confirmed by Cadenhead and Wagner [46] in their study of hydrogen adsorption on copper catalysts, the adsorption isotherm showed that the amount of hydrogen adsorbed was reduced drastically with increase of temperature and the isotherm reached an adsorption plateau only at the lowest temperature of the study of -196.7°C and they related the dissociation of hydrogen on copper to the impurities in the surface.

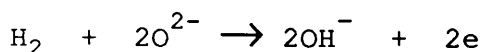
Furthermore, the dissociative adsorption of hydrogen could take place on a combined copper atom-nickel atom site with subsequent movement of the hydrogen atom on to the copper [46, 47]. This explanation is of particular interest in explaining the effect of the presence of traces of transition metal in such copper samples, and it might be that the study of the hydrogen adsorption on copper catalysts doped with transition metals as impurities in very low concentrations, was a definite alternative explanation of the behaviour of copper catalysts toward the adsorption of hydrogen.

1.3.2 The Adsorption of Hydrogen on Zinc Oxide Surfaces

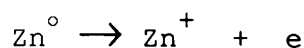
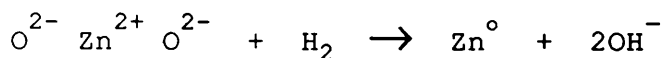
The hydrogen on zinc-oxide system has been the subject of many conductivity studies [48-50]. These studies showed that there was one type of hydrogen chemisorption at temperatures below 100°C which did not affect the conductivity of the oxide and another type of chemisorption at higher temperatures which increased the conductivity of the oxide.

Eischens *et al.* [48] suggested three general mechanisms for the increase in the conductivity of the zinc oxide surface as it is progressively exposed to hydrogen at higher temperatures. These are:

(i) A hydrogen chemisorption process which results in electron production;

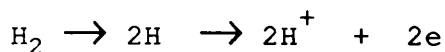


or the production of ionised excess zinc atoms;

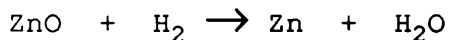


with a subsequent increase in the hydroxyl groups at higher temperature.

(ii) A mechanism based on the production of an electron via the route;



(iii) The suggestion that the increase in conductivity is caused by the reduction of the zinc oxide:



this reaction leaves ionised excess zinc atoms on the surface as in mechanism (i). Mechanism (iii) differs from mechanism (ii) in that the oxygen is removed as water.

In their study of the adsorption of hydrogen on zinc oxide, Nagarjuna et al. [51] conclude that the hydrogen chemisorbed below 50°C does not affect the zinc oxide

conductivity. They related this to the weak bond of hydrogen-zinc oxide at this temperature, in which the hydrogen atom is attached to the defect sites by one electron bonds, forming a complex where the hydrogen electron remains localized and, therefore, does not contribute to the change in conductivity.

Aharoni et al. [52] measured the activation energy for the adsorption of hydrogen on zinc oxide at room temperature (about 25°C). They found that the rate of hydrogen chemisorption decreased with the repeated use of the zinc oxide adsorbent, and the zinc oxide surface showed a small number of active sites with low activation energy together with a large area of sites with higher activation energy. They related this to surface heterogeneity effects.

Infrared spectroscopy studies [53-55] showed two types of hydrogen chemisorption at low temperature. The first is weak, fast and reversible, while the second type is stronger, fast and irreversible with neither having an effect on the conductivity of the oxide. Type one hydrogen chemisorption occurs on active sites confined in densely populated patches, while type two chemisorption is in a dissociated form with hydrogen bridged between neighbouring oxygen and zinc ions. However, four main types of hydrogen chemisorption can be distinguished; (i) rapid, reversible adsorption at room temperature; (ii) irreversible adsorption at room temperature; (iii) reversible adsorption at -196°C; (iv) high temperature adsorption which also

occurs to varying extents at room temperature. The (i) and (ii) adsorption processes are infrared inactive adsorption [56].

From the above studies, it is concluded that both zinc and oxygen are involved in the hydrogen chemisorption process but the nature of the active sites and the adsorption intermediates is still unclear.

1.4 THE ADSORPTION OF WATER

1.4.1 The Adsorption of Water on Copper Surfaces

Molecular water is believed to be adsorbed associatively at low temperature and, even at the adsorption of more than one monolayer, molecular water clusters into islands characterized by intermolecular hydrogen bonding.

Many studies [57-59] reveal that the knowledge of the interaction of the metal with water in an island form is not completely understood so as to make it difficult to draw any conclusion about the water-metal bonding.

Andersson *et al.* [60] found that water is adsorbed on copper (100) as a monomer at low temperature and low coverages, from their electron energy loss spectroscopy (EELS) vibrational spectra. Andersson *et al.* concluded that molecular water was adsorbed with the oxygen end toward the substrate and with its molecular symmetry axis tilted relative to the surface of the metal. However, upon

heating the surface, adsorbed water clusters into islands.

A similar conclusion was reached by Spitzer et al. [61] in their comparative study of the adsorption of water on a clean copper surface using UPS and XPS. They stated that only one species was adsorbed, that is molecular water. Upon heating, two species remained on the surface, these were water at low temperature and hydroxyl groups at higher temperatures.

However, up to 0.5 monolayer coverage of water, it was suggested that cluster formation is not the dominant effect and that molecular water is bonded to the surface in a configuration with the molecular plane normal to the surface.

The state of the molecular adsorption of water on the surface has a large effect on the surface work function. In the adsorption of a full monolayer of water, and at a submonolayer coverage, molecular water is adsorbed in a tilted geometry [62] and has a large effect on the work function of the copper (110) surface. However, at higher water exposure, multilayer adsorption was observed and accordingly this further adsorption caused a decrease in the work function. These results with many others [63-65] showed that the adsorption of water is structure sensitive and it has a large effect on the work function.

Physically adsorbed water at low temperatures could be desorbed upon heating, but when adsorbed at 300°C [63] it was desorbed only at temperatures above 500°C and this corresponded to the final chemisorption state.

The structure of copper surfaces has a large effect on the chemisorption state of water, indicated by the observation that both molecular water and hydroxyl groups are formed on the surface during the chemisorption of water on Cu (100) surface [64]. The formation of hydroxyl groups on a copper surface might be influenced by the presence of pre-adsorbed oxygen, [61, 64, 65]. During the adsorption of water on an oxygen covered surface, the molecular water could be bonded to the surface through its hydrogen atom. Therefore, the activation of hydroxyl bonds in molecular adsorbed water can be effected through a kind of hydrogen bonding with the chemisorbed oxygen at the surface.

Hydroxyl species formed at low temperatures are stable up to 100°C but above this temperature de-hydroxylation occurs. It is obviously very difficult to distinguish between hydroxyl groups formed by the exposure of an oxidised copper surface to water and those generated from the attack of oxygen on a molecular adlayer of water.

1.4.2 Water Adsorption on Zinc Oxide

The importance of the study of water chemisorption on zinc oxide is to decide whether water is adsorbed associatively or is dissociated into hydrogen and hydroxyl groups. Also, different strengths of interaction with the surface oxygen or zinc atoms might be expected depending on the surface structure.

Water can be chemisorbed on to the oxide surface at an

incompletely coordinated surface cation:

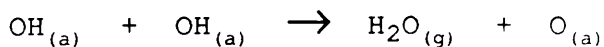


or it may be chemisorbed dissociatively on metal-oxygen sites:



The elements of water, hydrogen and hydroxyl groups are known to be the constituents of the oxide surface layer.

On the zinc oxide surface, hydrogen chemisorption sites of the type Zn-H and O-H, Zn^{2+} can be occupied by dissociatively adsorbed water [66, 67]. However, Atherton *et al.* [68] observed fundamental hydroxyl-stretching bands of surface OH groups on different zinc oxide low index surfaces which represent the dissociatively adsorbed water. These bands occur at 3670 and 3620 cm^{-1} and at 3550 and 3440 cm^{-1} , while the bands at 3550 and 3450 cm^{-1} were assigned as the asymmetric and symmetric hydroxyl-stretching fundamentals of associatively chemisorbed water. Bowker *et al.* [69] after exposing the zinc oxide to water found no desorption spectra in the temperature range 27-327°C that probably due to a low entropy factor for the reaction;



and a surface oxygen species paired with an anion

vacancy should be available. Accordingly, they concluded that vicinal hydroxyl species were formed. Recently, Zwicker and Jacobi ^[70] studied the adsorption of water on three low index (0001), (1010) and (1010) zinc oxide single crystal surfaces, and they concluded that the adsorption of water on zinc oxide interacts in a highly site specific manner and is stronger with zinc atoms than with oxygen surface atoms.

1.5 THE ADSORPTION OF CARBON MONOXIDE

1.5.1 The Adsorbed States of Carbon Monoxide on Metal Surfaces

The interaction of carbon monoxide with metal surfaces has been studied extensively in recent years. The study of the chemisorption of carbon monoxide on metal surfaces is very important, first because of the significant effect of the presence of carbon monoxide in various industrially important reactions such as methanol synthesis, the Fisher-Tropsch synthesis, and secondly, because of the use of carbon monoxide chemisorption for surfaces areas measurement and for studying the active site distribution on metal surfaces.

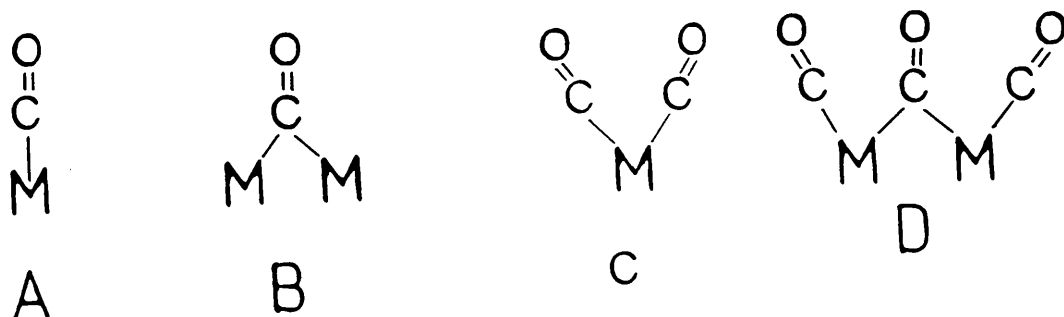
A review by Ford ^[71] has appeared in the past decade concerning the chemisorption of carbon monoxide on metal surfaces. Another review, by Sheppard and Nguyen ^[72] was concerned with the use of infrared spectroscopy in the study of carbon monoxide adsorption on supported group VIII

metals, and illustrated that infrared spectroscopy has been the main source of the evidence for the adsorption states of carbon monoxide on metal surfaces.

From organometallic chemistry, based on the early work of Eischens [73, 74] and his co-workers, comes most of the basic information on the spectroscopy of adsorbed carbon monoxide on metal surfaces. A band at 2143 cm^{-1} assigned to the C-O stretching frequency of the gaseous carbon monoxide was observed to shift to between 2100 cm^{-1} and 2000 cm^{-1} after the adsorption on the metal surface, when the carbon monoxide was bonded as a monodentate ligand. However, bidentate ligand formation was found to cause even greater shift in the band frequency to below 2000 cm^{-1} . These observations led Eischens et al. [73] to attribute the bands at above 2000 cm^{-1} to a "linear" carbon monoxide adsorption state on the surfaces (type A), and the bands below 2000 cm^{-1} to a "bridged" carbon monoxide bonded species (type B). However, many workers pointed out that the low frequency band could be caused by a change in the surface topography [75], while Harrod et al. [76] has suggested that the tailing of the broad band of chemisorbed carbon monoxide towards lower frequencies was due to a highly disordered surface, and to a sintering effect. The effect of oxygen as a permanent poison for the most active sites on the surface has also to be considered [75, 77], as well as support effects [77].

The adsorption of carbon monoxide on high area alumina supported rhodium was investigated by Kang et al. [78] and

they observed bands at high coverage at frequencies between 2095-2027 cm^{-1} and these bands were attributed to the adsorption of two carbon monoxide molecules bonded to a single metal atom (type C, D).

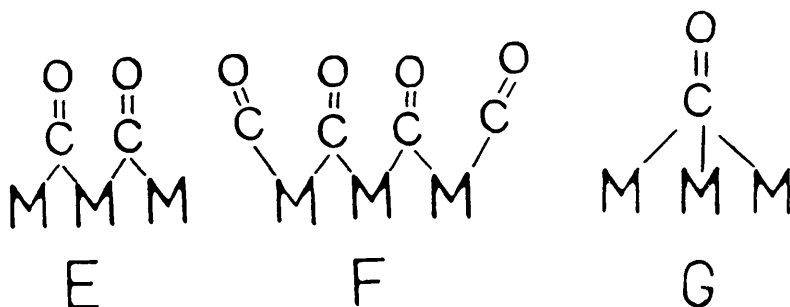


Three IR bands were observed by Haaland ^[79], the band at 2094 cm^{-1} was assigned to linear adsorption on surface terraces, (type A) that at 2045 cm^{-1} to linear adsorption on steps (type A) and the 1850 cm^{-1} band to bridged carbon monoxide. These bands were observed to be shifted to lower energy as the temperature increased.

The same assignments have been made by Tanaka and White ^[80] from their IR spectra for chemisorbed carbon monoxide on platinum supported by TiO_2 . From their results they showed that, on samples reduced at 200°C, two kinds of linear carbon monoxide species were observed, the first type of adsorption was assigned to platinum-terrace sites (2094 cm^{-1}) while the other was assigned to platinum-step sites (2077 cm^{-1}), although they observed a third band at 1854 cm^{-1} which was assigned to a bridged carbon monoxide species. With an oxidised sample the linear bands were shifted to higher frequencies of 2130 cm^{-1} and 2101 cm^{-1} ,

respectively, while the bridged carbon monoxide band was shifted to 1880 cm^{-1} .

However, Haaland [79] showed that the bridged carbon monoxide band at 1850 cm^{-1} was split into two bands after thermal desorption of carbon monoxide in the range $27\text{--}527^\circ\text{C}$. These lower band energies were assigned to carbon monoxide species adsorbed in 3-fold coordination (type E, F, G).



These observations are in accordance with the results of Hayden and Bradshaw [81] for carbon monoxide adsorption on platinum (111). Although infrared spectroscopy provides information on the adsorption form of carbon monoxide on metal surfaces, still the main experimental problem was that of preparing a sample with high adsorption capacity and acceptable infrared transmission. Two general approaches to this problem have been made. First, the use of supported metal samples [74, 78] and of evaporated metal films [82, 83]. These approaches have led to some valuable information about the nature of the chemisorption species. The difficulties in the use of supported metal are mainly because of the difficulties in spectral interpretation in the presence of the different supports, and also because of the use of hydrogen for reducing metal surfaces. The

hydrogen may dissolve in the metal and constitute an impurity which may change or alter the properties of the metal, and consequently, this change might produce some observable spectral changes [84]. On evaporated metal films the main difficulties have been those of contamination [82].

Yates and Garland [85] observed five distinct species of adsorbed carbon monoxide on nickel. Furthermore, it was established that the five absorption bands represented five distinct surface species. By observing independent variations in the intensities during various changes in the experimental conditions, these species, which occurred at frequencies of 3035, 2082, 2057, 1963, 1915 cm^{-1} respectively, were attributed to the adsorption type of the formula as detailed at A, B and D, respectively.

1.5.2 Chemisorption State of Carbon Monoxide on Copper Surfaces

The nature of the bonding of carbon monoxide to transition metal atoms in coordination complexes and on surfaces has been characterised by Blyholder [86]. The bonding was suggested to follow a donor-accepter mechanism, and carbon monoxide was bonded to the metal atom or atoms by means of stabilisation of the 5σ orbitals on mixing with metal molecular orbitals which were considered to be d-orbitals. He also pointed out that the electron donation from metal d-orbitals to a low energy π antibonding

orbital in carbon monoxide molecules may alter the linear position of adsorbed carbon monoxide, and this back donation may be enhanced for the adsorbed carbon monoxide on low coordination sites of the metal, which causes the shift in the infrared band position of adsorbed carbon monoxide molecules to lower frequency.

In the case of copper, because of the filled d-orbitals, an alternative possibility has been considered [78, 88, 89] in which the electron pair of the 5σ orbitals of carbon monoxide molecules forms a donor-acceptor bond with the partially filled 4s orbitals of the surface copper atoms. Although copper d-orbitals are filled, it has been proposed that the small promotion energy required for the carbon monoxide bonding with 4s-orbitals is reflected by a small heat of adsorption. This led to the suggestion of the use of low temperatures to obtain quantitative adsorption [90]. This postulate was examined by Isa et al. [91] who studied the adsorption of carbon monoxide on copper (100). The adsorption state of carbon monoxide at room temperature was attributed as $\text{CO}^{-\sigma}$ and the back donation into the antibonding orbital would have a significant importance to the carbon monoxide-copper bonding, while the adsorption state at -193°C was designated as $\text{CO}^{+\sigma}$ and the back donation was less important in the bonding. Room temperature adsorption suggests the occurrence of the rehybridisation of the metal electron, which contributes to the carbon monoxide adsorption on copper at room temperature and above, as transition metal characteristics.

This was similar to the above mentioned d-s promotion.

1.5.3 The Adsorption of Carbon Monoxide on Copper Catalysts

In recent years, considerable effort has been directed toward the study of the adsorption of carbon monoxide on copper catalysts. Indeed, infrared spectroscopy has contributed to the understanding of the adsorption state of carbon monoxide on copper catalysts using a variety of catalyst preparative methods and reductive procedures. These studies have been carried out either on single crystals, supported catalysts, or evaporated metal films. In all these studies a considerable variation in the vibrational spectra of adsorbed carbon monoxide has been observed in the frequency range of 2120 cm^{-1} - 2080 cm^{-1} . This variation appears to depend on the particle size, the completeness of copper surface reduction, and the effect of coadsorbed oxygen on the catalyst surface [92].

Bocuzzi et al. [93] showed the temperature and pressure dependence of bands due to adsorbed carbon monoxide on copper surfaces. The strong and narrow band at 2089 cm^{-1} was assigned to adsorption at stepped close-packed sites, while a broad and weak band at 2070 cm^{-1} was assigned to adsorption at corner or edge sites. These kinds of sites show a different reactivity towards adsorbed oxygen by a shift in the band towards a high frequency.

The surface potential of copper surfaces was found to

increase [94] after exposing the surface to carbon monoxide at -183°C up to a surface coverage of 0.25 monolayer, whereupon the potential decreases until the maximum surface uptake at low pressure ($\theta = 0.5$) was achieved. However, at high surface coverage, the high frequency band of adsorbed carbon monoxide, which appears at 2105 cm^{-1} , was found to change only slightly [95], while the surface potential decreased [96] significantly.

Surface potential measurements of adsorbed carbon monoxide on single crystal copper surfaces showed that it has similar characteristics to that of an evaporated film. That is the surface potential of copper (111) following the adsorption of carbon monoxide at -180°C was found to change significantly, the changes were found to be an increase to 0.47 V at low coverage which then decreased to 0.05 V at saturation coverage [97, 98]. On a copper (100) surface the rise was up to 0.23 V and subsequently decreased to 0.07 V, whereas on copper (110) the increase was 0.29 V decreasing to 0.18 V.

The infrared spectra of carbon monoxide chemisorbed on a variety of copper single crystals have provided information on the carbon monoxide-copper system. A single band at 2070 cm^{-1} due to adsorbed carbon monoxide on a copper (111) single crystal was observed at all coverages, and it has been ascribed to the adsorption of carbon monoxide at higher coverage by bridging to two copper atoms [97]. Also, two bands reported by Hayden et al. [99] appeared at 1830 and 1810 cm^{-1} for high coverages of carbon

monoxide on copper (111) as well as the high frequency band at 2070 cm^{-1} . However, Chesters et al. ^[100] observed bands arising from the linear and the bridge bonded carbon monoxide molecules on a copper (111) single crystal. A decrease in the linear carbon monoxide band from 2077 cm^{-1} at lower coverage to 2069 cm^{-1} at high coverage was also observed.

When carbon monoxide was adsorbed on a well-reduced supported copper sample the infrared spectra showed only one band at a frequency characteristic of linearly chemisorbed carbon monoxide ($2200\text{--}2000\text{ cm}^{-1}$), which was both temperature and pressure dependent. At high equilibrium pressure of 5 torr of carbon monoxide at room temperature ^[101], two bands appeared and attained their maximum intensity; the band at 2098 cm^{-1} was assigned to adsorbed carbon monoxide molecules on a "definite and ordered" surface which corresponded to linear bound carbon monoxide molecules, while the band at 2070 cm^{-1} has been assigned to carbon monoxide adsorbed on the "borderline" copper atoms of the particles.

Different copper species were identified as isolated atoms incorporated in the support following the adsorption of carbon monoxide on silica-supported copper catalysts. The adsorption bands were found to lie between $2113\text{--}2090\text{ cm}^{-1}$ on well reduced surfaces ^[102] and arose from linearly bound carbon monoxide. These bands were suggested to be adsorbed carbon monoxide on Cu^0 , while another band, at 2175 cm^{-1} , was assigned to weakly adsorbed carbon monoxide

bound to isolated Cu^+ ions. The position of the latter did not appear to vary with the metal loading or surface reoxidation.

The shift in the positions of the bands with surface coverage is consistent with the decrease in the heat of adsorption of adsorbed carbon monoxide. The heat of adsorption was found to decrease with coverage from 76 to 50 kJ mol^{-1} [103]. The heat of adsorption was also determined on single crystals. On copper (111) [104] it was found to be 50 kJ mol^{-1} , on copper (100) [103] 59 kJ mol^{-1} , and on copper (110) [105] 58 kJ mol^{-1} .

A decrease in the heat of adsorption from 50 to 22 kJ mol^{-1} with coverage was also observed by Kohler [102] for the carbon monoxide-silica supported copper system.

Measurements of the heat of adsorption of carbon monoxide on copper catalysts are, however, rather conflicting. Trapnell [106] determined the heat of adsorbed carbon monoxide on copper surfaces, and estimated it to be 38 kJ mol^{-1} at -80°C and high surface coverage, while Dell, Stone and Tiley [107] using reduced copper powder estimated a value of 70 kJ mol^{-1} at room temperature with a resulting 20% surface oxygen coverage. A further value for the heat of adsorption of 80 kJ mol^{-1} was calculated by Joyner *et al.* [108].

Evidence for strongly adsorbed species has been obtained by studying the adsorption of carbon monoxide on supported copper surfaces. Smith and Quets [94], after allowing carbon monoxide to adsorb at -196°C , found that

10% of the adsorbed carbon monoxide was desorbed with a heat of desorption of between 42 and 84 kJ mol⁻¹. If the adsorption occurred at higher temperature, an activation energy for desorption as high as 125 kJ mol⁻¹ was obtained. Parris and Klier ^[109] studied the chemisorption of carbon monoxide on Cu/ZnO catalysts, and concluded that carbon monoxide was irreversibly bonded at room temperature to the surface of the binary catalysts, thereby supporting the evidence for the existence of strongly adsorbed carbon monoxide species on copper catalysts. A copper cation (Cu⁺) species has been identified as the active site ^[8] for the adsorption of carbon monoxide. The heat of adsorption was calculated for the adsorbed carbon monoxide on these sites and found to be 75-110 kJ mol⁻¹ ^[88]. The copper cation (Cu⁺) associated with the metallic copper clusters forms the most active species in the commercial Cu/ZnO synthesis catalysts and these two species have qualitatively different carbon monoxide adsorption behaviour. The irreversible adsorption occurs at room temperature on the cation sites while reversible adsorption is on the metallic copper phase ^[110].

1.5.4 Carbon Monoxide Chemisorption State on Zinc

Oxide

Many studies have been reported on the adsorption of carbon monoxide on both zinc oxide powders ^[111] and zinc oxide single crystal surfaces ^[89, 112].

Gay et al. ^[89] reported that the adsorption of carbon

monoxide occurred reversibly at the coordinatively unsaturated zinc surface ions;



giving rise to an infrared band at 2191 cm^{-1} . The heat of adsorption was estimated to be $\sim 50 \text{ kJ mol}^{-1}$. This reversible adsorption was found not to affect or block type I hydrogen adsorption sites. These results with a constant heat of adsorption of 44 kJ mol^{-1} were confirmed by Ghcotti *et al.* [113], who found that, on samples slowly heated under vacuum at 400°C followed by admission of oxygen, carbon monoxide was reversibly and weakly adsorbed on zinc oxide. This adsorption state was characterised by a carbon monoxide band at 2183 cm^{-1} , and also resulted in the formation of a small amount of carbonate reversibly held on the surface.

Recently, in our laboratory as part of an investigation of copper-based catalysts properties, the adsorption of [^{14}C -] labelled carbon monoxide on zinc oxide was found to be negligible [114].

1.6 THE ADSORPTION OF CARBON DIOXIDE

1.6.1 The Adsorption of Carbon Dioxide on Copper Surfaces

In an ab-initio valence-bond calculation study, Freund

et al. [115] considered three different coordination geometries for the transition-metal complexes with coordinated carbon dioxide: pure carbon coordination, (which was considered unlikely) pure oxygen, and mixed oxygen-carbon coordinations. The bonding between carbon dioxide and a metal atom was considered to be in the form of the anion of carbon dioxide (CO_2^-).

Anderson [116], in his molecular orbital study of the interaction of carbon dioxide with copper (100), found that carbon dioxide molecules adsorbed weakly on the surface and the molecule rested in a μ -bridging position and was bonded through the mixing of copper d- and carbon dioxide π -orbitals.

Molecular carbon dioxide is found to bend with an $\text{O}-\text{C}-\text{O}$ angle of (120°) similar to excited state of free carbon dioxide molecule with bending angle of (122°). According to the calculation the μ -bridging position of carbon dioxide on Cu (100) involves two copper atoms with the distance of the carbon from the surface of 1.5° . The binding energy was estimated to be 46 kJ mol^{-1} .

The weak bonding of carbon dioxide on copper surface, as predicted by the above theoretical calculations has been confirmed experimentally. In their UPS-XPS study of the adsorption of carbon dioxide on evaporated copper film, Norton and Tapping [117] suggested the occurrence of physically adsorbed carbon dioxide. This postulate arose from their observation of little shift in the carbon and oxygen 1s binding energies of the adsorbed carbon dioxide,

and localised attenuation in the copper valence bonds with respect to the heat of adsorption which was estimated to be $<38 \text{ kJ mol}^{-1}$. More recently, Kinnaird et al.^[114] extensively studied the adsorption of carbon monoxide and carbon dioxide on freshly reduced, and partially and fully oxidised copper-based catalysts, by a radiotracer technique. They showed evidence^[114] for both weak and strong adsorption states of carbon dioxide on the copper component of catalysts reduced with hydrogen, and also detected both rapid and a very slow adsorption of carbon dioxide. The adsorption of carbon dioxide was not prevented by the presence of carbon monoxide on the surface, while on partially oxidised surfaces^[114] and at low coverages of surface oxygen, the amount of carbon dioxide adsorbed, and retained as strongly bound species, on the copper component was increased compared with that adsorbed on a freshly reduced surface. The adsorption of carbon dioxide on an oxidised surface in the presence of hydrogen showed enhanced amounts adsorbed and retained on the copper component. However, little adsorption of carbon dioxide was observed on the fully oxidised surface.

In contrast to the above studies, some early work showed no interaction of carbon dioxide with various copper catalysts. Within the experimental conditions used for one study, Stone and Tiley found^[118] no appreciable adsorption of carbon dioxide to occur on a reduced copper surface, but they did not indicate the adsorption temperature. Similarly, Collins and Trapnell found^[119] no

adsorption of carbon dioxide at -78°C on copper films sintered at 0°C or above, however, their copper films did have very low surface areas, which made it difficult to detect small amounts of adsorption.

Habraken et al. [120] found no adsorption of carbon dioxide on a copper (111) surface at temperatures of 24°C and 36°C and pressures of 10^{-3} torr.

In some of the above studies and many others [115, 117, 121-123, 105, 10], attention has been given to the possibility of the dissociative adsorption of carbon dioxide. On transition-metal surfaces the adsorption of carbon dioxide has been observed and has been interpreted to be due to the occurrence of dissociation of carbon dioxide into carbon monoxide and oxygen. The conclusion that carbon dioxide dissociated to carbon monoxide and oxygen was based on the observation of the identical behaviour of the adspecies to those of adsorbed carbon monoxide [121, 122] with respect to the different techniques used for this observation.

Wachs and Madix [105] studied the adsorption of carbon dioxide on a copper (110) single crystal at -93°C , and observed that on a oxygen-free copper surface greater than 99% of the adsorbed molecular carbon dioxide dissociated to carbon monoxide and oxygen, the activation energy for the formation of carbon monoxide was estimated to be 58 kJ mol^{-1} . Kinnaird et al. [114] reported evidence for the dissociative adsorption at room temperature of some of the carbon dioxide to adsorbed carbon monoxide and surface

oxygen, as well as the formation of surface carbonate by reaction of carbon dioxide with surface oxygen. Although, their observation of the dissociative adsorption of carbon dioxide was made as a result of long exposure of the catalyst to carbon dioxide during the build-up of the adsorption isotherms, only a small amount of carbon monoxide was detected in the gas phase analysis by gas-chromatography. However, Kleir ^[110] obtained indirect evidence that on carbon monoxide reduced copper-zinc oxide-alumina catalysts the surface could be re-oxidised by carbon dioxide during the adsorption of carbon dioxide at 250°C with the accompanying appearance of carbon monoxide. Carbon dioxide was found to dissociate at higher temperature in a radiotracer study by Grabke et al. ^[123] with an activation energy determined to be 53 kJ mol⁻¹.

1.6.2 The Adsorption of Carbon Dioxide on Zinc Oxide Surfaces

Carbon dioxide is a small molecule with acidic properties which has been used as a probe molecule for poisoning in catalytic reactions and for studies of basic surface sites.

Carbon dioxide adsorption on oxide surfaces leads to a variety of adsorbed species such as bicarbonate and carbonate ions that coordinate to surface metal ions in various ways. Bicarbonate species give rise to infrared bands at 1618, 1431 and 1230 cm⁻¹, according to the study of Taylor and Amberg ^[124], when carbon dioxide is adsorbed

on a zinc oxide surface. However, no such bands were observed by Malsuchita and Nokata [125] or by Atherton et al. [68]. This might be due to the relatively low stability of the bicarbonate species, which could result in it being removed from the surface before the spectrum had been recorded. In the above studies and also in the study of Matsushita [126] it was shown that the existence of unidentate, bidentate and bridge bonded adsorption complexes of carbon dioxide occurred on zinc oxide surfaces.

The adsorption capacity for carbon dioxide of zinc oxide surface was shown to increase with a decrease in the number of hydroxyl groups on the surface [127], while carbonate formation was related to the nature of the Zn-O cation-anion pair site. In a complete contrast with the above studies, Levy and Stenberg [128] measured the heat of adsorption of carbon dioxide on zinc oxide surfaces and found that the heat of adsorption varied linearly with the concentration of free zinc in the catalyst sample. Heats of adsorption were found to be between 87.9-125.6 kJ mol⁻¹ depending on the amount of excess zinc in the sample. Their measurements were carried out for adsorption at 300°C and the extent of dehydroxylation of the surface had to be considered; heats of adsorption of 71.7-87.9 kJ mol⁻¹ were found from the measurement of the adsorption isotherm [129]. Determination of the heat of adsorption of carbon dioxide on a zinc oxide surface by measuring the heat of immersion [130] of zinc oxide samples in water, and the

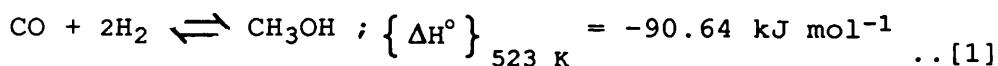
heat of immersion of zinc oxide sample with pre-chemisorbed carbon dioxide at different temperatures gave values of between 77.5-93 kJ mol⁻¹.

The effect of the interaction of carbon dioxide on the properties of zinc oxide has been investigated. Amiguiés and Teichner found [131] no change in surface conductivity during carbon dioxide exposure, while Hotan et al. [132] concluded that there is a ready establishment of a surface equilibrium during the chemisorption of carbon dioxide on clean zinc oxide (1010) surfaces near room temperature, and that there is an increase in the work function and corresponding decrease in the surface conductivity.

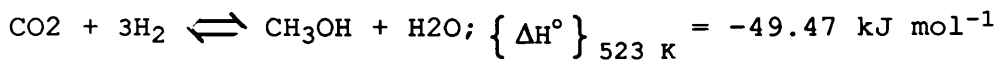
1.7 REACTIONS ON COPPER CATALYSTS

1.7.1 METHANOL SYNTHESIS

Methanol synthesis is a reaction of great importance in industry. It is, in general, the main product of the hydrogenation reaction of a mixture of carbon monoxide and carbon dioxide. The main synthesis reactions are shown in equations [1-3] with their thermodynamic values for reaction of the gas-phase components:



$$\left\{ \Delta G^\circ \right\}_{523 \text{ K}} = -25.34 \text{ kJ mol}^{-1}$$



...[2]

$$\left\{ \Delta\text{G}^\circ \right\}_{523 \text{ K}} = +3.30 \text{ kJ mol}^{-1}$$



..[3]

$$\left\{ \Delta\text{G}^\circ \right\}_{523 \text{ K}} = -28.64 \text{ kJ mol}^{-1}$$

Hydrogenation of carbon dioxide {reaction [2]} produces water as well as methanol. However, both carbon monoxide and carbon dioxide participate in reaction [3], the water-gas shift reaction, which is also catalysed by the synthesis catalysts (see section 1.7.2), so that both or either one of the carbon oxides can be the main source of carbon for methanol production. This subject has been of interest to many investigators in recent years (see section 1.7.1.1). Under the industrial conditions a mixture of carbon monoxide, carbon dioxide and hydrogen (10:10:80) undergoes reaction on a ternary catalyst of copper-zinc oxide-alumina (60:30:10) at 250°C and a pressure of 50 atm [133].

An early review by Natta [134] showed that copper based catalysts are active for the synthesis process from a mixture of carbon monoxide and hydrogen at 300°C and pressure of 100 atm. Although the copper catalyst is very

sensitive to poisoning during the reaction process, Natta found that polycrystalline copper is not active for this reaction, while a combination of copper and zinc oxide (about 30-40% copper) had good activity and the addition of a third component provided the catalyst with a resistance to ageing. Similar results were obtained by Klier ^[110] who investigated the activity of pure copper metal and zinc oxide and found that neither of the two, individually, can catalysed the synthesis reaction. However, the situation was different when they are used together.

The active sites on which the adsorption and consequently the hydrogenation take place are the subject of much debate (as detailed in section 1.2.1), as well as the reaction mechanism.

Many mechanisms have been proposed for the synthesis reaction, although the nature of the reaction intermediates and the nature of the adsorbed species are still not very clear. Formate and methoxy species have been identified ^[135] on a used methanol catalyst and the proposed mechanism postulated that formate, methoxy groups and methoxy are reaction intermediates bonded to the surface through the oxygen end. A different mechanism has been suggested by Herman *et al.* ^[5]. Involving carbonyl, formyl, hydroxycarbon, and hydroxymethyl intermediates bonded to the Cu^+ ion in the zinc oxide phase through carbon. He also proposed, that the zinc oxide surface is the active site for hydrogen adsorption, while copper nondissociatively adsorbed and activate carbon monoxide.

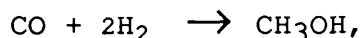
The catalyst deactivation in their experiment was explained by the reduction of Cu^+ to inactive copper metal. The hydrogenation of carbonyl species to a formyl species, was another proposed mechanism [136], formation of a methoxy species occurring as a result of further hydrogenation following the interaction between the formyl oxygen and a surface vacancy. The methoxy formation was claimed to be due to the increase in the oxygen vacancy bonding strength and the weakness of carbon bonding to the metal ion [136]. Following an *in situ* infrared study of the synthesis reaction, Edwards et al. [137] suggested a similar mechanism to that of Herman et al. [5]. Their mechanism was based on the adsorption of carbon monoxide on copper ion sites in the zinc oxide phase forming a carbonyl species, while molecular hydrogen is adsorbed on adjacent zinc-oxygen sites to form hydroxyl and hydride species. However, the hydroxyl and the hydride species were not very stable and were difficult to detect. The hydrogen might migrate to other sites forming stable hydroxyl species. The carboxyl species can insert into a hydroxyl group forming a bidentate formate species. The hydrogenation of formate is the next step, to form adsorbed formaldehyde on different sites from those occupied by the formate species, the formaldehyde is quickly hydrogenated to methoxy species and finally the hydrogenation of the methoxy species to methanol, which represents the rate determining step in the synthesis reaction mechanism. In contrast, infrared spectroscopy and temperature programmed desorption studies,

[138] both identified copper formate as the reaction intermediate in methanol synthesis. And the hydrogenation of the formate species was proposed as the rate-determining step. It is most interesting to note that it is a copper formate species which is identified in the above study while a formate on zinc oxide was identified in the study of Edwards et al. [137].

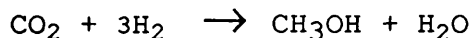
Chemical trapping techniques have been used to identify the synthesis reaction intermediates [139], on pure copper based catalysts and on catalysts promoted by metal oxides. From these studies formate species represent the first step in the reaction of carbon dioxide by insertion in hydride sites, while formate can be produced after the reaction of carbon monoxide with the hydroxy species on the oxide surface. The reaction of these formate species through bridged oxygenated and methoxy intermediates was considered to be the final step in the synthesis of methanol. The catalyst selectivity was influenced by the presence of metal oxide [139], and the extent of this effect depended on the nature of the promoting oxide, for example, metal oxides, (e.g. ThO_2 , Y_2O_3 , and In_2O_3) led mainly to the formation of methanol, while a sample promoted with SiO_2 gave mainly methane.

1.7.1.1 The Role of Carbon Dioxide in Methanol Synthesis

The classic methanol synthesis reaction (see section 1.7.1),



has been the subject of many studies as reviewed by Kung [136] and Klier [110]. Relatively little information has appeared in the literature concerning the alternative synthesis reaction, the hydrogenation of pure carbon dioxide.



Among the papers reporting on the synthesis of methanol from carbon dioxide, one reports the measurement of the catalytic activity of $\text{Cu}/\text{Al}_2\text{O}_3$ [140] assuming that carbon dioxide is indirectly converted to methanol, with carbon dioxide converted to carbon monoxide through the water gas shift reaction and then carbon monoxide is hydrogenated to methanol.

However, Klier *et al.* [6] demonstrated that the presence of carbon dioxide has the effect of stabilising the active site on the catalyst surface, while others suggest that carbon dioxide is converted to methanol with carbon monoxide acting as a source for carbon dioxide

[141]. In a recent review, Chinchen *et al.* [142] showed that the direct hydrogenation of carbon dioxide is the main source of methanol. In their review Chinchen *et al.* [142] explained their experimental results on methanol synthesis using a mixture of CO, CO₂ and H₂ containing ¹⁴C-CO₂. This mixture was passed over industrial Cu-ZnO/Al₂O₃ catalyst which had shown to be active for the synthesis reaction from CO : H₂ mixture. Their measurement of product yields and radioactivities showed clearly that the synthesis proceeded via carbon dioxide and they showed [142] that scrambling of ¹⁴C between carbon monoxide and carbon dioxide was negligible during the synthesis reaction. Formate was found to be involved in the synthesis and water gas shift reactions [142]. However, many researchers still feel that the hydrogenation of carbon monoxide is the dominant route to methanol. Indeed, Liu *et al.* [143] investigated the contribution of carbon monoxide and carbon dioxide to methanol synthesis using ¹⁸O-labelled carbon dioxide. They found that the rate of production of ¹⁸O-labelled methanol (from carbon dioxide) was 50% of the rate of ¹⁶O-labelled methanol production (from carbon monoxide) at 220°C, indicating that methanol is primarily produced from carbon monoxide hydrogenation.

An interesting observation was also made by Klier *et al.* [6] regarding the role of carbon dioxide in the synthesis reaction, namely that when the molar ratio of CO₂/CO was increased methane was produced, while no methane production was detected for the hydrogenation of carbon

monoxide. However, in this regard there are conflicting observations. First, Amenomiya ^[144] found no methane production from the reaction of carbon dioxide and hydrogen at temperatures below 297°C. Second, Liu et al. ^[145], recently studied the rate of methanol production, and their initial rate studies showed that the production rate of methanol increased as the ratio of CO₂/CO increased and that it had no maximum value.

Third, Schach et. al. ^[146] found that an optimum ratio of CO₂/CO exists, and that the inhibition of methanol production occurred beyond this ratio. Their results suggest that carbon dioxide inhibits the hydrogenation of carbon monoxide, but not its own hydrogenation to methanol. Liu et al. ^[145] also found that water inhibited carbon dioxide adsorption, but not carbon monoxide hydrogenation to methanol, in agreement with the various investigations of Schach ^[146] and Klier ^[6] regarding the influence of the reverse synthesis reaction.

The results of Schach et al. ^[146] and the oxygen labelled experiments of Liu et al. ^[143] indicate that carbon dioxide hydrogenation and carbon monoxide hydrogenation occur on different sites and they showed that whilst water inhibited the carbon dioxide hydrogenation it had no effect on the carbon monoxide hydrogenation.

1.7.2 WATER-GAS SHIFT REACTION (WGS)

The water-gas shift reaction:



is an important step in many industrial processes, including hydrogen production for ammonia synthesis.

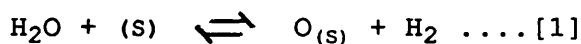
Commercial low temperature shift catalysts are all based on copper and zinc containing compounds, mostly supported on alumina or chromia. Catalysts are usually activated by a careful reduction, and most of the copper compound is brought into the metallic state. The active state may be considered tentatively to arise from the mixture of copper and zinc oxide components. However, the role of the support is to ensure stability which may also affect the activity [110].

The state of the copper in working catalysts is a subject of much controversy. For catalysts similar to those used in methanol synthesis (see section 1.2.1), it has been suggested [110, 147] that copper dissolved in zinc oxide is the active phase for this reaction. Campbell *et al.* [148], in a study of WGS reaction on copper (111) single crystal surface with a pressure of water of 10 torr and a pressure of carbon monoxide of 26 torr at temperature of 339°C, concluded that the surface was in a metallic form and relatively free from the adsorbed species even if the catalyst was preoxidised. They suggested that copper is the

active phase for this reaction.

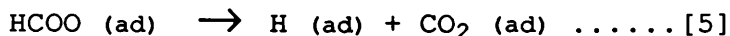
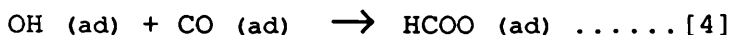
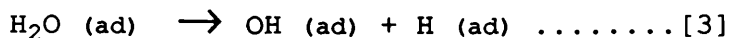
Copper-based catalysts containing zinc oxide as a "stabiliser or promoter" are used commercially as low temperature shift catalysts. However, the exact role of zinc oxide is not very clear [149-153]. Many studies [148-150] have investigated the nature of the active phase of the catalysts in water-gas shift and concluded that metallic copper is the active phase, while others suggested that copper ions in the metal-oxide lattice are important for the catalysis [110, 147].

A surface-redox mechanism has been suggested [110, 152, 153] where water, dissociatively adsorbed on the surface, produces hydrogen and surface oxygen, which is further consumed by carbon monoxide to produce carbon dioxide and a reduced surface according to the reactions:



where S represents the surface sites. In these two half reactions, the carbon monoxide shift conversion always acts as an oxygen transfer reaction [152] such that carbon monoxide is oxidised by water, with the catalyst acting as an oxygen transfer agent. Formate intermediates have been suggested as being involved in the water gas shift reaction [148] from the reaction of the dissociative products of adsorbed water under conditions of higher pressures and lower temperatures [152] similar to those used by Campbell

et al. [148]. The formate decomposition was determined to be the rate-controlling step:



The formate species is also claimed to be very important in both methanol synthesis and the shift reaction [138], since the formate species is produced by the adsorption of carbon dioxide and hydrogen on copper catalysts, but decomposes to carbon monoxide or is hydrogenated to methanol in the presence of hydrogen.

A redox mechanism was also suggested by Uchida et al. [154] to account for the observation that low temperature shift catalysts, containing low percentages of copper component, had a high specific activity. The smaller copper particles were suggested to be more easily oxidised than those of the methanol synthesis catalyst, which contains a higher copper content, and this allowed the redox mechanism to produce equilibrium yields rapidly. A similar conclusion was reached by Kuijpers et al. [155].

All the reported activation energies [148-150, 156] fall close to a value of 113 kJ mol^{-1} , and a kinetic study [148] of the shift reaction over a copper (111) single crystal found that the reaction was zero order in carbon monoxide and had a positive order with respect to water.

1.7.3 METHANOL DECOMPOSITION ON COPPER-BASED CATALYSTS

1.7.3.1 Methanol Decomposition on Copper Surfaces

The dehydrogenation and oxidation of alcohol over metal and metal oxide catalysts is a well studied reaction. This is primarily because of increasing industrial interest in the development of various reaction routes towards the production of a substitute for natural gas.

Methanol decomposition represents the simplest catalytic reaction of oxygen-containing organic compounds. Spectroscopic studies have shown convincingly that the decomposition process proceeds via sequentially formed methoxy and formate intermediates [157, 158]. Both of these intermediates are stable to approximately 90°C, but decompose at higher temperature to produce gaseous products, and a clean surface.

Methanol was found to be adsorbed associatively on copper surfaces at room temperature [158] forming a chemical bond with the surface via the oxygen lone-pair orbitals, and the higher exposure of the surface to methanol at this temperature was found to cause the formation of an adsorbed aldehyde which was stable under these conditions. Heating the surface produced the decomposition products of both methanol and formaldehyde, that is carbon monoxide, and hydrogen. In their UPS study of methanol decomposition on

copper and nickel Kojima *et al.* [158] related the production of HCHO to the lower affinity of hydrogen for the copper surface, two methanol hydrogens being removed during the adsorption process leaving an adsorbed hydrogen molecule and CH₂O on the surface. Nevertheless, the methoxy intermediate was found to be bound normally to the surface via the C-O axis [159], in agreement with Sexton's study [157] using electron energy loss spectroscopy (EELS), indicating that the methoxy molecule was oriented with the oxygen end towards the metal, and that the methoxy group was rather little perturbed by the adsorption. This result is in a complete contrast with an infrared study by Ryberg [160] on the vibration study of CH₃O on copper (100), it was concluded that the methoxy molecules were tilted on the surface.

From kinetic measurements and simultaneous measurements of surface potential, Myazaki *et al.* [161] concluded that the outer s-electron in copper is used for the bonding of methanol to the copper surface, through the oxygen end of the molecule. The intermediate products of the decomposition were suggested to be bound in a similar way to the surface, that is the formaldehyde was bonded to the copper surface through the oxygen. Moreover, formate was found to be the surface intermediate as revealed by the temperature programmed decomposition study by Sexton *et al.* [162] in a spectroscopic study of methanol decomposition on silver (110) [163]. These studies showed that formate is the most stable intermediate in the

decomposition process and its decomposition is the elementary step which has the highest free energy of activation within the overall mechanism. It was also shown that the formate decarboxylated to carbon dioxide.

The above results are in good agreement with study of the decomposition of methanol on Cu/ZnO oriented thin films [164] which showed that the decomposition products were carbon monoxide, carbon dioxide and hydrogen, and the formation of carbon dioxide was attributed to the decomposition of formate on copper clusters and on the copper cation sites dispersed on the zinc oxide surface.

The activity of the copper cation in Cu/ZnO catalysts was proposed by Klier [110], who suggested that the substitutionally dissolved Cu^+ cation on the zinc oxide surface was the active site in Cu/ZnO synthesis catalysts. An infrared spectroscopy study [165] of the adsorption of methanol on copper-based catalysts showed that methanol adsorbed dissociatively to produce methoxy species and hydroxyl groups, with an infrared frequency of 3524 cm^{-1} . The origin of the hydrogen in the observed hydroxyl group was examined by the use of deuterated methanol. This showed that the hydrogen comes from the hydroxyl hydrogen in the methanol feed-stock. The methoxy species was then converted to formate. This study concluded that the formate was adsorbed on the non-polar zinc oxide surface while methoxy groups were adsorbed on the polar zinc oxide surface. However, copper was found to be the major component influencing the activity of the catalyst, and zinc oxide

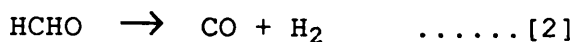
appeared to promote the stability and activity of the copper-based catalyst [166].

It was generally observed [167, 168] that, at low temperatures, methanol was adsorbed molecularly on copper catalysts. At these temperatures the non-bonding orbitals of oxygen were shifted to higher electron binding energies. This shift was indicative of a bonding interaction of methanol with the surface through the oxygen lone pair electrons, and molecularly adsorbed methanol decreased the work function, indicating the adsorption of the molecules through the negative end. However, Bowker and Madix [168] found that the adsorbed monolayer of methanol on copper (110) did not prevent the dissociative adsorption of oxygen at low temperatures ($\sim -140^{\circ}\text{C}$) which indicated that methanol dissociates on sites different from those of the adsorption of oxygen.

The binding energy of non-dissociatively adsorbed methanol on copper (110) was found to be in the range of 48-64 kJ mol^{-1} .

1.7.3.2 The Effect of Oxygen on the Decomposition Of Methanol on Copper Catalysts

Copper-based materials are regarded as dehydrogenation catalysts, the decomposition taking place in two stages as shown by Lawson and Thomson [169]



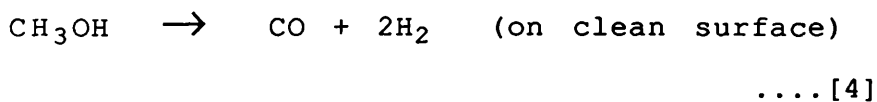
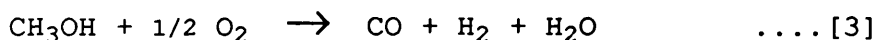
The extent of reaction [2] is found to depend upon temperature and the method of catalyst preparation .

The importance of oxygen in the decomposition reaction was extensively investigated by Lawson and Thomson [169], who measured its influence on the copper activity for methanol decomposition. They concluded that the reduction of copper oxide by hydrogen produced a catalyst which could be used to catalyse the decomposition of methanol, although the catalyst was either deactivated or poisoned after several reactions, whereas on partially oxidized copper film a significant decrease in the catalyst activity for the decomposition was noticed. However, copper catalysts in the form of wires or foils were found to be inactive for the decomposition although they could be activated by treatment with oxygen at higher temperature. It was suggested that the presence of oxygen on a copper catalyst is essential for it to be active for the decomposition reaction.

Copper catalysts have a high selectivity for oxidising methanol to aldehyde [105] by removing hydrogen from the hydroxyl group of alcohol without breaking the C-O bond. Furthermore, the methoxy group is a stable surface intermediate which was found to be responsible for the formation of the aldehyde. The methoxy species can be produced by the direct interaction of methanol with surface

oxygen. The UPS spectrum of the methoxy species was found to be different from that of methanol molecules adsorbed on copper (110) [171], following the heating of adsorbed methanol to moderate temperatures. The methoxy species was observed to be recombined with adsorbed hydrogen to form methanol due to the low rate of hydrogen recombination on copper (110), This resulted in a decrease in the rate of formation of aldehyde. However, since the surface oxygen could be easily removed, this could provide a low energy path way to remove the hydrogen through water formation [168] leaving the methoxy species to decompose to aldehyde and hydrogen. The aldehyde decomposed to carbon monoxide and hydrogen at 100°C [165]. The oxidative dehydrogenation of methanol in the presence of oxygen to form formaldehyde has been investigated by Sexton [157] who demonstrated that the methoxy intermediate is involved. The formaldehyde was found to be oxidised to carbon dioxide and hydrogen on a copper (110) single crystal [170].

At higher temperatures, the main steps in the oxidation reaction may be considered to be [105, 172]:



Reactions [4 and 5] are the conventional route of the steam reforming reaction which could be considered as part

of the oxidation process. It is well established [169, 173] that the presence of oxygen on copper surfaces influences the surface activity towards a high adsorption capacity for methanol in the decomposition [169] and the synthesis reactions [173]. Herman et al. [5] found that the partially oxidised copper surface was responsible for the catalyst activity in copper-zinc catalysts and the methanol decomposition was found to be the rate determining step in the steam reforming route [172]. Thus, the high catalyst activity must be due to the optimum state of the catalyst surface for the decomposition reaction.

1.7.3.3 Mechanism of Methanol Decomposition on Copper Surfaces

Methanol is decomposed into hydrogen, carbon monoxide and/or formaldehyde over a variety of metal catalysts and metal oxides [174]. On the surface of copper-zinc oxide-alumina catalysts, [175] methanol reacts readily. The reaction depends on the temperature. At 120-180°C primarily, methyl formate, dimethyl ether, and hydrogen are formed, whereas at the synthesis temperature of 220-280°C, carbon monoxide and hydrogen are the main products with some formation of methane, while in the presence of water it gives carbon dioxide and hydrogen [174]. However, there is evidence that in the absence of surface oxygen the decomposition of methanol does not occur at all [176, 156,

157, 177]. The intermediates observed in the decomposition reaction, as well as the final products depend on the temperature and the characterisation technique employed.

Sexton *et al.* [162] demonstrated that the clean surface of copper (110) single crystal was relatively unreactive, but adsorbed oxygen readily attacks the hydroxyl proton to generate the methoxy intermediate. They also found no evidence for the formation of methyl formate. However, a formaldehyde intermediate which was oxidised to carbon dioxide and hydrogen [170] was observed on a copper (110) single crystal surface. The reaction of methanol on copper-based catalysts [175] was investigated under non steady-state conditions at 250°C. Methanol was found to reduce the surface, forming carbon dioxide and hydrogen. The reduced sites after methanol interaction were oxidised by carbon dioxide at the decomposition temperature with the formation of carbon monoxide. A kinetic study of the decomposition reaction of methanol on copper wire [161] showed that the intermediates which exist in the reaction were initially formaldehyde and subsequently carbon monoxide and hydrogen, formed via a more stable intermediate, that is methyl formate.

A temperature programmed decomposition study [164] of the adsorbed methanol on model copper/zinc oxide surfaces showed that the adsorption of methanol on copper clusters does not require the presence of surface oxygen, and large carbon dioxide desorption peaks were observed at 237°C and 352°C. These results were attributed to the spillover of

hydrogen atoms on to oxygen anions of the zinc oxide support. As a result of this spillover, methoxy species were stabilised and remained on the copper clusters. The authors suggested that the two desorption peaks assigned to carbon dioxide were due to the decomposition of the formate species either on copper clusters (237°C peak) or at the copper cation sites dispersed on the zinc oxide surface (352°C peak). An infrared study ^[178] of the catalytic oxidation of methanol on a copper (100) single crystal showed that the methoxy species is the surface intermediate formed during the reaction, and that the reaction can be prevented by the presence of an excess of oxygen atoms or highly mobile methoxy species on the surface. However, this study also revealed that the reaction can only occur if empty nearest neighbour adsorption sites exist adjacent to the oxygen atom.

1.7.3.4 METHANOL DECOMPOSITION ON ZINC OXIDE SURFACES

Studies of methanol decomposition on pure zinc oxide are important, not only for scientific interest, but also as a prerequisite for understanding more complex real catalysts, the activity and selectivity of copper-based catalysts for the synthesis of methanol and to study the details of the decomposition of the various proposed reaction intermediates.

Methoxy and formate intermediates have been shown to be

involved in the decomposition of methanol [179, 180, 69] on zinc oxide surfaces. The methoxy species is developed during methanol adsorption at room temperature, and is converted to formate upon heating the catalyst surface.

A temperature programmed decomposition study [179] showed that the reaction occurred *via* a methoxy species and that this species decomposed at higher temperatures through hydrogen transfer to formate or formaldehyde, which were stabilised by unsaturated O^{2-} anions. The formaldehyde species was found to decompose at a temperature of $250^{\circ}C$ to produce hydrogen and either carbon monoxide or carbon dioxide.

Carbon monoxide was found to be produced mainly from the decomposition of formate while carbon dioxide was proposed to be derived from the reaction between methanol and formate species as indicated by infrared study of deuterated methanol [180]. The involvement of formate and formaldehyde have been confirmed by many other temperature programmed reaction spectroscopy studies [181-183]. These intermediates decompose to carbon monoxide and carbon dioxide in the rate determining step of the decomposition reaction.

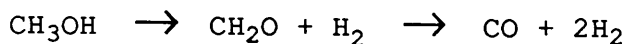
The formate is reported to be produced [69, 182] after nucleophilic attack on the formaldehyde carbon atom by surface oxygen.

The decomposition products of deuterated methanol decomposed on prismatic (1010), polar (0001) and two stepped 4(1010 X 0001) and 5(1010 X 0001) single-crystal

ZnO surfaces have been identified by Cheng et al. [181]. They found that in all cases the products are carbon monoxide, carbon dioxide and D_2 . CD_4 was produced on the prismatic and stepped surfaces but not on the polar surface. However, Bowker et al. [181] did not observe decomposition on the prismatic zinc oxide single-crystal face, and concluded that the polar face must have active sites for the decomposition. Robert and Griffin [189] studied the importance of the hydrogen adsorption sites on zinc oxide surfaces and found that methanol decomposed on these sites as well as at other sites. The methoxy intermediate was observed on all sites but with different decomposition temperatures which were higher on the hydrogen adsorption sites. The activation energy was estimated to be between 126-134 kJ mol^{-1} at both the hydrogen adsorption sites and the other sites. The methoxy species decompose to formate and hydrogen on all different sites, formate species decomposed at the same temperature (290°C) to produce hydrogen and carbon dioxide. The ratio of $\text{CO} : \text{CO}_2$ during formate decomposition is larger on hydrogen adsorption sites. At all sites the activation energy for this step was estimated to be 163 kJ mol^{-1} . The main conclusion of this work was that the presence of the sites of the type associated with the hydrogen adsorption on zinc oxide are not important for the decomposition of methanol on this surface, and consequently they are not essential for activity of Cu/ZnO synthesis catalysts.

Variation in the activation energy of the decomposition

reaction on zinc oxide surface was found to be dependent upon the consecutive decomposition steps [32, 33]:



of which the first step occurs at higher temperature and represents the rate-determining step. The variation in the activation energy was attributed to the change in the controlling step of the overall reaction, or due to the change in catalyst semiconductivity [32], and was in the range of 84-164 kJ mol⁻¹.

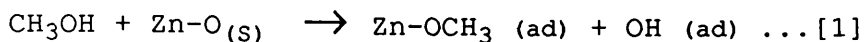
1.7.3.5 Mechanism of Methanol Decomposition on Zinc Oxide Surfaces

In the last section (1.7.3.4), it is clear that there is no complete agreement in the literature regarding the mechanism of methanol decomposition on zinc oxide. This disagreement arises mainly from the difference in the method of catalyst pretreatment, and from the techniques used in these studies. Despite, this conflict, many other studies have concluded that the methoxy species is the major intermediate during the decomposition step on zinc oxide surfaces. For example, infrared studies of zinc oxide powders by Ueno *et al.* [179] showed that methoxy species were involved in the methanol decomposition process. This species was observed to develop during the adsorption of methanol at room temperature on well out-gassed zinc oxide,

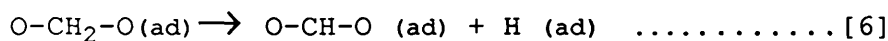
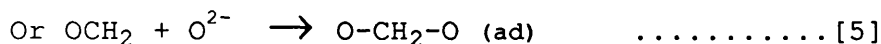
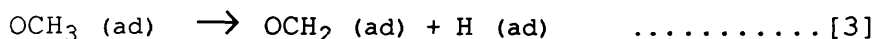
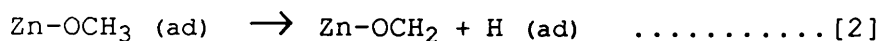
following heating of the surface up to 230°C. Bowker *et al.* [180] conducted a temperature programmed reaction study of zinc oxide powders which showed that the methoxy species decomposed to formate upon heating. Their observations, however, were based on the identified peaks in their TPD thermogram for the hydrogen and carbon monoxide after the adsorption of either methanol or formaldehyde. The kinetics of the formation of the formate intermediate were not very clear in the TPD thermogram of the methanol decomposition.

Other studies on various oriented zinc oxide single crystal surfaces [181, 186] have shown that methanol decomposition occurred through two channels on the (1010) and the stepped $\{4 * (1010), 5 * (1010)\}$ plane surfaces. The first channel led to the production of CH₄ at 150°C while the second produced carbon monoxide, carbon dioxide and hydrogen at 370°C. However, on the polar (0001) zinc oxide surface the decomposition occurred through different routes, one leading to the production of hydrogen, carbon monoxide, and CH₂O at 407°C, the other route to the production of carbon monoxide, carbon dioxide, hydrogen and water at 477°C. In these studies the decomposition of formate was assigned to both a surface process at 377°C on the prism surface and to surface processes at 477°C on the polar surface. These conclusions were reached after separate comparative experiments using CH₂O and HCOOH.

The above studies point to the dissociative adsorption of methanol and thus one might write the first decomposition step as:



Despite the fact that many studies have observed the formation of formaldehyde, the mechanism of this step is still unclear owing to a uncertainty as to whether the abstraction of the hydrogen atom occurs on the Zn^{2+} cation [187, 188] or on the O^{2-} anion [189].



From the proposed mechanism shown above, it is very clear that the presence of the anion (O^{2-}) is very important for the decomposition to proceed, and to overcome step [4], which occurs in the absence of the anion on the surface.

The formation of carbon monoxide and carbon dioxide which follow the formate decomposition are very clearly resolved despite the observation of these gases as adsorbed products. The reduction of the catalyst with carbon monoxide has been suggested to preclude the formation of carbon dioxide during methanol decomposition [33, 190].

1.8 POISONING OF METAL CATALYSTS

1.8.1 Introduction

The poisoning of metal catalysts is one of the most severe problems associated with the industrial applications of catalysts, and the understanding of the poisoning process is an important step in understanding and predicting catalyst behaviour and lifetime.

The poisoning is a form of catalyst deactivation caused by adsorption or deposition on, or the reaction of small amounts of material with the catalyst surface. The poison may be a contaminant in the gas stream, or it might be a reactant, intermediate or product of a desired or undesired reaction.

The most usual type of catalyst poisoning is caused by impurities, either present in the gas feed stream or formed by some process during reaction on the catalyst surface (reactants, or products and/or intermediates) [191, 192]. In both cases the poison becomes adsorbed on the active sites of the catalyst causing a fall-off in the catalytic activity towards the adsorption of the reactant(s). This process might be either temporary or permanent depending on how fast the poison can be removed from the catalyst surface [193]. However, when the reaction leads to two or more products, the poison can markedly alter the selectivity by reducing the rate of one of the reactions with respect to the other. Such a poison is described as a selective poison [191-193]. Small quantities of sulphur can,

for example, alter significantly the selectivity of Fischer Tropsch catalysts. Thus, McCarty et al. [194] showed that over a Co/ThO₂/Kieselguhr catalyst, there was an increase in the production of liquid hydrocarbons and a decrease in the yield of gaseous hydrocarbons, when a small amount of sulphur was present as gas phase H₂S in the reaction stream. From this observation, they concluded that the sulphur poisoning of the hydrogenation activity led to the formation of longer chain hydrocarbons. Also sulphur or aminated compounds can act as selective poisons for these reactions involving diolefinic or acetylenic compounds. It has been shown that the sulphided derivatives encourage isomerisation more than hydrogenation [195]. Another example of selectivity modification by poisoning is that due to Dalla Betta et al. [195] who have shown that the addition of H₂S to Ru, Ni or Rh catalysts during the methanation reaction reduces the activity, but interferes more severely with the hydrogenation reaction of carbon itself than with the carbon-carbon bond formation reaction. It also modifies the selectivity by altering it such that a greater yield of products of higher molecular weight is observed.

In discussing the main effects of adsorbed poisons on catalyst-adsorbate interactions, it is possible to imagine that poisons can cause various effects on the metal, and that the metal-poison bond could modify the properties of the metallic atom responsible for adsorption, in particular, its bonds with the nearest neighbouring atoms.

1.8.2 Poisoning of Copper Catalysts

A number of studies have shown that there are two main steps involved in sulphur uptake on copper, [197-201] as the coverage is increased. These steps are: (a) the adsorption of sulphur, on the highly coordinated sites on the catalyst surface and (b) sulphur adsorption which leads to the formation of a two-dimensional surface sulphide. Weak electronic transfer from the metal to adsorbed sulphur atoms has been observed from work function measurements made with sulphur covered surfaces [202]. These measurements showed that, although, the sulphur-metal bond is mainly covalent in character, electronic effects as well as geometric effects could be expected to influence the catalytic properties observed during the poisoning process. Furthermore, Bartholomew et al. [192] pointed out that there are two effects caused by adsorbed sulphur, that is the geometric blockage of active sites by sulphur and activity changes, which are attributable to surface restructuring.

Sulphur has been observed to be adsorbed very rapidly on copper [203] the high sticking probability showed there is no adsorption barrier and sulphur adsorbed dissociatively until the surface saturation limit has been reached. Sulphur was also found to adsorb on copper surfaces with a heat of adsorption generally 20-40% larger than that for bulk sulphide formation. [204] Nevertheless, more complicated sulphur containing compounds such as

dimethyl disulphide $(\text{CH}_3)_2\text{S}_2$ and methyl mercaptan (CH_3SH) , were found to be adsorbed on copper (100) [205] and on copper (111) [206] as molecules at low temperatures but to dissociate at room temperature. In contrast to this observation, dimethyl sulphide $(\text{CH}_3)_2\text{S}$ was found to adsorb reversibly and associatively on copper (100) [205] at -180°C . Interestingly, the adsorption of CH_3S on copper (100) has been compared with the adsorption of methoxy species on copper single crystal surfaces, where methoxy was found to decompose on copper (100) to formaldehyde. By contrast, the methyl mercaptide (CH_3S) species was found to be stable up to a temperature of about 80°C . No thioformaldehyde (CH_2S) was observed during the adsorption process [205], but, upon heating, the methyl mercaptide decomposes to form methane, hydrogen, ethane and adsorbed sulphur. The released sulphur atoms following the higher temperature decomposition process, block the surface toward further adsorption, altering the selectivity toward methane and ethane formation by enhancing the reaction of adsorbed hydrogen with oxygen and, therefore, changing the reaction probabilities of hydrogen-methyl and methyl-metal recombination.

Many reviews have dealt with the adsorption state of sulphur and catalyst poisoning in general. Those which deserve particular mention are due to Maxted, [207] Hegedus and McCabe, [208] Shelef, Otto and Otta [209], Bartholamew [192], Benard [201], and Kiskeinova [210]. All of these reviews have shown extensively the effect of the poison,

and in particular, sulphur as the most common catalyst poison on many catalytic reactions. They have also provided details on surface modification induced by poisons, and the adsorption of many poisons under various conditions have also been discussed.

1.8.2.1 The Sulphur-Copper Bond

The important condition for molecules to have a "poison effect" on a catalyst depends on its ability to create a strong chemisorption bond with the catalyst. This implies that molecules must form an actual chemical bond with the catalyst surface, and therefore, a transfer of electrons between the poison and catalyst that is compatible with the electronic structures of both the metal and the poison.

Generally, metals used in heterogeneous catalysts are all transition metals or on the limit of such a group, and their basic characteristic is that they have some available valence orbitals, that are donor or acceptor levels of the same energy. Covalent bonding between the metal and the proposed "poison" is possible with a large number of unsaturated molecules. In the formation of the catalyst-poison bond the lone pair electrons of poison atoms such as those of sulphur, oxygen, and nitrogen are involved. Thus, for example, according to Maxted ^[207] sulphur bonds to the transition metals during the chemisorption process *via* donation to metal d orbitals of the unshared electron pairs in the sulphur atoms. Electron spectroscopy studies ^[211]

have shown that the d orbitals of the metals are the ones involved in the chemical bonding between sulphur and transition metals such as Cu, Ag, Zn, Ga and In. This bonding also has an effect on the sulphur orbital energies; 3d and 4d orbitals are mainly involved in the bonding of copper and silver with 3p sulphur orbitals.

1.8.3 THE ADSORPTION OF HYDROGEN SULPHIDE ON COPPER-BASED CATALYSTS

1.8.3.1 The Adsorption of Hydrogen Sulphide on Copper Surfaces

A number of adsorption studies of hydrogen sulphide on copper catalysts [201, 199, 212, 215] have been reported. The results show that a dissociative adsorption of hydrogen sulphide occurs on copper surfaces. Domange and Oudar [199] studied the structure of an adsorbed sulphur layer on low-index copper faces in contact with a gaseous mixture of H₂ and H₂S. They demonstrated three different structures for the Cu (100)-sulphur system, a P(2 X 2) structure, a diffuse structure and a two dimensional structure. From the study of the adsorption of sulphur on (100), (111) and (110) copper single crystal surfaces they concluded [199] that a dissociative adsorption occurs through localised S²⁻ bonded to the highly coordinated surface sites in such a way that sulphur atoms are arranged in a rigid manner in the metallic substrate.

In a XPS study of the adsorption of H_2S on oxygen-covered copper (111), Moroney et al. [212] showed that, at low temperature, a dissociative adsorption occurs involving the adsorption of hydrogen with surface hydroxyl formation. Although in this XPS study no evidence was found for the formation of surface (SH) species during the adsorption process, the desorption of hydrogen following the adsorption of hydrogen sulphide at temperatures above $30^\circ C$ was found to be less than that of the adsorbed hydrogen sulphide [213]. At higher temperatures of $200^\circ C$ the reaction was found to proceed through bulk sulphidation with an activation energy estimated to be 32 kJ mol^{-1} . The rate of adsorption was found to decrease with increasing surface coverage and some hydrogen was desorbed at $-80^\circ C$.

The change in the surface area of copper-based catalysts induced by hydrogen sulphide adsorption was measured [214] at $300^\circ C$. Both copper and zinc oxide surface areas were found to decrease linearly with increasing exposure time. However, the decrease in the copper component was observed to be about 1.5 times greater than that of the zinc oxide component.

Recently, [215] an electron energy loss spectroscopy (EELS) study of hydrogen sulphide adsorption on copper (100) as a function of coverage and temperature showed that the adsorption of hydrogen sulphide was irreversible, with the formation of HS species following the dissociation of hydrogen sulphide, these findings were in complete contrast with those from the XPS study [212]. EELS study [215] which

showed that (HS) species formed only at low coverage and temperature, whilst physical adsorption occurs at higher coverages and the process was described as molecular adsorption.

The dissociation of hydrogen sulphide and the formation of sulphhydryl species (HS) has been found to occur below -100°C on most metal surfaces, including nickel (100) [216], platinum (100) [217] and copper (100) [215]. Furthermore, these species bind weakly to the surface and are easily desorbed. owing to the low binding energy of H-S in hydrogen sulphide. Hydrogen and hydrogen sulphide were found to be the only desorption products [212, 214] from the copper surface which is very similar to that observed on other metal surfaces. [215, 216]

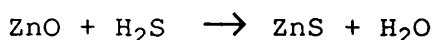
1.8.3.2 The Reaction Between Hydrogen Sulphide and Zinc Oxide

Methanol synthesis catalysts are very active with high selectivity, but they have a high sensitivity to poison. Thus careful purification of the gas feed is required in order to achieve the long production runs to meet the economic standard of the production of methanol.

The removal of sulphur from the natural gas by absorption at ambient temperature on activated charcoal or with molecular sieves has been widely used in North America [218]. Charcoal has its capacity enhanced by impregnation with transition metals such as copper, but frequent

regeneration of the absorbent with steam is required. However, if only hydrogen sulphide is present in the natural gas, then it is possible to use zinc oxide, which can remove hydrogen sulphide completely (~0.02 ppm).

The zinc oxide reacts almost completely with hydrogen sulphide to form zinc sulphide:



Kinetic studies [219] of the reaction of hydrogen sulphide with powdered zinc oxide have shown that the reaction is first order with respect to hydrogen sulphide concentration. Rapid and complete reaction was observed in the temperature range of 600-700°C, but at temperatures below 600°C the reaction stopped well before total zinc oxide conversion was obtained. The concentration of hydrogen sulphide has no effect on the overall reaction and no unexpected results were observed.

With both the low-temperature shift and methanol synthesis catalysts, the catalyst is very sensitive for the presence of the poison, although poisoning is not usually a significant problem in well-purified gas feeds. Zinc oxide is much more effective than alumina in picking up and holding typical poisons, such as sulphur. Sulphiding copper metal in copper-zinc oxide-alumina catalysts is very favourable at the synthesis temperature (table 1.1). It is, therefore important to remove any trace of sulphur before it contacts the catalyst surface. With the catalyst

containing zinc oxide, the removal of low levels can be achieved by trapping the sulphur as zinc sulphide, which is more stable than copper sulphide (table 1.1).

Table 1.1

Bulk thermodynamic data and the thermodynamic equilibrium constant for the reaction of H₂S with Cu and ZnO at 300°C

Reaction	H _f kJ mol ⁻¹	K
2Cu + H ₂ S \rightleftharpoons Cu ₂ S + H ₂	-59.4	3.26 X 10 ⁵
ZnO + H ₂ S \rightleftharpoons ZnS + H ₂ O	-76.6	7.2 X 10 ⁶

1.8.4 THE EFFECT OF SULPHUR ON THE ADSORPTION OF OTHER MOLECULES

1.8.4.1 The Effect of Sulphur on the Adsorption of Carbon Monoxide and Carbon Dioxide

Many studies have investigated the effect of adsorbed sulphur on the chemisorption of carbon monoxide on metal surfaces. However, none of these studies has addressed the effects of poisoning on carbon monoxide or carbon dioxide

chemisorption on copper catalysts. It has been shown that reactant-catalyst bonds can be weakened by sulphur. For example, the carbon monoxide-metal bond on iron and nickel catalysts is weakened in this way [220, 221].

In a UV photoemission spectroscopy study, Rhodin and Brucker [222], investigated the change in the molecular bonding of adsorbed carbon monoxide on iron in the presence of sulphur. They found that the carbon-oxygen bond has a stretched configuration similar to gaseous carbon monoxide when carbon monoxide becomes chemisorbed on sulphur-free surface. However, the presence of sulphur reduces both the forward-and back-donation of electrons between the chemisorbed carbon monoxide and the catalyst surface. This results in a relaxation of the carbon monoxide molecules toward the unstretched configuration. The electron bonding interactions between carbon monoxide and iron can be quenched to varying degrees by chemisorbed C, O, P and S with sulphur causing a completely unstretched configuration. Such an effect on bonding caused by adsorbed sulphur has also been observed by infrared spectroscopy. Rochester and Terrell [221] found that the strength of the chemisorption bond between carbon monoxide and nickel was weakened by sulphiding the metal.

The effect of three electronegative poisons (P, S, and Cl) on the chemisorption of carbon monoxide and hydrogen on nickel (100) has been investigated [223]. The presence of these electronegative atoms on the surface reduced the adsorption rate, the adsorption bond strength, and the

adsorption capacity of the surface. The magnitude of these effects increased with the increasing electronegativity in the sequence $P < S < Cl$.

Sulphur dioxide was used to examine its effect on the metal oxide activity toward the oxidation of carbon monoxide [224]. The results showed that on copper oxide and on copper chromite catalysts, sulphur dioxide adsorbed preferentially on the most active sites for the carbon monoxide oxidation reaction.

Recently, in our laboratory, Pettigrew [225] studied in detail the effect of hydrogen sulphide on the adsorption of both carbon monoxide and carbon dioxide on polycrystalline copper, copper-alumina and copper/zinc oxide/alumina. His results showed that the first amount of adsorbed sulphur reduced the adsorption capacity of the copper component to a large extent, as indicated by the adsorption isotherm of [^{14}C -] carbon monoxide, before and after the poison had been introduced. However, the decrease in the adsorption capacity continued with increasing amounts of added hydrogen sulphide, until after three doses of the poison little further effect on the isotherm was noticed, suggesting a site-blocking mechanism for the poisoning effect.

1.8.4.2 The Effect of Sulphur on the Catalytic Decomposition of Methanol

Little information has appeared in the literature concerning sulphur poisoning of the methanol decomposition

reaction on metal surfaces.

A significant effect of sulphur on the kinetics and mechanism of the decomposition reaction has recently been observed on nickel (100). The nature of sulphur modification of methanol reaction was determined [226, 227] by comparison of temperature programmed spectra of the products formed, following methanol adsorption on clean and poisoned nickel surfaces. The reaction was found to be modified by sulphur, not only with respect to the amounts of methanol adsorbed on the surface, but also with regard to the distribution of products.

The presence of sulphur acted as a modifier of the surface reaction of methanol, by altering the reaction path from one forming hydrogen and carbon monoxide on clean surface to one resulting in the production of formaldehyde and hydrogen on the sulphided nickel surface.

In an early work with very simple experimental arrangement, Ghosh *et al.* [228] investigated the effect of various poisonous substances when mixed with methanol, on the velocity of the methanol reaction on reduced copper oxide containing 0.1% ceria. The velocity on clean and CS₂ poisoned surfaces for the formation of formaldehyde and carbon monoxide from methanol was determined, and it was found that the velocity of the hydrogenation reaction was slightly increased. While the velocity of the formaldehyde decomposition to hydrogen and carbon monoxide was almost halved. This effect increased as the amount of poison was increased.

1.8.4.3 Sulphur Poisoning of Methanol Synthesis Catalysts

Like the LTS catalysts, the low-temperature methanol synthesis catalysts are very sensitive to sulphur poisoning (see 1.8.4.4). However, the presence of water is an important difference in the operating conditions. The inlet gas to a methanol reactor is almost dry [218]. Thus, if there is any sulphur component in the synthesis gas, zinc oxide, which is present in the synthesis catalyst, will function as an efficient adsorbent guard. As a result, the presence of sulphur does not cause as much of a problem for methanol catalysts as it does for LTS catalysts.

However, in the synthesis plant based on the gasification of heavy oil, sulphur may cause serious problems [218], that is because of the difficulty in removing carbonyl sulphide (COS) efficiently by the conventional absorbents. However, this can be overcome by the use of special conversion catalysts converting the carbonyl sulphide to hydrogen sulphide, which can be adsorbed on zinc oxide, instead of allowing it to be hydrogenated to methyl mercaptan, which would be strongly chemisorbed on the active sites, thereby causing a rapid decline in the activity.

1.8.4.4 Sulphur Poisoning of the Water Gas Shift Reaction

Copper-based catalysts are very active for the conversion of carbon monoxide in an ammonia synthesis stream into carbon dioxide and hydrogen at low temperatures (see section 1.7.2).

The most common cause of poisoning for the low temperature shift catalysts is chloride, and since the active component of the catalyst (copper) is present in the form of reduced metal, sulphur poisoning can be expected. Some interesting results have been reported recently for poisoning of this type of catalyst [218]. Poison profiles in the bed are steep, which suggests that the rate of poison adsorption may be diffusion limited. Furthermore, on a thermodynamic basis of the stability of adsorbed sulphur and the bulk sulphide formation on the components of copper and zinc oxide of the low temperature shift catalyst (see section 1.8.3.2), it has been suggested that an increase in the amount of "free" zinc oxide in the catalyst reacts with the sulphur forming the more thermodynamically stable zinc sulphide and hence the sulphur will retain in a well-defined concentrated layer of the catalyst bed. However, many studies have shown that sulphur poisoning is cumulative in nature and the poisoning of the catalyst activity depends on the total amounts of adsorbed sulphur [229]. A homogeneous adsorption of sulphur has been indicated and both of the active copper and zinc oxide

components of the catalysts, were sulphided.

Campbell et al. [230, 231] characterised the sulphur poisoning of the low shift catalyst and concluded that the poisoning mechanism occurred by a simple site-blocking mechanism. The ratio of surface to bulk atoms of the active species in the low temperature shift-catalyst depends on the crystallite size [232, 333], and it is generally about 0.5%. As the catalyst contains about 30% copper, approximately 0.1 wt% of sulphur is required to poison the catalyst severely. However, owing to the presence of zinc oxide more than 0.1% sulphur could be adsorbed before the total loss of activity occurred, while, due to the reaction of sulphur with zinc oxide, the poisoning is only temporary [232] as indicated by the restored catalyst activity after the poison admission had been stopped. The formation of cuprous sulphide requires a 3 ppm H₂S concentration while the formation of zinc sulphide requires 5×10^{-3} ppm H₂S concentration. Thus, sulphur is expected to react with zinc oxide, and sulphur has little effect on the water gas shift reaction catalysts.

CHAPTER TWO

OBJECTIVES OF THIS STUDY

The aim of the present work is to understand in detail the adsorption properties of methanol, carbon monoxide, carbon dioxide, and hydrogen sulphide on copper-based catalysts in a pulse flow system. This study also aimed to provide information about the effects of sulphur poisoning on the catalytic activity of copper-based catalysts. In order to achieve the objectives, the following studies were undertaken on copper supported on alumina and commercially prepared copper/zinc oxide/alumina, zinc oxide and alumina catalysts;

(1) The adsorption and decomposition of methanol on clean and hydrogen sulphide poisoned surfaces.

(2) The adsorption of both (^{14}C -) carbon monoxide and unlabelled carbon monoxide on unpoisoned and hydrogen sulphide poisoned surfaces.

(3) (^{14}C -) carbon dioxide adsorption on unpoisoned and hydrogen sulphide poisoned surfaces.

(4) The adsorption of (^{35}S -) hydrogen sulphide on each of the above mentioned surfaces.

(5) An FTIR investigation of the interaction of methanol and carbon monoxide with copper-based catalysts.

By using of different types of catalyst and their

individual components, it was attempted to identify the roles of the individual components and compare these roles with the combined effects as observed with the complex copper /zinc oxide/ alumina catalyst.

The aim of the methanol decomposition experiments was to examine the decomposition products on copper-containing catalysts, and to determine the effects of varying extents of hydrogen sulphide poisoning on the decomposition reaction.

The FTIR study was aimed to provide information concerning methanol interaction with the various catalysts and the nature of the reaction intermediates and hence to establish a mechanism for the decomposition reaction.

The objective of the studies of carbon monoxide and carbon dioxide adsorption on clean and poisoned surfaces, was to gain an insight into the extent of the adsorption in a pulse flow system, the strength of adsorption, hydrogen sulphide poisoning effects and, finally, to compare these effects with results obtained from a static system using similar catalysts.

Hydrogen sulphide adsorption is examined in order to determine the adsorption characteristics in terms of relative strengths of the adsorption and the extent of uptake on the various catalysts.

CHAPTER THREE

EXPERIMENTAL

3.1 MATERIALS AND GASES

3.1.1 Materials

Supported copper catalysts were supplied by ICI plc. Both the binary Cu/Al₂O₃ catalyst and the ternary Cu-ZnO/Al₂O₃ catalyst were prepared by the co-precipitation method [218]. The binary catalyst was prepared by precipitating copper carbonate and aluminum hydroxide from a nitrate solution. As prepared copper carbonate was calcined at 300°C to decompose the copper carbonate to copper oxide. The ternary catalyst (LTS catalyst) was prepared by precipitation at pH7 from a solution containing the three metal nitrates. The precipitated catalyst prepared by using this method has the required composition as well as the smallest obtainable particle size. Also, this kind of catalyst has a relatively low bulk density, reduced impurity levels and a high resistance to sulphur poisoning [218].

For the preparation of zinc oxide, attempts have been made to develop zinc oxide as an absorbent with a high

porous volume having a large internal surface area. However, this material inherently possesses a low density and little mechanical strength. In order to overcome this problem, ICI developed a zinc oxide absorbent material which consists of zinc oxide with a small amount of foreign support material, which is either a carbonate or silicate cement [218]. This oxide was mainly prepared for the purpose of the removal of hydrogen sulphide from crude oil and hydrocarbon feedstocks.

The zinc oxide material used in this study was ICI type 75-1.

It is important to mention that both $\text{Cu}/\text{Al}_2\text{O}_3$ and $\text{Cu-ZnO}/\text{Al}_2\text{O}_3$ were supplied in pellets form. These pellets were crushed and ground before being used.

The composition and the experimentally measured areas for the catalysts used in this study are shown in table 3.1.

Table 3.1

The catalyst composition and surface area

Catalyst	Cu (%)	ZnO (%)	Al ₂ O ₃ (%)	Cu Surface area m ² /g	BET area m ² /g
Cu/Al ₂ O ₃	64	-	36	11	-
Cu-ZnO/Al ₂ O ₃	60	30	10	32	82
ZnO	-	>90	-	-	73.33
Al ₂ O ₃	-	-	-	-	-

The alumina sample used in this study was similar to that used for the preparation of copper-based catalysts(the support). It was prepared by the same way.

3.1.2 Gases

AnalaR methanol was distilled over magnesium metal (10 g/L) to remove any trace of water which may have been present.

The methanol was further distilled over molecular seive, before being transferred to the reservoir connected to the vacuum line, through trap-to-trap cycle of freeze-thaw-pumping, in order to remove any gaseous impurities, such as, air.

The reducing agent used was 6% hydrogen in nitrogen (BOC Ltd, commercial grade), used without any further purification. The gas was specified by the manufacturer as being of high purity (99.98% pure).

Helium (BOC Ltd) was used as carrier gas for the gas chromatography, (^{14}C -), and (^{35}S -) adsorption studies; methanol decomposition experiments, and during the FTIR-spectroscopic study of these catalysts. The helium purity was quoted as being 99.9%.

Carbon monoxide (BOC Ltd) was specified as 99.5% pure.

All gases were used directly from the cylinders without any further purification. No impurities were detected by gas chromatography in any of the gases used for the various experimental procedures.

Carbon dioxide (BOC Ltd) was admitted directly to the vacuum line from the cylinder and was further purified by cycles of freezing at liquid nitrogen temperatures, followed by pumping. Following this procedure, no impurities were detected by gas chromatography.

3.2 THE APPARATUS

The apparatus used in methanol decomposition and ^{14}C -adsorption studies consisted of three parts joined together to form a pulsed-flow system. It consisted of: (i) a vacuum line, constructed from Pyrex glass which was used (in all

studies) for the storage of pure gases and for pressure measurement; (ii) a sampling system for introducing measured samples of methanol vapour or other gases into the helium stream, and finally, (iii) provision for the analysis of gaseous compounds by gas chromatography. Each of these parts is described in detail below, including the reaction vessel.

3.2.1 The Vacuum System

The apparatus consisted of a high vacuum glass system as shown in figure [3.1]. The pumping section consisted of a mercury diffusion pump backed by an oil rotary pump. The pressure obtained within the system during operating conditions was $\leq 10^{-4}$ Torr as measured by the Pirani vacuum gauge (vacustat) which was connected to the end of the manifold. High pressures, up to 760 torr, could be measured by the mercury manometer.

Three-two litre storage vessels (V_1 - V_3) were connected to the secondary manifold via 2 mm vacuum taps. These storage bulbs were used for storing non-radiolabelled gases. The bulbs can be filled with the required pressure of specific gas by flowing the gas, from a high pressure cylinder, through tap (A) and into one of the evacuated bulbs.

The dried methanol was transferred to the reservoir

(V5) as a vapour via tap (A). The vapour was condensed into the reservoir using liquid nitrogen. Once the required volume of methanol had been transferred to the reservoir, a cycle of freezing and evacuation was followed to ensure the removal of any gaseous impurities, e.g. air.

The radiolabelled gas was stored in one litre bulb (V4), which had a side-arm for the attachment of ampoules of any radioactive gas (mainly $^{14}\text{C-CO}$ or CO_2).

All gases could be introduced to the reaction vessel in a controlled manner, after measuring the gas pressure on the manometer.

3.2.2 The Flow System (Sampling System)

The flow-pulse system was constructed from stainless steel tubing and three-way valves as shown in figure [3.2]. The sample loop (S1) with a volume of $0.201 \pm 0.05 \text{ cm}^3$ could be evacuated using the three-way valve (1) which was connected to the main manifold of the vacuum system via tap [B in figure 3.1]. A measured pressure of the required gas could be introduced to the catalytic reactor or to the chromatograph, by filling the sample loop, and then switching valves (2) and (3) to allow the gas to pass through the catalyst bed, or valve (5) to by-pass the catalyst bed and admit the sample to the gas chromatograph for calibration purposes. The sampling system was connected

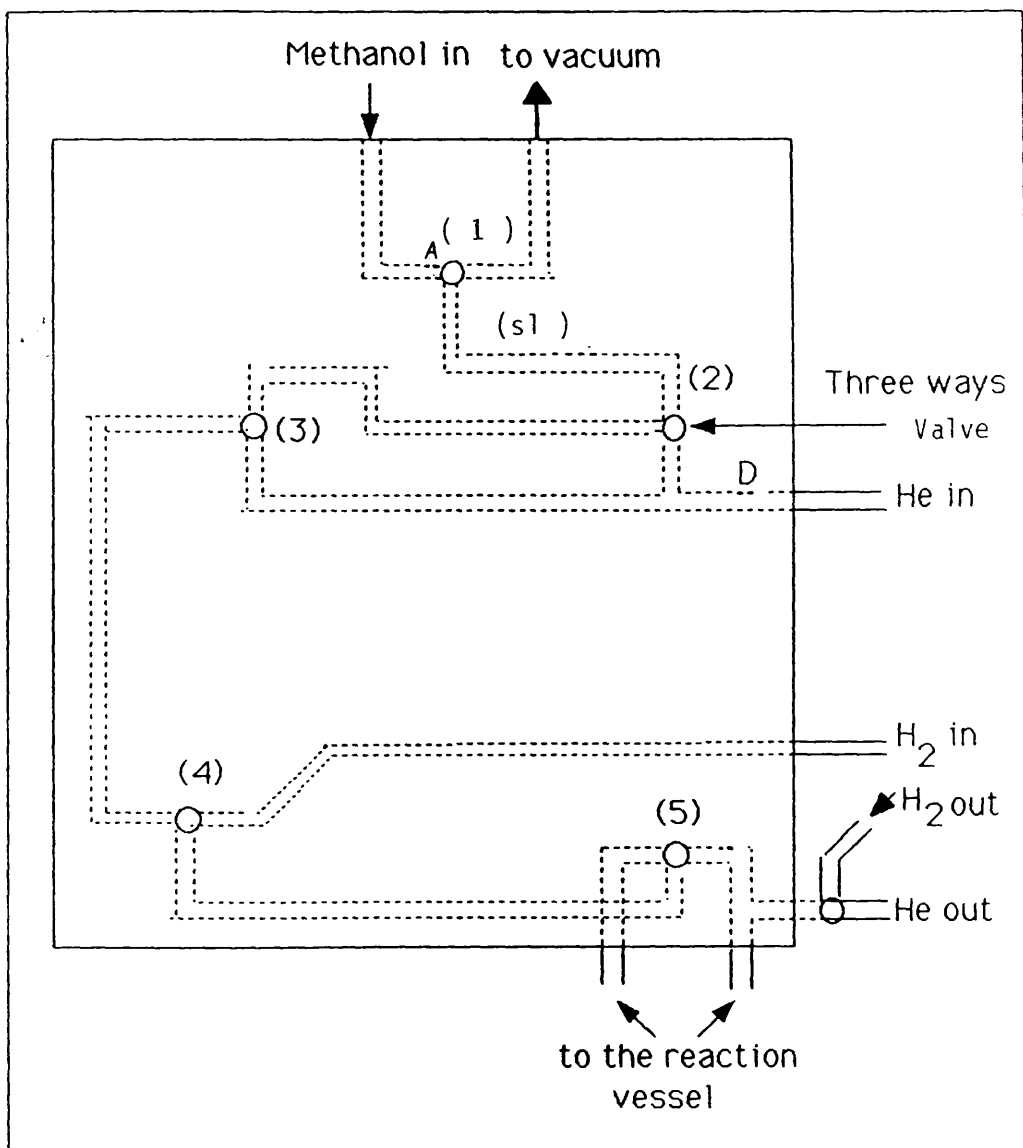


Fig.3.2 The Sampling system

to the reaction vessel using stainless steel tubing and glass-metal connections. The reaction vessel itself was constructed from Pyrex glass in a U-shape.

The catalyst sample was held on a glass sinter in the middle of the vessel shown in figure [3.3].

3.2.3 The Analytical System

Gas analysis was carried out using a (Pye Unicam series 204) gas chromatograph. This was equipped with a thermal conductivity detector which could be used to detect and quantitatively determine hydrogen, carbon monoxide, carbon dioxide, water, methanol, methane, and hydrogen sulphide.

The analyses were made using a stainless steel tube column, 110 cm long and 2 mm internal diameter, containing 1.7089 g of activated spheron carbon (CMS-S), 80-100 mesh. The column was operated at 50°C using helium as a carrier gas at a flow rate of \approx 32 ml/min. A typical trace for a mixture of H₂, CO, CH₄, CO₂, H₂O and CH₃OH is shown in figure [3.4].

The gas chromatograph was used to determine quantitatively the gaseous reaction products formed during methanol decomposition. To make this possible the sensitivity factor for each gas was measured by admitting a

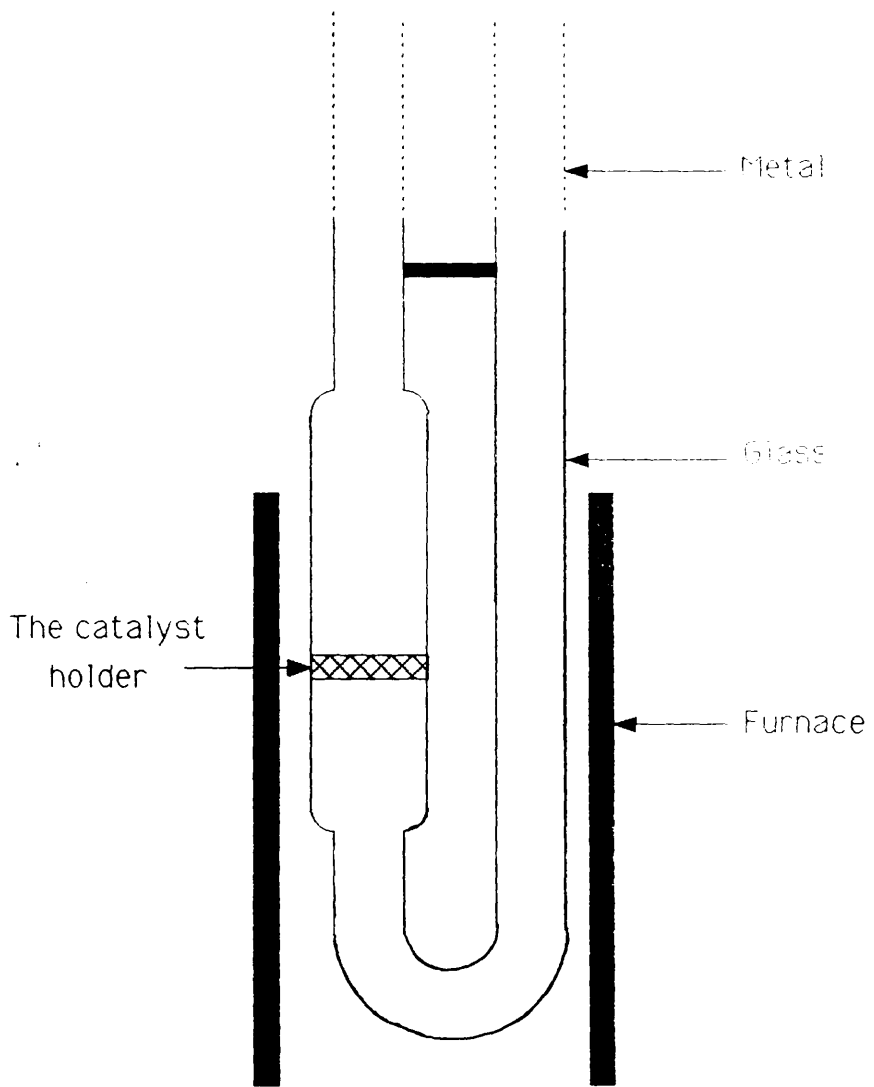


Fig.3.3 The reaction vessel

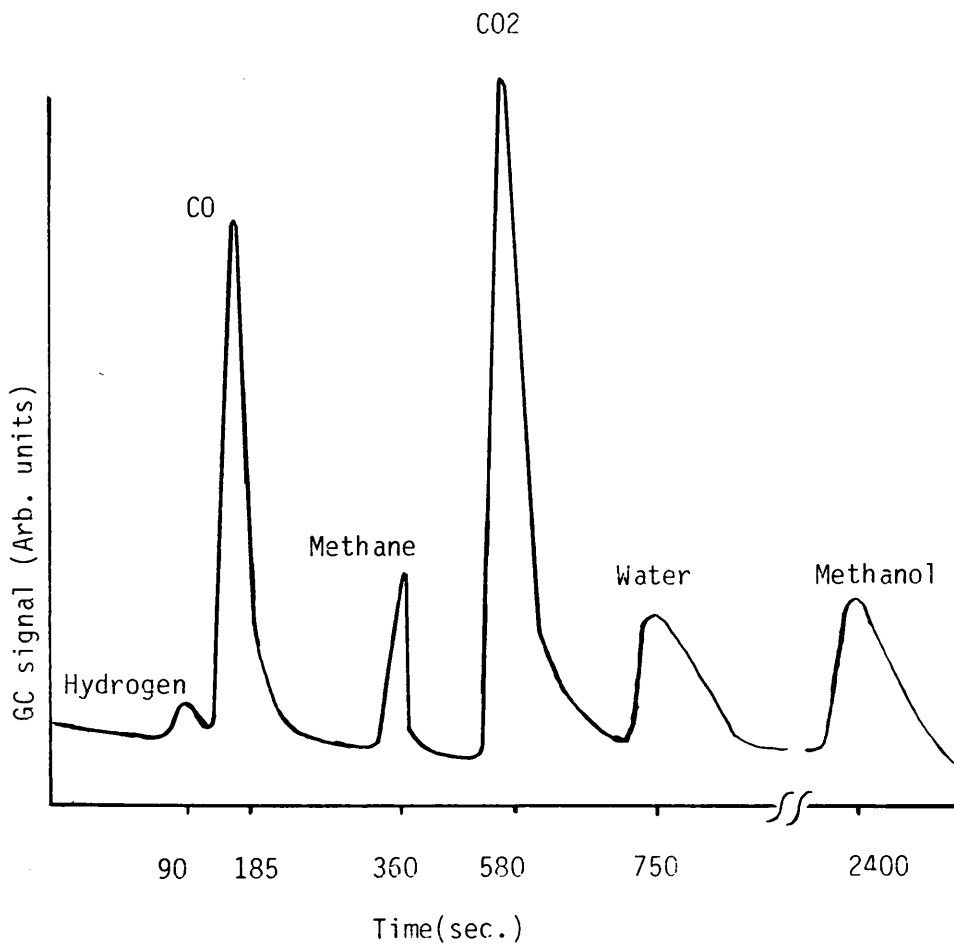


Fig.3.4 Chromatograph trace for a mixture of gases.

number of different calibration pulses of the gas to the column. The area under each peak was measured and a plot of peak area against gas pressure of the sample, as shown in figure [3.5], was obtained. The slope of this line was a measure for the sensitivity of the chromatograph. The retention time of each gas is shown in table 3.2.

Table 3.2

The retention time of different gases passed through the chromatograph column

Gases	Retention time (sec)
H ₂	90
CO	185
CO ₂	580
CH ₄	360
H ₂ O	750
CH ₃ OH	2400

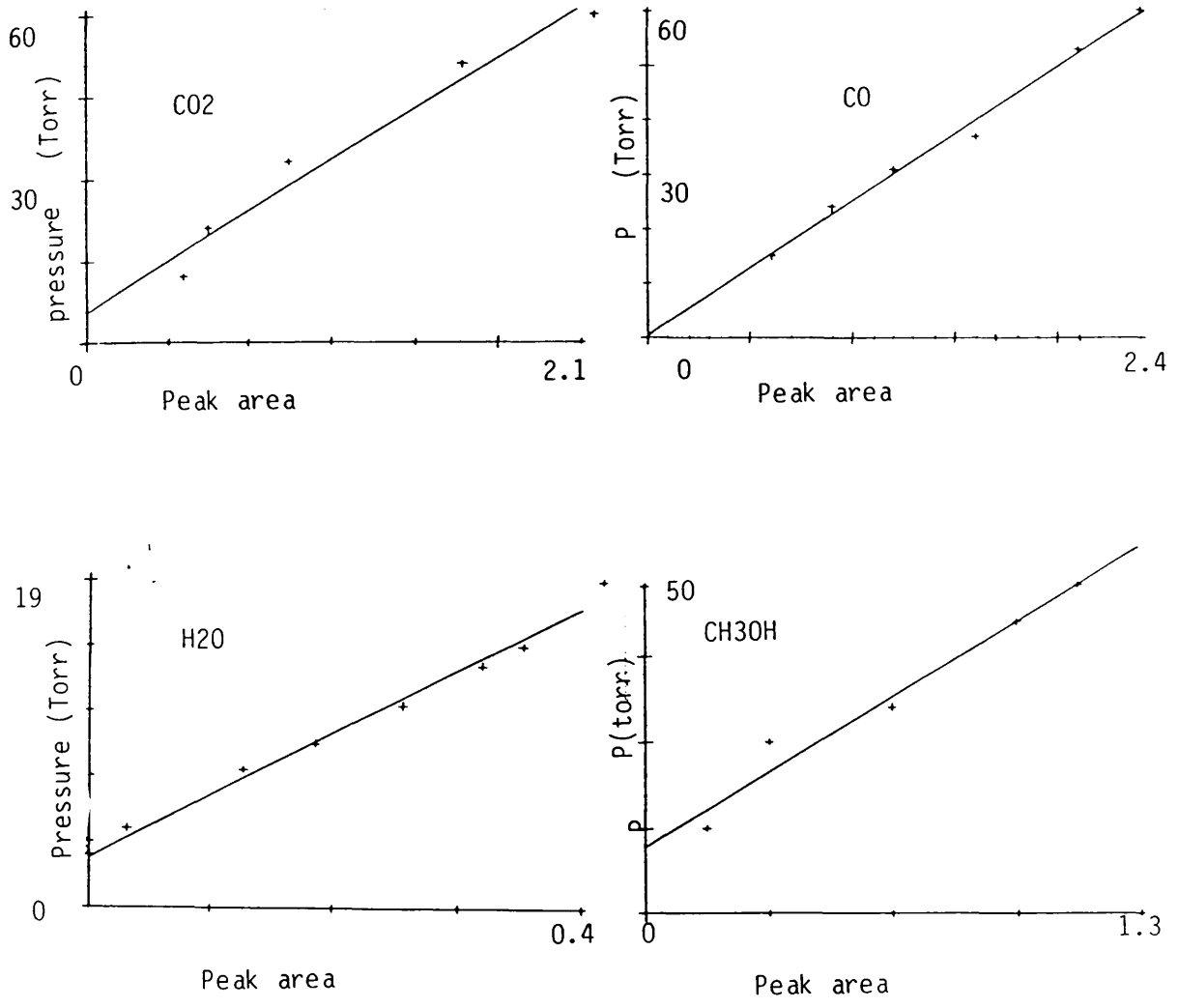


Fig.3.5 Chromatograph calibration curves.

3.3 THE EXPERIMENTAL PROCEDURE

3.3.1 Catalysts Treatment And Activation

In the methanol decomposition experiments the first catalyst used was an alumina supported copper. In the light of the preliminary results obtained in this part of the work (chapter four) a number of activation procedures were used to ensure that in every case a reproducible surface was generated. In the first method, the catalyst sample was reduced, using the method specified by the manufacturer, in a continuous flow of 6% hydrogen in nitrogen. The flow rate was about 25 ml per minute at 180°C for about 14 hours, then at 200°C for 2 hours. However, this reduction procedure was not completely effective as shown by the amounts of oxygen-containing compounds obtained from the reaction of methanol with the catalyst surface. A further step (second method) was added to the reduction procedure to remove the last trace of oxygen. In this step the catalyst was treated in a carbon monoxide stream at a flow rate of 7 ml per minute at 250°C for half an hour, instead of the final two hour reduction in hydrogen at 200°C.

In the third method, the catalyst was heated to 250°C in a stream of carbon monoxide, flowing at a rate of 7 ml per minute and held at this temperature for about 14 hours.

After the completion of each reduction, the catalyst

was flushed in a stream of helium to remove any residual gas. The catalyst, could then be used for an experiment. In some methanol decomposition experiments and in the adsorption of carbon monoxide, carbon dioxide and the adsorption of $^{35}\text{S-H}_2\text{S}$, all the catalyst samples were reduced under flow of 6% hydrogen in nitrogen, 25 ml per minute at 250°C for about 14 hours, as a fourth method.

The copper-zinc oxide/alumina catalyst was activated in several ways. (i) The catalyst was reduced under a stream of 6% hydrogen in nitrogen at a flow rate of 25 ml per minute at temperature of 180°C for 14 hours followed by two hours at 200°C .

(ii) The catalyst was reduced in 6% hydrogen in nitrogen with the same flow rate as in (i), but with the temperature set to 250°C for 14 hours. (iii) The catalyst was reduced using carbon monoxide at a flow rate of 7 ml per minute and at a temperature of 250°C for about 14 hours.

Both zinc oxide and alumina, which were in a powdered form, were treated by the same method using 6% hydrogen in nitrogen stream at a flow rate of 25 ml per minute at 250°C for about 14 hours followed by flowing helium at the same temperature for about another hour.

3.3.2 Experimental Procedure

A typical weight of 0.10 to 0.16 g of the catalyst was placed in the reaction vessel shown in figure [3.3]. The catalyst was then reduced by one of the methods described above.

A measured pressure of methanol vapour was expanded into the vacuum line to fill the secondary manifold, and the pressure measured by the manometer. At the same time evacuation of the sample loop was carried out via the three-way valve (A) in figure [3.2]. This valve was left open for a few minutes for evacuation while valves (2) and (3) were directed towards the "sweep sample" and "by pass" respectively, to ensure the continuous flow of helium through the gas chromatograph. The sample loop was filled with methanol (or one of the other gases) by changing the direction of valve (A) toward the sampling direction for about 2 minutes to ensure that the sample loop is filled with the gas at the measured pressure.

Valve (A) was then closed while changing the direction of valves (2,3) towards the "by pass" and "sweep sample" positions respectively, a few seconds after closing valve (A). Following this procedure the helium swept the sample to the reaction vessel (valve 5) and over the catalyst.

3.3.3 Analysis of Reactant and Products

The gas chromatograph was pre-set to the temperatures for each operating part, as listed in table 3.3, while the gas chromatograph output signal was recorded using a chart recorder operated with a full-scale deflection of 0.5 V with a chart speed of 500 mm per an hour.

Table 3.3

The operation temperatures of different gas chromatography parts

Part	Temperature °C
Column	50
Injection	200
Detector	150

The reaction products were carried out of the reaction vessel by the helium stream to be separated by the chromatograph column and detected by thermal conductivity detector.

The reaction products were then analysed by the chromatograph. The area under each peak was measured and

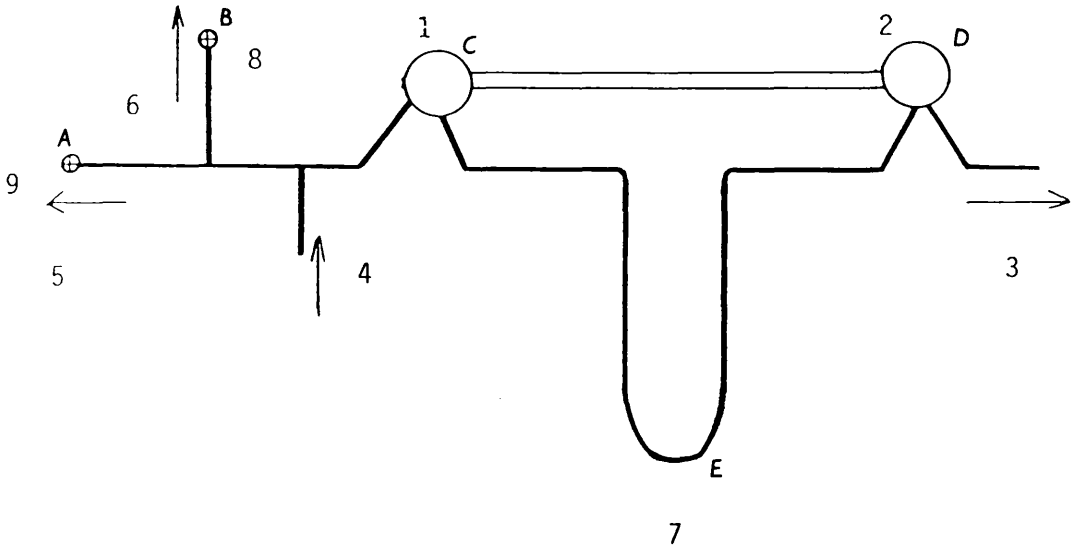
then converted to a quantity using a calibration factor taking into account the chromatograph sensitivity.

3.4 $^{35}\text{S}-\text{H}_2\text{S}$ PULSE SYSTEM

3.4.1 The Flow System

The adsorption study of $^{35}\text{S}-\text{H}_2\text{S}$ was carried out using a glass flow system shown schematically in figure [3.6]. Cylinder helium was used as the flow gas, flow rate being controlled by Negretti-Zambra pressure flow regulator.

The main feature of the flow system was the two three-way valve (C and D) which allows the carrier gas to either flow through the sample loop or to by-pass the sample loop (E) directly to the reaction vessel. The pulse system was connected to the main vacuum line through taps A and B. Tap A, connected to the main manifold, allowed the evacuation of the sample loop, while tap B, which was connected to the secondary manifold, allowed the introduction of a pulse of hydrogen sulphide at a measured pressure. After evacuation of the sample loop, a pulse could be admitted to the sample loop by leaving tap B open to the manometer; the helium flowing through the by-pass. The measured sample was allowed to expand in to the glass tube between tap C and tap D (with tap A closed). Then, the expanded sample was introduced to the sample loop by freezing it at liquid



- 1,2 three way valves
- 3 To the reaction vessel
- 4 Helium in
- 5 To vacuum
- 6 To manometer
- 7 The sample loop
- 8,9 Two way valves

Fig.3.6 (35-S) H₂S pulse flow system.

nitrogen temperature. The sample was then allowed to warm up and expand in the sample loop before tap C and D were changed in order to allow the flow to be rediverted through the sample loop to the reaction vessel.

3.4.2 The Reaction Vessel

The reaction vessel was constructed from Pyrex glass with two side-arms, the first for the gas inlet; the other for the gas outlet, as shown in figure [3.7]. The inlet side arm was connected via a B10 cone to a U-shaped tube which contained the catalyst during the reduction procedure. This tube was surrounded by a furnace for heating during reduction. The inlet tube was connected by a similar arrangement to the pulse system. This arrangement allowed the turning of the U-shaped holder (the U tube) through an angle of 180° in order to release freshly reduced catalyst directly into the reaction vessel. The catalyst was held on a glass sinter in the reaction vessel. During the use of powdered samples, the reaction vessel had to be positioned in a vertical position. The height of the reaction vessel was 35 cm and its diameter 2.5 cm.

A Geiger-Muller tube was fitted in each end of the reaction vessel. The Geiger-Muller tubes were held in position by means of B29 glass cones fitted with feed-through wires which were used to connect the tubes to the

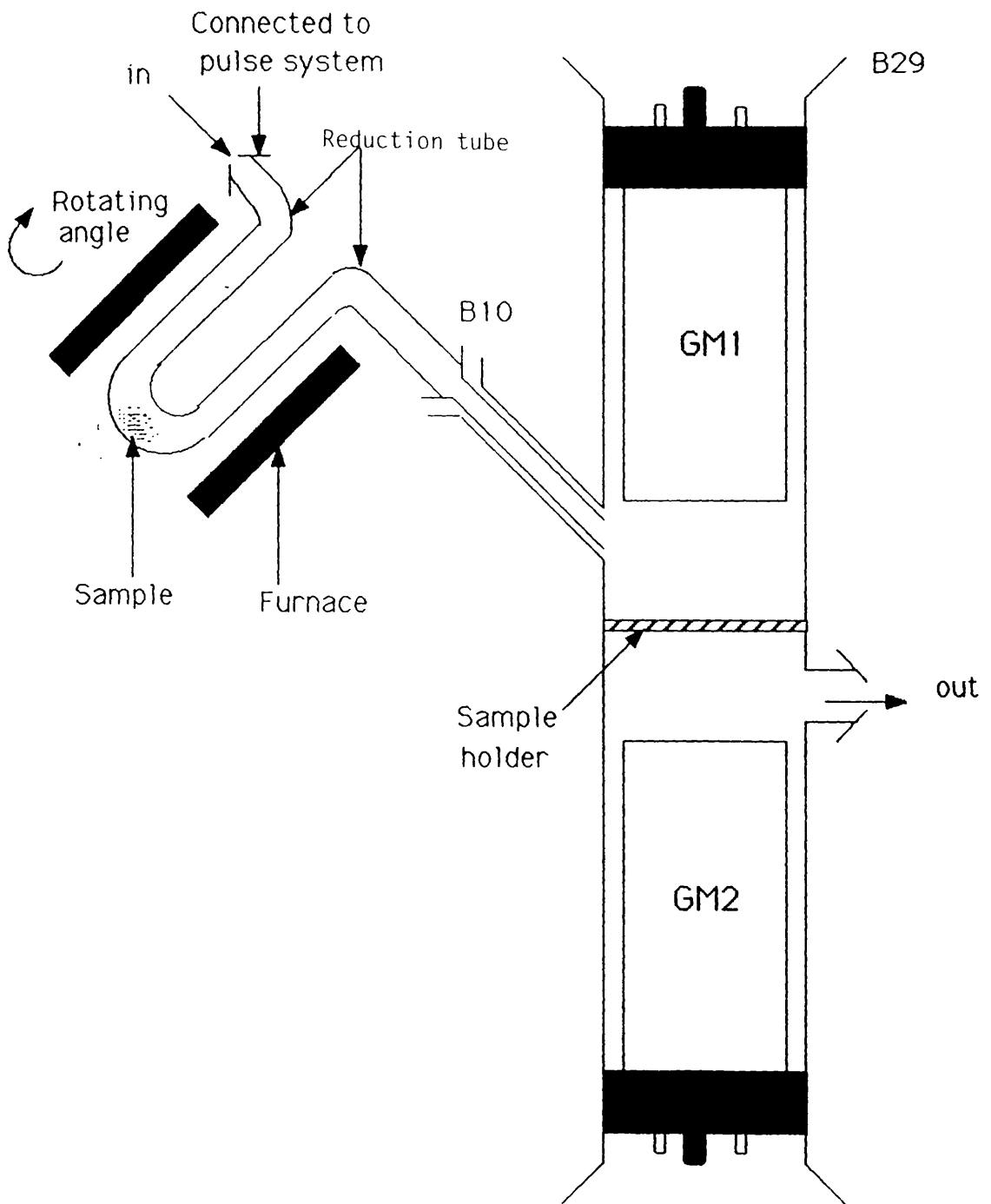


Fig.3.7 (35-S)-Hydrogen sulphide monitoring system

scaler-counter system.

3.4.3 The Geiger-Muller Counter

Samples of H₂S labelled with (³⁵S) were counted using Geiger-Muller tubes. The pulses from the counters were recorded by electronic scaler-timer (SR-5).

In a GM counter, no counts are recorded until the applied potential is large enough to reach the Geiger threshold after which the count rate begins to rise rapidly until a plateau is reached where the count rate increases only very slightly with voltage [figure 3.8].

Plateau regions were determined for each Geiger-Muller used by measuring the count rate from a cesium-137 source as a function of voltage [figure 3.8]. The working voltage was set in the middle of the plateau region. For both counters the working voltage was taken as 450 V. Under these conditions both counters were found to be stable and to give error-values on counting which lay within the calculated statistical deviation.

During the experimental measurements the output of the scaler ratemeter could not be used directly for adsorption analysis since a number of corrections had first to be made

(a) Background count rate.

This was measured before any adsorption analysis began

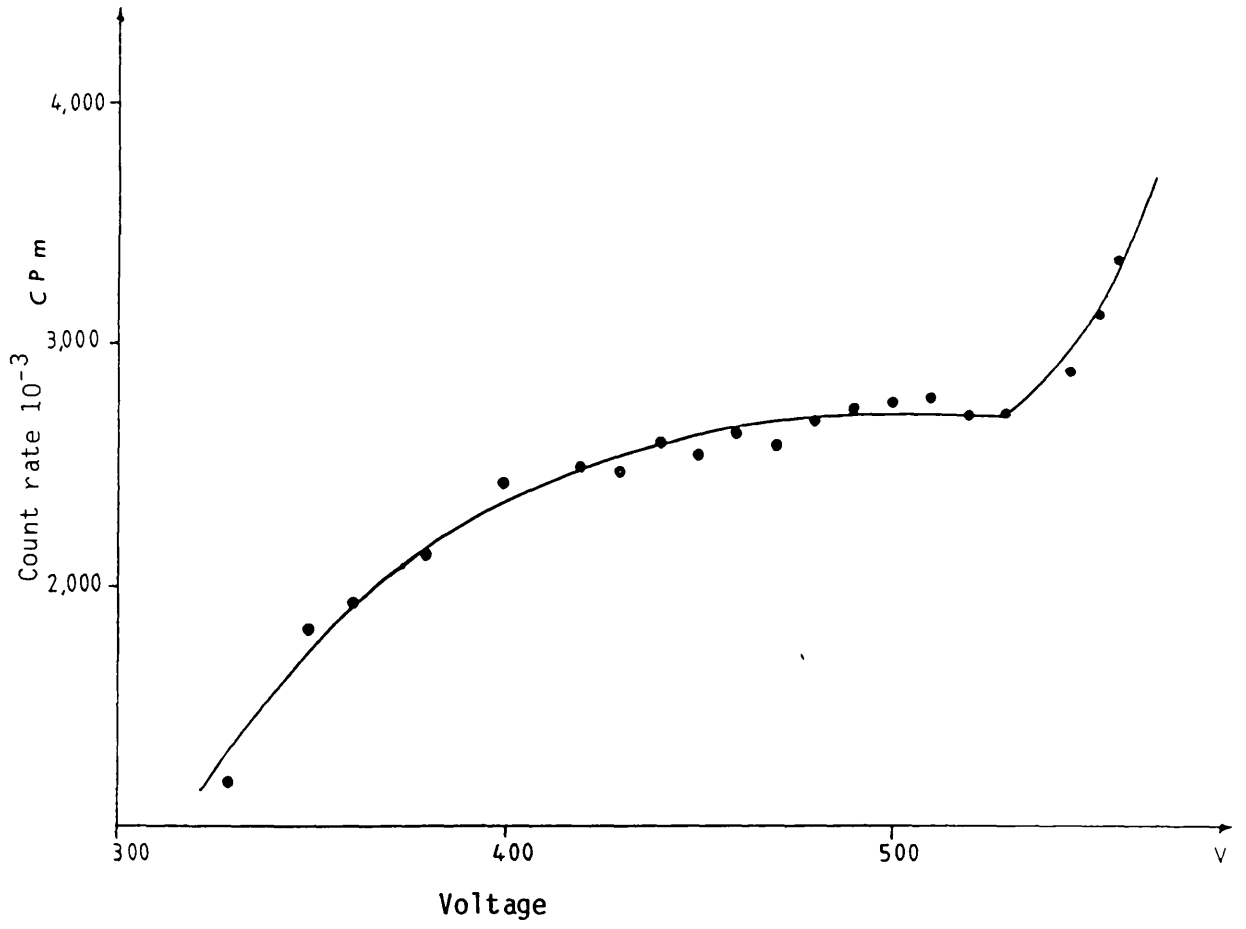


Fig.3.8 GM plateau curve

and was subtracted from the scaler-ratemeter output.

(b) Dead-time corrections.

The ions generated by an ionising event at the anode in a Geiger-Muller counter are spread along the entire length of the anode wire. This prevents the counter from counting another event until the positive ions migrate to the cathode. The time for this to occur is termed the counter dead-time and is a significant source of error when large count rates are observed.

The true count rate, N_t , can be related to the observed count rate, N_o , by use of the expression:

$$N_t = \frac{N_o}{1 - N_o T} \quad \dots\dots(1)$$

Where T is the counter dead-time. The dead-time can be determined by rearranging equation (1) into the form:

$$T = \frac{N_t - N_o}{N_t \cdot N_o} \quad \dots\dots(2)$$

The dead-time was calculated to be approximately 5.2×10^{-4} sec. All count rates were therefore corrected according to equation (1).

3.5 ¹⁴C-EXPERIMENTAL

3.5.1 Isoflo Scintillation Counting

The Isoflo scintillation counter is a microprocessor based, high efficiency scintillation monitoring system used for the analysis of radioactivity in a continuously flowing liquid or gas medium. It was designed mainly for use with HPLC and liquid chromatography. It has the ability to enhance the scope of data taken and significantly reduce the time and material consumed in analysing elements by conventional methods.

The Isoflo detector consists of high voltage amplifiers, two single channel analysers with scalers and a timer.

The flow cell is placed in a low background, light-tight lead chamber, [figure 3.9] where it is surrounded by two high performance photomultiplier tubes set 180° apart and operating in a coincidence mode to reduce any electronic noise. The two photomultipliers are surrounded by lead shielding to reduce the background. Voltage control for the phototube and the two channel analyser controls are independently adjustable to give optimum counting conditions for each isotope used.

A teflon coil cell was used in this study because it has a high beta-particle counting efficiency, figure [3.9].

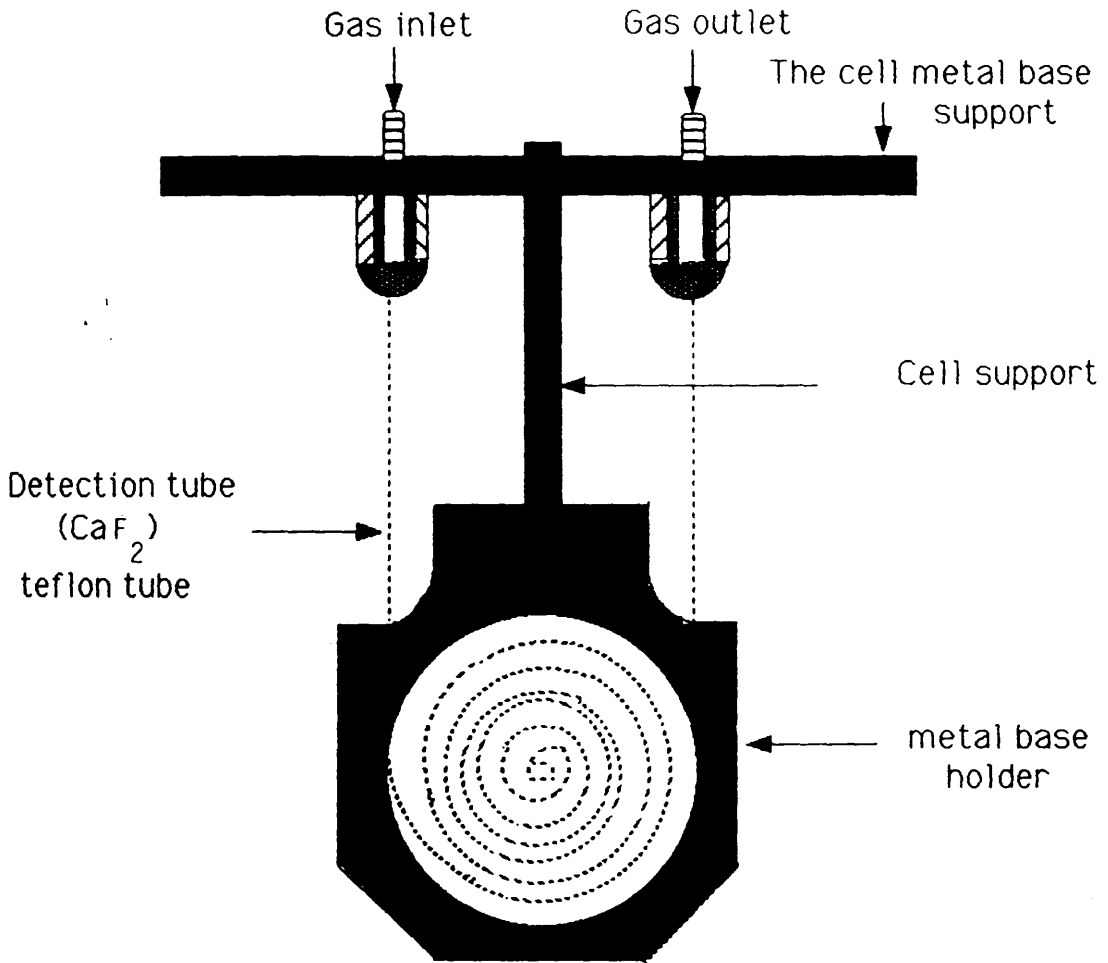


Fig. 3.9 Isoflo scintillation counter flow cell

The coil was held in a reflecting frame which was designed to have a range of internal volumes between 0.5-2 ml. The sensitivity of a packed flowcell is determined by the total surface area and optical properties of the solid scintillator granules presented according to the radioactive sample. As well as the effect of the flowcell volume, this in turn will determine the discrimination between peaks.

During the measurements, the effluent gas from the chromatograph column flows through the flow cell, the two photomultiplier tubes adjacent to the cell detect the photons emitted from the cell, while the coincidence techniques record only the events which occur in the photomultipliers within the coincidence time of the instrument. The emitted pulses of light that are detected in the Isoflo are converted by the photomultiplier tubes to pulses of electronic charge. These charges are then processed electronically and subsequently counted.

During ^{14}C -carbon monoxide or ^{14}C -carbon dioxide experiments, the required weight of catalyst was loaded into the reaction vessel [figure 3.3] and reduced using the same procedure as explained in section (3.4.1). Successive pulses of a labelled gas were then introduced to the reactor and the adsorption isotherm determined. The gases, after passing through the catalyst bed, were analysed and separated by the gas chromatograph. The outlet gas from the

chromatograph column then passed through the Isoflo cell, where the activity of the gas was quantified. The results were either stored on disk or printed directly in the form shown in figure [3.10]

The Isoflo scintillation counter was coupled to a personal computer with programming facilities to process the scintillation signals to produce a radiochromatograph as shown in figure [3.10].

Following the measurement of gas activity by the scintillation counter, the activity of an adsorbed amount of labelled gas could be determined as follows. A measured pulse, usually similar to the pressure used in each experiment, was introduced directly to the Isoflo cell by "by-passing" the catalyst bed, and the activity was measured. During the ^{14}C -adsorption experiment (with the specific activity of the gas kept constant) some of the gas molecules will be adsorbed on the catalyst surface, while the remaining gas activity was determined by the scintillation counter. The difference in the activity between the calibration pulse and an adsorption pulse was used to determine the activity and hence the amount of gas adsorbed on the catalyst surface. From the accumulated sum of the amounts of gas, adsorbed after each pulse the extent of the adsorption could be measured and an adsorption isotherm could be determined.

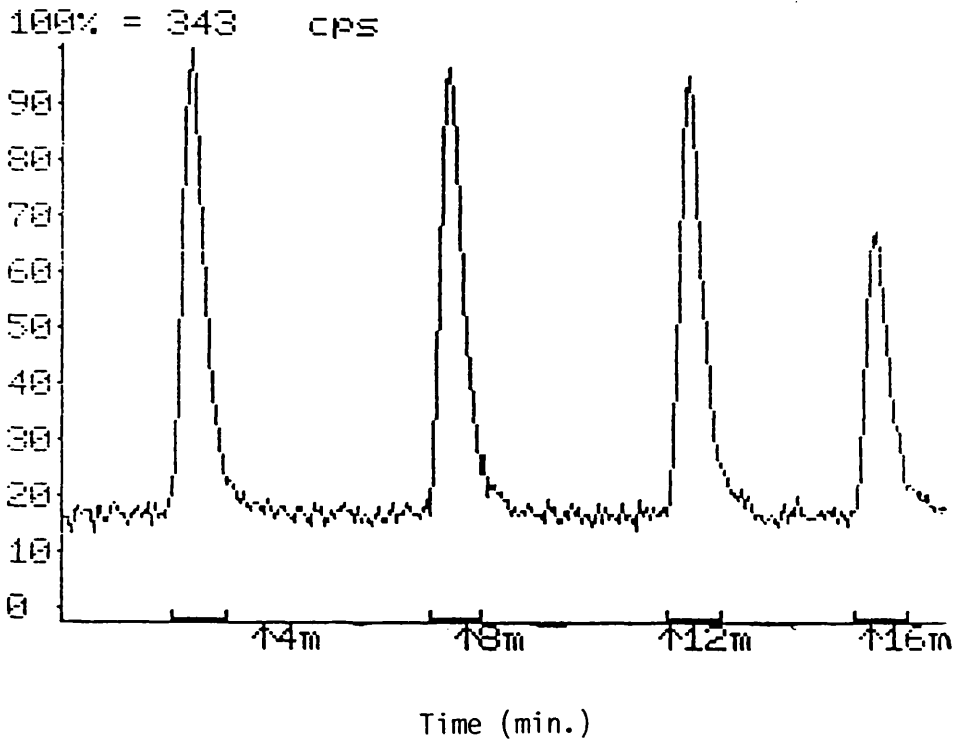


Fig.3.10 (14-C) Carbon monoxide radiochromatogram

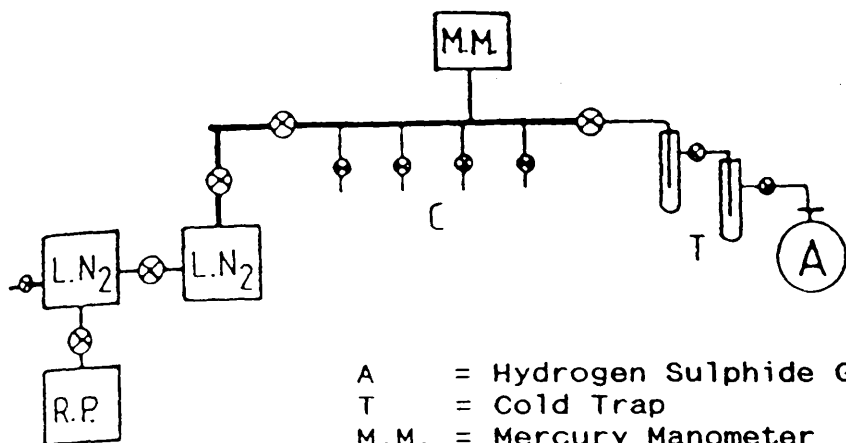
3.6 PREPARATION OF LABELLED GASES

3.6.1 [^{35}S -] Hydrogen Sulphide Preparation

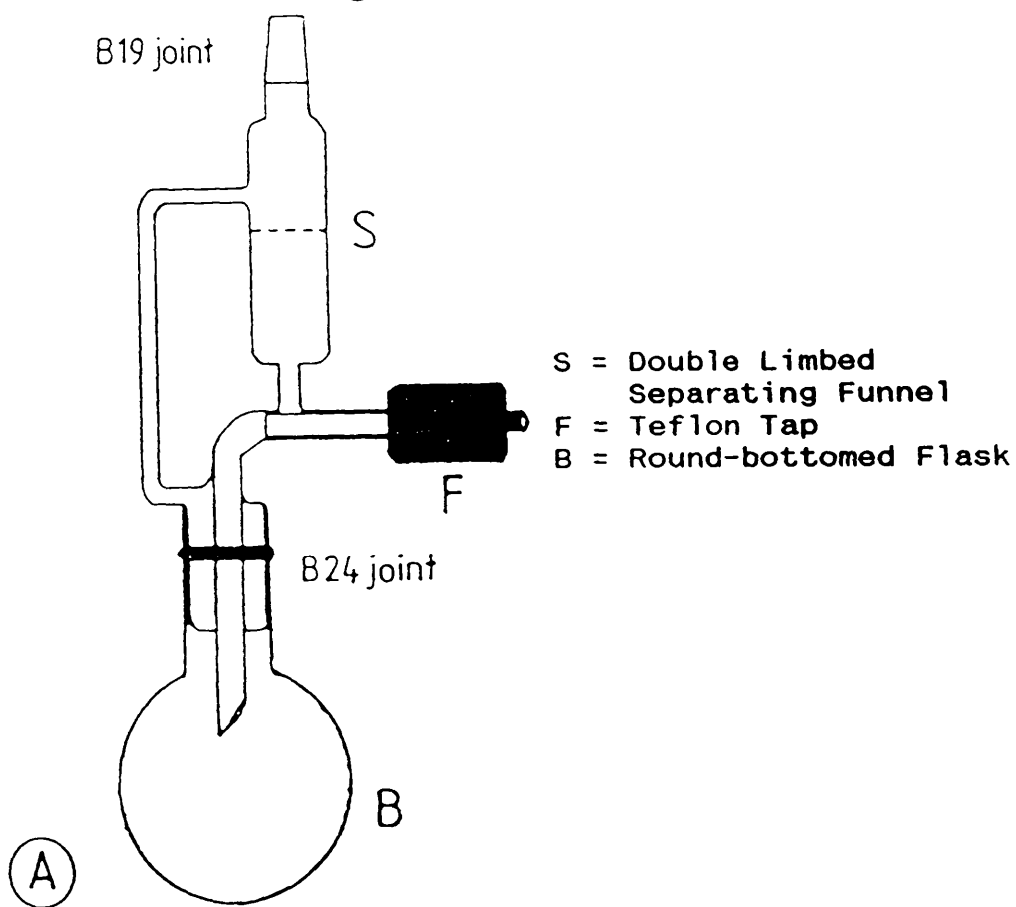
Labelled [^{35}S -] hydrogen sulphide was prepared using the glass vacuum line shown in figure [3.11]. The vacuum system consisted of the gas generator, which contains a double limbed separating funnel (S), and a Teflon tap F which allowed acid to drop into the round-bottomed flask containing labelled sulphur $^{35}\text{S-Na}_2\text{S}$.

The generated $^{35}\text{S-H}_2\text{S}$, was dried by passing through liquid nitrogen traps containing P_2O_5 before being stored in traps within the vacuum system. The vacuum was generated within the system using a rotary oil pump and liquid nitrogen trap. The vacuum as well as the pressure of the generated gas was measured by the mercury manometer.

Hydrogen sulphide was generated by reaction of labelled [$^{35}\text{S-Na}_2\text{S}$] sodium sulphide with diluted sulphuric acid or hydrochloric acid at room temperature. The labelled [^{35}S -] Na_2S was obtained from Amersham International in the solid form. This was dissolved in a 2 ml aqueous Na_2S solution (5 gm Na_2S dissolved in 50 ml distilled water) and transferred using a 1 ml syringe to the gas generator [B in figure 3.11] (part A). The diluted acid was then dropped gently in to the ^{35}S -container using the Teflon tap F. The generated



- A = Hydrogen Sulphide Generator
- T = Cold Trap
- M.M. = Mercury Manometer
- C = B14 Collecting Joints
- L.N = Liquid Nitrogen Traps
- R.P. = Rotary Pump
- ⊗ = Stopcock



- S = Double Limbed Separating Funnel
- F = Teflon Tap
- B = Round-bottomed Flask

Fig.3.11 (35-S)Hydrogen sulphide preparation line

gas was collected in a series of small traps, which contained P_2O_5 for drying purposes, which were held at liquid nitrogen temperature for about 25 minutes. The traps were then allowed to warm up and the gas was expanded into the manifold, the pressure being measured by the mercury manometer. The gas was then frozen into a container fitted with stopcocks and transferred to the main vacuum system where a trap-to-trap distillation was carried out using liquid nitrogen. Finally, the labelled [^{35}S -] hydrogen sulphide was stored in 1 litre bulb attached to the main vacuum system and diluted with known pressure of unlabelled hydrogen sulphide to achieve the desired specific activity.

3.6.2 The Preparation of [^{14}C -] Carbon Monoxide and Carbon Dioxide

3.6.2.1 The Preparation of [^{14}C -] Carbon Monoxide

[^{14}C -] carbon monoxide was prepared by reduction of [^{14}C -] carbon dioxide (1 mci batches), with metallic zinc. The metallic zinc was in a form of pellets of about 5 mm in diameter, which were made from a moistened mixture composed of 95% (w/w) zinc dust and 5% (w/w) Aerosil silica. Silica was used to increase the porosity of the reductant and to prevent clogging. The zinc pellets were dried in an air

oven ($\sim 120^\circ\text{C}$) for about 48 hours before being introduced into the converter. The apparatus, which was used for this preparation process is shown in figure [3.12].

A batch of [^{14}C -] carbon dioxide was attached to the B14 side-arm and the converter was degassed for about 24 hours at 400°C . The zinc pellets were heated by means of an electric furnace, the current being controlled by a Variac controller. The temperature was measured with a chromel-alumel thermocouple attached to the side of the converter inside the furnace, the thermocouple being connected to a Comark electronic thermometer. [^{14}C -] carbon dioxide was introduced into the converter by breaking the break-seal of the ampoule using stainless steel balls and an external magnet. The apparatus was left at 400°C for 72 hours to allow circulation of [^{14}C -] carbon dioxide through the zinc pellets and to ensure complete reduction of the [^{14}C -] carbon dioxide at this temperature to [^{14}C -] carbon monoxide. Any unconverted [^{14}C -] carbon dioxide was trapped in the cold finger using liquid nitrogen. The [^{14}C -] carbon monoxide thus formed was allowed to expand in to a 1 litre storage bulb and was diluted with non-radioactive carbon monoxide to the required specific activity.

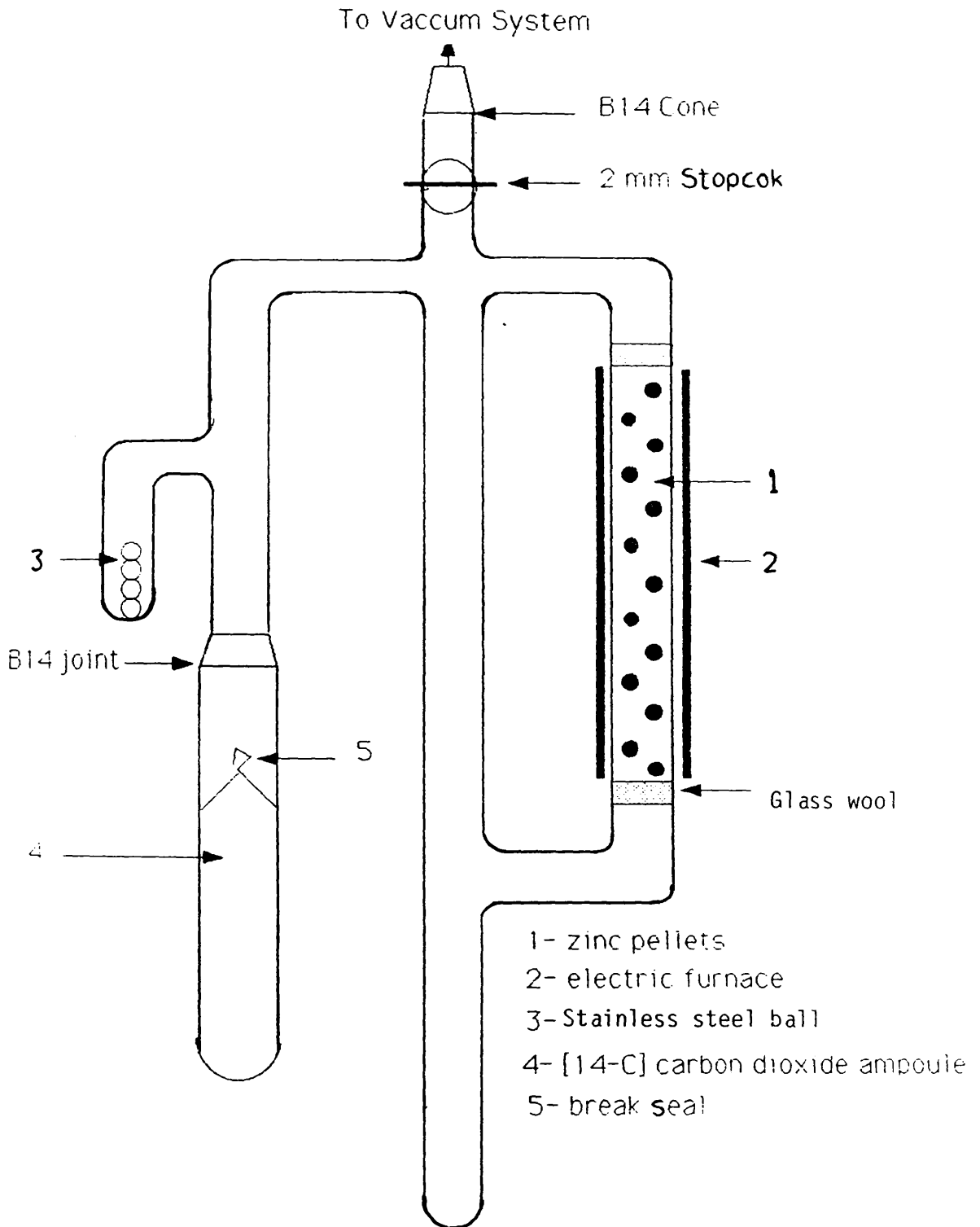


Fig.3.12 (14-C)Carbon monoxide preparation line

3.6.2.2 The Preparation of [^{14}C -] Carbon Dioxide

[^{14}C -] carbon labelled carbon dioxide (2 mmol, 1 mci) was also prepared by the addition of hydrochloric acid (35.4 w/w%) to a sample of [^{14}C -] labelled barium carbonate ($\text{Ba}^{14}\text{CO}_3$). It was dried by trap-to-trap distillation over P_2O_5 at liquid nitrogen temperatures and was then diluted using dried unlabelled carbon dioxide to give suitable working count rate of 330 ± 18 counts/s/mmol.

Tests showed that a linear relationship between the count rate and pressure was obtained. The IR spectra of the prepared [^{14}C -] carbon dioxide showed two bands at 2350 and 680 cm^{-1} due to carbon dioxide and there was no indication of any other impurities.

3.7 IN *Situ* FTIR SPECTROSCOPY, EXPERIMENTAL PROCEDURES

The adsorption of methanol and carbon monoxide were examined by FTIR spectroscopy using a Nicolet 5-DXC instrument at 2 cm^{-1} resolution. The purpose of such an investigation was essentially to identify the surface species adsorbed on the surface of the various copper catalysts and to examine the effects (on any surface species formed) of various treatments, such as heating or helium flushing over any period of time. Both $\text{Cu}/\text{Al}_2\text{O}_3$ and

Cu-ZnO/Al₂O₃ were examined by diffuse reflectance spectroscopy using a DRIFT accessory (collector type as supplied by spectra-Tech Inc.) because of the high copper loading which makes the sample very dark and impossible to examine by transmission infrared spectroscopy. The diffuse reflectance accessory consists of 4 flat and 2 aspherical mirrors, and an alignment mirror as shown in figure [3.13]. The two aspheric mirrors are off-axis ellipsoids which focus and collect infrared energy with a 6X beam condensation. However, at the focus, the beam of the FTIR spectrophotometer has a 3-18 mm spot size, therefore, the spot size within the DRIFT accessory is between 0.5-3.0 mm in size. The sample holder (a cup in the shape of a boat) could be removed from the top of the collector by sliding apart the ellipsoid mirrors. The cell was connected to a flow system fitted with a three-way valve to allow for the introduction of more than one gas. The catalyst samples were heated to the required temperature by an internal cartridge heater powered by a Variac controller. The temperature was monitored by a chromel-alumel thermocouple placed beneath the centre of the catalyst cup.

During the FTIR experiments the procedure was as follows; a background spectrum was recorded using KBr as a diffuse reflector in the instrument. A catalyst sample was then loaded into the sample cup, sealed inside the environment chamber, and reduced in a flow of 6% hydrogen

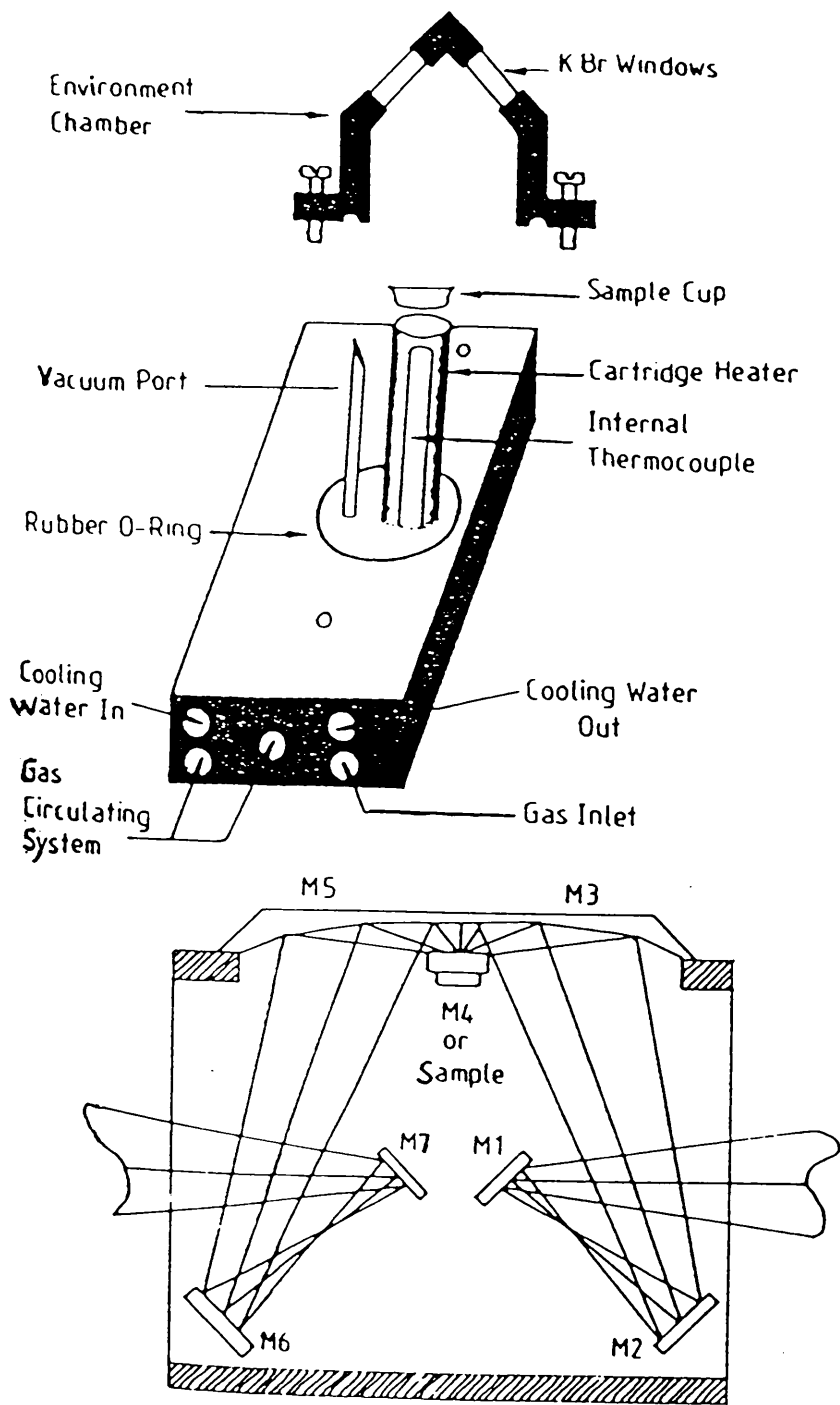


Fig.3.13 Diffuse reflectance IR cell

in nitrogen (25 ml/min) at 200°C for 3 hours, followed by flushing with helium at the same temperature for about 20 minutes. The experiment was then carried out at the required temperature. The gases (the adsorbate) were introduced in flow mode for 15 minutes at a flow rate of 25 ml/min, followed by flushing with helium for 10 minutes, the spectrum was recorded immediately after this and again after various treatments.

Liquid methanol was introduced using a (10 μ l) microsyringe whilst the catalyst sample was subjected to the same treatment (such as, heating at elevated temperature or under helium flow) before recording the spectrum of the adsorbed species.

The adsorption of methanol on samples of ZnO and Al₂O₃ was investigated using an *in situ* flow IR cell as shown in figure [3.14].

The sample wafer was held in a glass holder which was positioned in the centre of the flow cell. The outer body of the Pyrex/borosilicate glass cell was surrounded by a Nichrome-wire furnace capable of heating the sample wafer to 450°C. This temperature was monitored by an electronic thermometer (electronics Ltd.-1602 Cr/Al) coupled to a chromel-alumel thermocouple located in a thermowell which terminated close to the sample wafer. Two KBr windows (25 x 4 mm, spectra-Tech Inc.), sealed in stainless steel rings

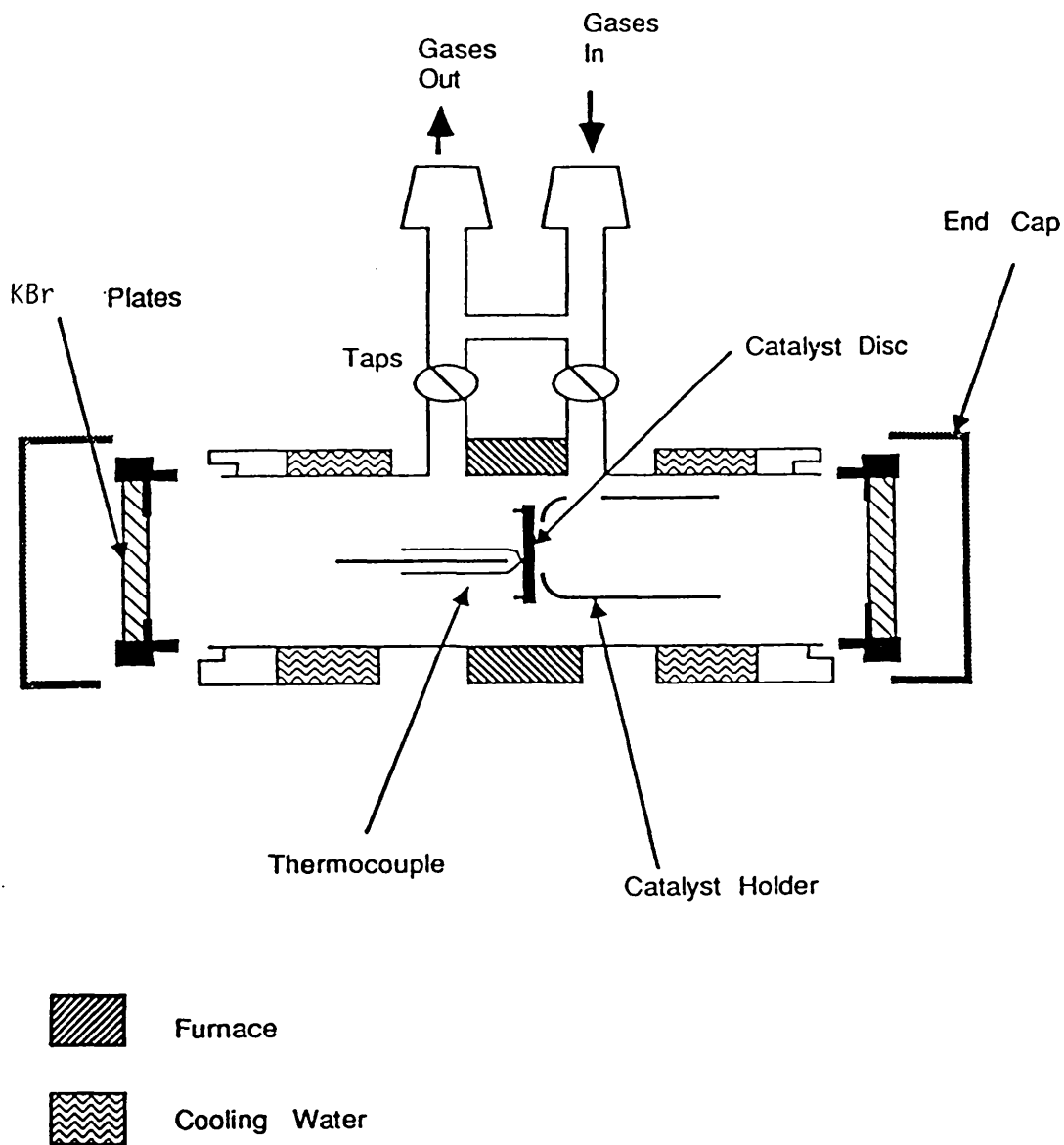


Fig.3.14 In-situ FTIR flow cell

with Araldite adhesive were fitted to both ends of the flow cell by stainless steel threaded flanges. The sleeves holding the windows were surrounded by water coolant jackets in order to prevent thermal shock to the KBr windows.

Catalyst powder (~0.07 gm) was pressed into thin self-supporting wafers using pressures of about 520 kg cm⁻². The wafers were then placed in the IR flow cell and reduced in 6% hydrogen in nitrogen, (flow rate 25 ml/min) at 300°C for 3 hours followed by helium flushing for 15 minutes at the reduction temperature before the sample temperature was set at a required value under the helium flow.

3.8 Treatment of the Results

The results presented in this thesis were treated as follows;

(a) pressure measurements; each chromatograph peak was traced several times using a planimeter and the average area determined. This area was then converted to pressure using the calibration curves, and number of moles were calculated using the equation:

$$n = \frac{PV}{RT}$$

Whereas n, number of moles, P; pressure of a pulse in

torr, V; the sample loop volume $(0.201)\text{cm}^3$, R; gas constant $(6.24 \times 10^4) \text{ cm}^3 \text{ torr K}^{-1} \text{ mol}^{-1}$ and T; room temperature (298 K).

Number of moles then converted to molecules by multiplying by Avogadro's constant $(6.022 \times 10^{23} \text{ molecules mol}^{-1})$.

(b) calculation of adsorbed sulphur coverage on the catalyst surface. Metal surface areas (table 3.1) were calculated on the basis that 1×10^{19} copper atoms are exposed by 1 m^2 of copper surface [141,225]. The surface coverage of adsorbed sulphur on the copper component of the catalyst was calculated by taking the ratio of the number of poison molecules (calculated as in {a} above), admitted to the catalyst, to the calculated number of copper surface atoms in the sample.

CHAPTER FOUR

METHANOL DECOMPOSITION ON CLEAN AND HYDROGEN SULPHIDE POISONED COPPER-BASED CATALYST SURFACES

4.1 DECOMPOSITION OF METHANOL ON CLEAN AND POISONED SURFACES

Data on the conversion of methanol over $\text{Cu}/\text{Al}_2\text{O}_3$, $\text{Cu-ZnO}/\text{Al}_2\text{O}_3$, ZnO and Al_2O_3 will be presented in this chapter. The effect of hydrogen sulphide adsorption on the extent of methanol decomposition over these catalysts will also be considered.

It was found that the progress of the reaction was strongly dependent on the conditions of catalyst reduction. As a direct consequence, it was decided to probe the precise role of the reduction procedure; the results of this investigation are included in the following sections.

4.2 METHANOL DECOMPOSITION ON CLEAN SURFACES

4.2.1 The Decomposition of Methanol on $\text{Cu}/\text{Al}_2\text{O}_3$ Surface

Catalysis over a freshly reduced $\text{Cu}/\text{Al}_2\text{O}_3$ (64 wt% Cu) catalyst yielded carbon dioxide, carbon monoxide and hydrogen as products of methanol interaction. The amount of carbon dioxide found varied according to the method of the

catalyst surface reduction (as mention in section 2.2).

Typically, 0.16 g of catalyst was reduced in a stream of 6% H₂ in N₂ at 180°C for 14 hours followed by heating for a further 2 hours at 250°C.

Figures [4.1 and 4.4] illustrate variation of the yields of carbon monoxide and carbon dioxide with methanol pressure. At lower methanol pressure (<ca. 40 torr) the concentrations of carbon monoxide and carbon dioxide in the gas phase remain constant (~89% and ~11% for carbon dioxide and carbon monoxide respectively).

On increasing the methanol pressure, the carbon monoxide concentration increased while the concentration of carbon dioxide decreased; the drop in the carbon dioxide concentration corresponds directly to the increase in carbon monoxide production.

The variation of carbon monoxide and carbon dioxide production with the number of methanol pulses was studied at a constant pressure of methanol (87 torr) and a reaction temperature (250°C), as shown in figure [4.2]. The concentration of carbon dioxide decreased, while the amount of carbon monoxide liberated increased with the number of reactions.

The yield of carbon monoxide and carbon dioxide as a function of temperature is shown in figure [4.3]. Reactions at different temperatures were studied in random order. At lower temperatures (<ca. 250°C), the concentration of carbon dioxide was very high (>80% of reaction products) with smaller amounts of carbon monoxide formed; as the

Fig: 4.1

Methanol Decomposition on Reduced (0.156g)
Copper/Alumina Catalyst at 250°C

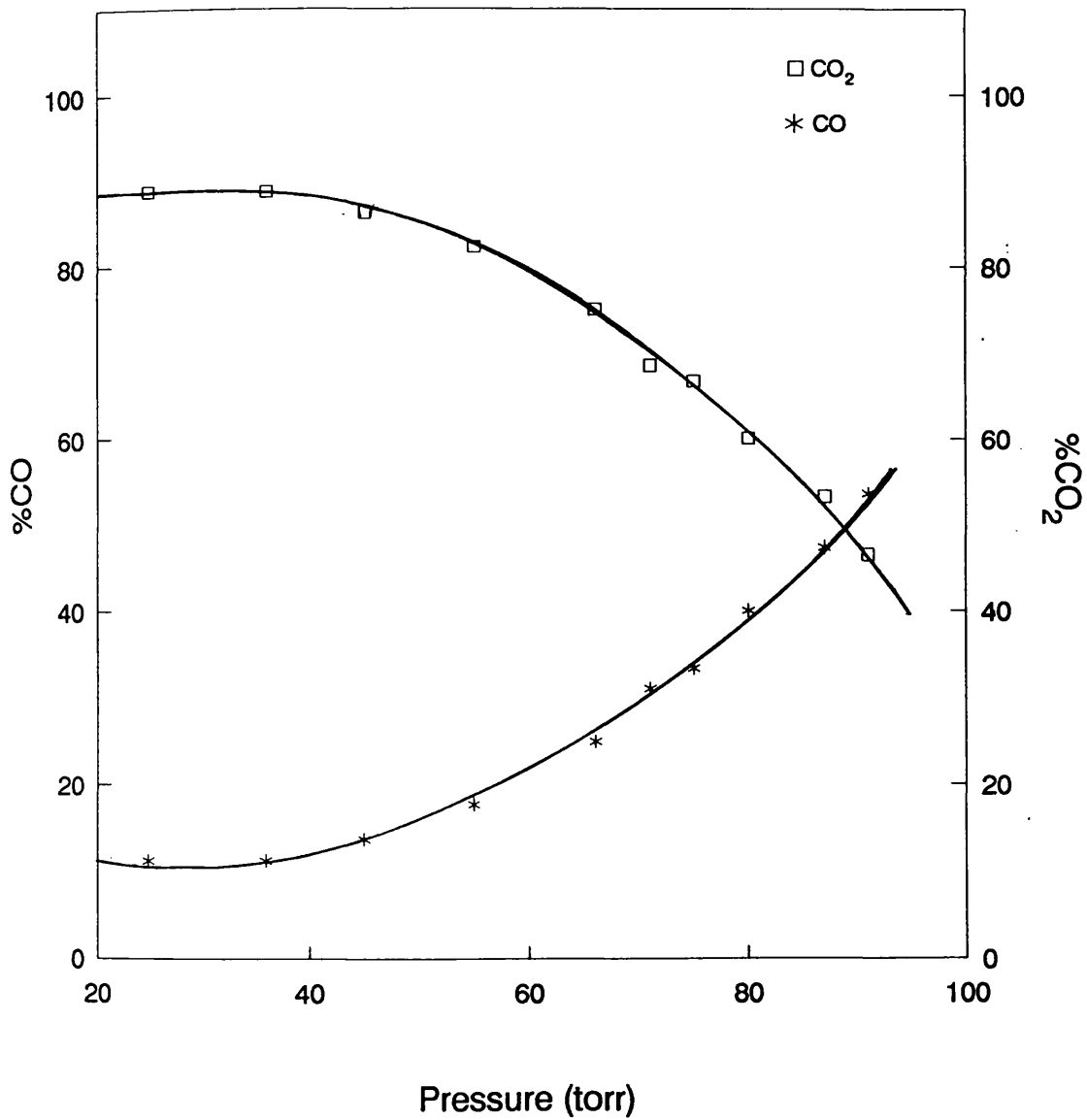


Fig: 4.2

Methanol Decomposition on Reduced
Copper/Alumina Catalyst (0.156g),
Methanol Initial Pressure 87 Torr
Reaction Temperature 250°C

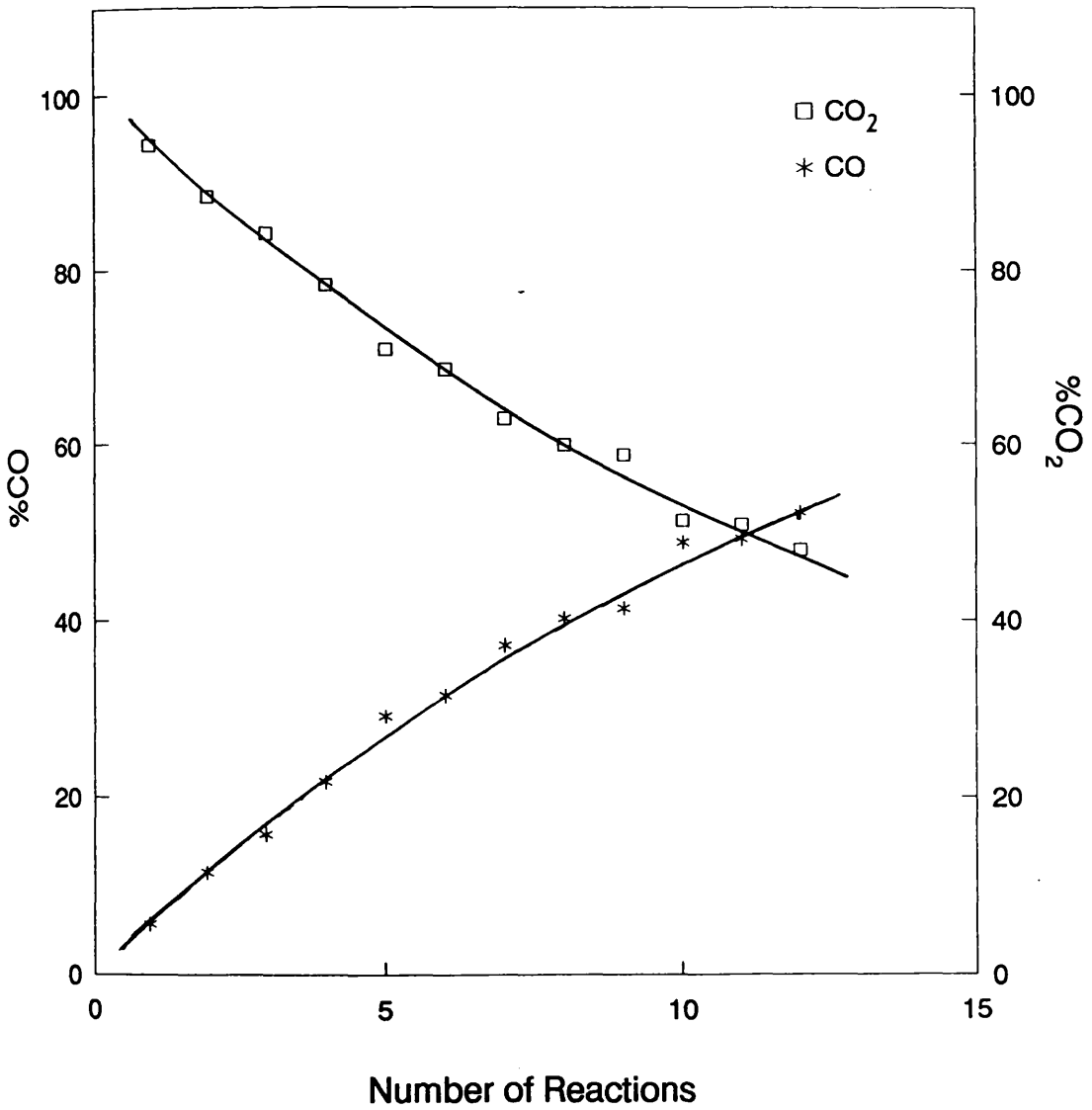


Fig: 4.3

Methanol Decomposition on Reduced
Copper/Alumina Catalyst (0.156g),
Methanol Initial Pressure 87 Torr

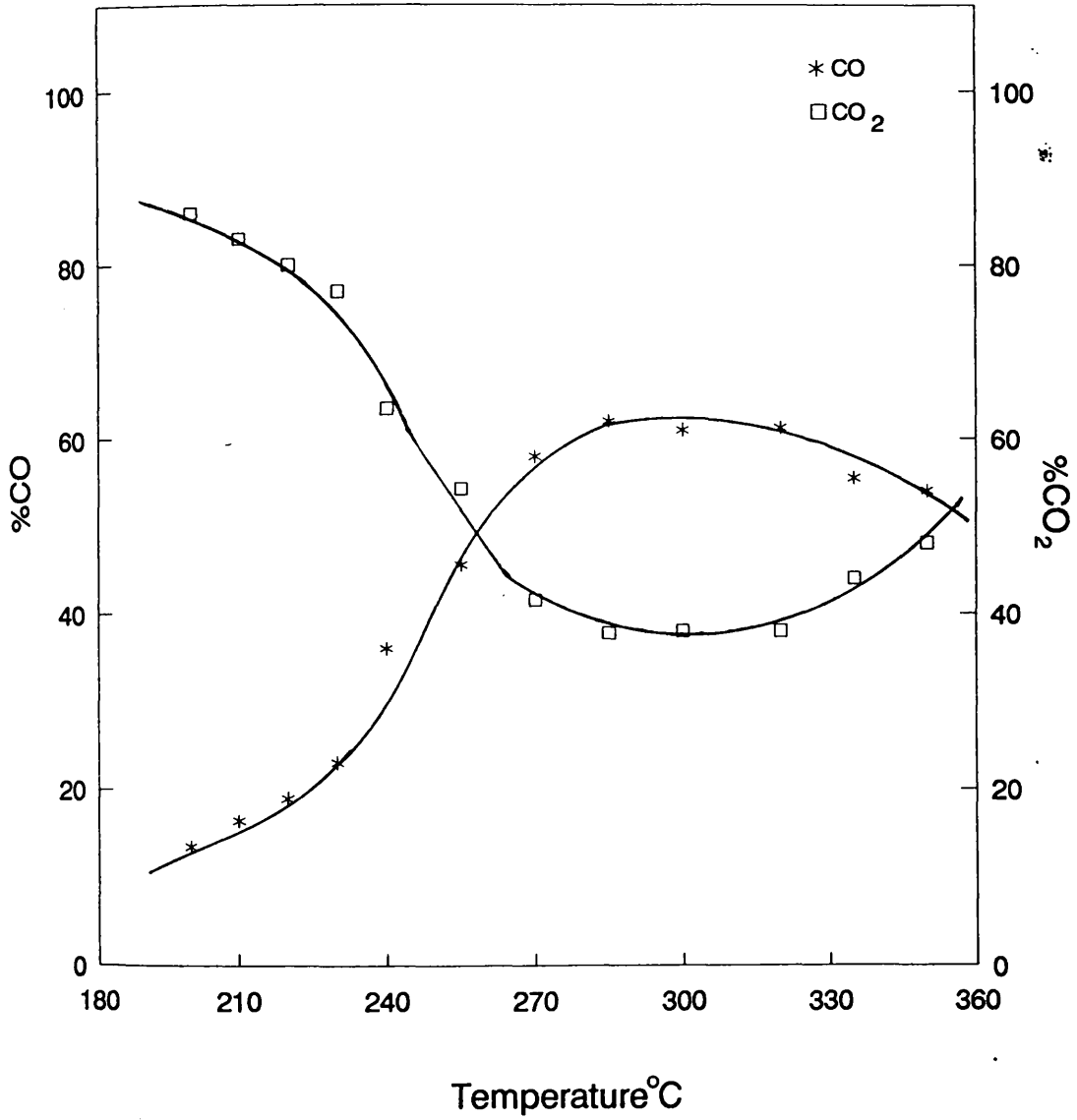
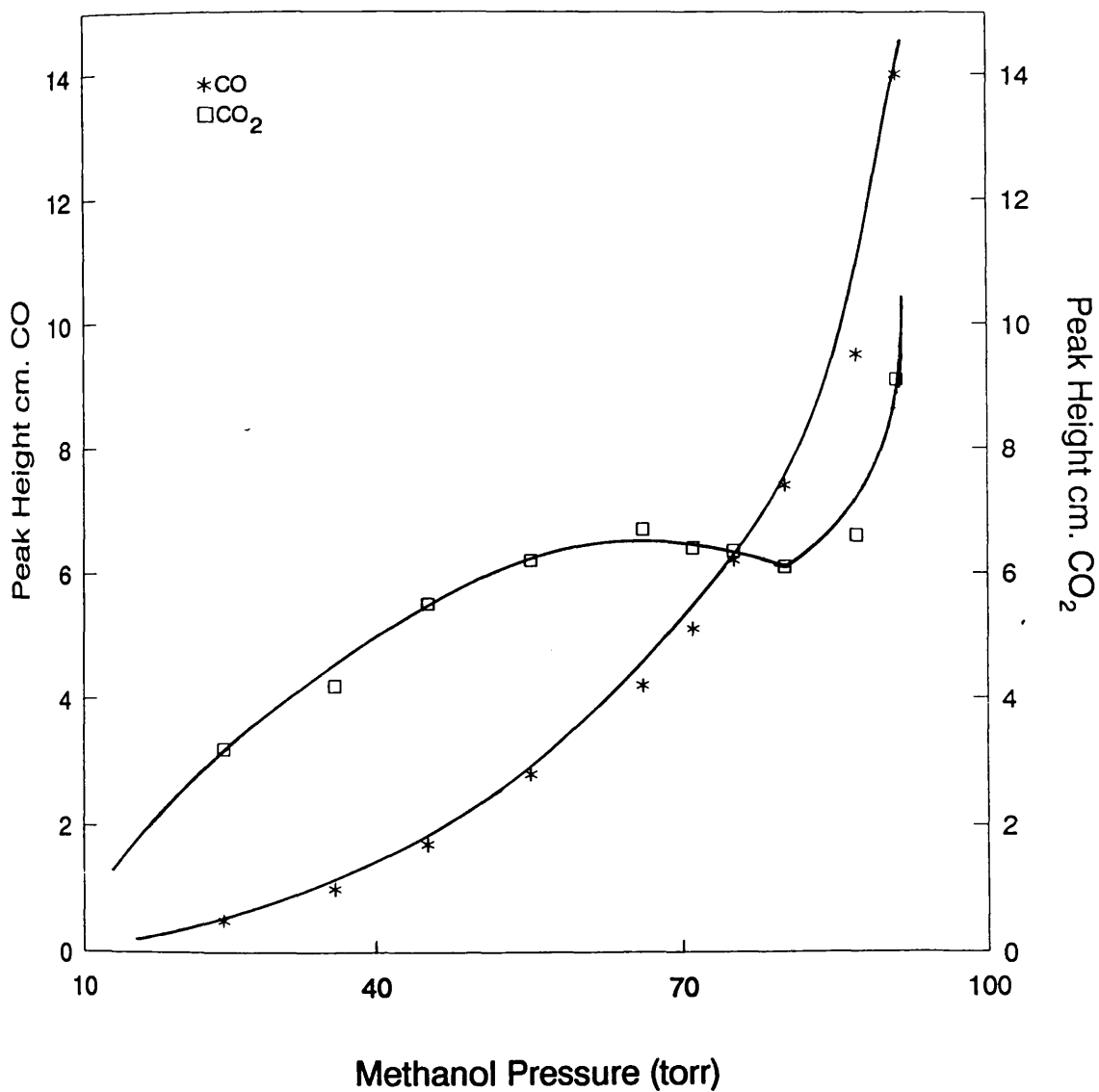


Fig: 4.4

Methanol Decomposition on Reduced
Copper/Alumina Catalyst (0.156g) at 250°C



temperature increased, the carbon dioxide concentration decreased while the amounts of carbon monoxide produced were enhanced. At temperatures higher than 260°C the situation was reversed in that the concentration of carbon monoxide formed was higher than that of carbon dioxide. The concentration of the products remained substantially unchanged up to a temperature of 340°C, at which point the carbon monoxide concentration began to decrease with a corresponding increase in the concentration of carbon dioxide. The effect of methanol initial pressure and the reaction temperature on the decomposition product distributions are presented in table 4.1. Tables 4.1-4.5 show the effect of both methanol initial pressure and reaction temperature from separate experiments on methanol decomposition, in which one of them was varied while the other was kept constant.

Table 4.1

Products distribution at various methanol pressures and reaction temperatures on Cu/Al₂O₃ surface

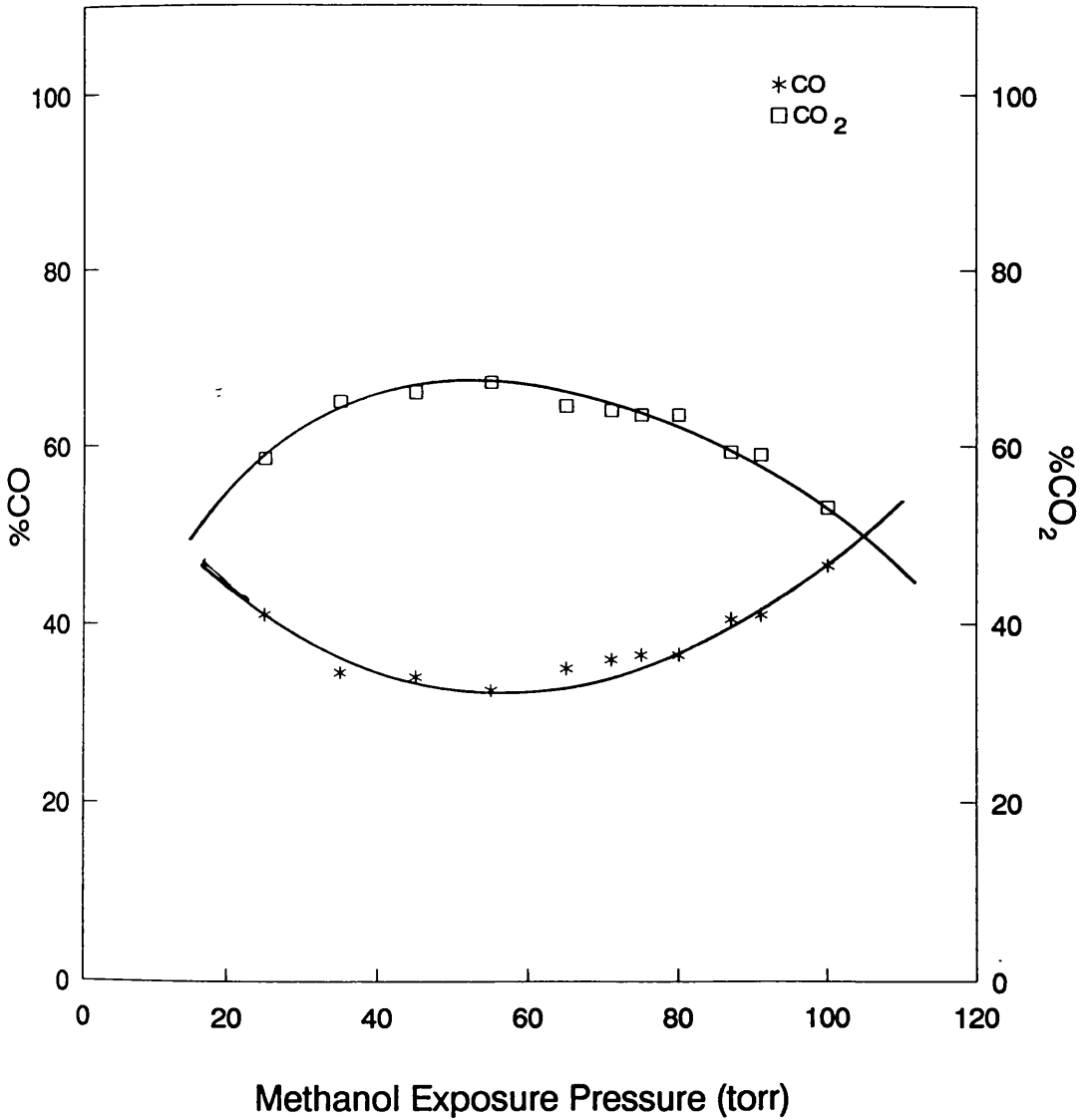
Methanol initial pressure Torr	% yield		Reaction temperature °C	% yield	
	CO	CO ₂		CO	CO ₂
25	11.2	88.5	200	13.84	86.15
45	13.63	86.36	220	19.62	80.00
66	24.99	75	240	36.37	63.62
75	33.35	66.64	270	58.22	41.77
80	40	60	285	62.00	37.95
91	53.54	46.45	335	55.37	44.26

The amounts of carbon dioxide and carbon monoxide formed during methanol decomposition over a Cu/Al₂O₃ catalyst reduced in a 6% hydrogen in nitrogen mixture at 180°C for 14 hours followed by 30 minutes flowing of carbon monoxide are shown in figure [4.5]. It can be seen that the nature of the plot is similar to figure [4.1], but the amounts of both carbon monoxide and carbon dioxide produced are lower. The yield percent of both carbon monoxide and carbon dioxide were lower than that of figure [4.1]. Nevertheless, the carbon dioxide concentration was still higher than that of carbon monoxide and again fell at higher methanol pressures. Thus, the nature of the reduction procedure strongly affects the catalysis.

The role of reaction temperature in influencing carbon

Fig: 4.5

Methanol Decomposition on Reduced
Copper/Alumina with Both 6% Hydrogen in
Nitrogen and Carbon Monoxide at 250°C



monoxide and carbon dioxide production over a carbon monoxide pretreated catalyst is presented in figure [4.6]. Here, the amount of carbon dioxide formed decreased as the reaction temperature was increased up to temperature of 245°C, while the amount of carbon monoxide formed increased in the same temperature range. At a temperature of 245°C, the amounts of carbon monoxide produced become higher than those of carbon dioxide, but both gases reached a steady state at temperatures greater than 290°C.

Reducing the catalyst surface with pure carbon monoxide for 14 hours at 250°C following reduction using 6% hydrogen in nitrogen, also generated a catalytically active surface. Figure [4.7] illustrates the variation of carbon monoxide and carbon dioxide yields as a function of methanol initial pressure; carbon monoxide is formed at a higher concentration from the outset of the reaction, indicating a complete surface reduction (of Cu^{2+}) by carbon monoxide.

By increasing the methanol pressure, at a constant temperature of 250°C, a slow increase in carbon dioxide formation was observed. At higher methanol pressures (>70 torr), carbon monoxide increased linearly. This increase was accompanied by a small increase in the amount of carbon dioxide. Interestingly, at higher methanol pressures the concentration of carbon monoxide was noticeably higher than that of carbon dioxide.

The effect of reaction temperature on the extent of methanol decomposition on the $\text{Cu}/\text{Al}_2\text{O}_3$ catalyst reduced overnight in carbon monoxide is shown in figure [4.8]. It

Fig: 4.6

Methanol Decomposition on Copper/Alumina
Sample (0.156g) Reduced with 6% Hydrogen
in Nitrogen and Carbon Monoxide
Methanol Initial Pressure 90 Torr

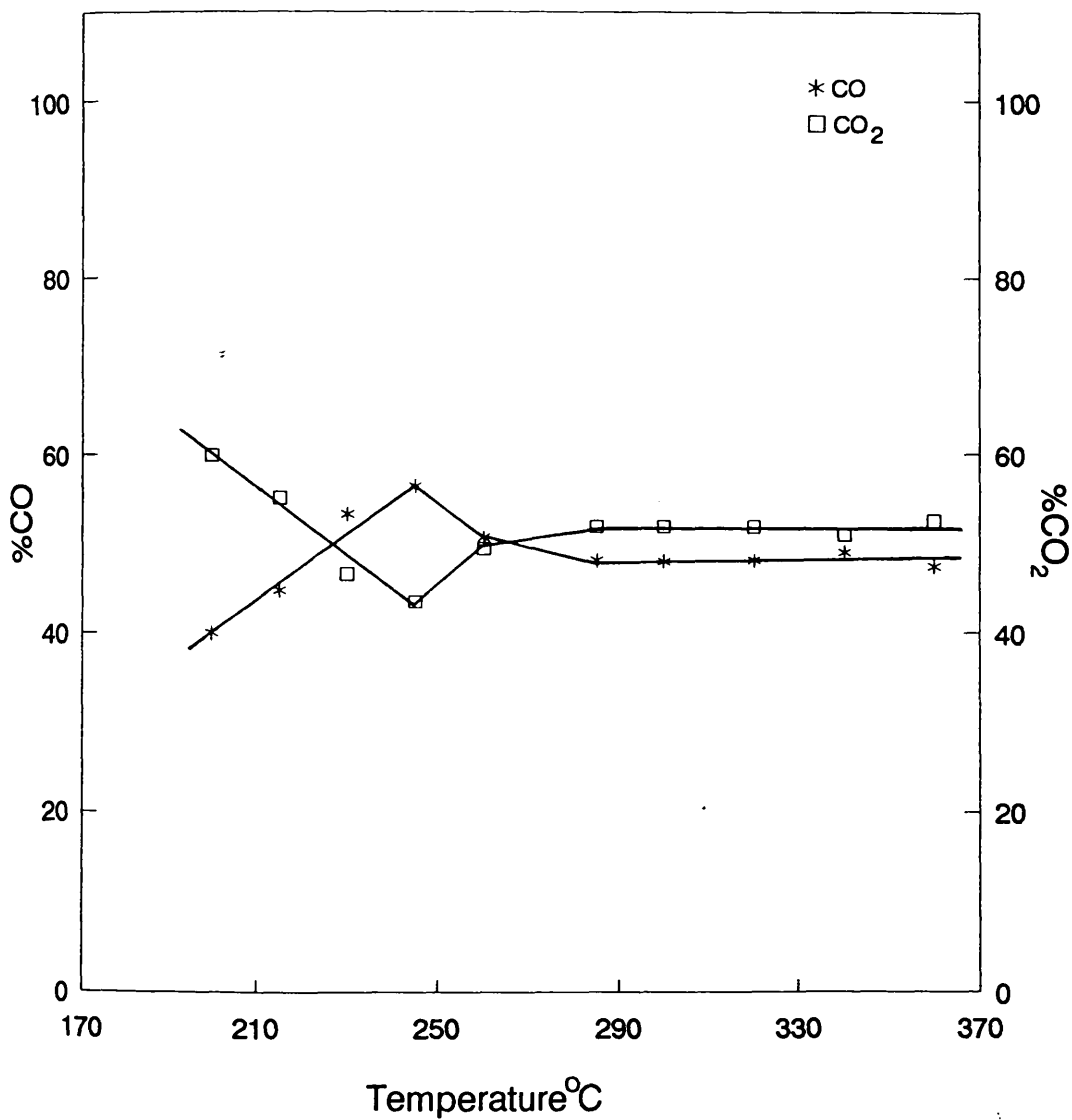


Fig: 4.7
Methanol Decomposition on Copper/Alumina
Sample (0.156g) Reduced with 6% Hydrogen
in Nitrogen and Carbon Monoxide
Reaction Temperature 260°C

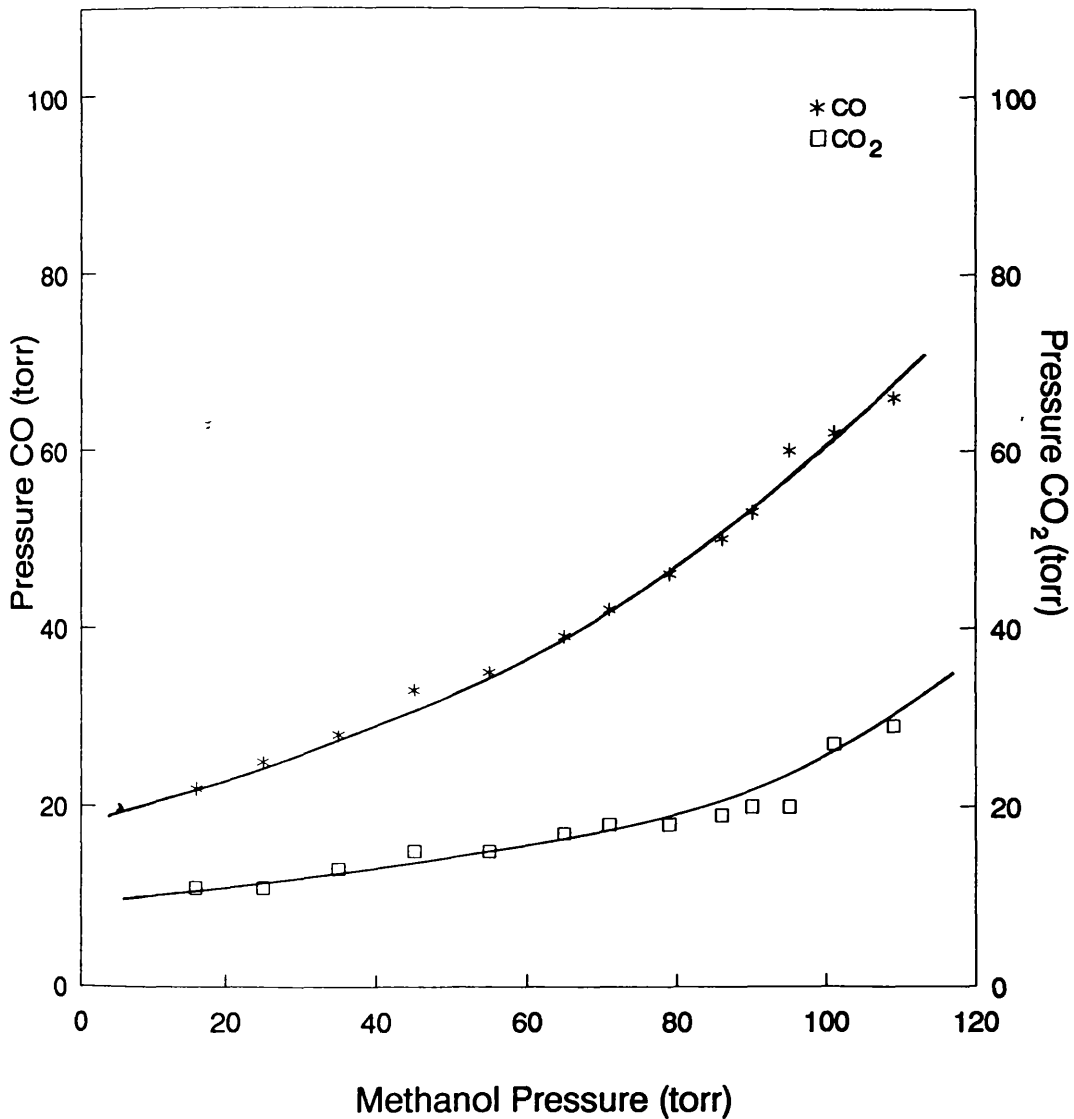
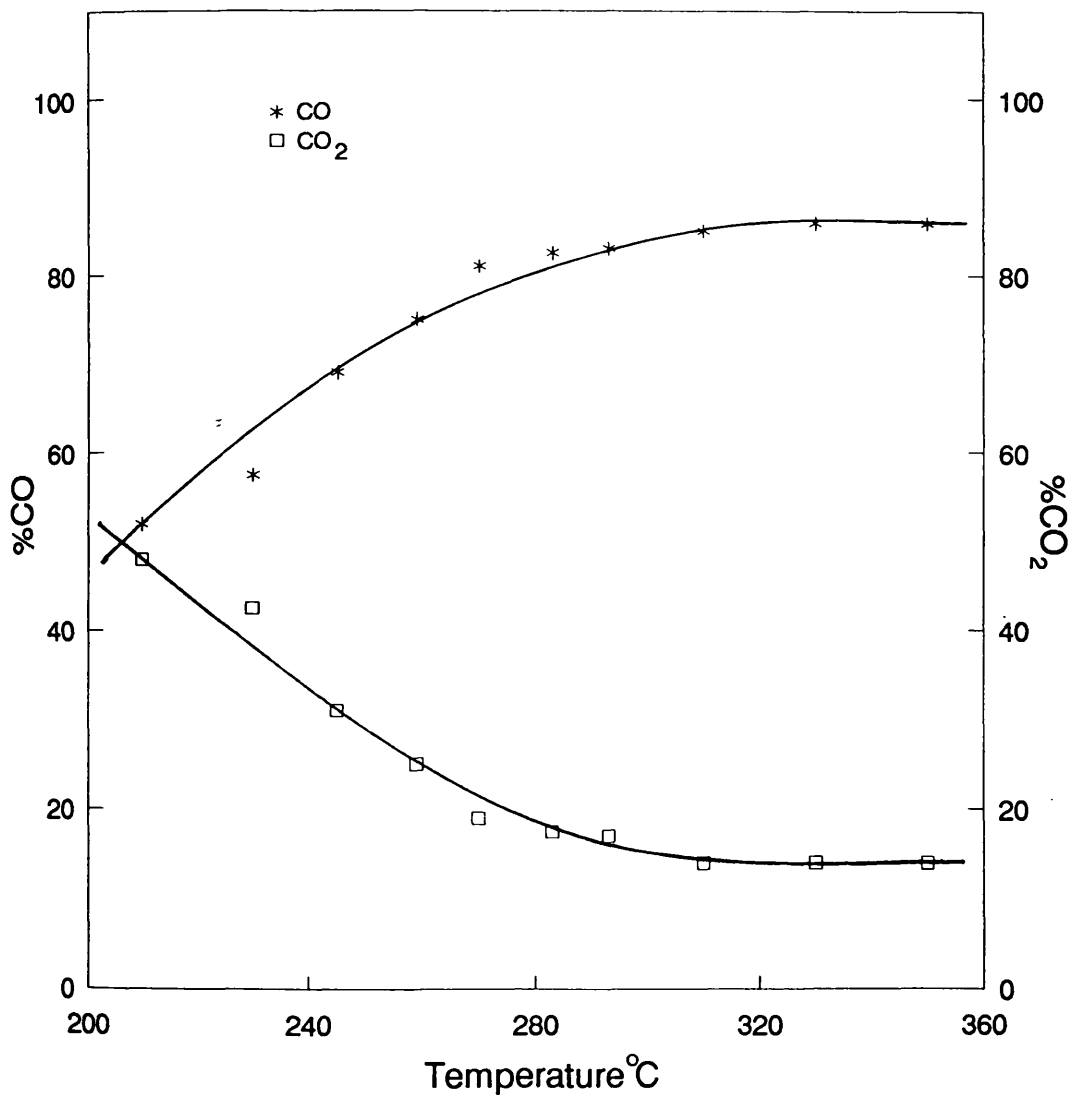


Fig: 4.8

Methanol Decomposition on Copper/Alumina
Sample (0.156g) Reduced with 6% Hydrogen
in Nitrogen and Carbon Monoxide at 250°C
Methanol Initial Pressure 110 Torr



can be clearly seen that carbon monoxide formation increased with reaction temperature, reaching a steady state at 300°C. Conversely, the level of carbon dioxide produced decreased with the total methanol exposure, yielding a much lower steady state conversion at temperatures in excess of 300°C.

The interaction of carbon monoxide with a catalyst surface reduced with 6% hydrogen in nitrogen at 180°C for 14 hours followed by 2 hours reduction in hydrogen at 200°C was then considered. Figure [4.9] shows that the carbon monoxide interacting with the catalyst surface generated carbon dioxide, which increased in concentration as the pressure of carbon monoxide was increased. Employing this catalyst for methanol decomposition resulted in the formation of carbon monoxide as the primary product. The results of the carbon monoxide interaction serve as an indication of incomplete reduction of the active catalyst surface.

The effects of methanol pressure and the reaction temperature on the decomposition of methanol on a surface reduced with carbon monoxide are presented in table 4.2.

Fig: 4.9

Carbon Monoxide Adsorption on Reduced
Copper/Alumina Catalyst Sample (0.156g)
with 6% Hydrogen in Nitrogen
Adsorption Temperature 250°C

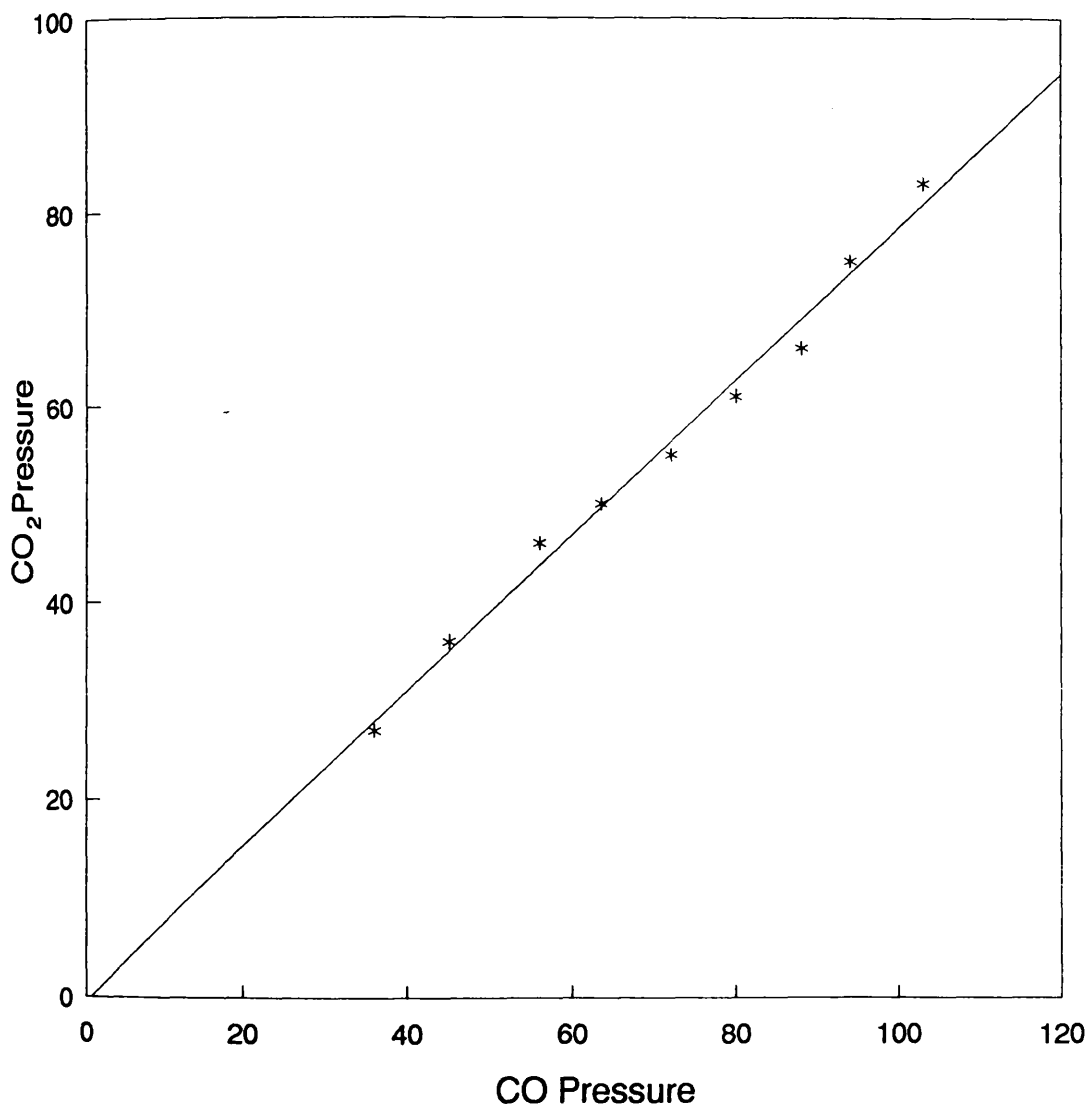


Table 4.2

Effect of methanol initial pressure and reaction temperature on the products distribution during the interaction of methanol over a (64% Cu) Cu/Al₂O₃ reduced with carbon monoxide at 250°C for 14 hours

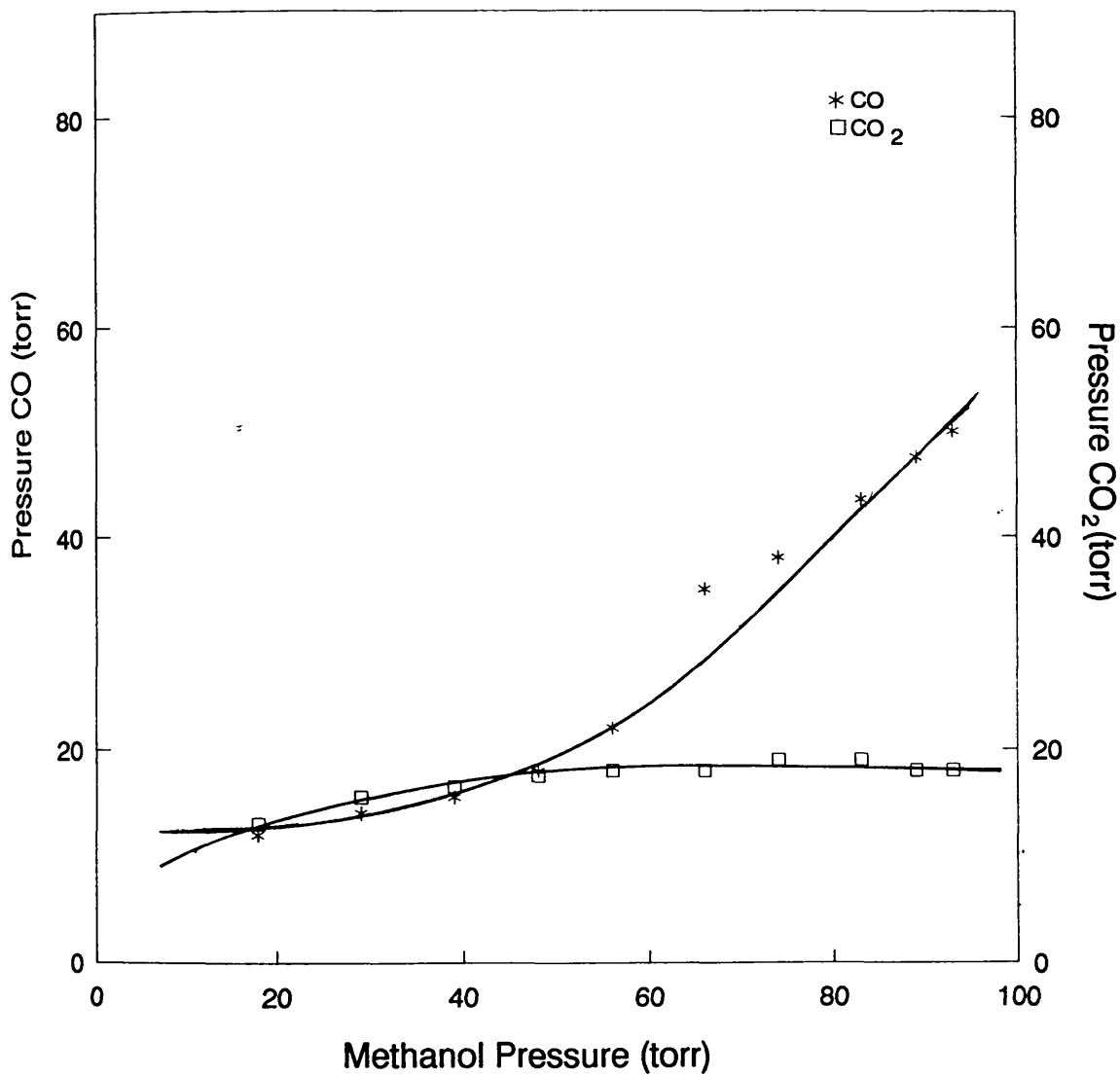
Methanol initial pressure Torr	% yield		Reaction temperature °C	% yield	
	CO	CO ₂		CO	CO ₂
25	69	30	210	51.8	48.2
45	68	31	245	73.1	26.9
65	69	30	270	76.4	23.5
79	71.8	28	283	81.8	18.00
90	72	27	330	85.9	14.00
101	69	30	350	85.9	14.00

4.2.2 Methanol Decomposition on Cu-ZnO/Al₂O₃ Surface

On freshly reduced Cu-ZnO/Al₂O₃ (in 6% hydrogen in nitrogen at 250°C for 14 hours) methanol decomposed mainly to carbon monoxide with only a small amount of carbon dioxide. Initially, the amount of carbon dioxide produced was higher but, with increasing methanol pressure the production of carbon monoxide increased. As shown in figure [4.10], increasing the methanol pressure, enhanced the concentration of carbon monoxide formed while the amounts

Fig: 4.10

Methanol Decomposition on Copper-Zinc Oxide/
Alumina Catalyst Sample Reduced with
6% Hydrogen in Nitrogen at 250°C
Reaction Temperature 300°C



of carbon dioxide produced remained unchanged. However, the total amounts of carbon monoxide and carbon dioxide generated as the methanol pressure was increased (up to 90 torr) were observed to be in the ratio of 1 : 0.2 and was lower than the total amount of methanol introduced as a pulse at 300°C.

Carbon dioxide, which was found to be the main decomposition product, decreased in concentration as the reaction number increased using a constant methanol pressure of 90 torr and reaction temperature of 300°C, [figure 4.11]. Initially, the CO : CO₂ ratio was 1 : 3.6; after the repeated use of the catalyst this ratio (after ten reactions) was 2.3 : 1 with the result that carbon monoxide was the main product and its concentration was almost 2.5 times higher than that of carbon dioxide.

Using the same reduction procedure as above, the reaction of methanol as a function of temperature was studied. Both products carbon dioxide and carbon monoxide concentrations were increased as the temperature increased, as shown in figure [4.12]. At lower temperatures up to 260°C; the carbon dioxide concentration was higher than that of carbon monoxide, i.e. at elevated temperatures the carbon monoxide concentration increased more rapidly than carbon dioxide, both components reached a steady state at temperature of 320°C with carbon monoxide being the major product. The effects of reaction temperature and methanol initial pressure on the products distribution are presented in table 4.3.

Fig: 4.11

Methanol Decomposition at 300°C on Reduced
Copper - Zinc Oxide/Alumina (0.156g) with
6% Hydrogen in Nitrogen at 250°C
Methanol Initial Pressure 90 Torr

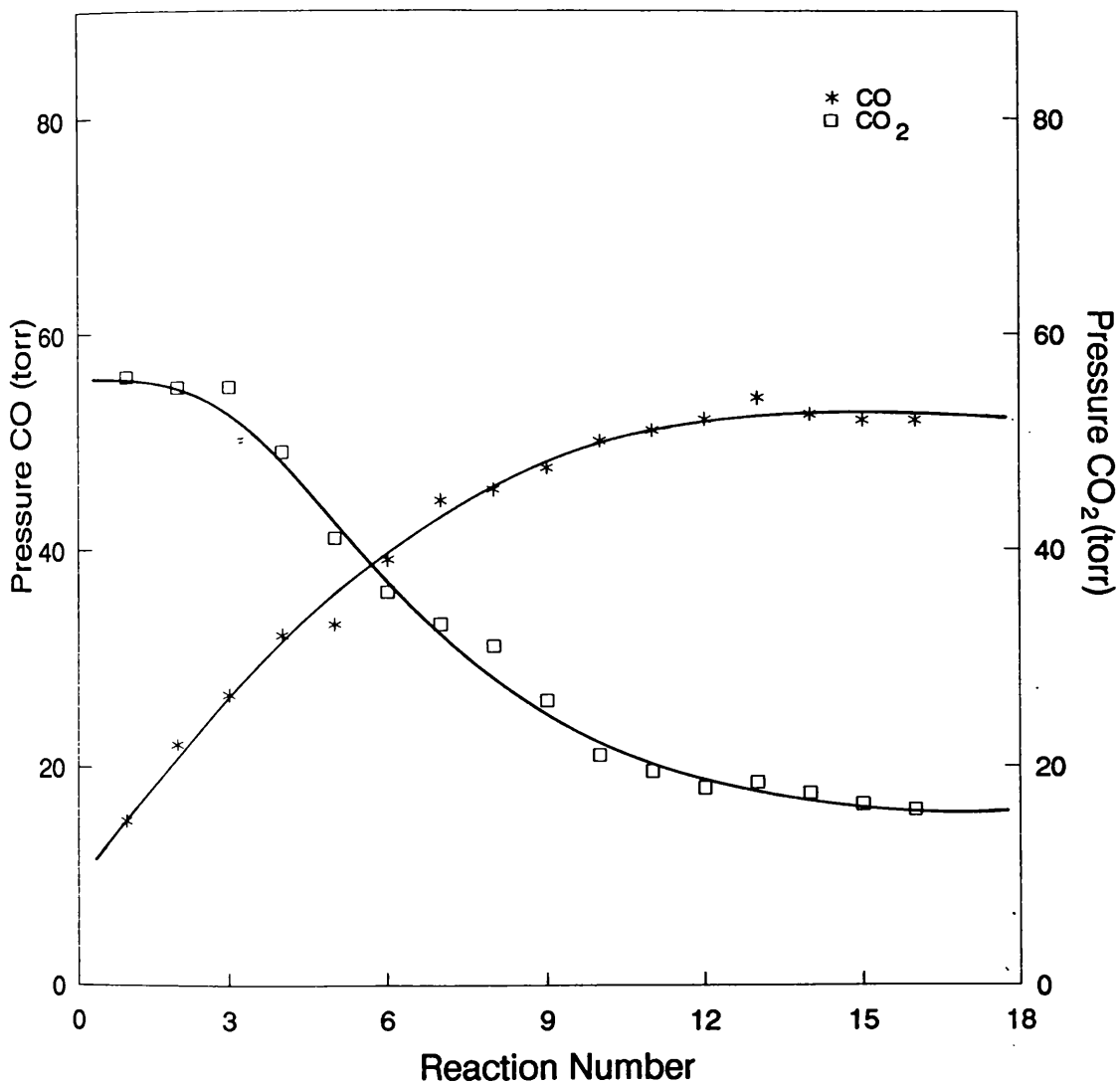


Fig: 4.12

Methanol Decomposition at 250°C on Reduced
Copper - Zinc Oxide/Alumina (0.156g) with
6% Hydrogen in Nitrogen at 250°C
Methanol Pressure 92 Torr

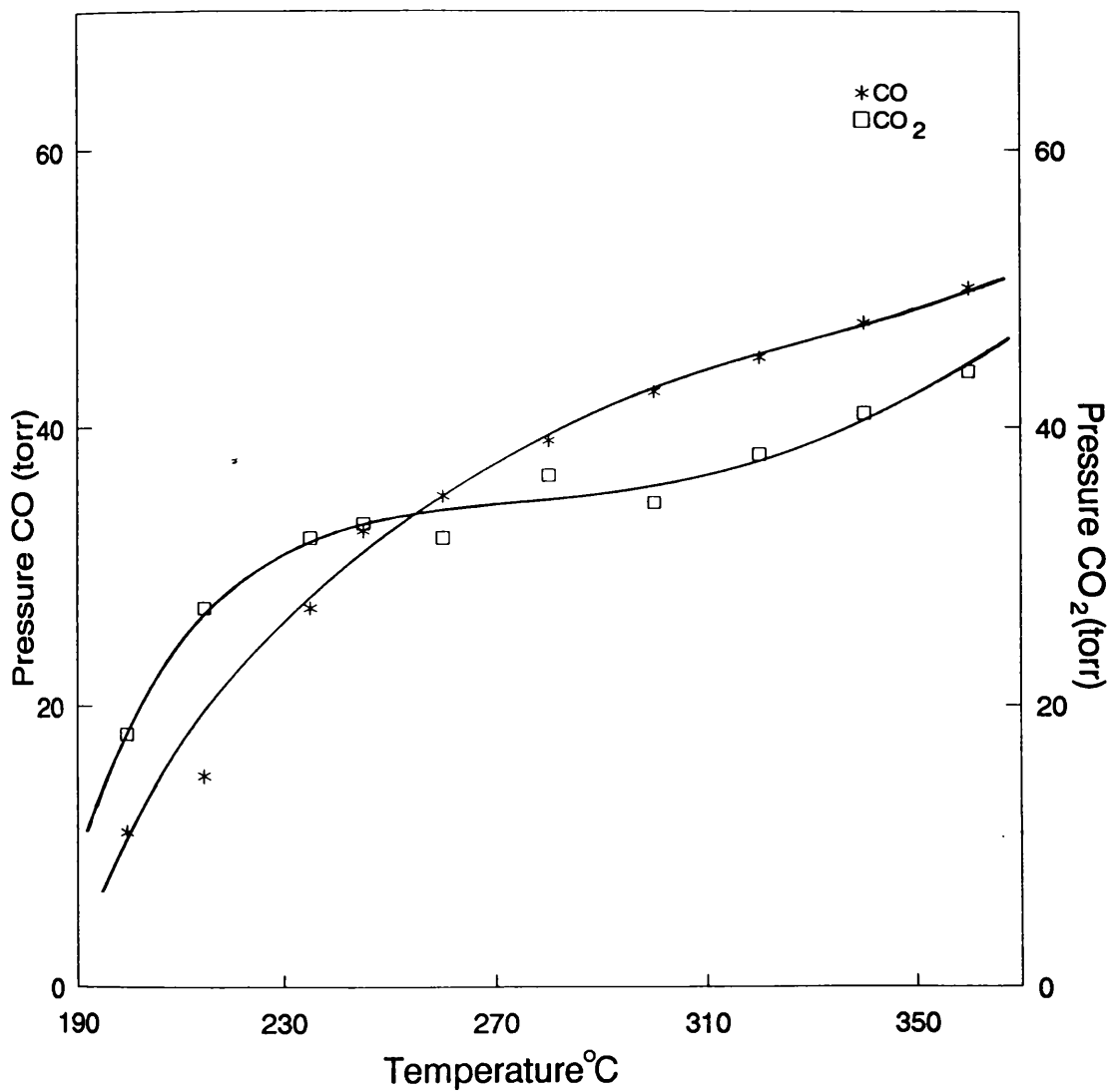


Table 4.3

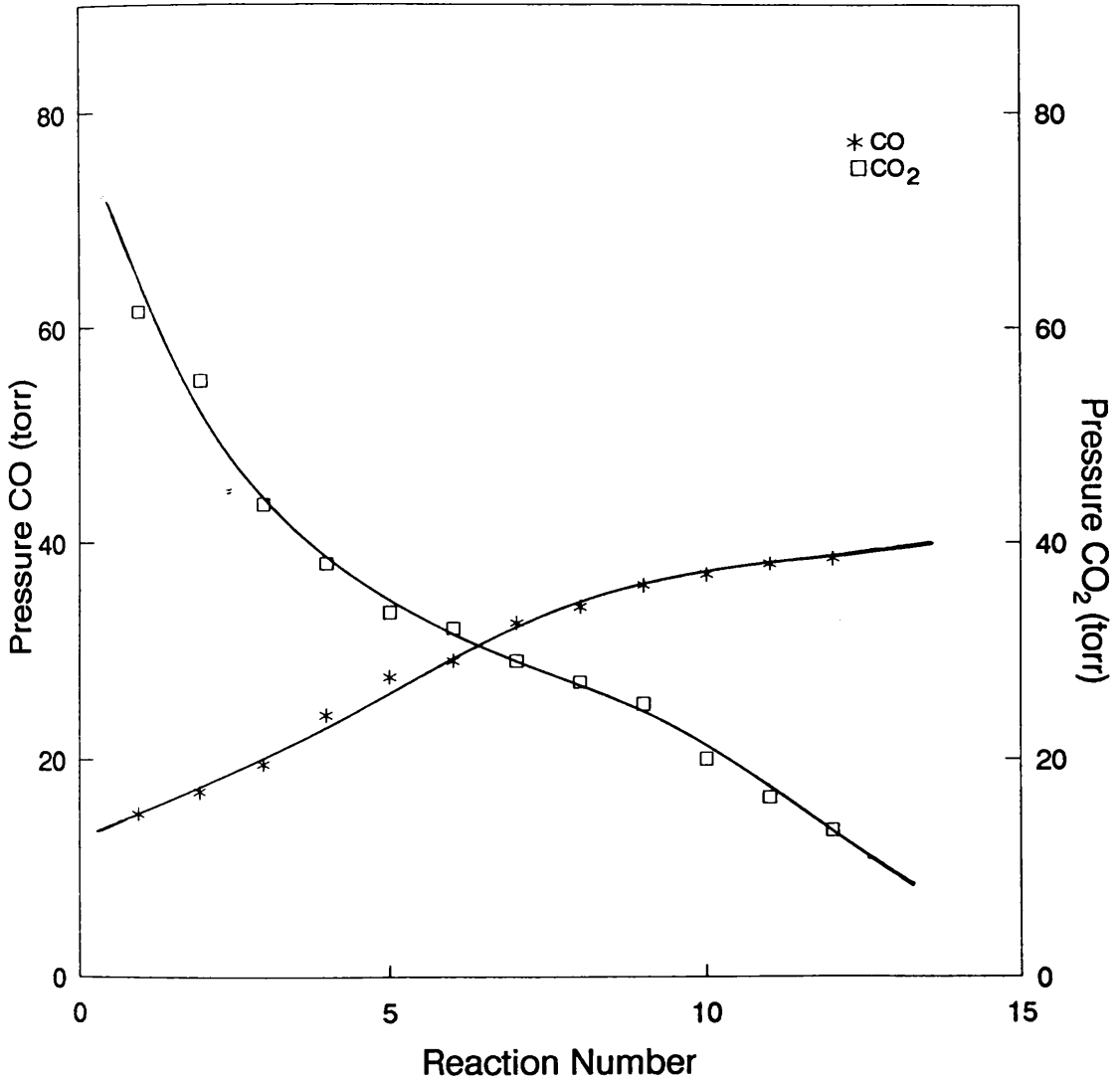
Effect of reaction temperature and methanol initial pressure on the decomposition products distribution on (60% Cu) Cu-ZnO/Al₂O₃ reduced with 6% H₂ in N₂ at 250°C for 14 hours

Methanol initial pressure Torr.	Products pressure Torr.		Reaction temperature °C	Products pressure Torr.	
	CO	CO ₂		CO	CO ₂
24	14	15.5	200	11	18
48	18	17.5	230	27	32
66	35	18	260	35	32
74	38	19	300	42.5	34.5
89	47.5	18	340	47.5	41
97	50	18	380	50	44

In order to investigate the effect of the reduction procedure on the product distribution, a sample of Cu-ZnO/Al₂O₃ catalyst was reduced in 6% hydrogen in nitrogen at 180°C for 14 hours followed by 2 hours reduction at 200°C. This method is used commercially to reduce this catalyst for the methanol synthesis reaction. The results of such a treatment are presented in figure [4.13]. At the initial stages of the reaction (methanol pressure = 100 torr, temperature 300°C) carbon dioxide production was at a

Fig: 4.13

Methanol Decomposition at 300°C on
Reduced Copper - Zinc Oxide/Alumina with
6% Hydrogen in Nitrogen at 180°C Followed
by 2 Hours at 200°C Methanol Pressure 100mm Mercury



maximum with a ratio of CO : CO₂ of 1 : 4.1. As the reaction number increased, the concentration of carbon dioxide decreased while the carbon monoxide concentration increased. The amount of carbon dioxide formed after 12 reactions was approximately 4.5 times lower than that at the beginning of the experiment, while the amount of carbon monoxide produced after the same number of reactions was 2.5 times higher than that during the initial stage of the reaction.

Reducing this catalyst with pure carbon monoxide at 250°C for 14 hours resulted in a much lower concentration of the products of the decomposition of methanol to carbon monoxide and hydrogen, with trace amounts of carbon dioxide, than those produced from hydrogen treated catalyst in terms of carbon balance in both methanol pulse and the number of carbon atoms in the products. These observations are presented in figure [4.14], which shows the increase in carbon monoxide formation as the initial pressure of methanol is increased. Trace amounts of methane were also observed at higher pressures of methanol. Results at different temperatures, obtained over the Cu-ZnO/Al₂O₃ sample reduced only with carbon monoxide, are shown in figure [4.15]. At lower reaction temperatures the carbon monoxide concentration was lower than expected from a methanol pulse pressure of 98 torr.

The amount of carbon monoxide formed increased as the reaction temperature increased, while no change in the trace carbon dioxide formation was observed. At higher

Fig: 4.14

Methanol Decomposition on Reduced Copper - Zinc Oxide/
Alumina Catalyst Sample with CO
at 250°C
Methanol Initial Pressure 98 Torr

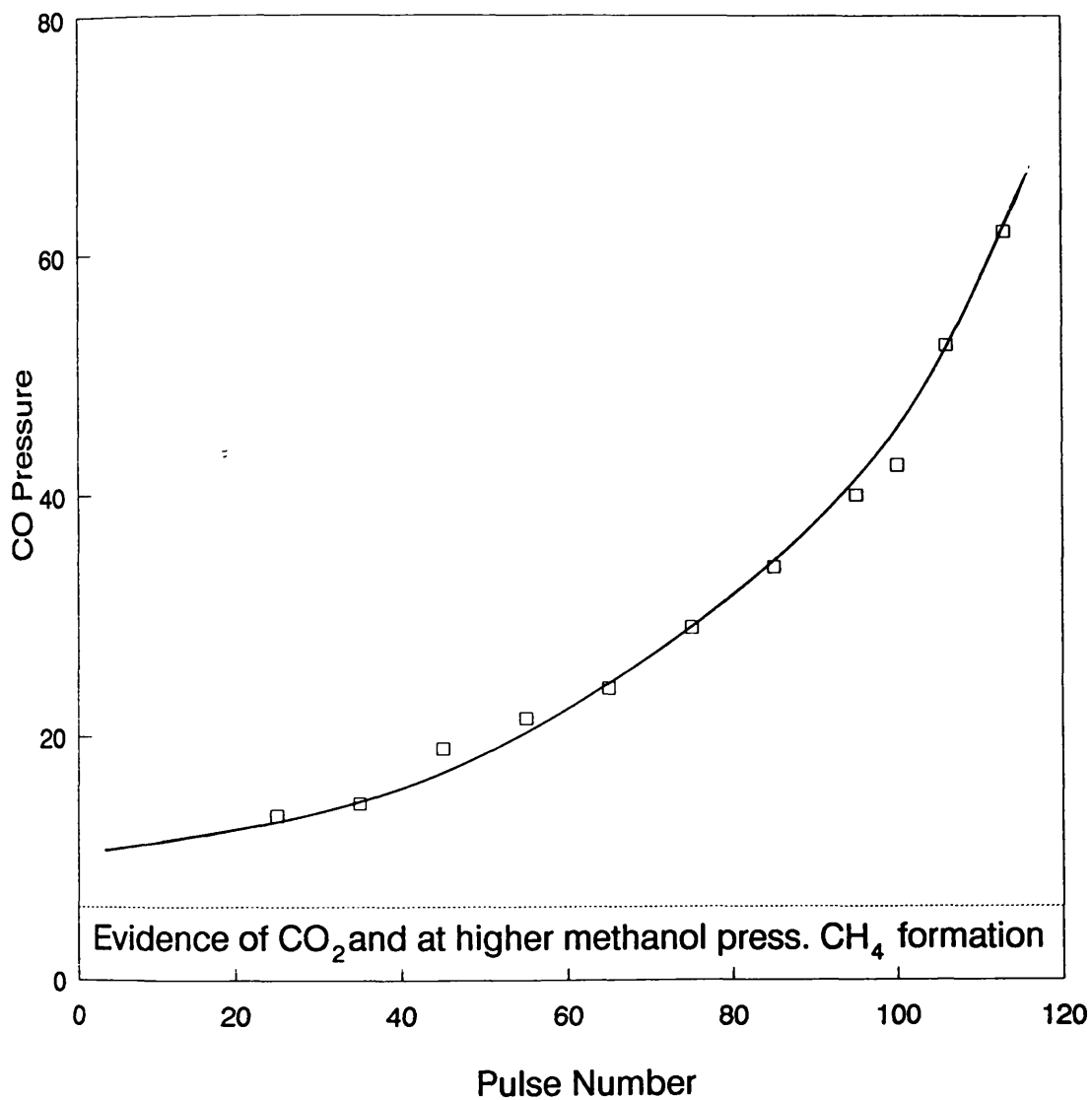
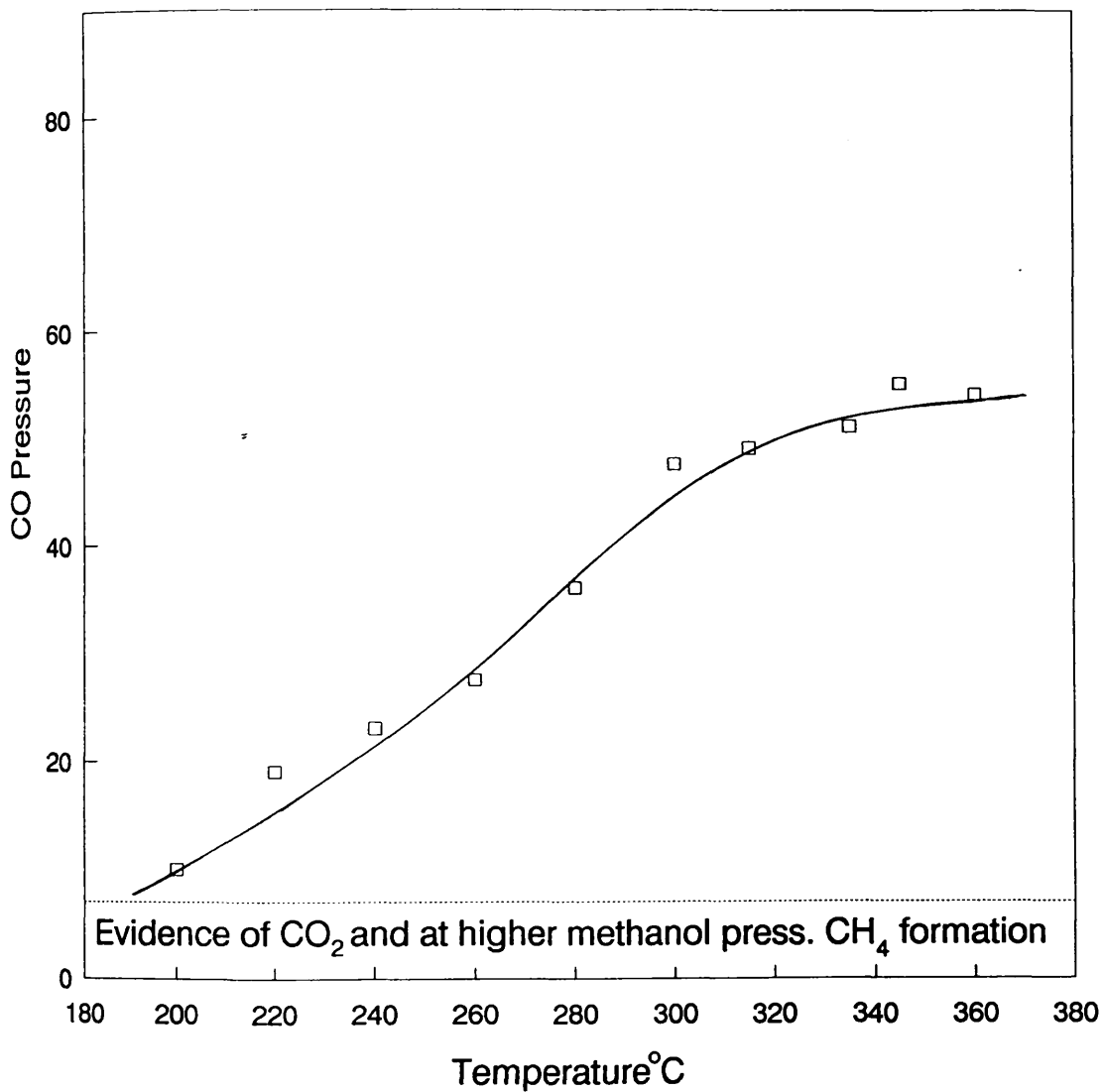


Fig: 4.15

Methanol Decomposition on Reduced Copper - Zinc Oxide/
Alumina Catalyst Sample with CO at 250°C

Methanol Initial Pressure 98 Torr



temperature ($>280^{\circ}\text{C}$) traces of methane were observed.

The effect of variations of the initial pressure of methanol and reaction temperature on the product distribution obtained with Cu-ZnO/Al₂O₃ reduced with carbon monoxide are presented in table 4.4.

Table 4.4

The product distribution on Cu-ZnO/Al₂O₃ reduced with CO only

Methanol initial pressure Torr.	Products pressure Torr.			Reaction temperature $^{\circ}\text{C}$	Products pressure Torr.		
	CO	CO ₂	CH ₄		CO	CO ₂	CH ₄
25	13.5	t	-	200	10	t	t
45	19	t	-	240	23	t	-
65	24	t	-	280	36	t	t
85	34	t	t	300	47.5	t	t
100	42.5	t	t	330	51	t	t
113	62	t	t	360	59	t	t

t = trace amount

4.2.3 Methanol Decomposition on ZnO surface

Reducing a ZnO catalyst sample with 6% hydrogen in nitrogen at 180°C and using the reduced sample for methanol

decomposition, showed that the main decomposition product was carbon dioxide. Interestingly, reducing the catalyst sample with carbon monoxide resulted in a conversion of the oxide to metallic zinc which, in turn, proved to be inactive in the decomposition reaction.

Figure [4.16] depicts the product distribution resulting from the reduction of a zinc oxide sample at 250°C under a stream of 6% hydrogen in nitrogen for 14 hours. Carbon dioxide which is expected to form on oxide surfaces was at a maximum yield at the beginning of the reaction; its concentration decreased with the number of reactions under the same conditions. Carbon monoxide formation increased to reach a ratio of CO₂ : CO of 1 : 8 after 13 reactions. Both carbon monoxide and carbon dioxide yields reached a steady state. However, a change in the colour of the catalyst sample, from grey to dark blue was observed at the top of the catalyst bed indicating a reduction of the oxide to metallic zinc, presumably by reaction with the carbon monoxide formed from methanol. At low methanol pressure (<50 torr), carbon dioxide was also found to be formed in higher concentrations [figure 4.17] which then decreased very slowly to constant value of about 13 torr at a reaction temperature of 360°C. In contrast, the carbon monoxide concentration increased with the increase in the initial pressure of methanol; the CO₂ : CO ratio was 1 : 3.4 at a methanol initial pressure of 110 torr. In this case, the carbon dioxide concentration was at its minimum with negligible changes observed during the

Fig: 4.16

Methanol Decomposition at 360°C on
Reduced Zinc Oxide Sample (0.1g) with
6% Hydrogen in Nitrogen at 250°C
Methanol Initial Pressure 100 Torr

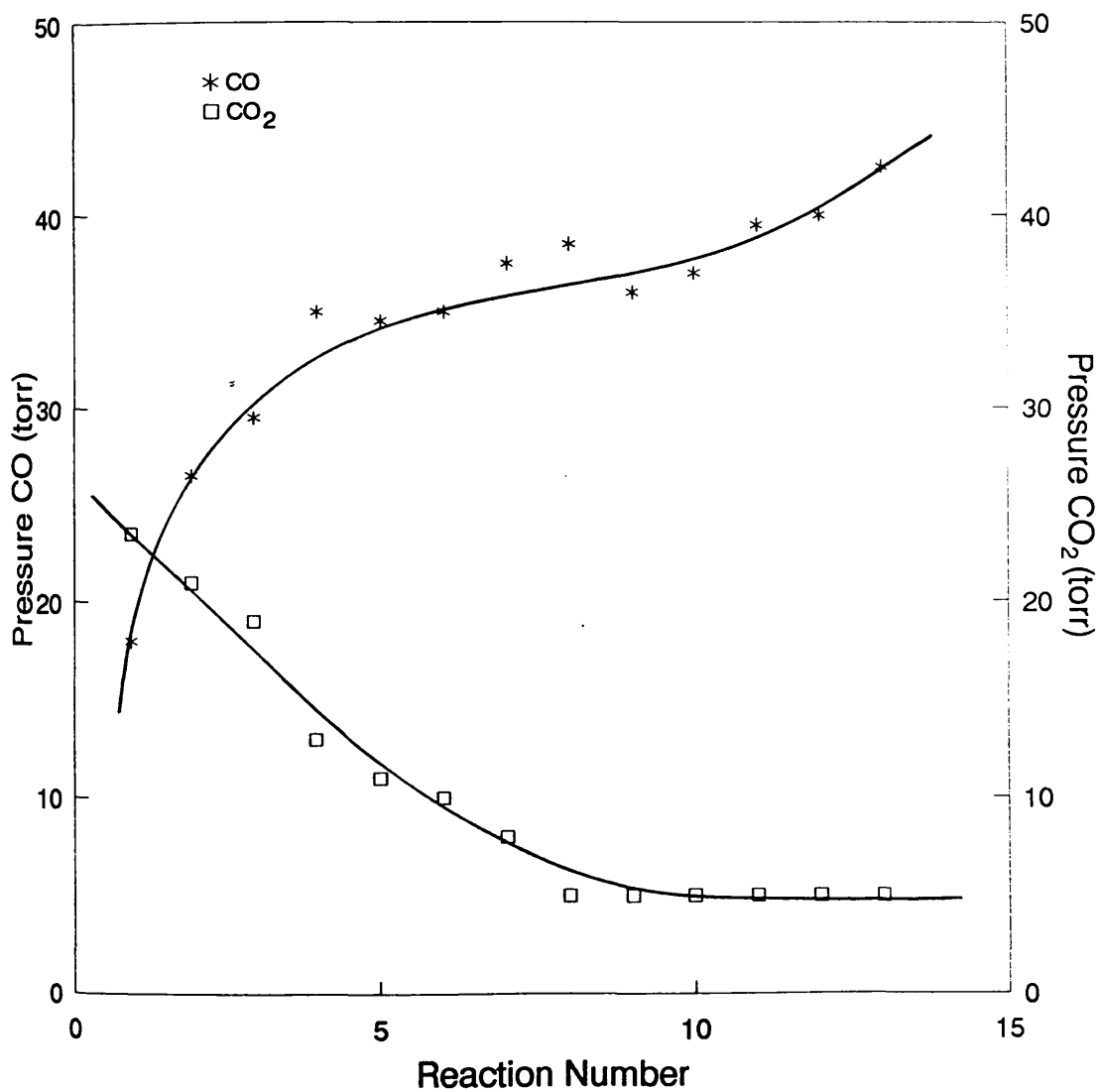
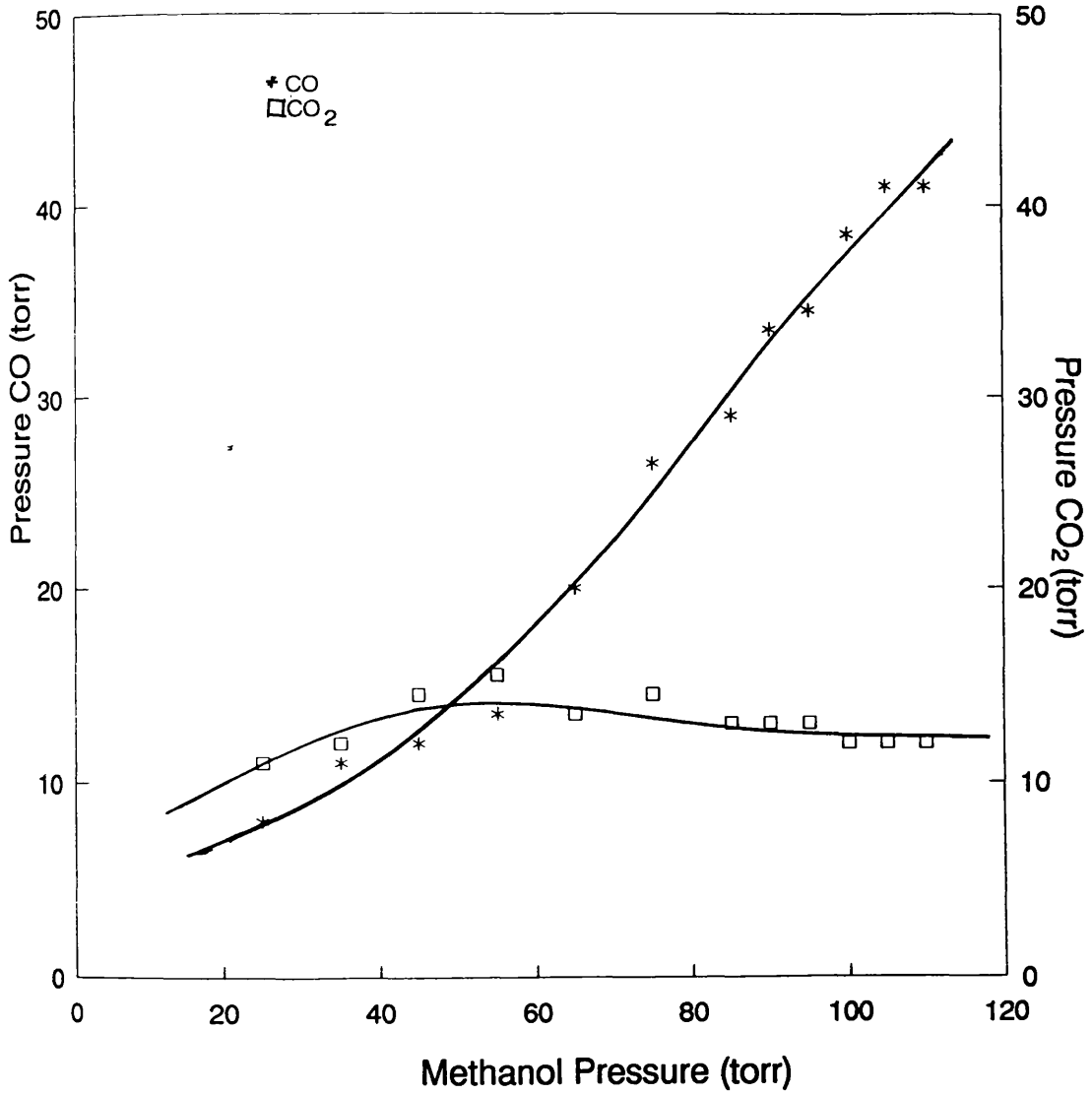


Fig: 4.17

Methanol Decomposition at 360°C on Reduced Zinc Oxide
Sample with 6% Hydrogen in Nitrogen at 250°C



reaction. A change in the catalyst colour at the top of the sample bed was also observed on the conclusion of this reaction.

No significant changes were observed by monitoring the reaction of methanol as a function of reaction temperature. As shown in figure [4.18], carbon dioxide formation was at its highest level at lower reaction temperatures (300-360°C), its concentration increased up to 360°C, above which the yield decreased reaching a steady state value at high temperature (420°C). The carbon monoxide concentration increased and attained a steady state at the same temperature. However, at this temperature small amounts of methane were detected. The formation of these trace amounts of methane occurs at the maximum formation of both carbon monoxide and carbon dioxide. Under these conditions, the change in the catalyst colour was even darker compared with the previous experiment.

The products distributions as a function of both methanol initial pressure and the reaction temperature are presented in table 4.5. It can be observed that carbon monoxide reached its maximum value at 380°C and pressure of 92 torr; carbon monoxide value corresponds to the increase carbon monoxide concentration shown in figure [4.17].

Fig: 4.18

Methanol Decomposition on Reduced Zinc Oxide
Sample with 6% Hydrogen in Nitrogen at 250°C

Methanol Initial Pressure 92 torr

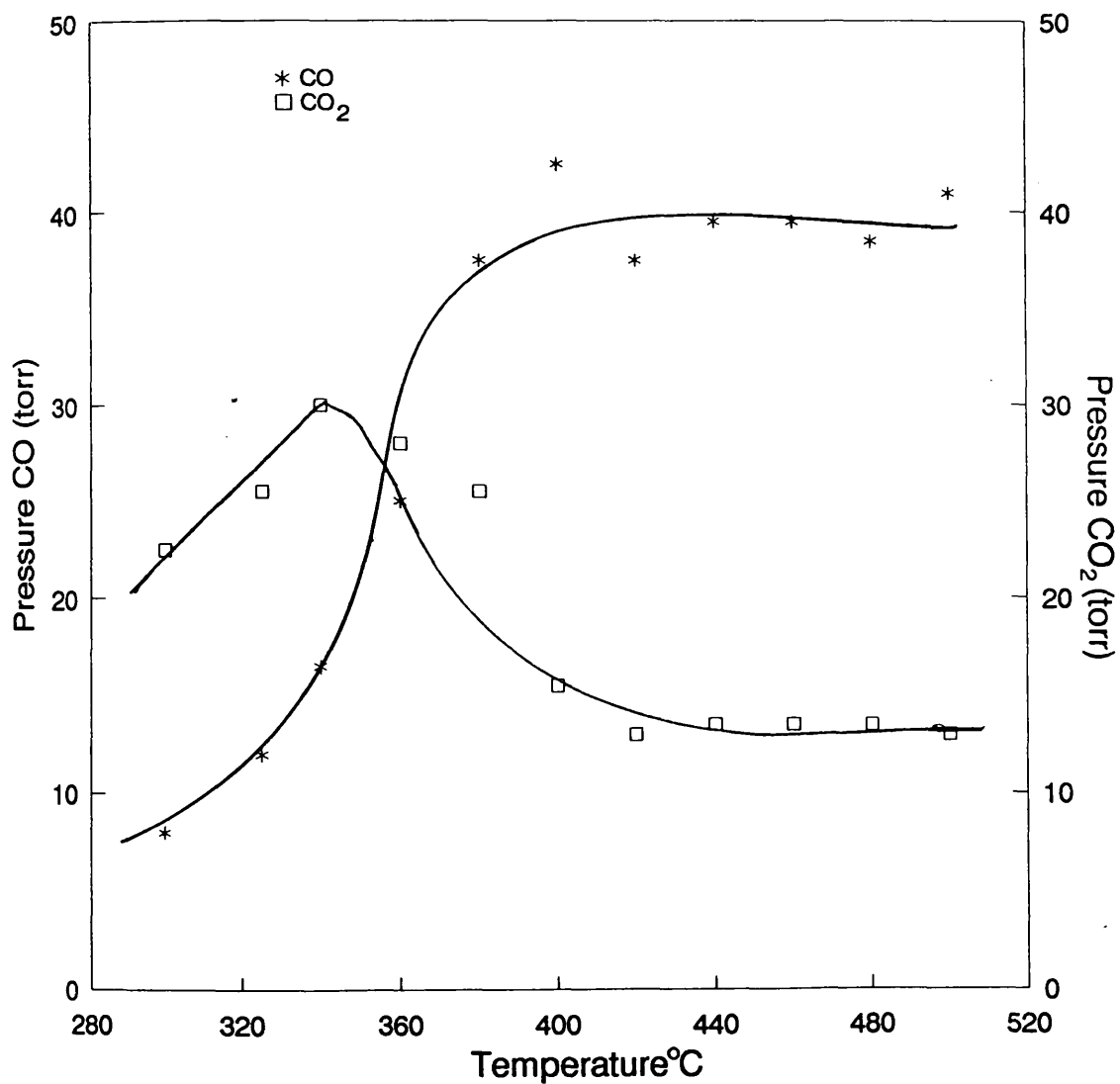


Table 4.5

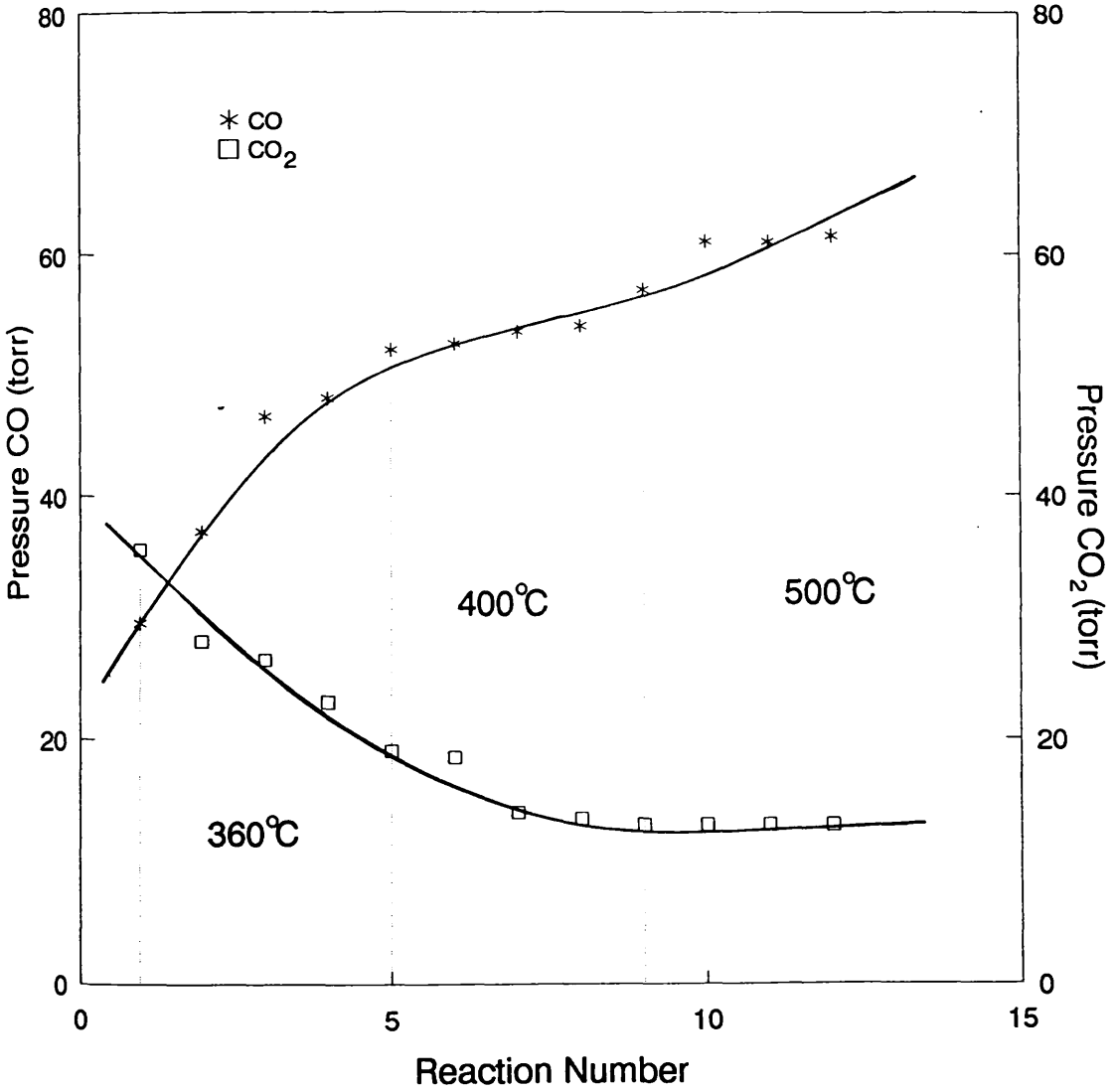
products distribution during methanol decomposition on ZnO catalyst

Methanol initial pressure Torr.	Products pressure Torr.		Reaction temperature °C	Products pressure Torr.	
	CO	CO ₂		CO	CO ₂
25	8	11	300	8	22.5
45	12	14.5	340	16.5	30
65	20	13.5	380	37.5	25.5
85	29	13	440	39.5	13.5
95	43.5	13	480	38.5	13.5
110	41	12	500	41	13

Figure [4.19] demonstrates that the same conclusions are reached by studying the decomposition reaction as a function of temperature, and following the change in the product distributions with the number of methanol pulses introduced to the catalyst bed at a given temperature. In this case, amounts of methane are also observed at high temperatures. In a similar way, the concentration of carbon monoxide increased with the increase of the reaction temperature and reaction number; at higher temperature and reaction number, the formation of carbon monoxide reached its steady state. Carbon dioxide formation was suppressed and reached its steady state at higher temperatures. The ratio at this point is CO₂ : CO ; 1 : 4.6. Higher temperature (>500°C) reactions produced a severe colour

Fig: 4.19

Methanol Decomposition on Reduced Zinc Oxide
Sample with 6% Hydrogen in Nitrogen at 250°C
Methanol Initial Pressure 92 Torr



change in the catalyst indicating the presence of metallic zinc which was not active for the decomposition reaction.

4.2.4. Methanol Decomposition on Al_2O_3 Surface

It was also decided to study the role of the alumina support in promoting methanol decomposition.

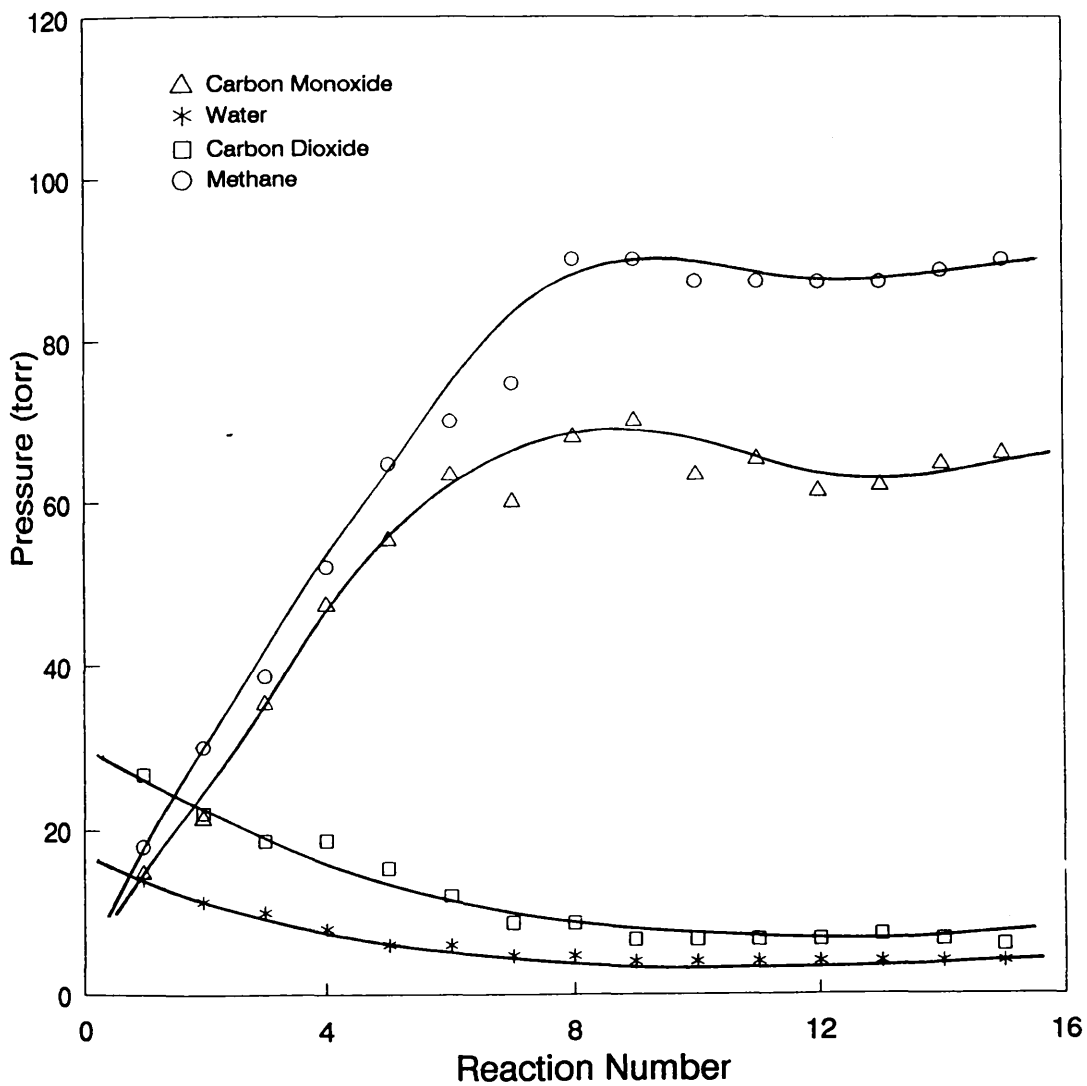
A high surface area ($>80 \text{ m}^2/\text{g}$, 0.15 g) alumina sample was treated in 6% hydrogen in nitrogen at 250°C for 14 hours. The freshly treated sample was inactive towards methanol decomposition at temperatures $<200^\circ\text{C}$; only traces of carbon monoxide and water were observed.

At higher temperatures ($>200^\circ\text{C}$), the amounts of carbon monoxide and water produced increased and traces of carbon dioxide were detected. At more elevated temperature ($>400^\circ\text{C}$) methanol was converted over the alumina surface producing methane, carbon monoxide, carbon dioxide and water.

Carbon monoxide and methane production increased with repeated reactions, whereas the carbon dioxide and water decreased in concentration. A steady state conversion was observed for all four products after ca. 11 reactions. Figure [4.20] shows the concentration changes with reaction number.

Fig: 4.20

Methanol Decomposition on Reduced
Alumina Sample (0.1g) with 6% Hydrogen in
Nitrogen at 250°C Reaction Temperature 450°C
Methanol Initial Pressure 110 Torr



4.3 METHANOL DECOMPOSITION ON H₂S POISONED SURFACES

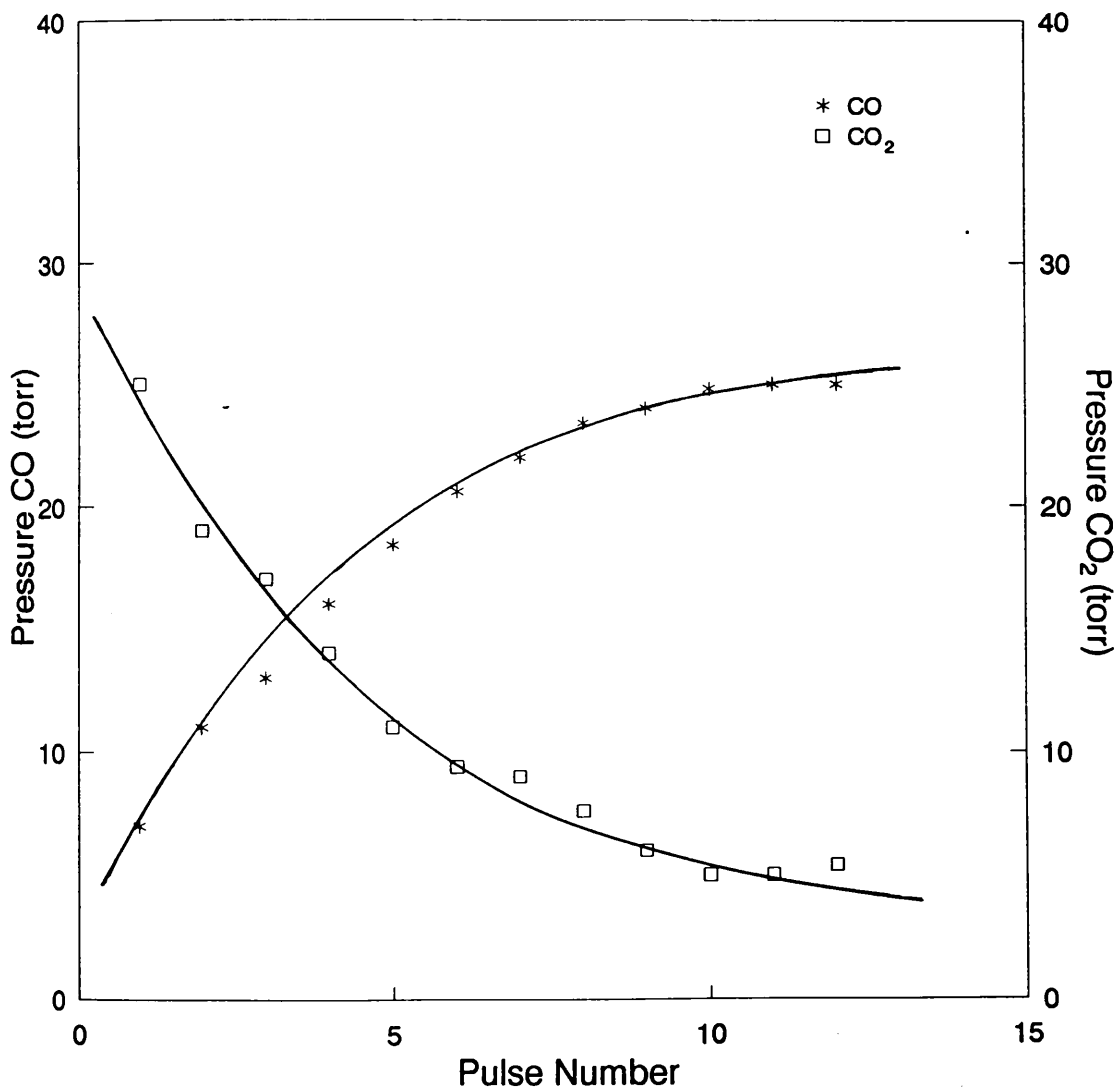
In this section the effect of hydrogen sulphide poisoning on the interaction of methanol with freshly reduced surfaces is considered. The catalyst surfaces were reduced as usual in 6% hydrogen in nitrogen. Hydrogen sulphide and methanol pulses were introduced in a controlled manner.

4.3.1 Effect of H₂S Poisoning on the Catalytic Decomposition of Methanol on a Cu/Al₂O₃ Surface

The Cu/Al₂O₃ sample (0.15 g) was reduced in 6% hydrogen in nitrogen (25 ml/min) at 250°C overnight. On completion of reduction, a measured pulse of hydrogen sulphide (100 torr) was introduced to the catalyst surface at the reaction temperature (250°C). The decomposition reaction of methanol was then followed by introducing measured pulses of methanol (95 torr). Figure [4.21] shows a typical plot of methanol conversion versus pulse number for the reaction over the H₂S poisoned Cu/Al₂O₃ sample. It is very clear that hydrogen sulphide lowers the overall catalyst activity. Whereas, a dramatic fall in the catalyst activity was clearly observed, no change in the catalyst selectivity was noticeable. Nevertheless, the yield of both carbon dioxide and carbon monoxide were markedly suppressed compared with the activity of the clean surface. Traces of water were detected at the beginning of the reaction. In

Fig: 4.21

Methanol Decomposition at 250°C on Reduced
Copper/Alumina Sample then Poisoned with
Hydrogen Sulphide 12%



addition, a small amount of methane was formed after several reactions and undecomposed or unreacted methanol was also observed after a number of reaction cycles. The relationship between the amounts of carbon dioxide and carbon monoxide formed was identical to that observed for unpoisoned Cu/Al₂O₃ surface.

Initially, carbon dioxide was formed at higher concentrations which eventually were lowered to a steady state as the reaction number increased, while carbon monoxide concentration increased and also reached a steady state. It is obvious from figure [4.21] (when compared with figure 4.2) that pretreatment of Cu/Al₂O₃ with H₂S inhibits methanol decomposition. After ten reactions, the relative concentrations of the products were in the ratio of CO₂ : CO of 1 : 4.5.

Increasing the amount of poison on the surface suppressed the catalyst activity of Cu/Al₂O₃ towards methanol decomposition to a greater extent. Figure [4.22] illustrates that there was a linear decrease in the production of carbon monoxide and carbon dioxide with increasing adsorption of H₂S. It should be noted that the data shown in figure [4.22] were taken after ten pulses of methanol had been introduced so as to allow the catalyst to reach a steady state. From figure [4.22], a 0.15 surface coverage of sulphur lowers the catalytic activity to ca 46%. Table 4.6 also serves to illustrate the effect of various uptakes of sulphur on the relative amounts of carbon monoxide and carbon dioxide produced.

Fig: 4.22

The Amounts of Carbon Monoxide, Carbon Dioxide and Hydrogen formed in the Decomposition of Methanol at 250°C on Copper/Alumina poisoned with varying Amounts of Adsorbed Sulphur at 250°C

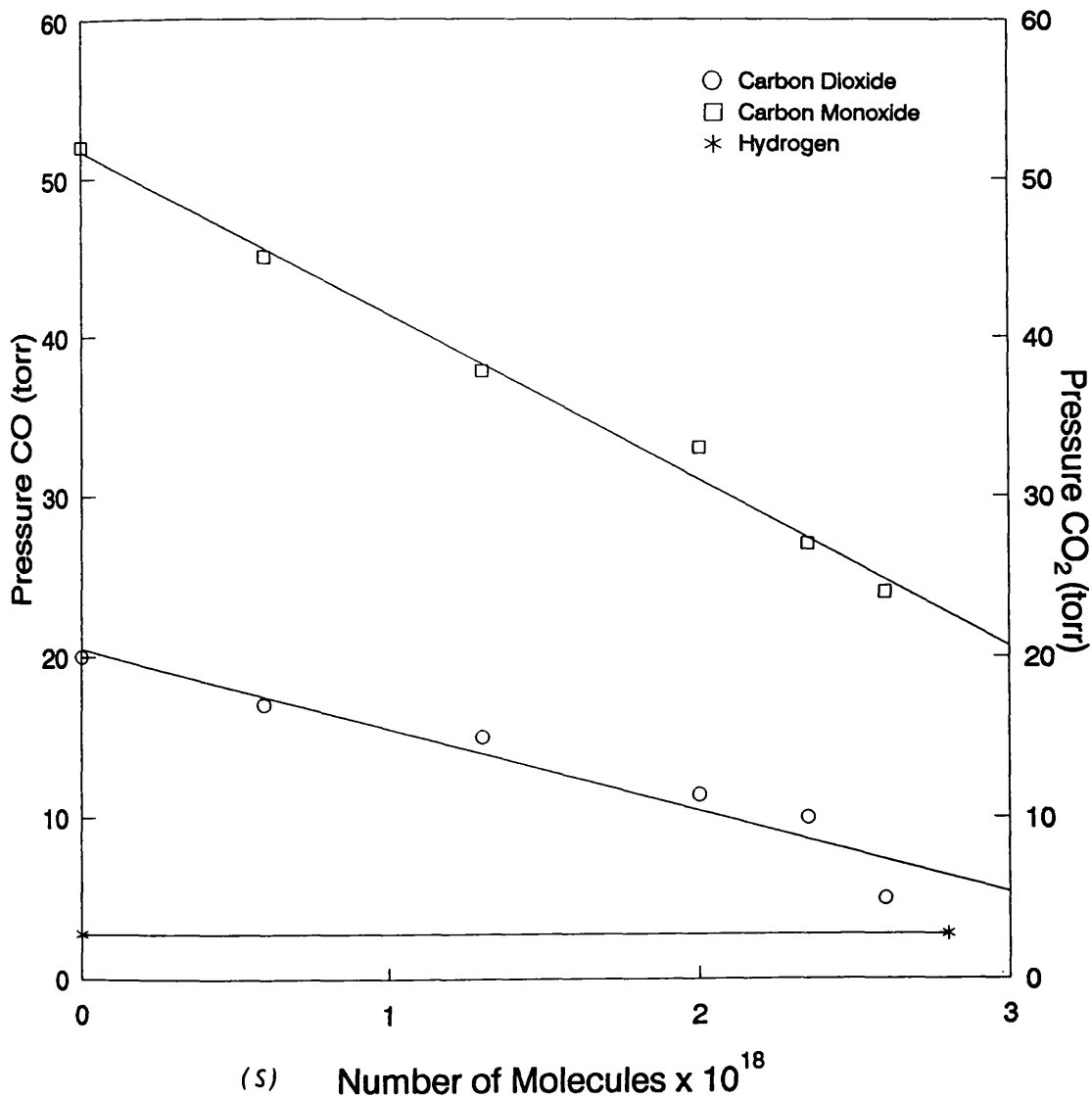


Table 4.6

Effect of various amounts of adsorbed sulphur on the relative amounts of carbon monoxide and carbon dioxide formed during methanol decomposition on Cu/Al₂O₃ at 250°C and methanol initial pressure of 95 torr.

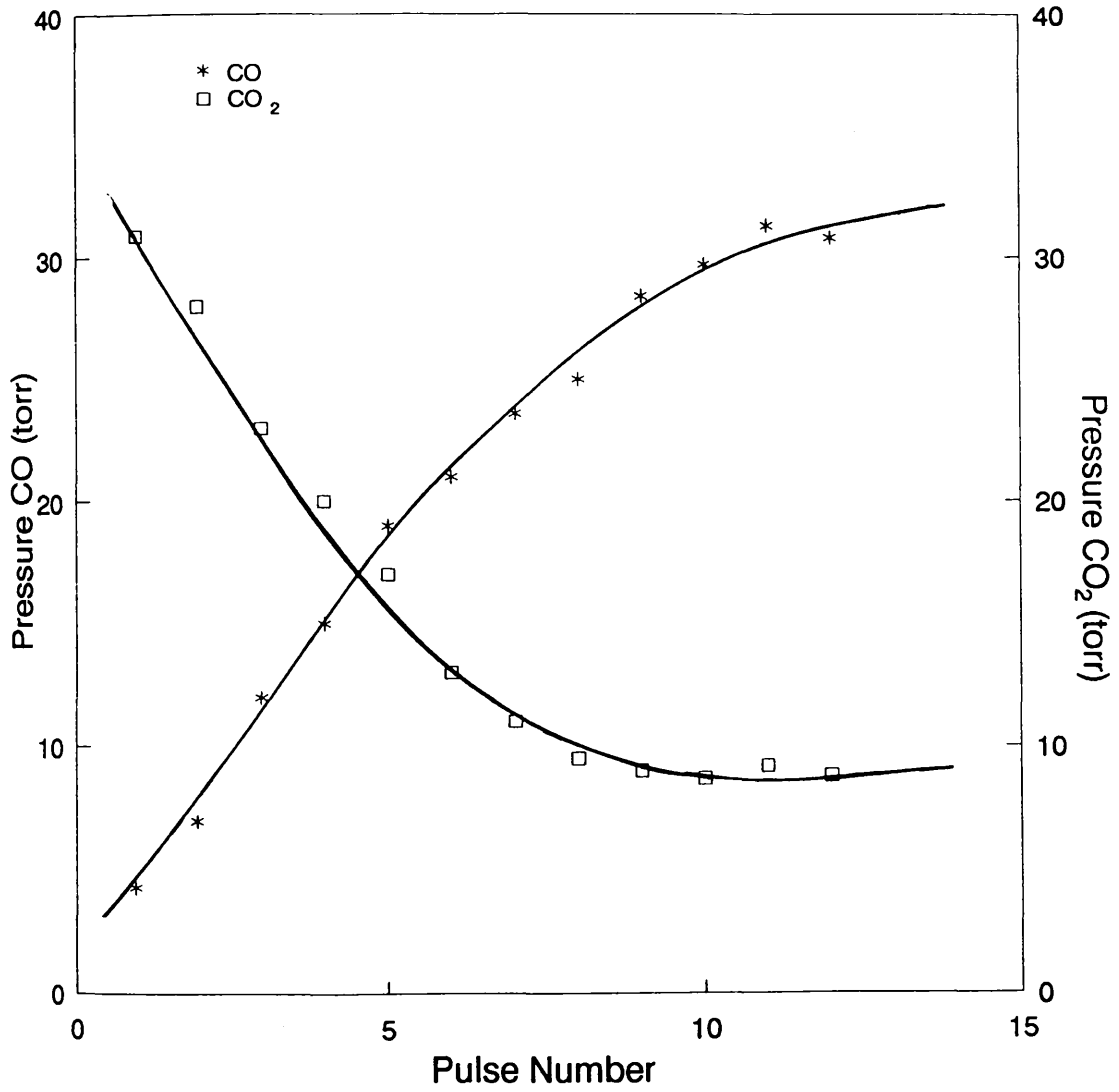
No. of adsorbed sulphur atom X10 ¹⁸	Products pressure Torr.	
	CO	CO ₂
0	52	20
0.66	45	17
1.33	37.8	15
2.33	27	10
2.66	24	5

4.3.2. Effect of Hydrogen Sulphide Poisoning on Methanol Decomposition on Cu-ZnO/Al₂O₃

A sample of Cu-ZnO/Al₂O₃ was exposed to the amounts of hydrogen sulphide corresponding to a $\theta_s = 0.15$, after it had been reduced in 6% hydrogen in nitrogen for 14 hours at 250°C. Figure [4.23] shows that the catalyst activity, in terms of the product distributions, was greatly affected by adsorbed sulphur; at the initial stage of the reaction, both carbon dioxide and carbon monoxide were produced in smaller amounts than those formed on clean surface [see figure 4.11]. For the unpoisoned surface the CO : CO₂ ratio was 1 : 3.6, as also found in the decomposition on poisoned

Fig: 4.23

Methanol Decomposition at 250°C on
Hydrogen Sulphide poisoned Copper -
Zinc Oxide/Alumina Sample



Cu-ZnO/Al₂O₃ catalyst sample.

The concentration of both gases formed varied empirically in the same way as with the clean surface; the carbon dioxide concentration decreased with time to reach a steady state, while carbon monoxide concentration increased with time eventually reaching a steady state value. After ten reactions the CO : CO₂ ratio was 1 : 0.31, which is equal to that for unpoisoned surface. Both the ratio in the initial stages of the experiment and at the steady state are indicative of the inhibiting influence of H₂S adsorption on methanol decomposition.

In figure [4.24] the effect of various amounts of preadsorbed sulphur on the catalytic activity of Cu-ZnO/Al₂O₃ are presented. The figure clearly depicts a decrease in the amounts of both carbon monoxide and carbon dioxide formed on the surface when poisoned with different amounts of hydrogen sulphide.

Each point in figure [4.24] was obtained from a separate experiment conducted to measure the effect of a fixed amount of preadsorbed sulphur on the steady state catalyst activity (after ten reactions). The catalytic activity decreased as the amount of preadsorbed sulphur increased; at a surface coverage of about 0.15, the activity fell to about 20%. The effect of various amounts of preadsorbed sulphur on the relative amounts of carbon monoxide and carbon dioxide formed, are given in table 4.7.

Fig: 4.24

The amounts of Carbon Dioxide, Carbon Dioxide and Hydrogen formed in the Decomposition of Methanol ay 250°C on Copper - Zinc Oxide/Alumina poisoned with varying amounts of adsorbed Sulphur

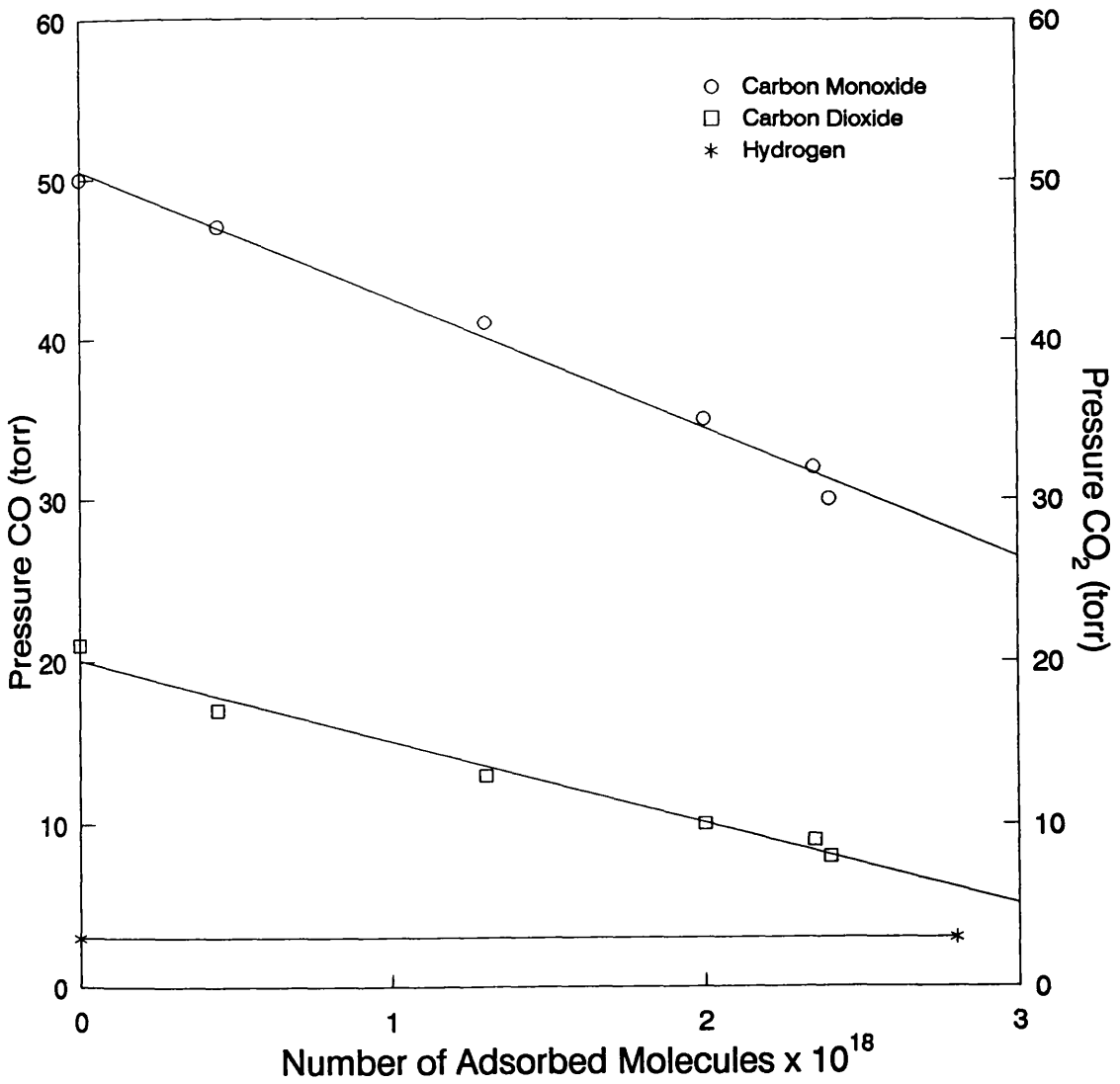


Table 4.7

Effect of various amounts of preadsorbed sulphur on the products distribution of methanol decomposition on Cu-ZnO/Al₂O₃ at 250°C

No. of adsorbed sulphur atom X 10 ¹⁸	Products pressure Torr.	
	CO	CO ₂
0	50	21
0.66	47	17
1.33	41	13
2.33	32	9
2.66	30	8

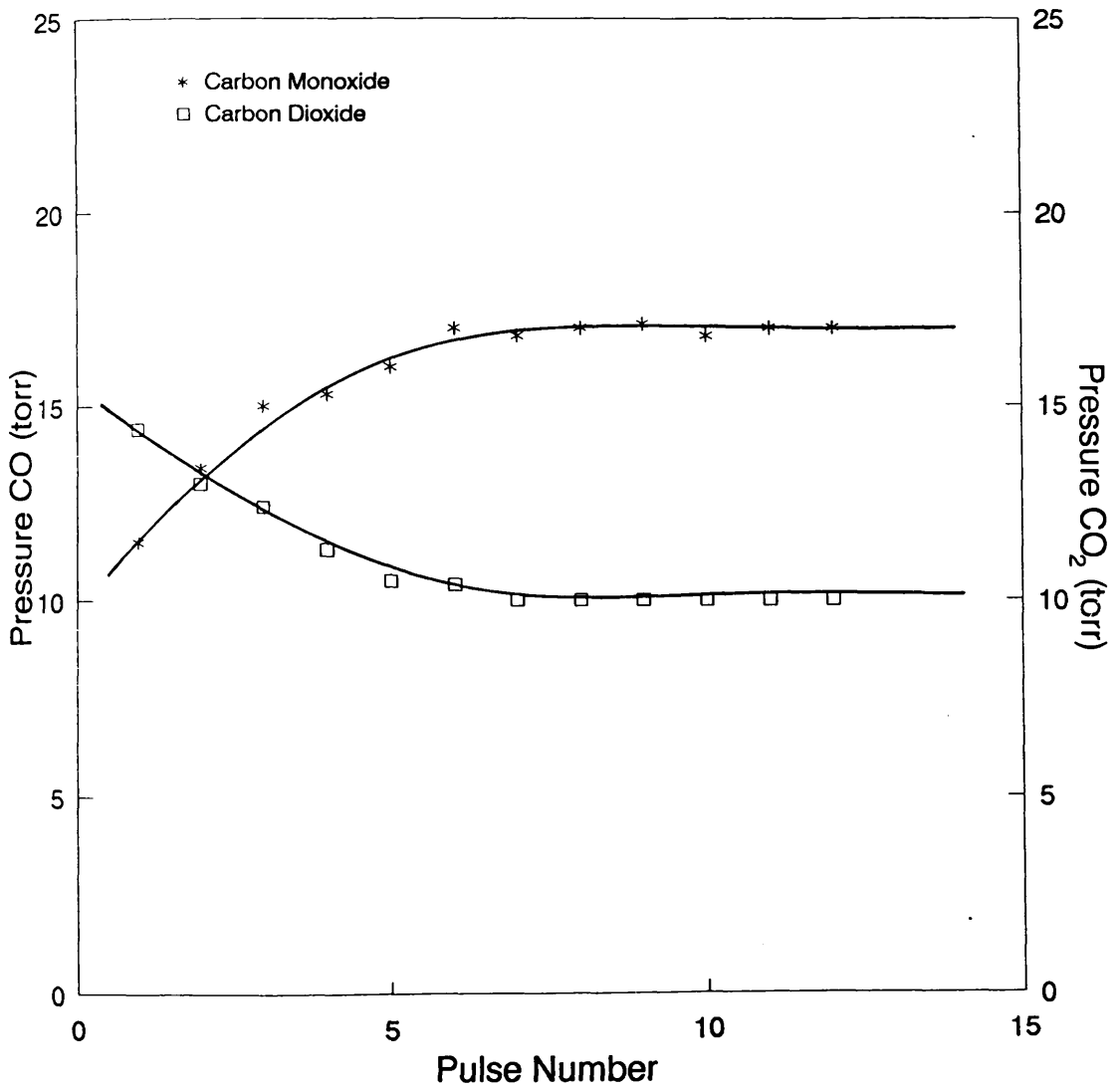
4.3.3 Methanol Decomposition on ZnO Surface Poisoned With Hydrogen Sulphide

In this experiment, a sample of ZnO (0.15 g), pretreated under the usual conditions, was exposed to hydrogen sulphide (four pulses, 100 torr each) and used to catalyse methanol decomposition.

Figure [4.25] shows the decrease in the concentration of carbon monoxide and carbon dioxide produced. It is clear that methanol decomposed mainly to carbon monoxide, the concentration of which increased with time. This increase

Fig: 4.25

Methanol Decomposition at 360°C on Zinc Oxide
Sample Poisoned with Hydrogen Sulphide



also eventually resulted in the attainment of a steady state conversion; the situation is reversed in the case of carbon dioxide formation, but, a steady state was also reached.

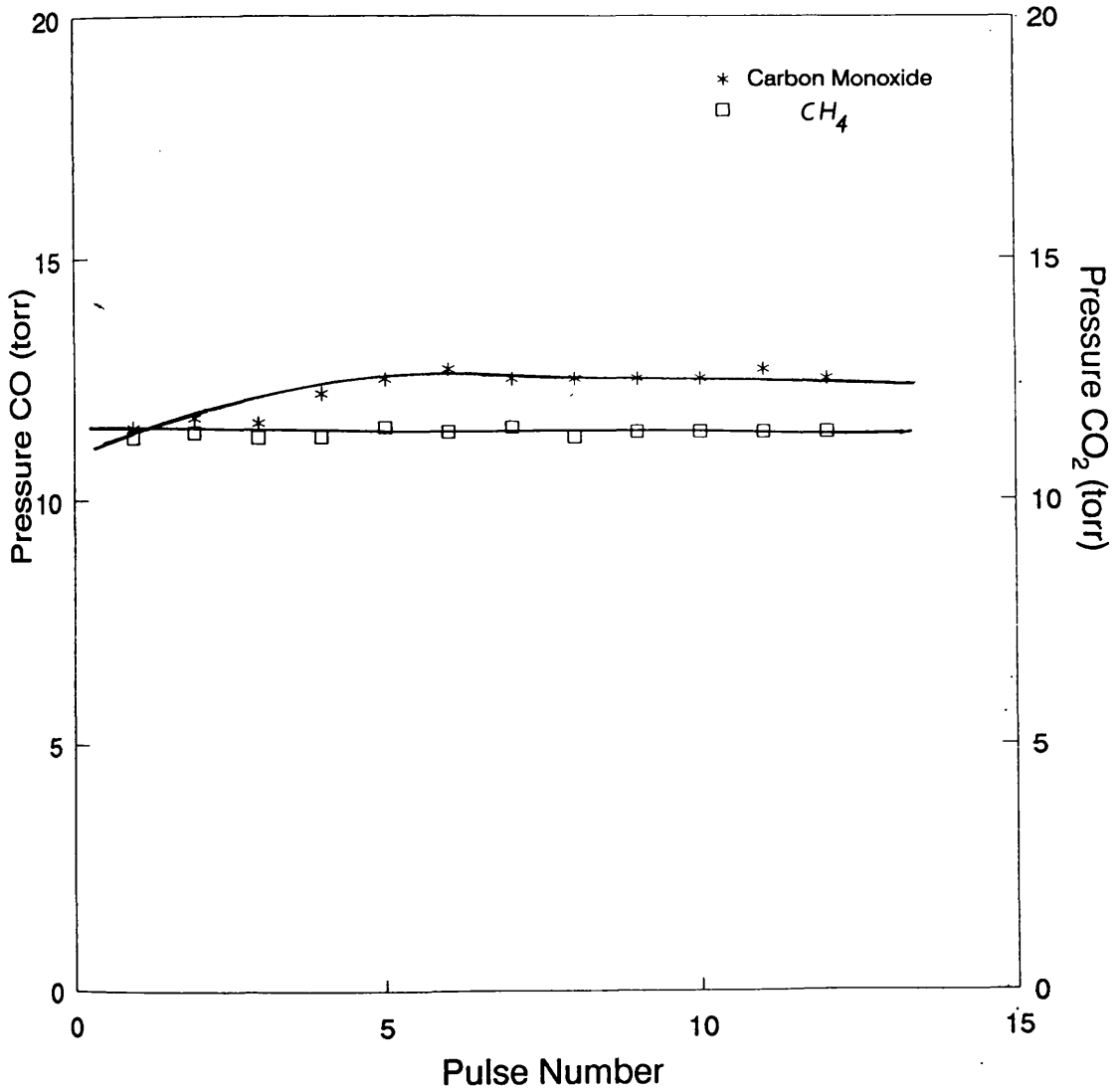
The ratio of CO_2 : CO at this steady state was found to be 1 : 1.7 compared with unpoisoned surface ratio of 1 : 8. Thus, as in the case of the previously studied copper supported catalysts, the extent of methanol decomposition is inhibited by H_2S adsorption. However, during the adsorption of sulphur on the hydrogen treated oxide surface, a peak was detected in the chromatograph which was assigned to water and must be due to the interaction of hydrogen sulphide with zinc oxide forming zinc sulphide and water. No hydrogen sulphide was detected by the chromatograph which is indicative of the complete adsorption or reaction of hydrogen sulphide on zinc oxide.

4.3.4 The Decomposition of Methanol on Al_2O_3 Surface Poisoned with Hydrogen Sulphide

A substantial decrease in alumina activity for methanol decomposition was observed on a surface poisoned with hydrogen sulphide (2 pulses, 100 torr each) at 450°C . Figure [4.26] clearly illustrates that methanol was mainly decomposed to carbon monoxide and methane; no water or carbon dioxide were detected. It can also be seen that the concentration of both carbon monoxide and methane were stable, with no appreciable change in their concentration

Fig: 4.26

Methanol Decomposition at 450°C on Alumina
Sample Poisoned with Hydrogen Sulphide



as the number of pulses increased. Furthermore, the carbon monoxide concentration was slightly higher than that of methane over the range of pulses. In any case, the poisoned surface exhibited much lower conversions relative to the unpoisoned samples. The amount of methane produced on the poisoned surface was about seven times less than that formed on a clean surface, while the carbon monoxide yield was reduced to ca. one-fifth on the poisoned alumina surface.

Hydrogen sulphide was found to have an overwhelming effect on the catalytic activity of copper-based catalyst, the relevant experimental catalytic data for the range of samples studied are summarised in table 4.8.

Table 4.8

products distribution of methanol decomposition on Cu/Al₂O₃ and Cu-ZnO/Al₂O₃ at 250°C, ZnO at 360°C and Al₂O₃ at 450°C. Catalysts surfaces are reduced in 6% H₂ at 250°C, and on H₂S poisoned samples

Catalysts	Products on clean surfaces (torr) ^a			Products on poisoned surfaces (torr) ^a		
	CO	CO ₂	CH ₄	CO	CO ₂	CH ₄
Cu/Al ₂ O ₃	52	18	-	24	5	t
Cu-ZnO/Al ₂ O ₃	50	21	t	30	8	-
ZnO	37	5	t	17	10	t
Al ₂ O ₃	63	9.2	83	12.5	-	11.3

a = Trace of hydrogen formed in all experiments

t = trace

CHAPTER FIVE

THE ADSORPTION OF CARBON MONOXIDE AND CARBON DIOXIDE ON CLEAN AND POISONED COPPER-BASED CATALYST SURFACES

5.1 CARBON MONOXIDE ADSORPTION ON CLEAN AND POISONED COPPER-BASED CATALYSTS

The adsorption/desorption of both carbon (^{14}C -) labelled and unlabelled carbon monoxide on copper-based catalysts was studied.

In this section the results obtained during the adsorption study on both clean and hydrogen sulphide poisoned surfaces will be presented. It should be noticed that the number of adsorbed/desorbed molecules of carbon monoxide are calculated per g of catalyst, while in the relevant figures this is presented as molecules per catalyst sample used in the experiments.

5.1.1 The Adsorption of Carbon Monoxide on Clean and Poisoned $\text{Cu}/\text{Al}_2\text{O}_3$ Surfaces

Adsorption isotherms of ^{14}C -labelled and unlabelled carbon monoxide on freshly reduced and poisoned $\text{Cu}/\text{Al}_2\text{O}_3$ surfaces were studied at room and higher temperatures, using an Isoflo flow scintillation counter to measure the

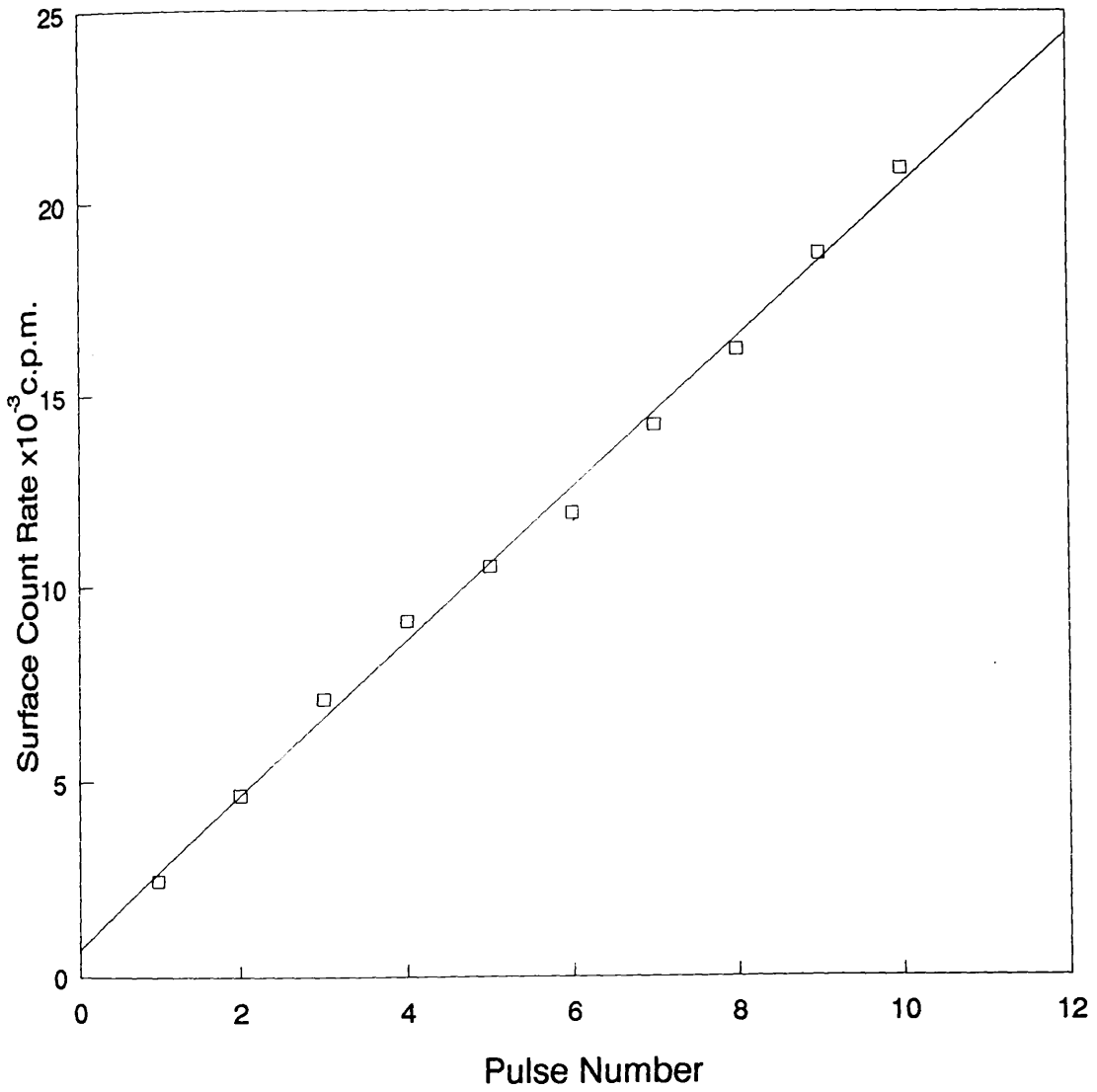
labelled carbon monoxide activity, and gas chromatography to determine the pressure of the carbon monoxide gas in the reactor eluant. ^{14}C -carbon monoxide adsorption was studied by admitting successive pulses of the gas to the reaction vessel. In the case of ^{14}C -carbon monoxide adsorption, the eluant gas phase activity was monitored by the scintillation counter and hence the amount of activity left on the surface could be deduced. Figure [5.1] plots the variation in the surface activity at 250°C as a function of the number of pulses.

The ^{14}C -carbon monoxide adsorption isotherm thus obtained [figure 5.1] exhibits a rapid rise in surface activity as the number of admitted pulses are increased. However, no plateau region was observed. Rather, the plot continues to increase linearly over the range of pulses. Gas phase analysis revealed the presence of only carbon dioxide from each of the ten pulses. This suggests the occurrence of a reaction between carbon monoxide and surface oxygen left on the surface following the reduction with 6% hydrogen in nitrogen (25 ml/min) at 250°C for 14 hours. However, if the amount of ^{14}C -carbon monoxide was increased by admitting more pulses, the gas phase analysis showed the presence of both ^{14}C -carbon dioxide and ^{14}C -carbon monoxide. This behaviour for carbon monoxide interaction with copper surfaces is similar to that found during methanol decomposition (chapter four).

Room temperature adsorption of unlabelled carbon

Fig: 5.1

^{14}C -Carbon Monoxide Adsorption on
Copper/Alumina (0.1g) Reduced with
6% Hydrogen in Nitrogen at 250°C



monoxide on a freshly reduced $\text{Cu}/\text{Al}_2\text{O}_3$ surface resulted in an initial increase in the number of adsorbed carbon monoxide molecules followed by a secondary phase characterised by a slow increase in carbon monoxide uptake, [figure 5.2]. Gas phase analysis showed carbon monoxide to be the only gas present. Figure [5.2] also showed the effect of hydrogen sulphide poisoning on the adsorption of carbon monoxide on another sample of the same catalyst. Although, the actual shape of the isotherm is identical to that obtained for the unpoisoned surface the overall effect of hydrogen sulphide pretreatment is to lower the number of adsorbed carbon monoxide molecules. The effect of hydrogen sulphide poisoning was shown to be only on the surface capacity toward the adsorption of carbon monoxide. On a surface poisoned with 0.12 coverage of adsorbed sulphur the decrease in the amount of carbon monoxide adsorbed on the surface was found to be about 25%.

The difference in the amounts of carbon monoxide adsorbed on the clean and poisoned surfaces at room temperature is shown in table 5.1.

Fig: 5.2

Carbon Monoxide Adsorption on clean and
Hydrogen Sulphide poisoned Copper/Alumina
at Room Temperature

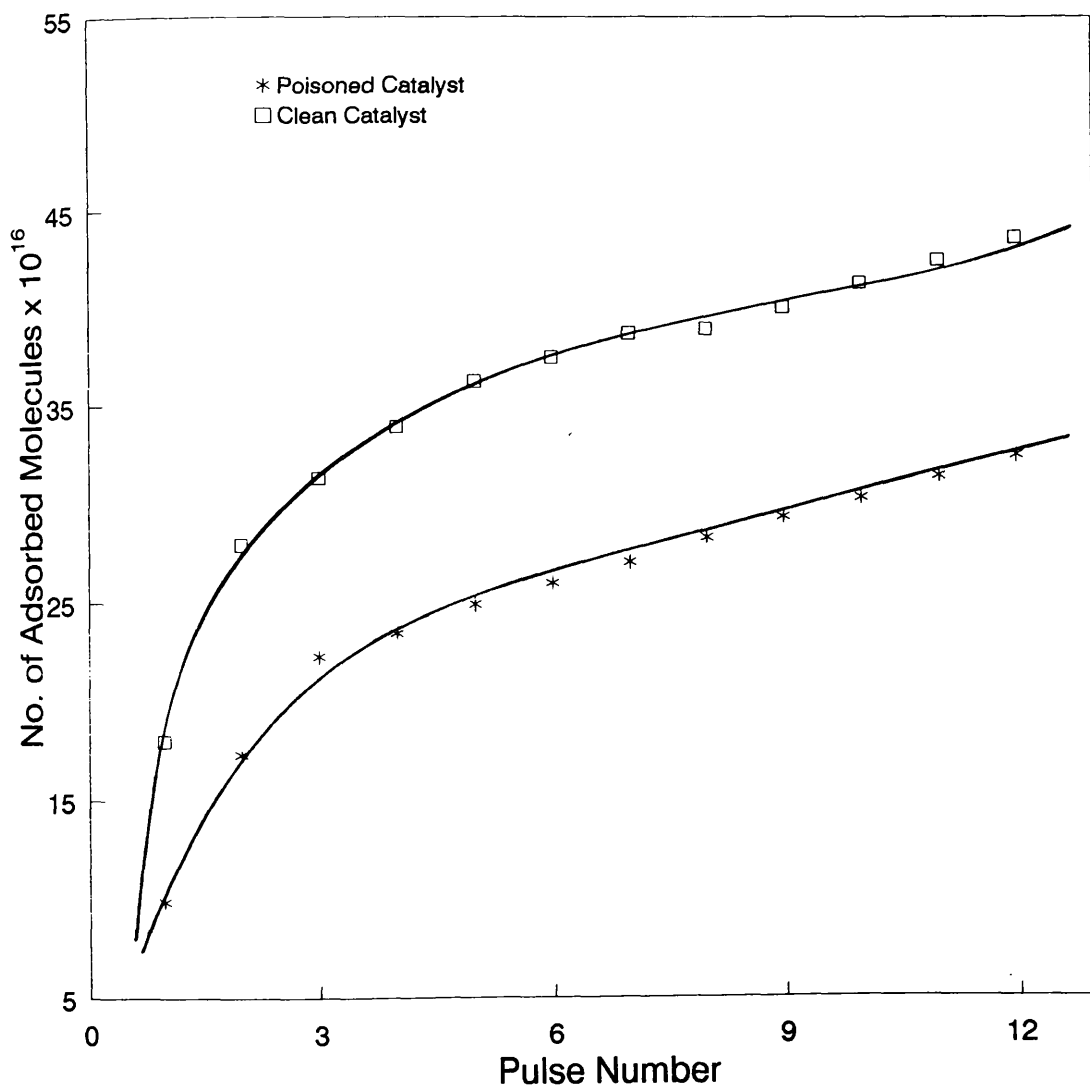


Table 5.1

The effect of H₂S pretreatment on the amount of carbon monoxide (g/catal)⁻¹ adsorbed at room temperature on a sample of 0.15 g of Cu/Al₂O₃ catalyst

Catalyst (0.15 g)	No. of Adsorbed molecules X 10 ¹⁸	
	Initial phase	Secondary phase
Clean Cu/Al ₂ O ₃ surface	1.06	2.165
Poisoned Cu/Al ₂ O ₃ sample	0.625	2.03

Passing a stream of helium (30 ml/min) over the poisoned sample at room temperature for 1 hour did not serve to increase the amount of carbon monoxide adsorbed when more pulses were subsequently admitted to the catalyst surface.

Heating the non-sulphided catalyst surface after room temperature adsorption of carbon monoxide resulted in two distinctive desorption peaks, the first, which was small and sharp, occurred at 200°C the second, a large and broad peak, occurred at 300°C. The total amount of carbon monoxide desorbed was ca. 2.165 X 10¹⁸ molecules per g/catalyst which compares with 2.718 X 10¹⁸ adsorbed molecules (g/catalyst) at room temperature after 12 pulses.

The amount of carbon monoxide retained on the surface after temperature treatment was ca. 20% of the initial uptake. These results suggest that two adsorbed states of carbon monoxide exist on Cu/Al₂O₃; a relatively weakly adsorbed species which was desorbed at 200°C and more strongly held species which was either desorbed at 300°C or retained on the surface, [figure 5.3 solid line].

Similar results were obtained for the poisoned surface as represented by the broken line in figure [5.3]. However, the two characteristic desorption peaks arise at lower temperatures in the case of the poisoned catalyst, ie. at 180°C and 270°C. From the desorption experiment, a total of 1.353×10^{18} molecules per g/catalyst were desorbed from the poisoned surface compared with 2.165×10^{18} molecules per g/catalyst desorbed from the clean surface. Thus, 34% of the total number of adsorbed carbon monoxide molecules were retained on the poisoned surface as a strongly adsorbed species. Figure [5.3] also shows that on the poisoned surface a noticeable decrease in the size of the second desorption peak was obtained with a corresponding increase in the first desorption peak's size. Although, both peaks were evident of the adsorption state of carbon monoxide, sulphur diminished and weakened the strongly adsorbed state. The effect of sulphur poisoning is summarised in table 5.2.

Fig. 5.3:

Desorption of CO Following adsorption
at RT on clean(—) and H₂S poisoned(---)
Cu/Al₂O₃

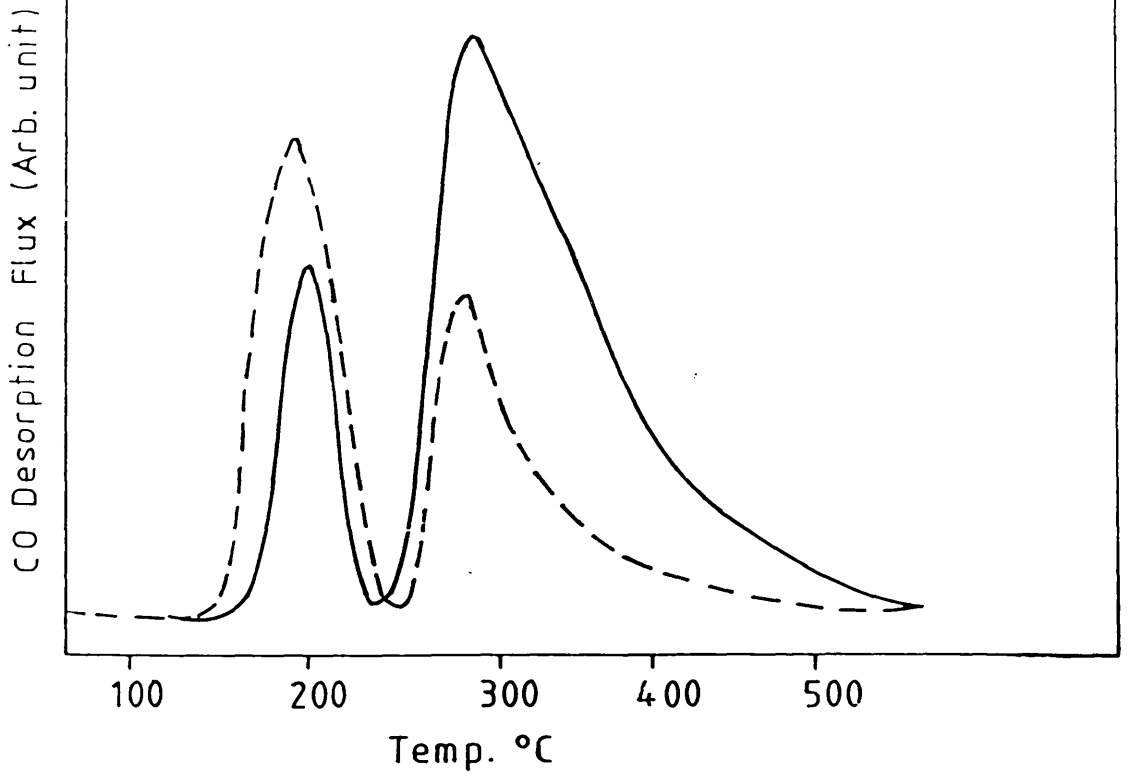


Table 5.2

The extent of carbon monoxide desorption (per g/catal.) from freshly reduced and poisoned Cu/Al₂O₃ catalyst heated under a stream of helium (25 ml/min), temperature rate 30°C/min.

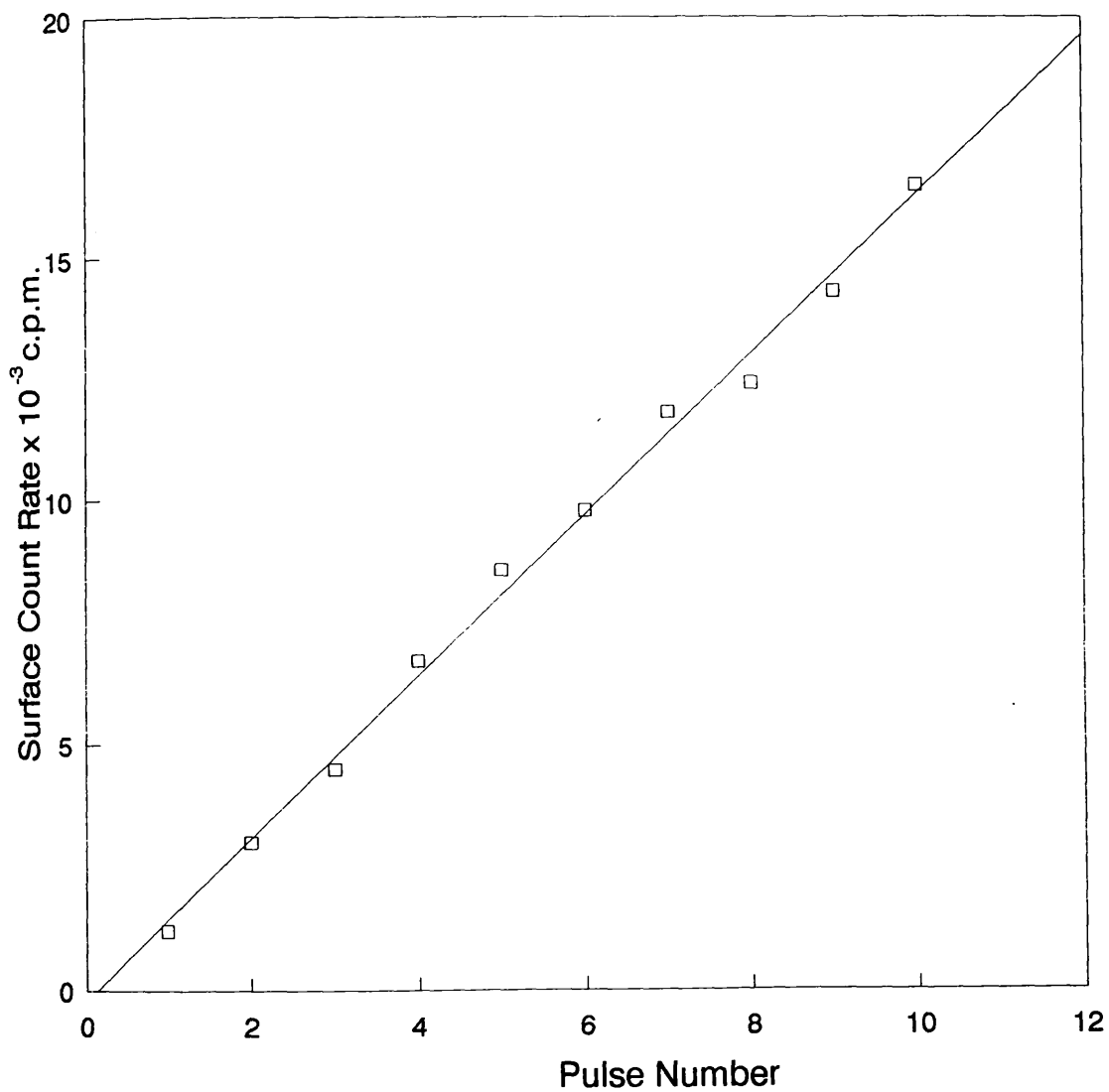
Catalyst (0.15 g)	No. of Adsorbed molecules X 10 ¹⁸		Desorption Temperature °C
	Adsorbed	Desorbed	
Freshly reduced Cu/Al ₂ O ₃ surface	2.718	2.165	200,300
Poisoned Cu/Al ₂ O ₃ sample	2.031	1.353	180,270

5.1.2 The Adsorption of Carbon Monoxide on Clean and Poisoned Cu-ZnO/Al₂O₃ Surfaces

Figure [5.4] illustrates the isotherm resulting from the adsorption of ¹⁴C-carbon monoxide at 250°C on a Cu-ZnO/Al₂O₃ sample reduced in 6% hydrogen in nitrogen stream (25 ml/min) for 14 hours at 250°C. The isotherm shows a linear increase in the surface count rate with successive pulses of ¹⁴C-carbon monoxide; this relationship is identical to that observed with the Cu/Al₂O₃ sample [see figure 5.1].

Fig: 5.4

^{14}C -Carbon Monoxide Adsorption on Copper - Zinc Oxide/Alumina
(0.1g) Sample Reduced with 6% Hydrogen in Nitrogen at 250°C

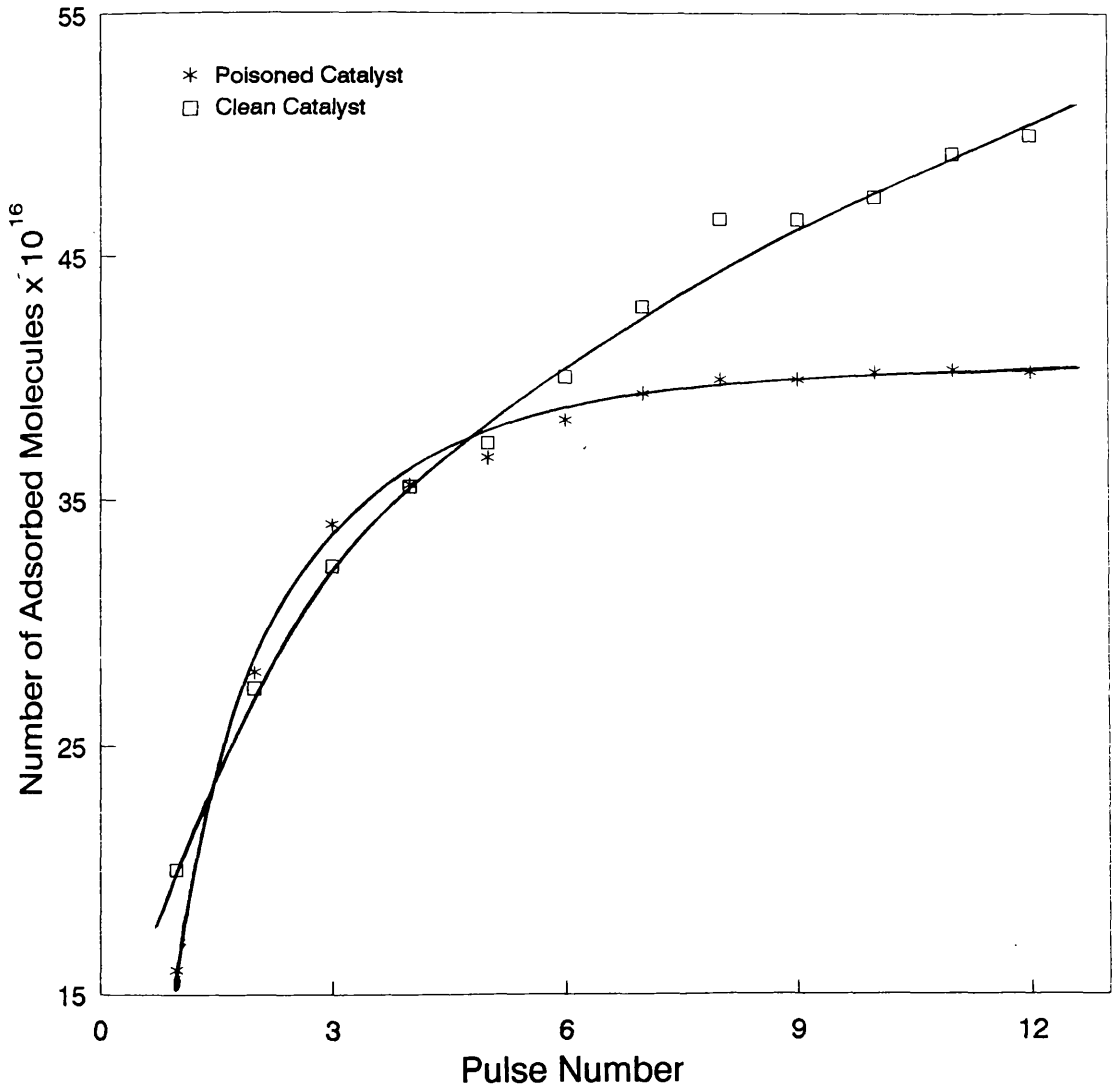


Gas phase analysis revealed that most of the admitted ^{14}C -carbon monoxide was converted to carbon dioxide under these conditions. However, after ten pulses, trace amounts of ^{14}C -carbon monoxide were detected. The concentration of gas phase ^{14}C -carbon monoxide was found to increase with further pulses.

Room temperature adsorption of unlabelled carbon monoxide resulted in the behaviour shown in figure [5.5], that is an initial rapid uptake of carbon monoxide followed by a secondary slower adsorption. Nevertheless, the adsorption isotherm did not attain a plateau but exhibited a slow continuing adsorption. The adsorption isotherm on Cu-ZnO/Al₂O₃ poisoned with hydrogen sulphide to an extent of 0.12 surface coverage of sulphur is also shown in figure [5.5]. The adsorption isotherm obtained exhibited the same rapid initial increase in adsorbed carbon monoxide until a plateau region was reached. This plateau corresponds to the saturation level of the poisoned surface with carbon monoxide. The total amount of adsorbed carbon monoxide on the poisoned surface is less than that on the freshly reduced sample; 2.531×10^{18} molecules per g/catalyst being adsorbed on the poisoned surface compared with 3.093×10^{18} molecules per g/catalyst adsorbed on the clean sample. In addition, in the initial stage of the isotherm adsorption increased in a similar way for both the clean and poisoned surfaces; the initial adsorption on the clean surface was 1.25×10^{18} molecules per g/catalyst which compares with

Fig: 5.5

Carbon Monoxide Adsorption on clean and Hydrogen Sulphide poisoned Copper - Zinc Oxide/Alumina at Room Temperature



1.031×10^{18} molecules per g/catalyst for the poisoned sample, with about 20% decrease in the adsorbed amounts.

Heating the clean catalyst surface in a similar way to that described for Cu/Al₂O₃ catalyst (see section 5.1.1) resulted (as with Cu/Al₂O₃) in desorption peaks at 260°C and 330°C. As in the Cu/Al₂O₃ study, the former peak is small and sharp while the other is much larger. However, in contrast to the Cu/Al₂O₃ case, the second peak exhibited a small shoulder at 400°C [figure 5.6 solid line], which can be attributed to a decomposition of the surface carbonate species presented in this kind of catalyst according to the preparation method (see section 2.1.1).

The picture for carbon monoxide desorption from the poisoned sample is presented in figure [5.6 broken line]. Two peaks also appeared during the heat treatment of the poisoned catalyst surface, at 270°C and 380°C. The shoulder observed for the clean surface was not apparent in this case. Whilst only 11% of the carbon monoxide adsorbed on the clean surface at room temperature was retained on the surface, following the thermal desorption, as a strongly held species, ca. 37% of the total amount adsorbed on the poisoned surface was retained as strongly bound species. The results are presented in table 5.3.

Fig. 5.6:

Desorption of CO, following adsorption at RT on clean (—) and H₂S poisoned Cu-ZnO/Al₂O₃

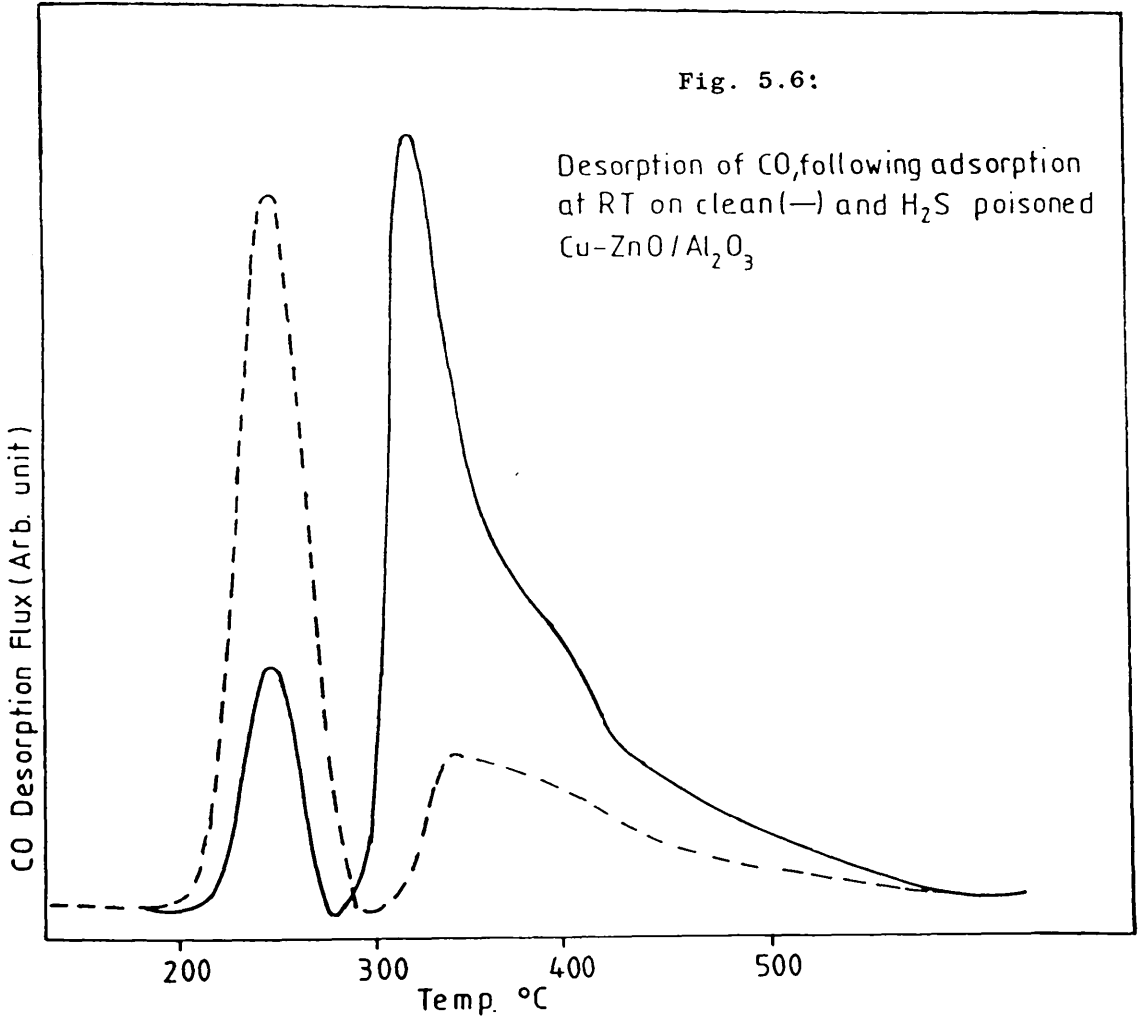


Table 5.3

The extent of carbon monoxide desorption (per g/catal.) on clean and H₂S poisoned Cu-ZnO/Al₂O₃

Catalyst (0.15 g)	No. of Molecules X 10 ¹⁸		Desorption temperature °C		
	Adsorbed	Desorbed	1st Peak	2nd Peak	3rd Peak
Clean Cu-ZnO/Al ₂ O ₃ sample	3.093	2.768	260	330	400
Poisoned Cu-Zn/Al ₂ O ₃	2.531	1.593	270	380	-

5.1.3 The Adsorption of Carbon Monoxide on Unreduced Cu/Al₂O₃ and Cu-ZnO/Al₂O₃ surfaces

There was no observable adsorption of carbon monoxide on unreduced samples of Cu/Al₂O₃ and Cu-ZnO/Al₂O₃ at room temperature. At temperature higher than 100°C, all the carbon monoxide admitted to the catalyst surface was converted to carbon dioxide. This was mainly due to the reaction of carbon monoxide with unreduced copper (i.e. CuO) in both catalysts.

5.2 THE ADSORPTION OF CARBON MONOXIDE ON OXIDE SURFACES

The adsorption of carbon monoxide on the zinc oxide and alumina surfaces was studied. Both surfaces were treated with 6% hydrogen in nitrogen under similar conditions to those used for the reaction on Cu/Al₂O₃ and Cu-ZnO/Al₂O₃ namely at 250°C for 14 hours at a flow rate of 25 ml/min, before being used to investigate the extent of carbon monoxide adsorption.

5.2.1 Carbon Monoxide Adsorption on a Zinc Oxide Surfaces

A typical isotherm for the adsorption of ¹⁴C-carbon monoxide on zinc oxide at 250°C is presented in figure [5.7]. The isotherm is characterised by initial increase in the surface count rate followed by plateau region which represents a saturation by ¹⁴C-carbon monoxide. Figure [5.8] illustrates the same adsorption isotherm for unlabelled carbon monoxide at room temperature; in both cases the surface is saturated after 8 pulses. Although the total amount of carbon monoxide adsorbed at room temperature is estimated at 0.847×10^{18} molecules (g. catal⁻¹), it was noted that most of the adsorbed carbon monoxide had been removed if the succeeding pulses was delayed for about five minutes. Further adsorption

Fig: 5.7

^{14}C -Carbon Monoxide Adsorption on Zinc Oxide
(0.05g) Reduced with 6% Hydrogen in Nitrogen
at 250°C Carbon Monoxide Pressure = 33 Torr

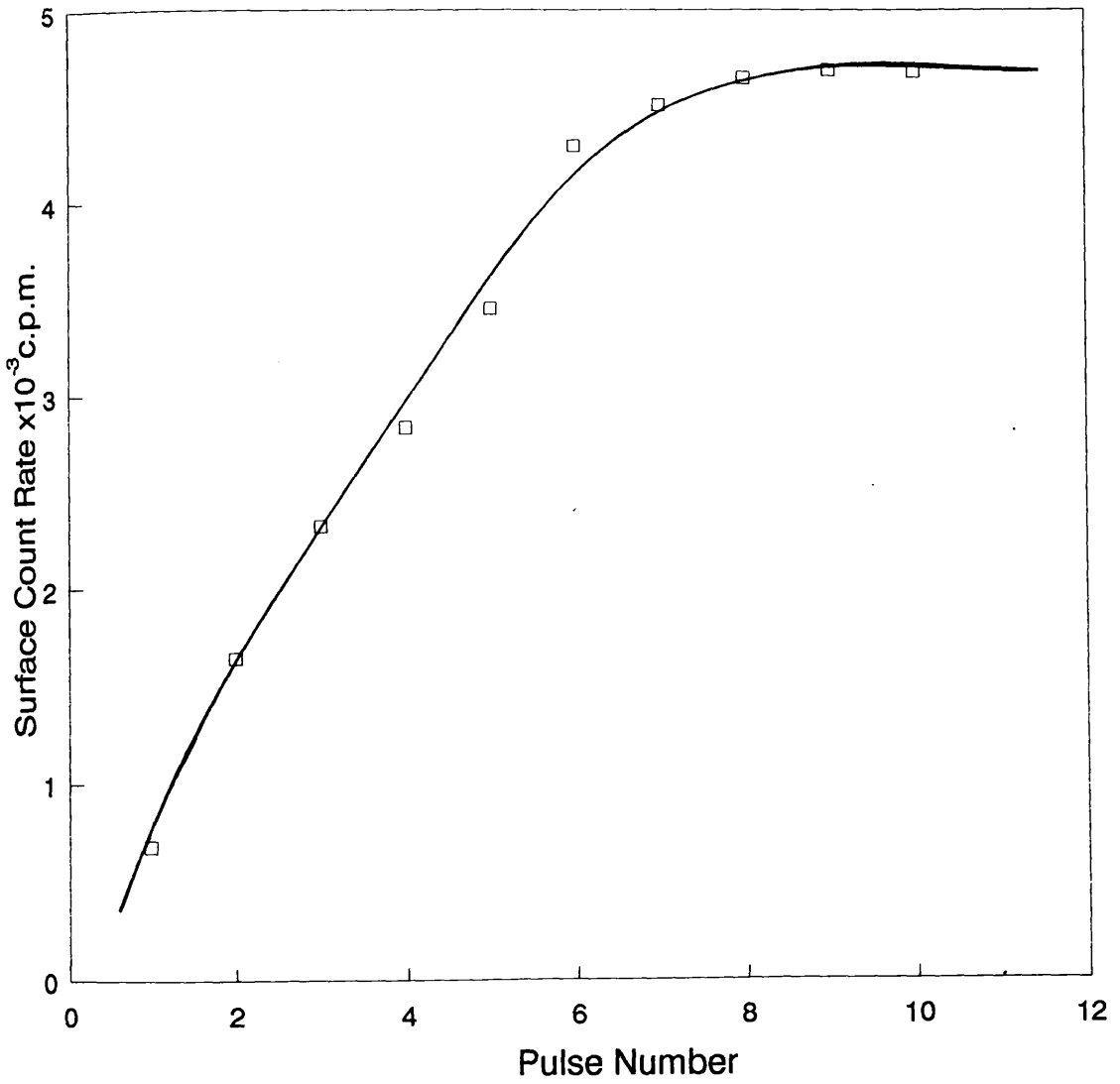
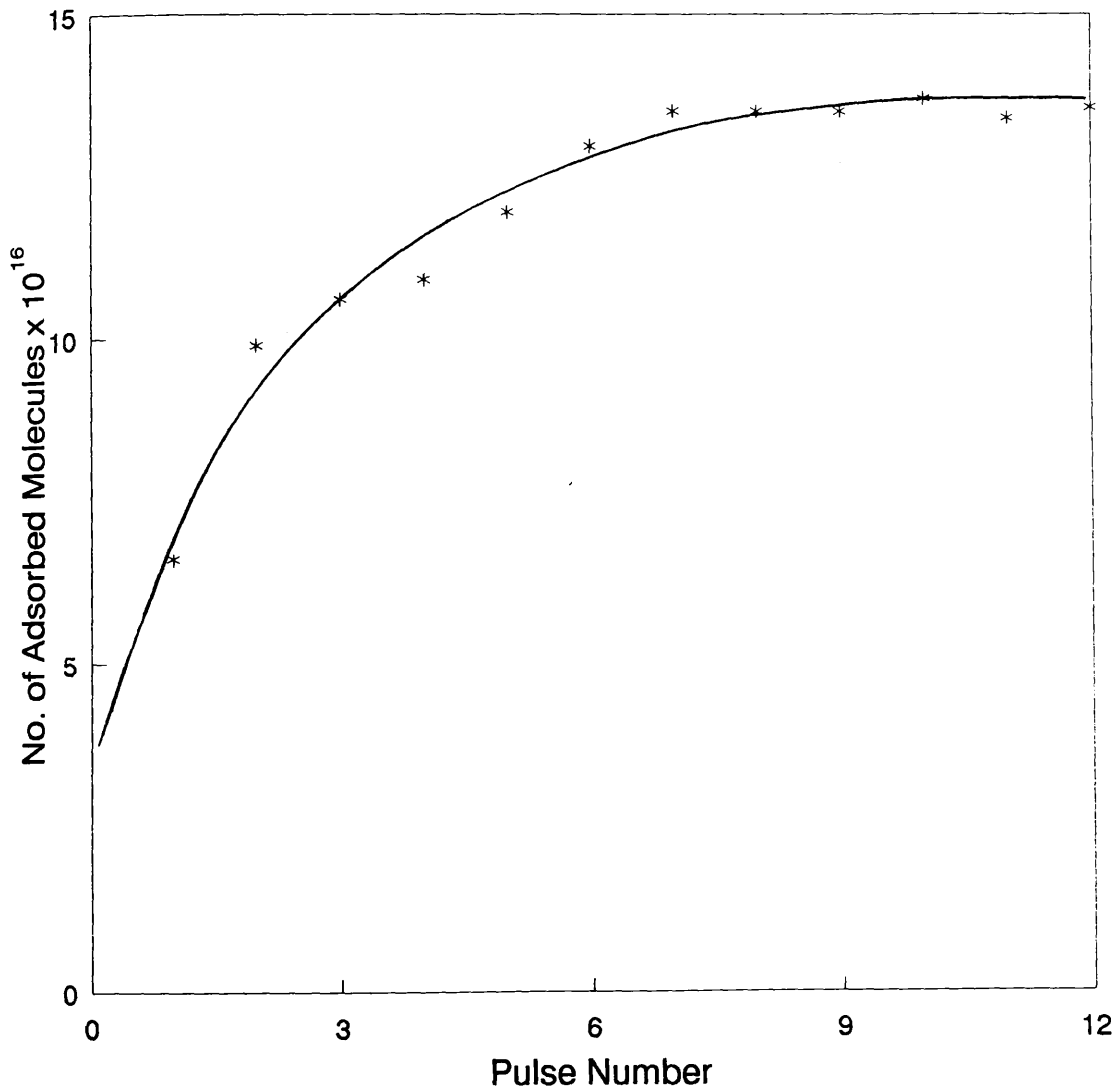


Fig: 5.8

Carbon Monoxide Adsorption on Zinc Oxide (0.5g)
at Room Temperature Sample Reduced with
6% Hydrogen in Nitrogen at 250°C



experiments revealed that carbon monoxide was indeed very weakly bonded to the zinc oxide surface. The desorption experiments revealed no peaks up to ca 500°C. These results were supported by adsorption data obtained on an AnalaR zinc oxide sample which showed no adsorption of carbon monoxide at either room or higher temperature (100°C). Analysis of the gas phase by gas chromatography revealed the presence of only carbon monoxide.

5.2.2 ^{14}C -Carbon Monoxide Adsorption on an Alumina Surface

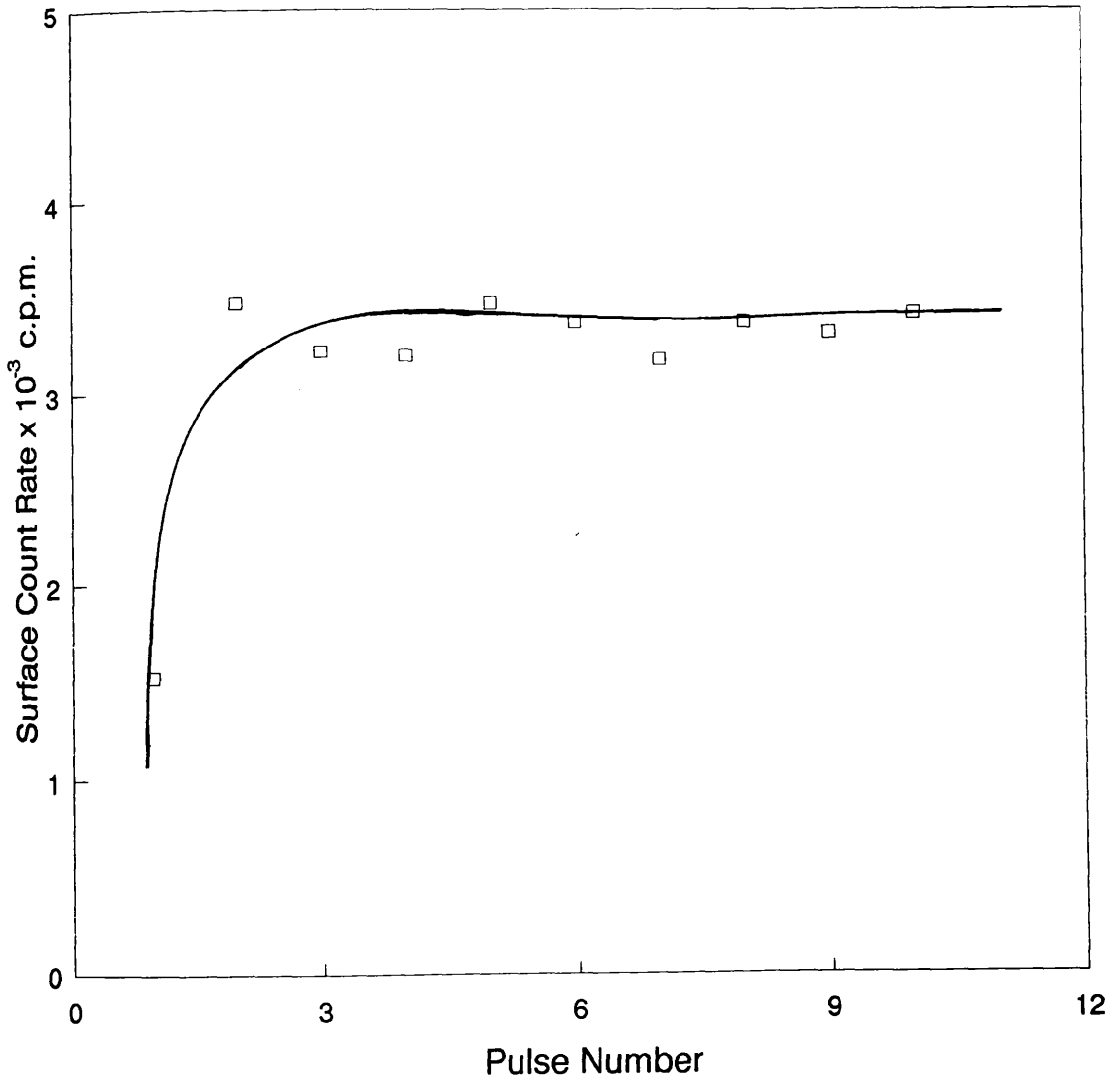
It is well documented in the literature ⁽¹¹⁴⁾ that there is no significant adsorption of carbon monoxide on alumina surfaces. Nevertheless, as can be seen from figure [5.9], the alumina surface was saturated with ^{14}C -carbon monoxide directly after the initial pulse of 33 torr in a volume of 0.204 cm³ at 250°C. This means that the alumina surface was saturated with only 2.24×10^{18} carbon monoxide molecules (g/catal.) as there is no further increase in the surface count rate (plateau region).

5.3 ^{14}C -CARBON DIOXIDE ADSORPTION ON COPPER-BASED AND RELATED CATALYSTS

The adsorption of ^{14}C -carbon dioxide on Cu/Al₂O₃, Cu-ZnO/Al₂O₃, ZnO and alumina catalysts was investigated by gas chromatography and the Isoflo scintillation counter.

Fig: 5.9

^{14}C -Carbon Monoxide Adsorption on
Alumina (0.05g) at 250°C Sample
Reduced with 6% Hydrogen in Nitrogen
at 250°C CO Pressure = 33 Torr



The results obtained from these studies will be detailed in the following sections. The effect of hydrogen sulphide pretreatment on the catalyst surfaces has also been investigated.

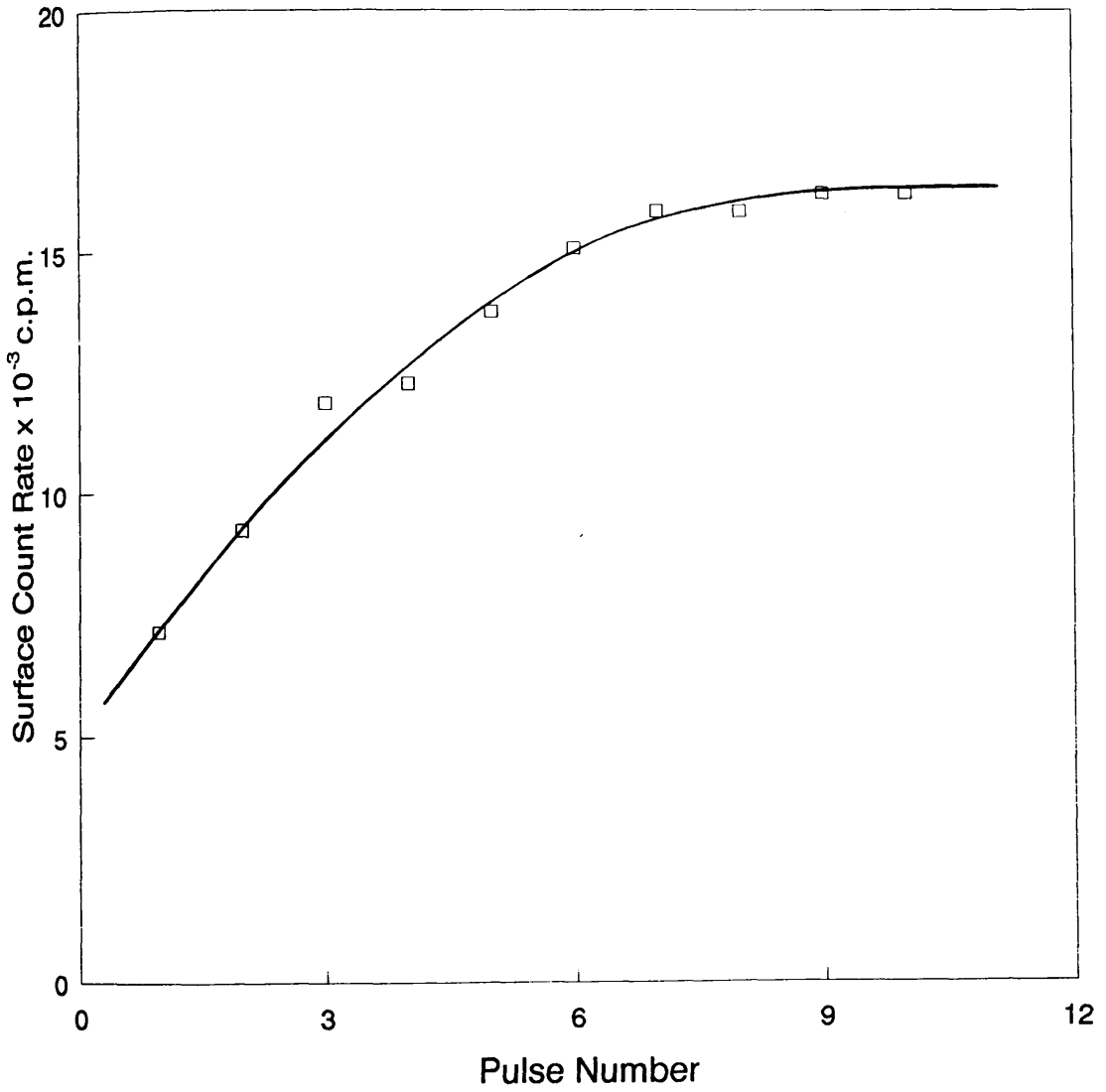
5.3.1 The Adsorption of ^{14}C -Carbon Dioxide on a $\text{Cu}/\text{Al}_2\text{O}_3$ Surface

The adsorption of ^{14}C -carbon dioxide was measured on a $\text{Cu}/\text{Al}_2\text{O}_3$ catalyst reduced either in a stream of 6% hydrogen in nitrogen (25 ml/min) at 250°C for 14 hours or carbon monoxide (flow rate 7 ml/min) under the same conditions. These pretreatments were followed by 45-60 minutes flushing in helium (32 ml/min) at the reduction temperature before the adsorption measurements.

A typical adsorption isotherm for ^{14}C -carbon dioxide on $\text{Cu}/\text{Al}_2\text{O}_3$ is shown in figure [5.10]. The adsorption was carried out at 250°C . A rapid increase in the surface count rate was again observed. Gas chromatographic analysis of the effluent gas after the first two pulses revealed only trace amounts of ^{14}C -carbon dioxide, which is indicative of an almost complete uptake. The catalyst surface reached the equilibrium state after the introduction of eight pulses of ^{14}C -carbon dioxide, at which point no further adsorption was observed; the total uptake was 5.25×10^{18} molecules

Fig: 5.10

^{14}C -Carbon Dioxide Adsorption at 250°C
on Copper/Alumina Reduced with 6% Hydrogen
in Nitrogen at 250°C



(g.catal⁻¹). By comparison, the carbon monoxide reduced sample [figure 5.11] exhibited a lower saturation level, ie. 4.5×10^{18} molecules (g.catal⁻¹). It is clear from figure [5.11] that the surface was saturated after five pulses of ¹⁴C-carbon dioxide. It should also be noted that the actual variation of surface count rate with pulse number followed the same trend regardless of the reducing agent.

A plot of the surface count rate as a function of ¹⁴C-carbon dioxide pulse pressure (under helium flow of 32 ml/min) is shown in figure [5.12]. The results are identical to the isotherm for ¹⁴C-carbon dioxide adsorption at room temperature [figure 5.13]. At room temperature an increased quantity of carbon dioxide is required to saturate the surface, ca. 5.625×10^{18} molecules (g.catal⁻¹). The relevant results are presented in table 5.4.

Fig: 5.11

^{14}C -Carbon Dioxide Adsorption at 250°C Carbon Monoxide
Reduced Copper/Alumina at 250°C overnight
 ^{14}C -Carbon Dioxide Pressure = 86 Torr

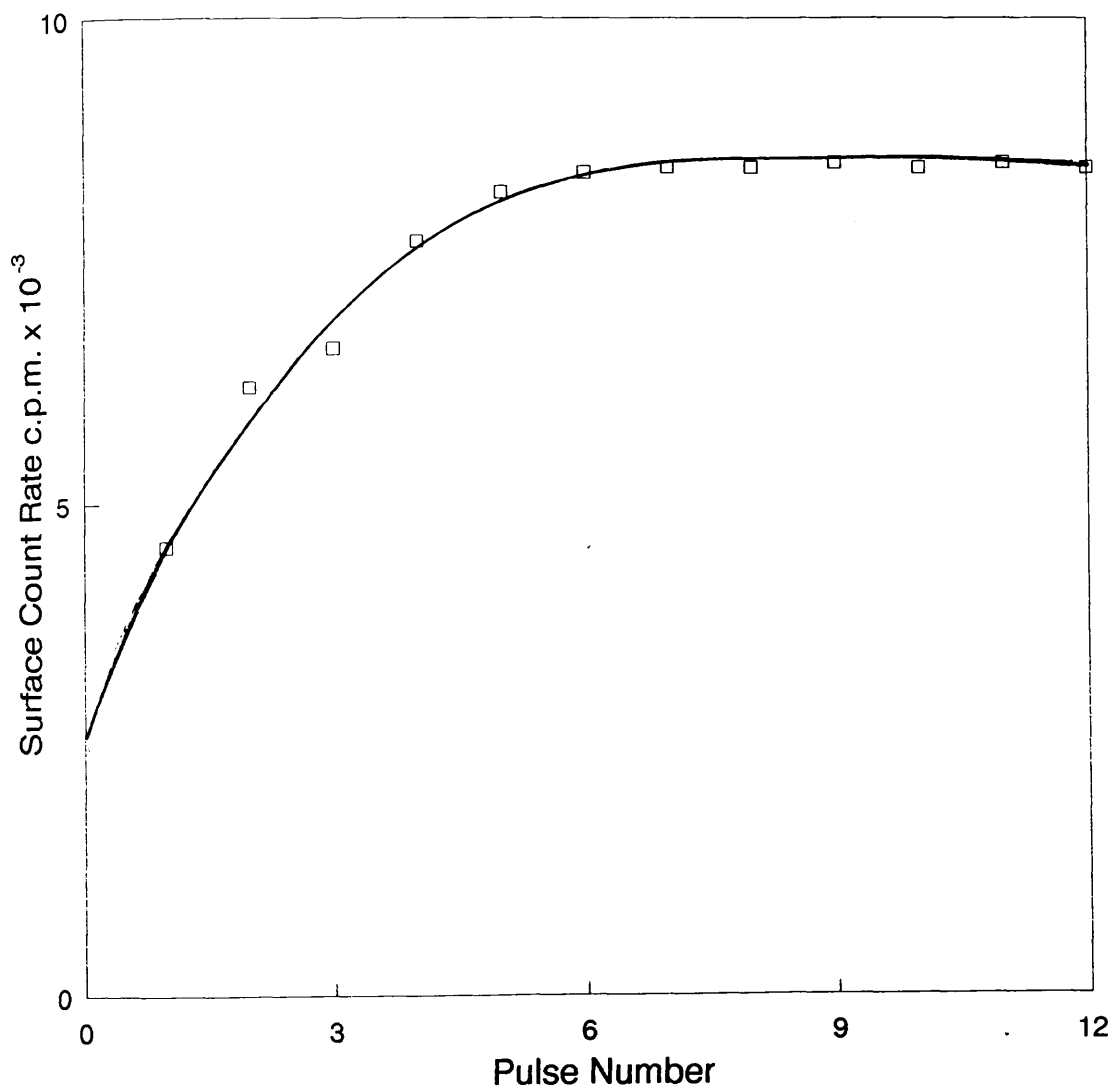


Fig: 5.12

^{14}C -Carbon Dioxide Adsorption at Room Temperature
Reduced Copper/Alumina with 6% Hydrogen
in Nitrogen at 250°C

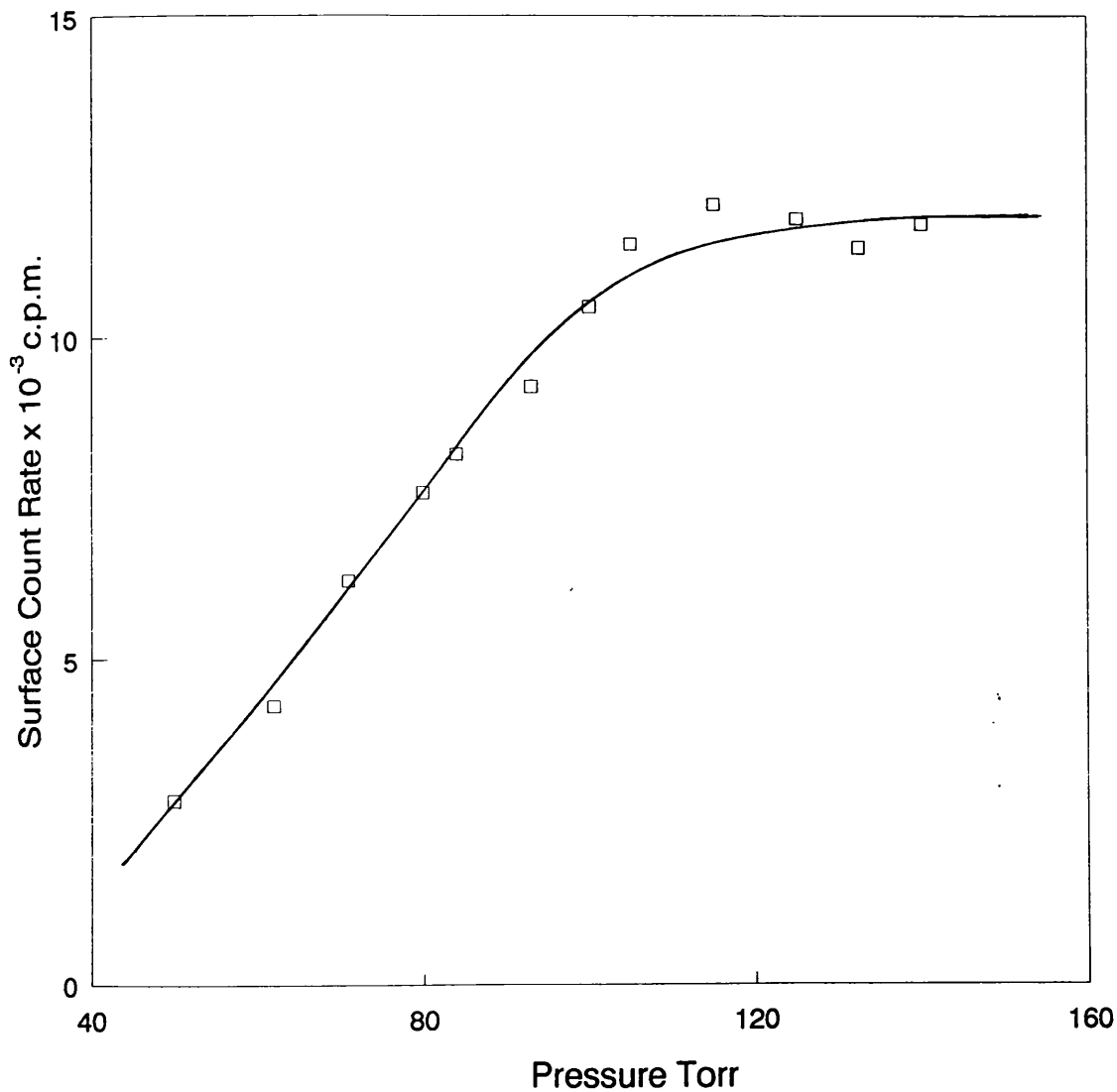


Fig: 5.13

^{14}C -Carbon Dioxide Adsorption on clean and Hydrogen Sulphide poisoned Copper/Alumina at Room Temperature

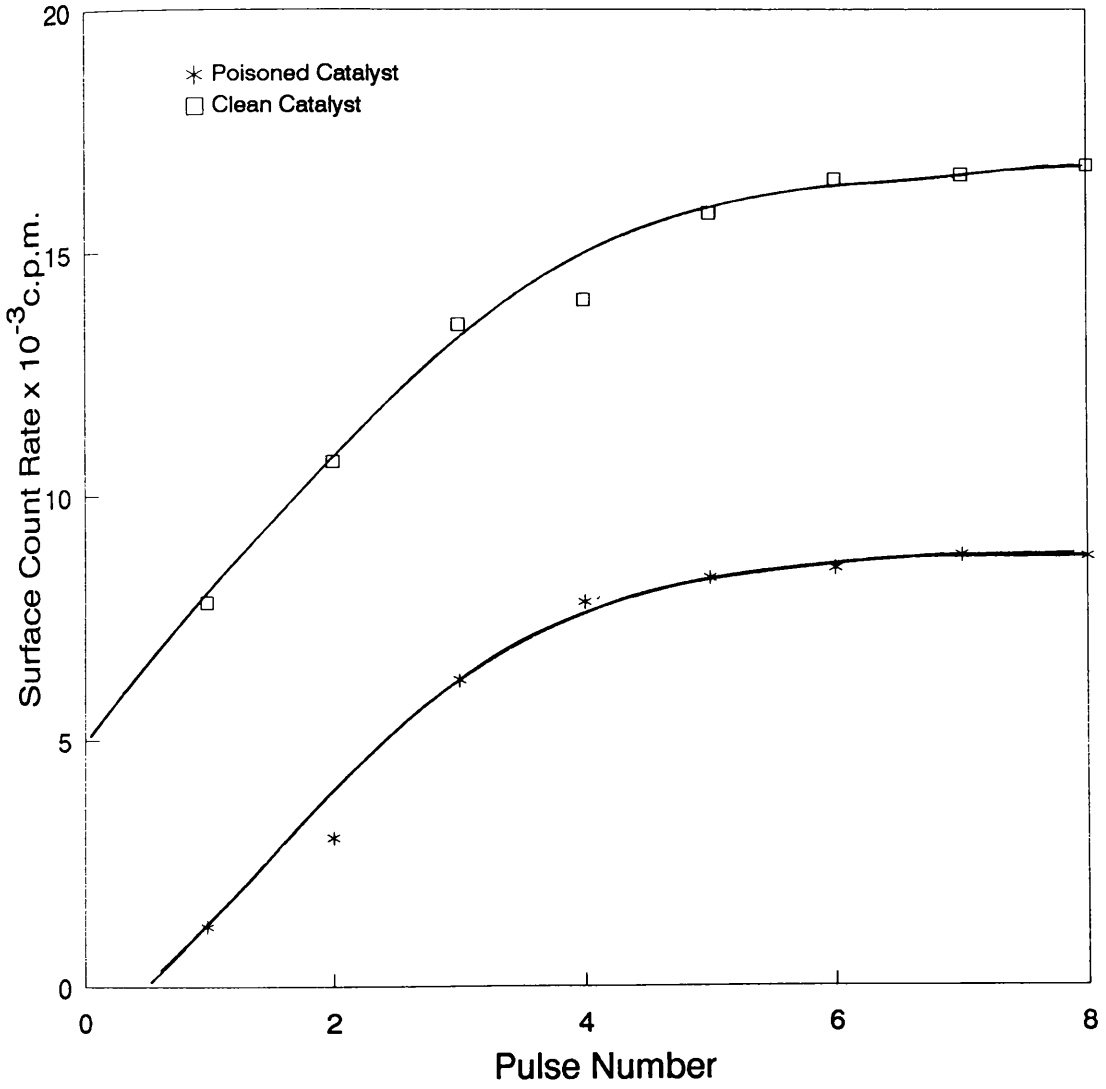


Table 5.4

The effect of the surface reduction procedure and adsorption temperature on ^{14}C -carbon dioxide adsorption (molecules per g/catal.) on $\text{Cu}/\text{Al}_2\text{O}_3$
 Weight of catalyst = 0.15 g

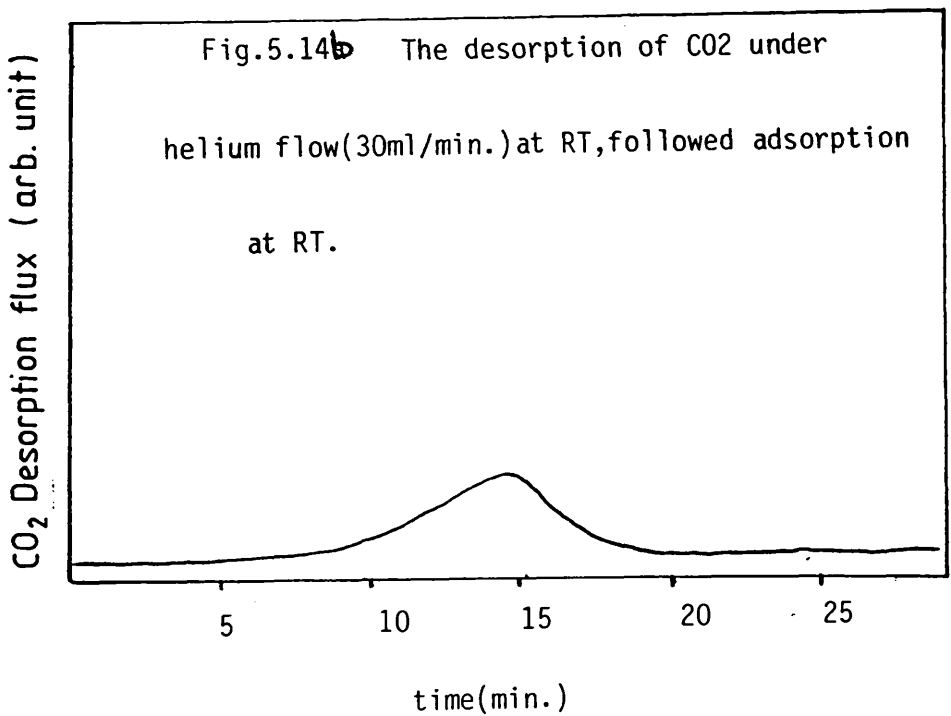
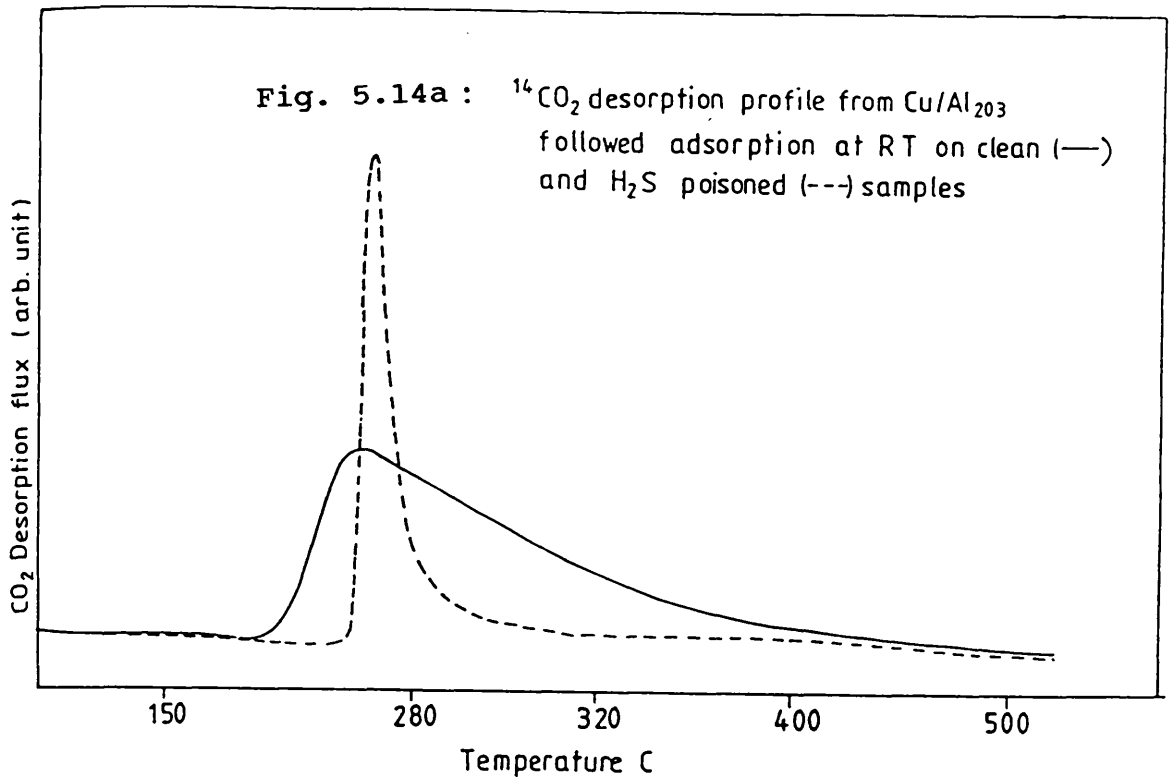
Surface reduction procedure at 250 °C	No. of adsorbed molecules X 10 ¹⁸	Adsorption temperature °C
6% H ₂ in N ₂	5.25	250
CO flow stream	4.5	250
6% H ₂ in N ₂	5.625	RT

As shown earlier in this section, the number of ^{14}C -carbon dioxide molecules necessary for a surface saturation increased at lower adsorption temperature. The adsorption isotherm at room temperature (also shown in figure [5.13]) was reproducible yielding a value of ca. 5.687×10^{18} molecules (g.catal⁻¹) at saturation.

The catalyst surface was heated under a helium flow (30 ml/min), and a rate of ca. $30^\circ\text{C min}^{-1}$. Using the gas chromatograph to detect the desorbed ^{14}C -carbon dioxide species and the Isoflo scintillation counter to determine

the desorbed gas activity. Under these conditions, ca. 90% of the adsorbed ^{14}C -carbon dioxide was desorbed generating a broad peak in temperature range of 170-400°C, as shown in figure [5.14a] (the solid line) of the chromatograph trace, it is clear that ^{14}C -carbon dioxide is adsorbed in two forms with the range of calculated ΔH_{ad} : a weakly bound species which is desorbed at lower temperature and a strongly held species which is suggested by the broad tailing of the desorption peak. The presence of a strongly bound species was also confirmed by the Isoflo desorption trace, figure [5.15]. The extent of desorption as measured by both techniques is in excellent agreement; 90% detected by the gas chromatograph as a desorbed species and 88% by the Isoflo flow scintillation counter.

As a further extension of this study, the extent of room temperature desorption of ^{14}C -carbon dioxide from a $\text{Cu}/\text{Al}_2\text{O}_3$ sample left under a stream of helium (30 ml/min) for 1 hour was measured; Ca. 20% of the adsorbed carbon dioxide was found to be removed. As is observed in figure [5.14b], a broad tailing peak is again evident. There is thus considerable evidence for the existence of two different adsorbed species on the copper component.



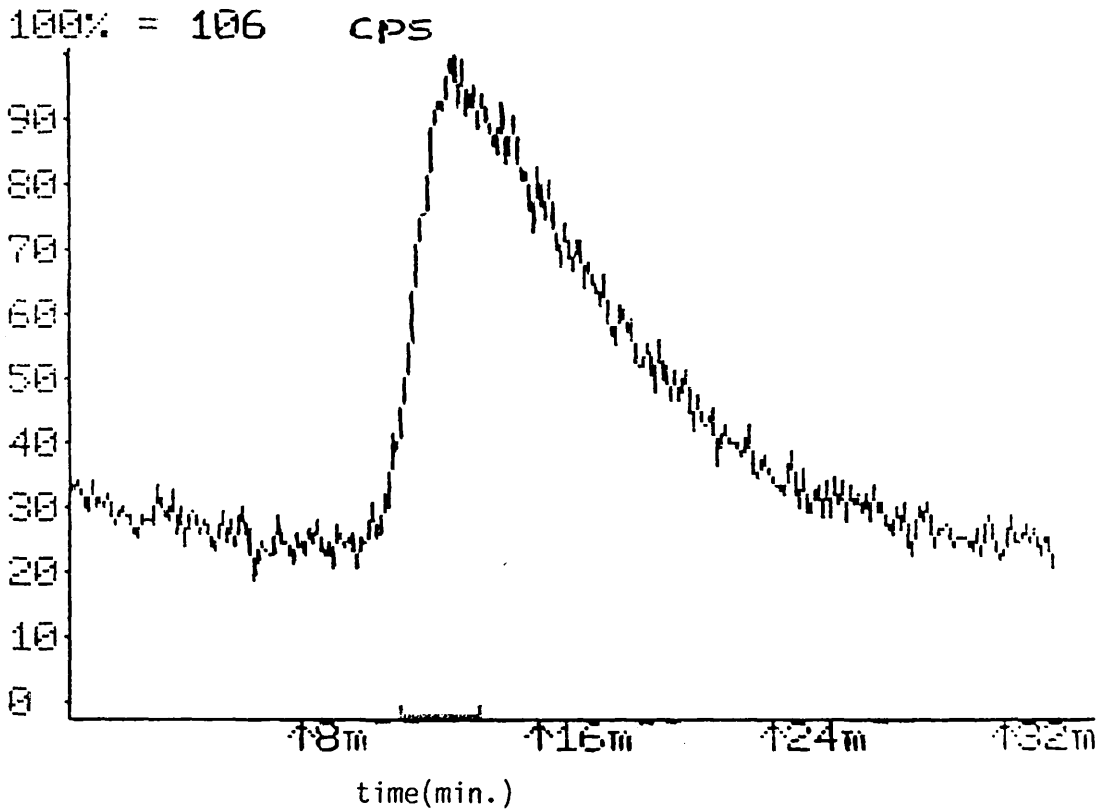


Fig. 5.15

The Isoflo desorption Profile of $^{14}\text{C-CO}_2$,
 following adsorption at RT on clean $\text{Cu/Al}_2\text{O}_3$
 surface.

5.3.2 ^{14}C -Carbon Dioxide Adsorption on H_2S Poisoned $\text{Cu}/\text{Al}_2\text{O}_3$ Surface

The ^{14}C -carbon dioxide adsorption isotherm on a reduced sample poisoned to the extent of ca. 0.13 surface coverage by hydrogen sulphide is presented in figure [5.13]. The isotherm is typified by the now characteristic increase in surface count rate followed by a plateau achieved at saturation; in this case, saturation was achieved after ca. 4 ^{14}C -carbon dioxide pulses. Comparison with the adsorption isotherm on the clean surface reveals a significant decrease in the catalyst surface capacity for adsorbed ^{14}C -carbon dioxide as a result of hydrogen sulphide poisoning. In fact, a 45% decrease in the surface count was observed. The catalyst surface uptake of ^{14}C -carbon dioxide molecules was also decreased, whereas, ca. 3×10^{18} ^{14}C -carbon dioxide molecules (g.catal^{-1}) were adsorbed on the poisoned surface, compared with 5.687×10^{18} adsorbed molecules (g.catal^{-1}) on a clean sample.

Heating the poisoned catalyst surface, after the adsorption had been completed, at $30^\circ\text{C}/\text{min}$ to 500°C while monitoring the desorbed species by both the gas chromatograph and the Isoflo flow scintillation counter resulted in a sharp peak presented in figure [5.14a] (dotted line) and figure [5.16], for the chromatography and the Isoflo traces respectively. It should be noted that there is no evidence of tailing in either trace which is

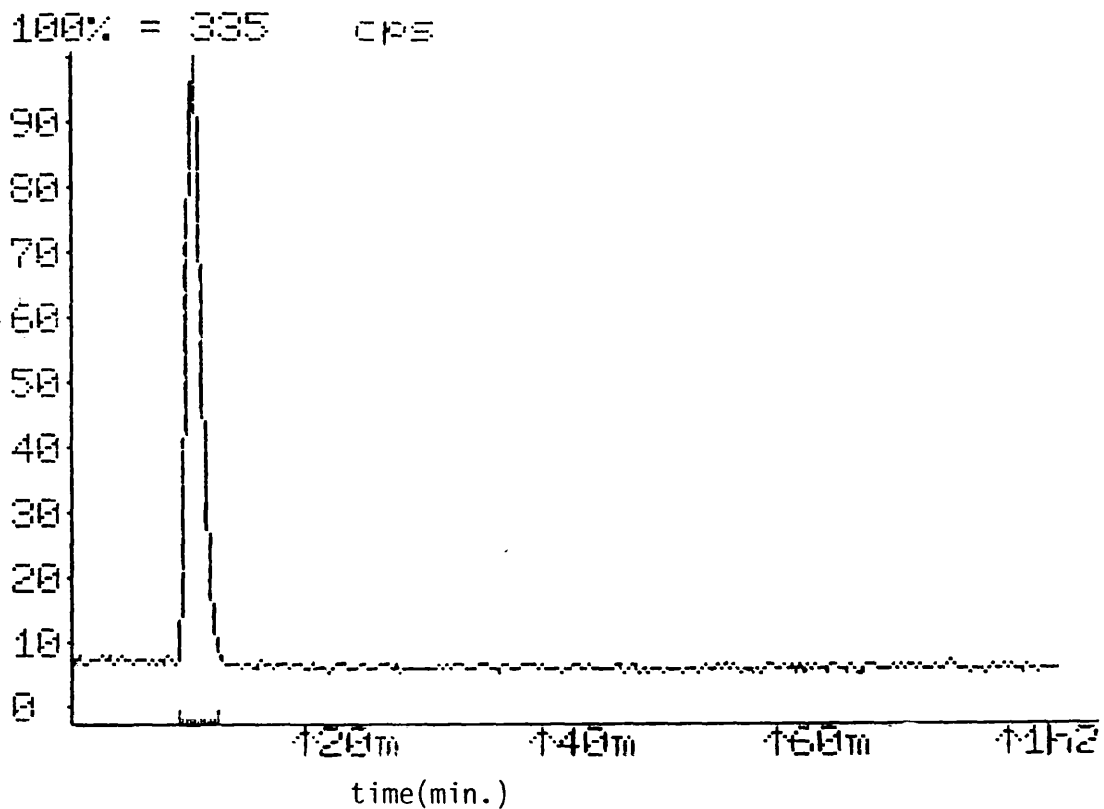


Fig. 5.16

Isoflo desorption Profile of $^{14}\text{C}-\text{CO}_2$ following adsorption at RT on poisoned $\text{Cu}/\text{Al}_2\text{O}_3$ catalyst.

diagnostic of the sole presence of the weakly adsorbed ^{14}C -carbon dioxide species on the poisoned surface. From the gas chromatography trace, it is estimated that ca. 2.84×10^{18} molecules were desorbed from the surface; ca. 6% of the total adsorbed ^{14}C -carbon dioxide remained on the surface. Adsorption data on both clean and poisoned $\text{Cu}/\text{Al}_2\text{O}_3$ surfaces are given in table 5.5.

Table 5.5

The effect of adsorbed sulphur on the adsorption of ^{14}C -carbon dioxide (molecules per g/catal.) on $\text{Cu}/\text{Al}_2\text{O}_3$ surface at room temperature

Catalyst (0.15 g)	No. of molecules $\times 10^{18}$		% Retained
	Adsorbed	Desorbed	
Freshly reduced $\text{Cu}/\text{Al}_2\text{O}_3$	5.687	5.187	10
Poisoned $\text{Cu}/\text{Al}_2\text{O}_3$	3	2.83	6
Reduced $\text{Cu}/\text{Al}_2\text{O}_3$ (Room temperature desorption)	5.625	4.531	80

5.3.3 Adsorption Isotherms of ^{14}C -Carbon Dioxide on Clean and Poisoned $\text{Cu-ZnO}/\text{Al}_2\text{O}_3$ Surfaces

The adsorption of ^{14}C -carbon dioxide was also studied on $\text{Cu-ZnO}/\text{Al}_2\text{O}_3$ samples reduced in either a stream of 6%

hydrogen in nitrogen (25 ml/min) or carbon monoxide (7 ml/min) at 250°C for 14 hours. The catalyst surface was then flushed with helium for 45-60 minutes prior to determining the adsorption isotherm at a chosen temperature.

Figure [5.17], depicts the isotherm obtained from the adsorption of ^{14}C -carbon dioxide at 250°C on a hydrogen in nitrogen reduced Cu-ZnO/Al₂O₃ sample. In contrast with the previous case, a rapid increase in the surface count rate was followed by much more gradual increase in the secondary region of the isotherm; surface saturation was not observed under these conditions. An estimated 9.462×10^{18} molecules (g.catal⁻¹) were adsorbed on the surface. In comparison, the catalyst sample activated in a stream of carbon monoxide (flow rate 7 ml/min) exhibited greater uptake of ^{14}C -carbon dioxide, namely 12.343×10^{18} molecules (g.catal⁻¹). Moreover, the adsorption isotherm attained a plateau after 5 pulses, figure [5.18].

Interestingly, the Cu-ZnO/Al₂O₃ surface becomes saturated with adsorbed ^{14}C -carbon dioxide species more rapidly at room temperature than for adsorption at elevated temperatures. The adsorption/desorption behaviour of ^{14}C -carbon dioxide on Cu-ZnO/Al₂O₃ at room temperature was examined on a sample activated with 6% hydrogen in nitrogen at 250°C. The ^{14}C -carbon dioxide adsorption isotherm at room temperature for the freshly reduced Cu-ZnO/Al₂O₃ sample is presented in figure [5.19]; surface saturation was reached

Fig: 5.17

^{14}C -Carbon Dioxide Adsorption at 250°C on Copper -
Zinc Oxide/Alumina (0.156g) Sample Reduced
with 6% Hydrogen in Nitrogen at 250°C

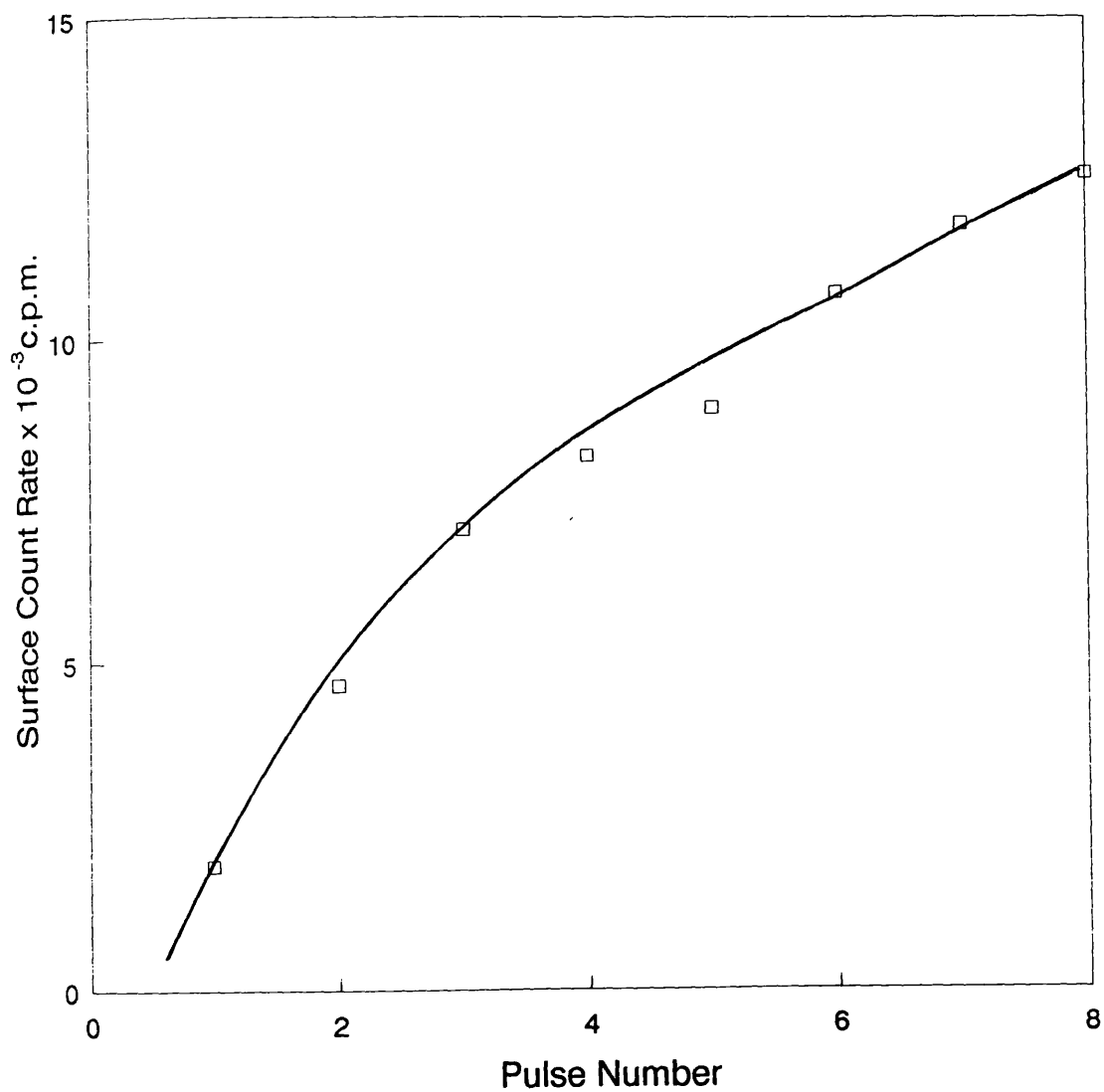


Fig: 5.18

^{14}C -Carbon Dioxide Adsorption at Room Temperature
on Copper - Zinc Oxide/Alumina (0.156g)
Sample Reduced with Carbon Monoxide at 250°C

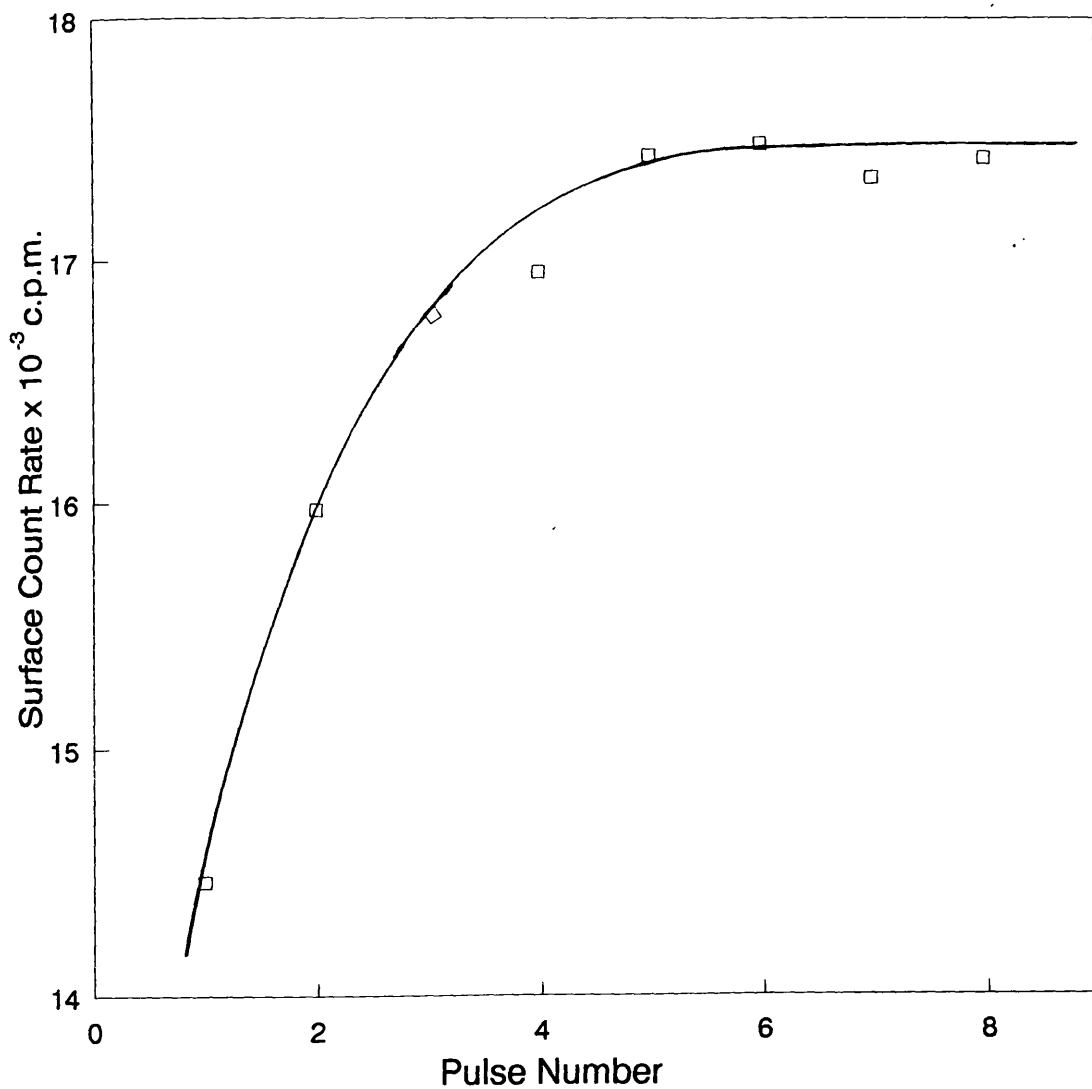
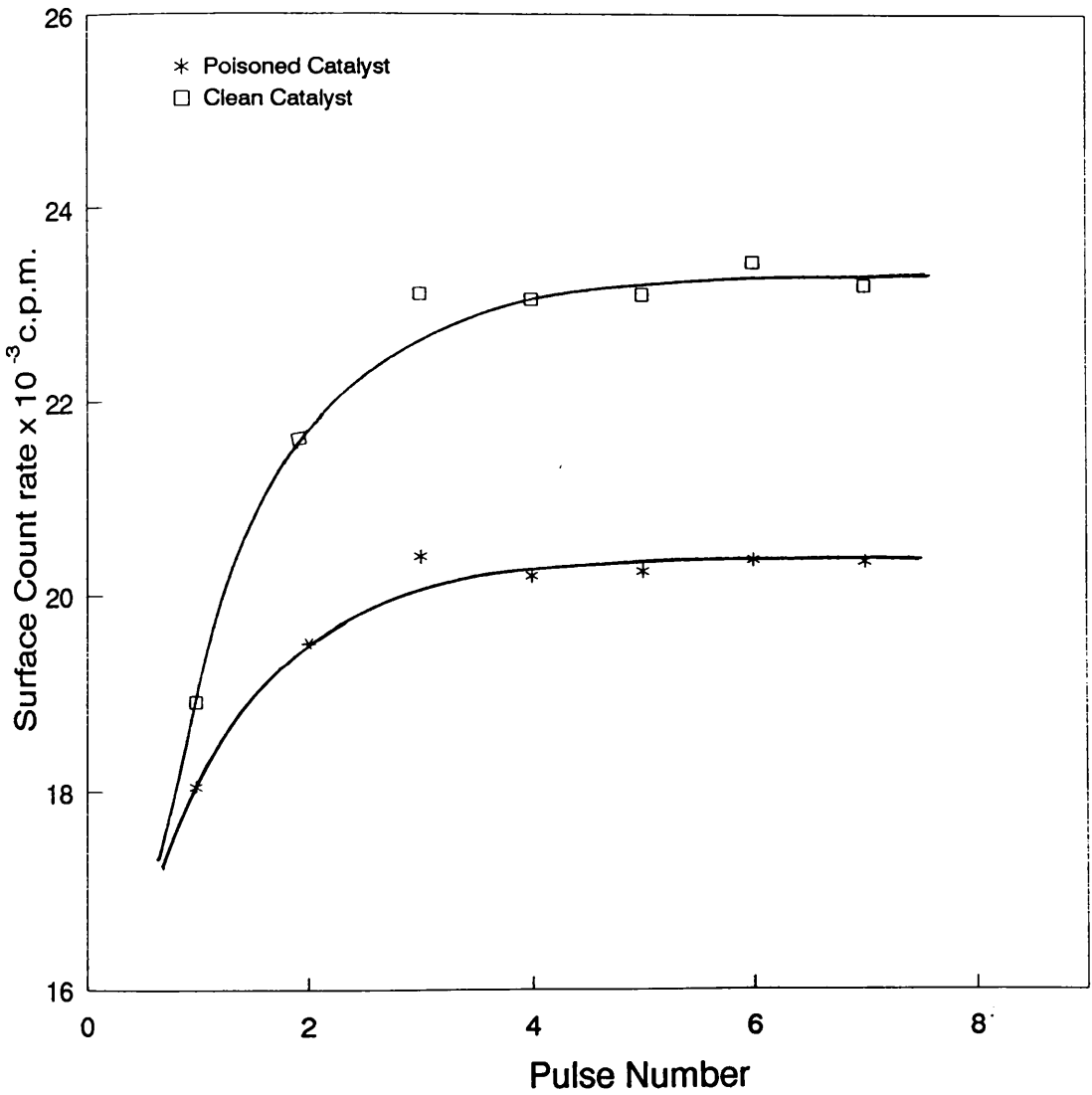


Fig: 5.19

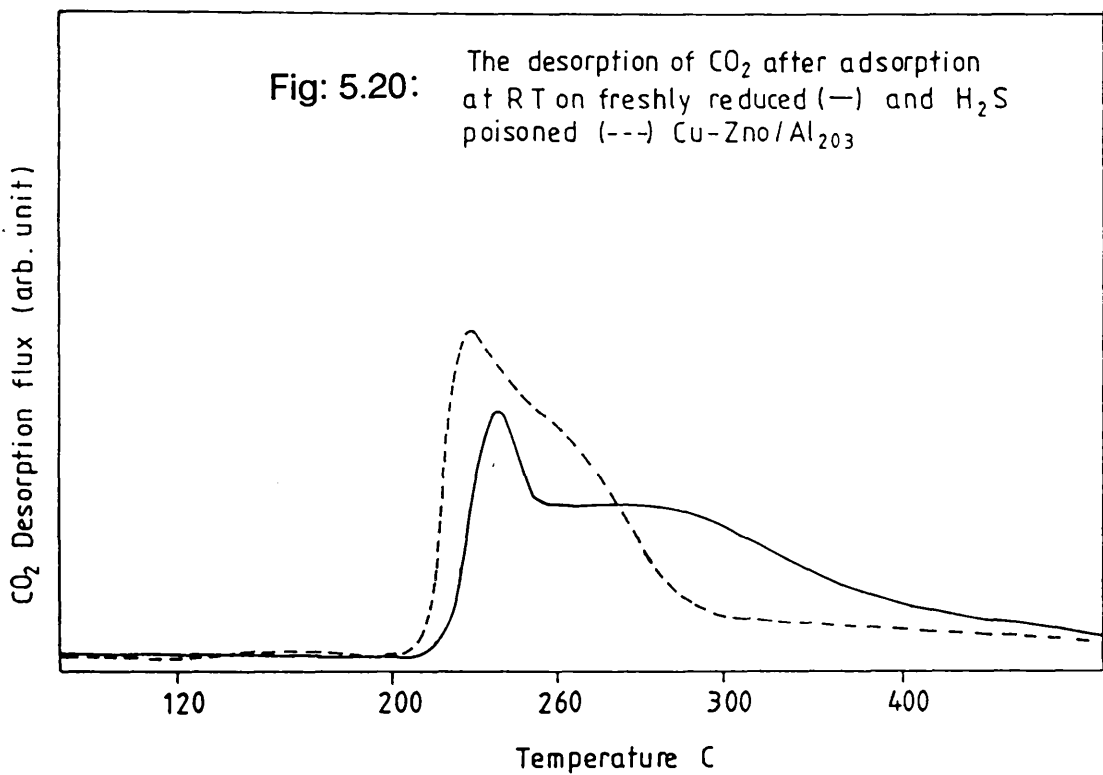
^{14}C Carbon Dioxide Adsorption on clean and Hydrogen Sulphide poisoned Copper - Zinc Oxide/Alumina at Room Temperature



after 3 pulses. ^{14}C -carbon dioxide adsorption on the hydrogen sulphide poisoned catalyst produced a similar isotherm but as expected, the adsorption capacity was lower; 9.725×10^{18} compared with 7.618×10^{18} molecules (g.catal^{-1}) adsorbed on the poisoned surface (0.13 H_2S coverage), which represents a decrease of ca. 22% in uptake. This value is in good agreement with the 20% decrease in the surface count rate obtained from the adsorption isotherm on clean and poisoned $\text{Cu-ZnO/Al}_2\text{O}_3$ samples [figure 5.19].

5.3.4 ^{14}C -Carbon Dioxide Desorption from Clean and H_2S poisoned $\text{Cu-ZnO/Al}_2\text{O}_3$ Catalyst Surfaces

The $\text{Cu-ZnO/Al}_2\text{O}_3$ surface which had been precovered at room temperature with ^{14}C -carbon dioxide was heated in a controlled manner (ca. $18^\circ\text{C}/\text{min}$), and the amounts of species desorbed were determined as previously described. The desorption profile obtained from the clean surface (figure [5.20], solid line) showed two poorly resolved peaks. Desorption commences at ca. 210°C with the second arising as a tail of the first and appearing at ca. 255°C . This tailing effect is evident over the temperature range $255\text{--}380^\circ\text{C}$. A total of ca. 7.812×10^{18} molecules (g.catal^{-1}) was desorbed from the surface leaving ca. 20% of the original ^{14}C -carbon dioxide uptake on the surface as a strongly adsorbed species. This two step desorption is also



evident from the Isoflo flow desorption spectrum [figure 5.21]. Again one can conclude that two distinct adsorption states for ^{14}C -carbon dioxide exist on $\text{Cu-ZnO/Al}_2\text{O}_3$.

The desorption of ^{14}C -carbon dioxide from a hydrogen sulphide poisoned (0.13 surface coverage) $\text{Cu-ZnO/Al}_2\text{O}_3$ sample was studied. Figure [5.20] (dotted line) details the desorption profile resulting from gas chromatographic analysis. The desorption profile is markedly different from that obtained for the unpoisoned surface in that (i) the first desorption peak is more intense and occurs in a lower temperature range, ie. $200\text{-}240^\circ\text{C}$ and (ii) the second desorption peak again appears as a broad shoulder of the first and occurs over the lower temperature range ($250\text{-}285^\circ\text{C}$).

After the desorption of ^{14}C -carbon dioxide from the poisoned $\text{Cu-ZnO/Al}_2\text{O}_3$ surface only ca. 8% ^{14}C -carbon dioxide species were retained on the surface. Similar results were observed from the Isoflo studies, figure [5.22]. The overall results obtained from these desorption studies are summarised in table 5.6.

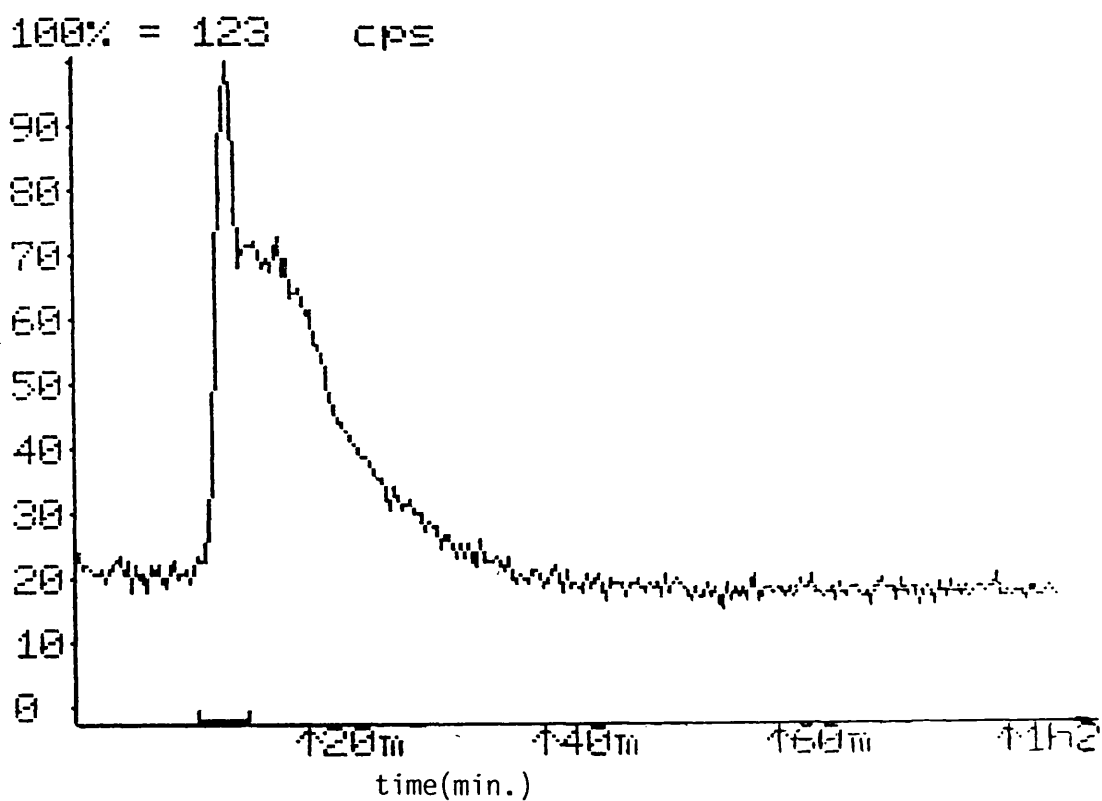


Fig: 5.21

Isoflo desorption Profile of $^{14}\text{C-CO}_2$ following adsorption at RT on clean Cu-ZnO/Al₂O₃ catalyst.

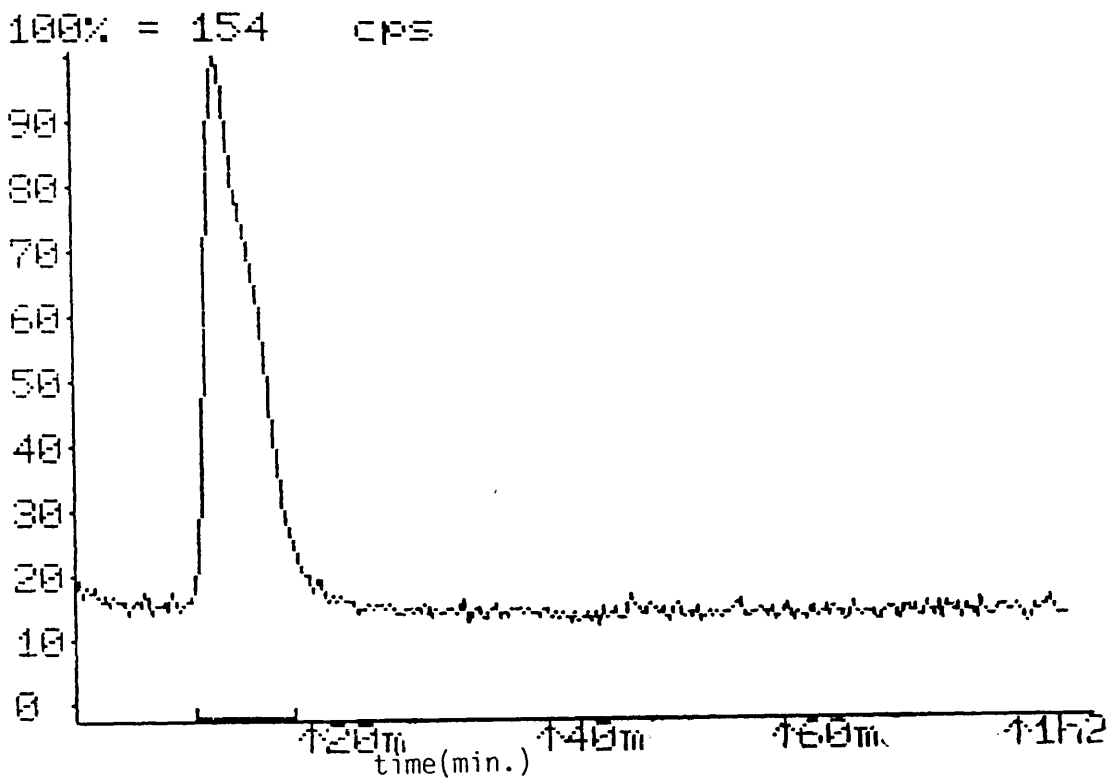


Fig: 5.22

Isofluorine desorption Profile of $^{14}\text{C}-\text{CO}_2$ following adsorption at RT on poisoned Cu-ZnO/Al₂O₃ catalyst.

Table 5.6

The extent of ^{14}C -carbon dioxide desorption (molecules per g/catal.) from a range of Cu-ZnO/Al₂O₃ catalysts

Catalyst (0.15 g)	Reducing agent	Adsorption temperature °C	No. of molecules X 10 ¹⁸		Adsorption temperature °C
			Adsorb.	Desorb.	
Cu-ZnO/Al ₂ O ₃	6% H ₂ in N ₂ at 250 °C	250	9.463	7.312	200-390
Cu-ZnO/Al ₂ O ₃	CO at 250 °C	RT	12.343	11.062	200-380
Cu-ZnO/Al ₂ O ₃	6% H ₂ in N ₂ at 250 °C	RT	9.725	7.812	210-380
Poisoned Cu-ZnO/Al ₂ O ₃	6% H ₂ in N ₂ at 250 °C	RT	7.618	7.031	200-280

5.3.5 The Adsorption of ^{14}C -Carbon Dioxide on Clean and Poisoned ZnO Catalyst

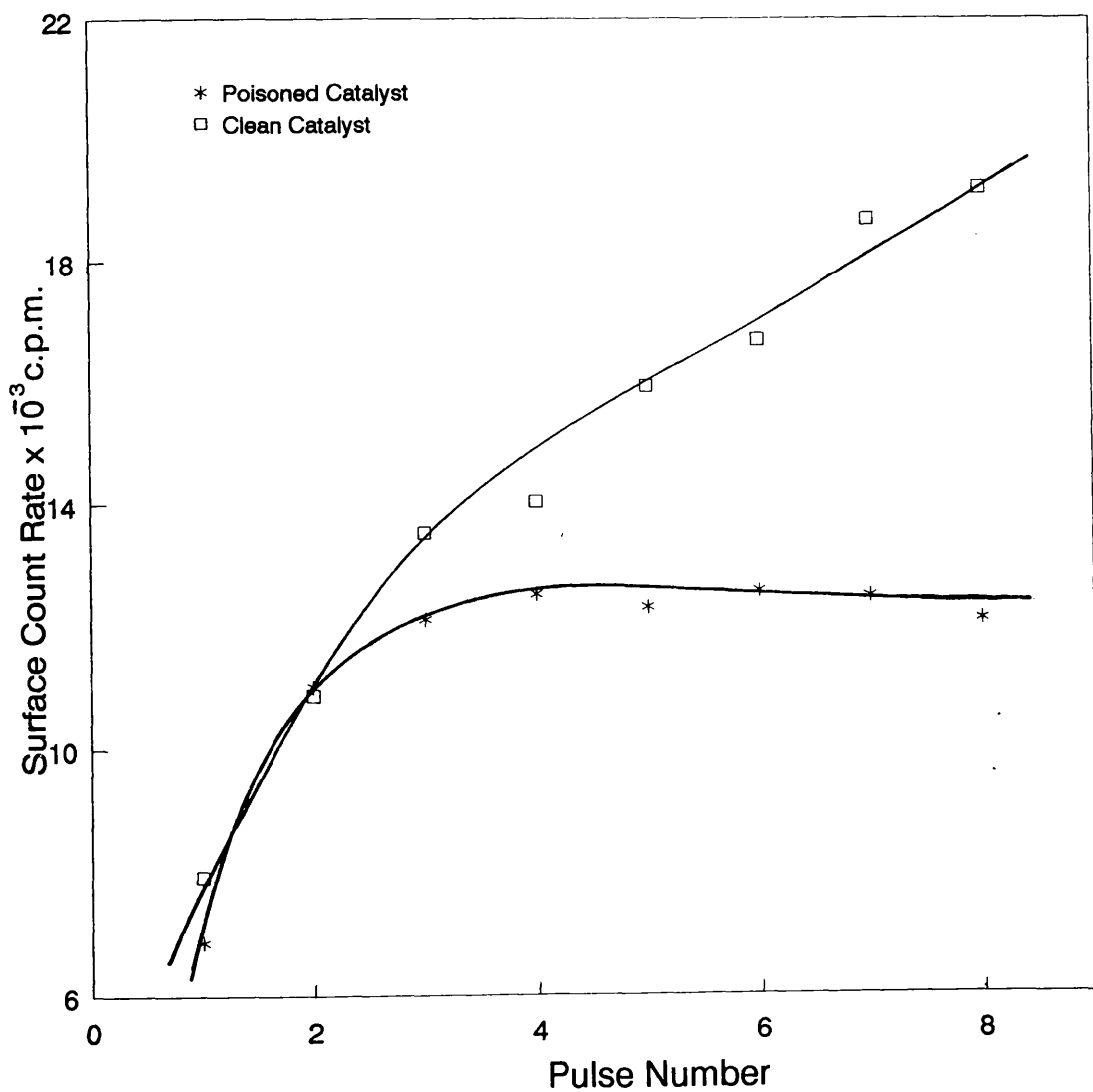
Two zinc oxide samples were used to investigate the extent of ^{14}C -carbon dioxide adsorption at different temperatures. Both samples were activated in 6% hydrogen in nitrogen (25 ml/min) at 250°C for 14 hours. The first catalyst (zinc oxide 75-1) exhibited negligible adsorption of ^{14}C -carbon dioxide at 250°C or room temperature. In the case of the second catalyst sample (basic zinc carbonate), there was no significant adsorption at 250°C, but the catalyst exhibited a high uptake of ^{14}C -carbon dioxide at

room temperature; no gas phase ^{14}C -carbon dioxide was detected over the first three pulses. figure [5.23] shows the adsorption isotherm of ^{14}C -carbon dioxide at room temperature. The surface count rate increased slowly over the first three pulses of ^{14}C -carbon dioxide. This step was then followed by a linear increase in the surface count rate. At a higher exposure (after eight pulses), the catalyst surface was saturated and no further increase in the surface count rate was observed.

As in the case of $\text{Cu}/\text{Al}_2\text{O}_3$ and $\text{Cu-ZnO}/\text{Al}_2\text{O}_3$, adsorption/desorption on a ZnO surface was also monitored by the gas chromatography and the Isoflo. In figure [5.24] (solid line) and figure [5.25], the desorption profiles of adsorbed ^{14}C -carbon dioxide at room temperature from ZnO obtained from both techniques are presented. It can be seen that desorption occurs in the temperature range ca. $320\text{-}680^\circ\text{C}$. The desorption profile is characterised by an initial small broad peak ($320\text{-}450^\circ\text{C}$) followed by a sharper peak ($450\text{-}680^\circ\text{C}$). The latter peak may be due to the carbonate species present in the catalyst during the preparation procedure, particularly as this large peak was not detected by the Isoflo, indicating that there was no ^{14}C -carbon dioxide containing species associated with this peak [figure 5.25]. The desorption data revealed that ca. 51% ^{14}C -carbon dioxide was retained on the surface as strongly held species.

Fig: 5.23

^{14}C -Carbon Dioxide Adsorption on Clean And Hydrogen Sulphide poisoned Zinc Oxide at Room Temperature



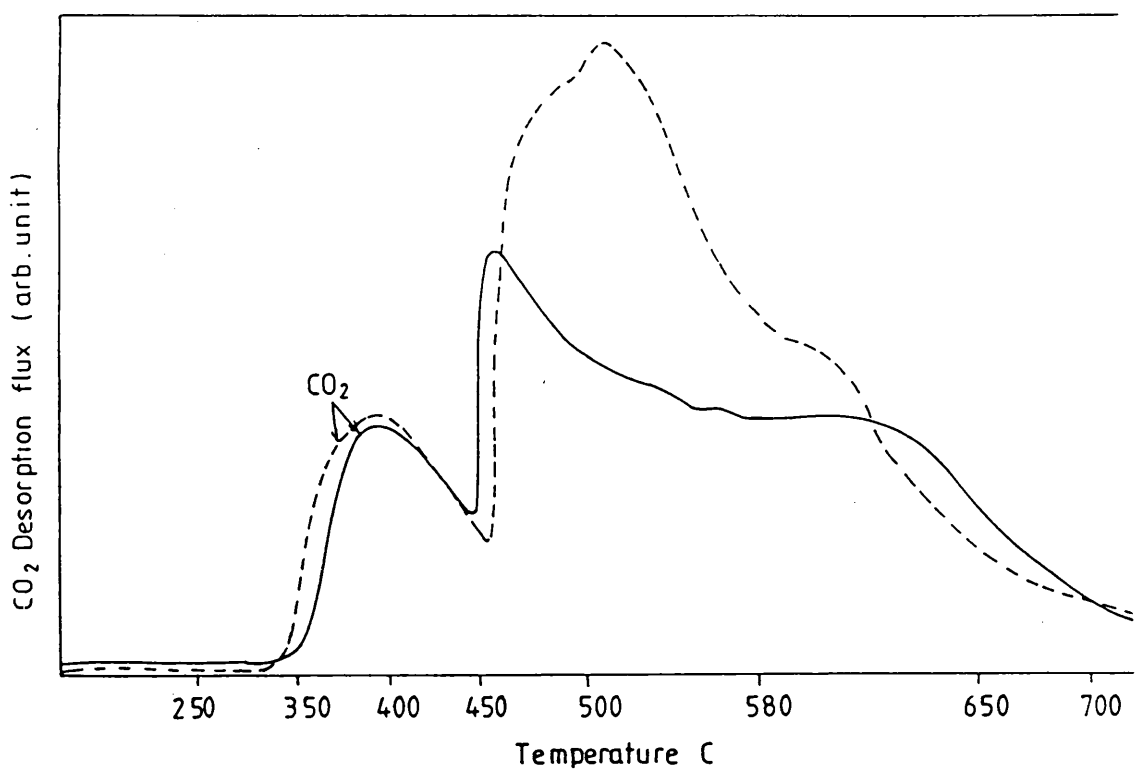


Fig. 5.24 (¹⁴C) CO₂ Desorption from ZnO following adsorption at RT on clean (—), and H₂S poisoned (---) samples.

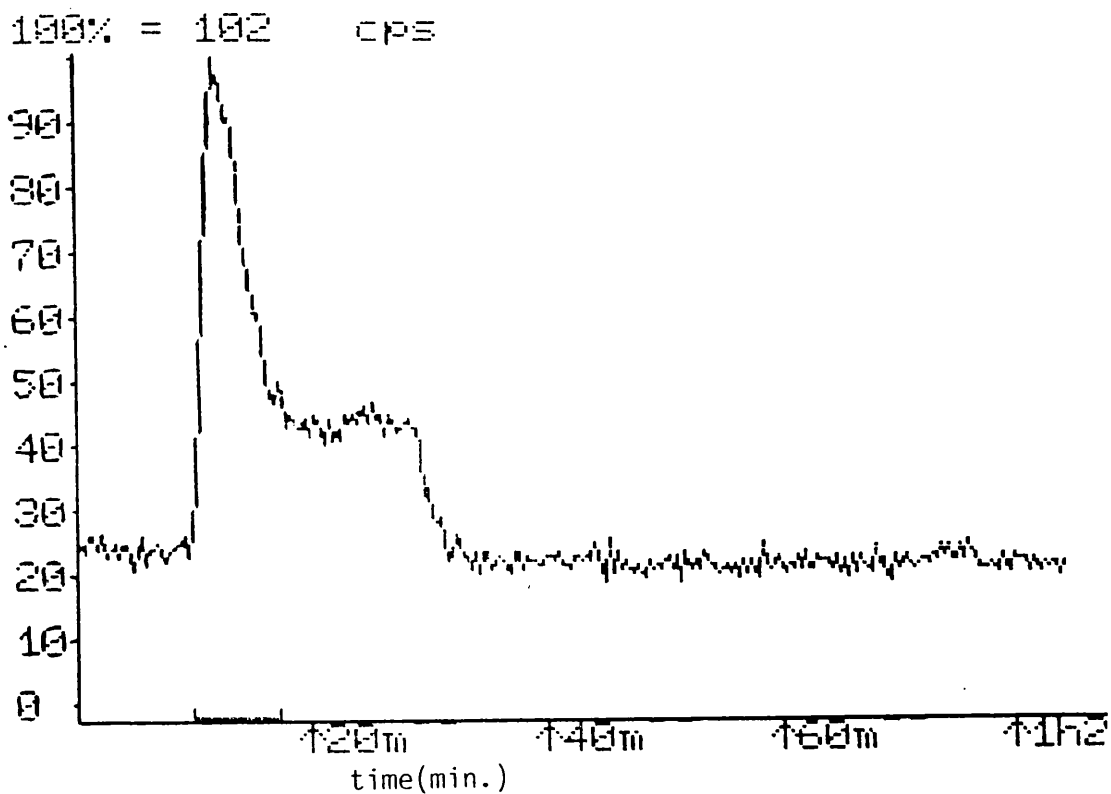


Fig: 5.25

Isofluorescence desorption Profile of $^{14}\text{C}-\text{CO}_2$ following adsorption at RT on clean ZnO surface.

On a ZnO sample poisoned with H₂S, the adsorption isotherm is presented in figure [5.23]. Prior to the adsorption of ¹⁴C-carbon dioxide, the 6% hydrogen in nitrogen reduced catalyst was flushed with helium (30 ml/min) for ca. one hour at 250°C, the temperature lowered to room temperature and four pulses of hydrogen sulphide (100 torr each) were introduced to the catalyst surface. The adsorption isotherm [figure 5.23] showed a similar initial increase in the surface count rate followed by a flattening of the curve as no further increase in the surface count rate was observed. A 16% decrease in the ¹⁴C-carbon dioxide surface capacity resulted from the hydrogen sulphide poisoning. Heating the preadsorbed hydrogen sulphide poisoned surface generated desorption profiles which were very similar to those observed for the unpoisoned sample, figures [5.26, 5.27]. This treatment removed 90% of the adsorbed ¹⁴C-carbon dioxide species. The room temperature Isoflo desorption profiles [figures 5.25, 5.26] reveal a ca. 19% decrease in ¹⁴C-carbon dioxide adsorption on the poisoned surface. It should be noted that the secondary large desorption peak in both chromatograph traces has not been considered as a separate peak.

The pertinent adsorption data are summarised in table 5.7.

Region:
100% = 79.3 cps

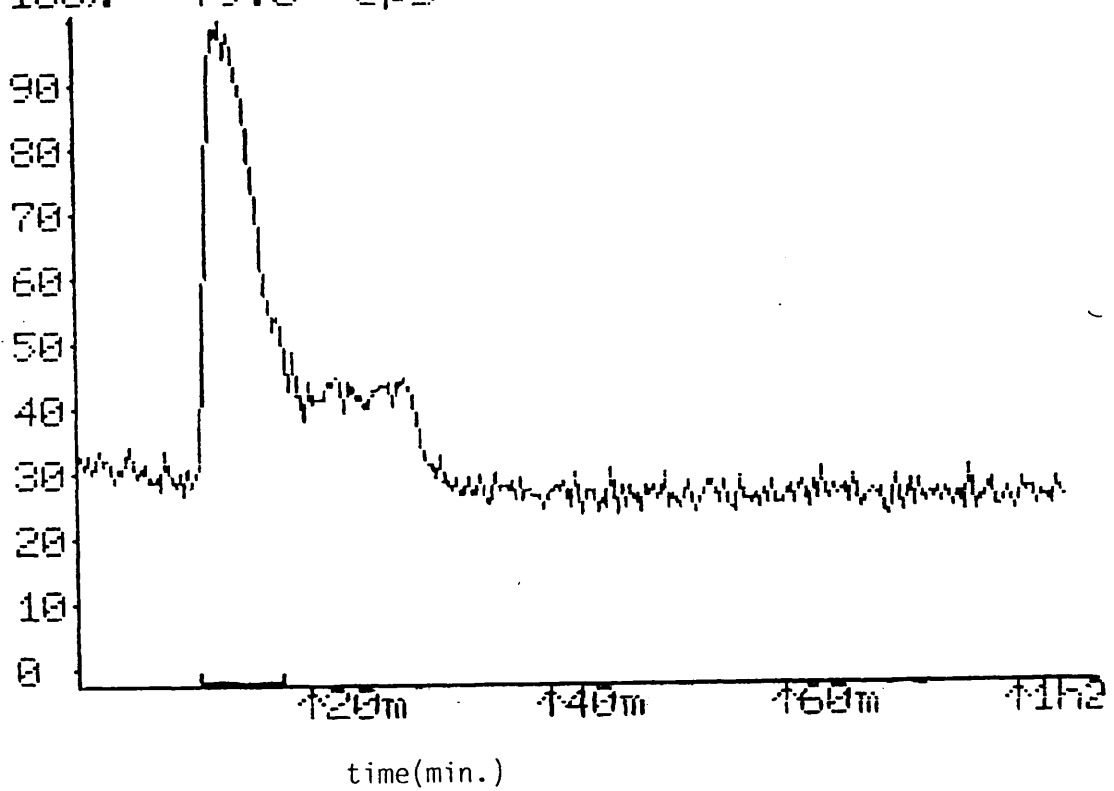


Fig: 5.26

Isofluorescence desorption Profile of $^{14}\text{C-CO}_2$ following adsorption at RT on poisoned ZnO surface.

Fig: 5.27

^{14}C -Carbon Dioxide Adsorption on Clean and Hydrogen Sulphide poisoned Alumina at Room Temperature

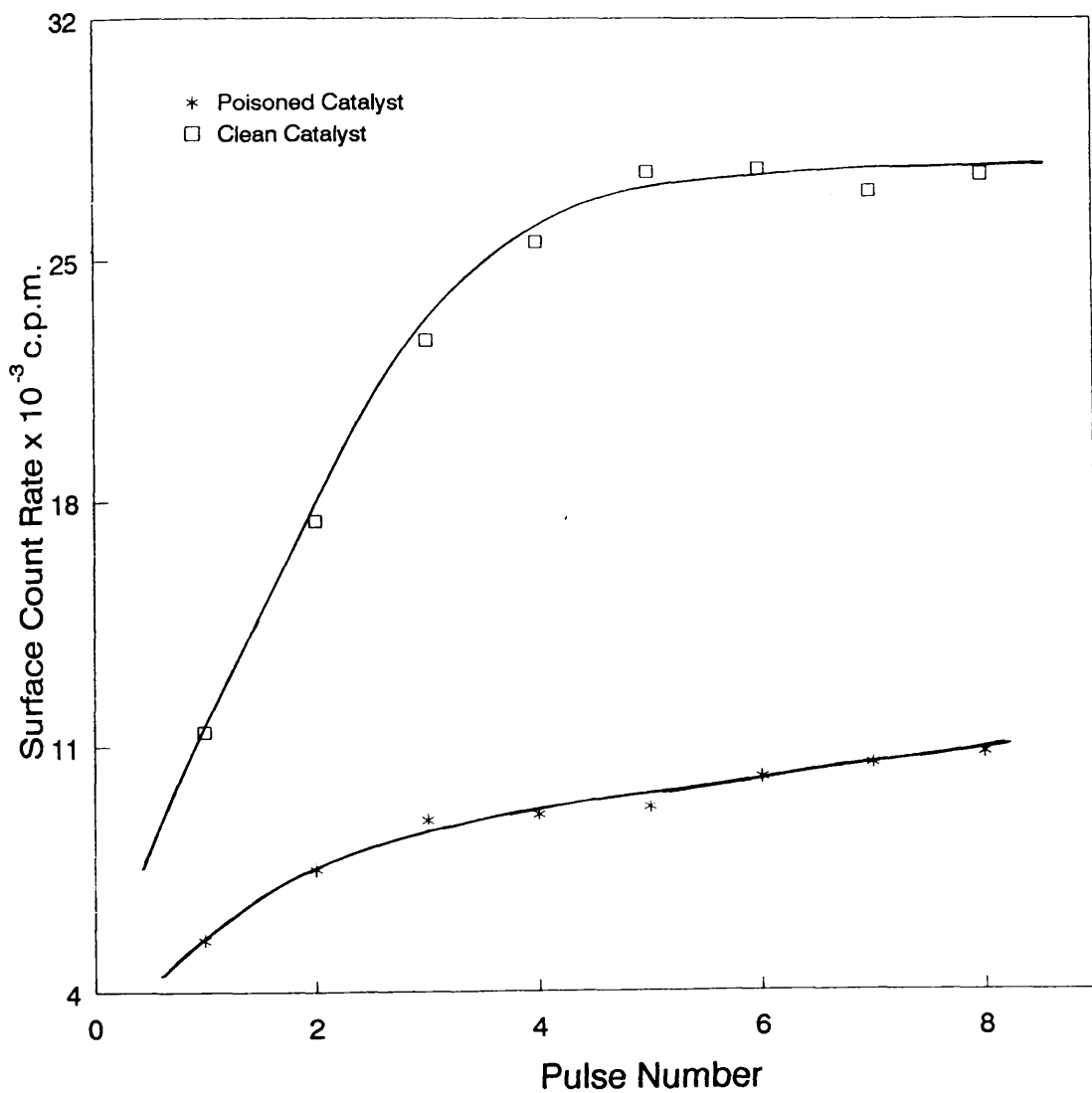


Table 5.7

The effect of H₂S on the adsorption capacity of ZnO for ¹⁴C-carbon dioxide (molecules per g/catal.)

Catalyst (0.15 g)	No. of molecules X 10 ¹⁸		Desorption temperature °C	Desorbed Gas phase count C.P.S
	Adsorbed	Desorbed		
Clean ZnO	6.243	3	320-680	31215
poisoned ZnO	5.412	4.9	300-650	25412

5.3.6 The Adsorption of ¹⁴C-Carbon Dioxide on Clean and H₂S Poisoned Alumina Surfaces

Figure [5.27] shows the adsorption isotherm of ¹⁴C-carbon dioxide on a freshly reduced alumina surface at room temperature. The adsorption isotherm clearly shows that alumina is saturated with adsorbed ¹⁴C-carbon dioxide (over the first 5 pulses). A broad desorption peak [figure 5.28] was obtained on heating the catalyst surface; this desorption peak occurs in the range 180-380°C and corresponds to the removal of ca. 92% of the adsorbed ¹⁴C-carbon dioxide. The Isoflo desorption trace, shown in figure [5.29], also shows a single broad peak.

As in the previous studies, hydrogen sulphide poisoning

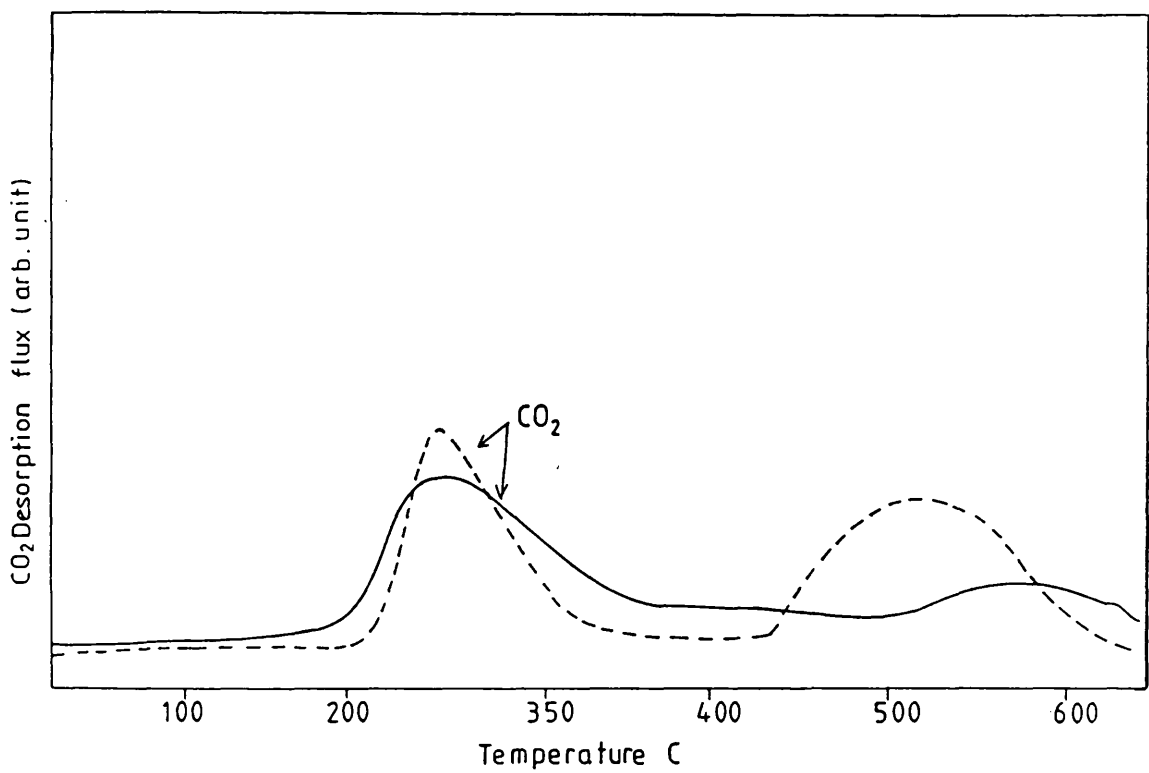


Fig. 5.28 (^{14}C) CO_2 desorption from Al_2O_3 following adsorption at RT on clean (—), and H_2S poisoned samples.

100% = 87.3 cps

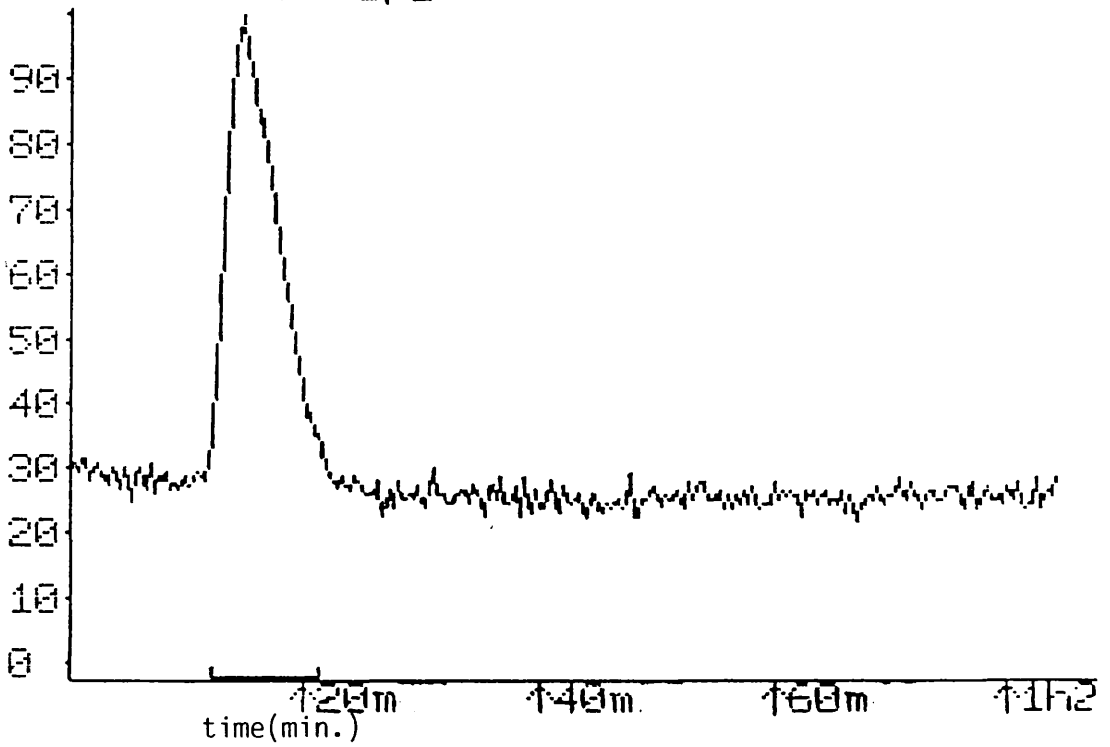


Fig: 5.29

Isofluorescence desorption Profile of $^{14}\text{C}-\text{CO}_2$ following adsorption at RT on clean Al_2O_3 surface.

on the alumina markedly lowered the extent of ^{14}C -carbon dioxide adsorption, figure [5.27]; a slight increase in the surface count rate was observed after the admission of one pulse of ^{14}C -carbon dioxide followed by the immediate attainment of a saturation level, which is 65% less than that measured for the unpoisoned sample. Desorption studies generated a gas chromatography peak at 270°C , figure [5.28] (broken line); a second broader peak (in the temperature range $430\text{--}630^\circ\text{C}$) which arose for both poisoned and non-poisoned samples, can again be attributed to residual carbonate presented on the catalyst surface after preparation. The absence of a second band in the Isoflo traces supports this hypothesis [figure 5.29, 5.30]. The retention of a trace amount (ca. 5% of the original) of ^{14}C -carbon dioxide on the poisoned surface must be due to the removal of sulphur from the alumina surface during the helium flushing step. This compares with a 30% decrease in the desorbed gas phase activity as inferred from the radiotracer studies, figure [5.29 and 5.30]. The estimated values for adsorbed/desorbed ^{14}C -carbon dioxide molecules (g.catal^{-1}) as well as the desorbed gas phase count rate on both clean and poisoned alumina samples are given in table 5.8.

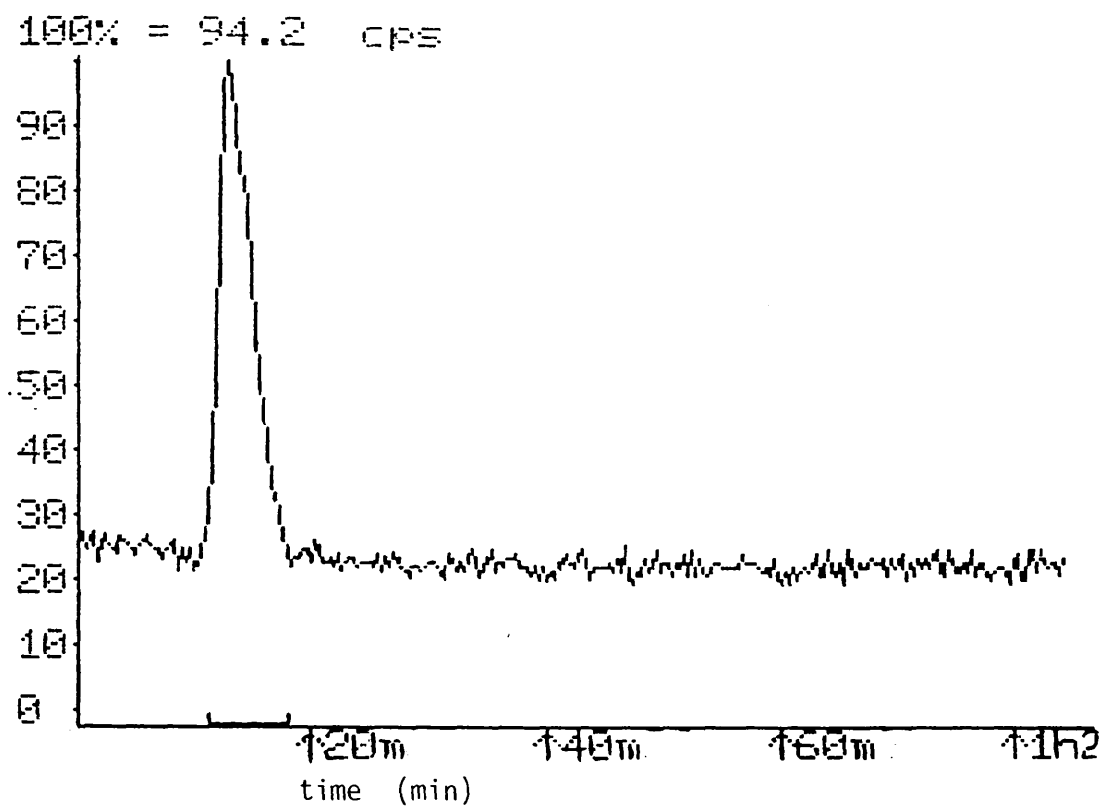


Fig: 5.30

Isoflo desorption Profile of $^{14}\text{C}-\text{CO}_2$ following adsorption at RT on poisoned Al_2O_3 surface.

Table 5.8

The estimated values of adsorbed and desorbed ^{14}C -carbon dioxide on clean and poisoned alumina surfaces

Catalyst	No. of molecules X 10^{18}		Desorption temperature $^{\circ}\text{C}$	Desorbed Gas phase count
	Adsorbed	Desorbed		
Reduced alumina Sample	8.118	7.487	270	32155
H_2S poisoned alumina sample	3.918	3.743	270	22744

CHAPTER SIX

RADIOTRACER STUDY OF THE ADSORPTION OF ^{35}S - HYDROGEN SULPHIDE ON COPPER-BASED CATALYST SURFACES

The pulse flow system employed to study the adsorptive capacity of copper-based catalysts and related surfaces has been described in section 3.3.

The catalyst samples were activated with and without precalcination in a helium stream.

6.1 THE ADSORPTION OF ^{35}S - H_2S ON COPPER BASED CATALYSTS

In this section the adsorption of ^{35}S - H_2S on $\text{Cu}/\text{Al}_2\text{O}_3$ and $\text{Cu-ZnO}/\text{Al}_2\text{O}_3$, will be presented.

6.1.1 Adsorption of ^{35}S - H_2S on $\text{Cu}/\text{Al}_2\text{O}_3$ Surfaces

During the study of the adsorption of ^{35}S - H_2S , a sample (0.36 g) of catalyst was reduced in a flow of 6% hydrogen in nitrogen at 250°C for 14 hours and the catalyst sample was then left under helium flow (15 ml/min) for one hour, then the temperature was lowered to room temperature prior to adsorption of ^{35}S - H_2S . ^{35}S - H_2S was admitted in measured pulses (1.434×10^{21} molecules per pulse) to the catalyst surface under a slow flow of

helium (5-10 ml/min). The surface and gaseous activities were monitored by the Geiger-Muller tubes located on each side of the reaction vessel [figure 2.9]. The $^{35}\text{S-H}_2\text{S}$ adsorption isotherm at room temperature on reduced $\text{Cu/Al}_2\text{O}_3$ sample is shown in figure [6.1]. A rapid increase in the surface count rate was observed as the amount of adsorbed sulphur increased. Indeed, the catalyst surface adsorbed all the admitted $^{35}\text{S-H}_2\text{S}$ as shown by the linear increase in the surface count rate, with a corresponding absence of the gas phase count as the number of $^{35}\text{S-H}_2\text{S}$ pulses increased. At a surface sulphur coverage (θ_s) of 0.219 the gas phase count rate became higher than the GM tube background count, and increased linearly with further $^{35}\text{S-H}_2\text{S}$ pulses. In the same pulse range (ca. 9-15) the surface count rate reached a plateau suggesting a surface saturation with $^{35}\text{S-H}_2\text{S}$. At this point the surface coverage (θ_s) was calculated to be 0.4.

Leaving the catalyst under a helium flow (15 ml/min) for ca. 24 hours had a negligible effect on the surface count suggesting that $^{35}\text{S-H}_2\text{S}$ is strongly adsorbed on $\text{Cu/Al}_2\text{O}_3$.

The results obtained for the adsorption of $^{35}\text{S-H}_2\text{S}$ on $\text{Cu/Al}_2\text{O}_3$ are summarised in table 6.1.

Fig: 6.1

³⁵Sulphur - Hydrogen Sulphide Adsorption on Copper/Alumina Catalyst Reduced with 6% Hydrogen in Nitrogen at 250°C for 14 Hours. Adsorption at room Temperature. Pulse Size 2.5 Torr

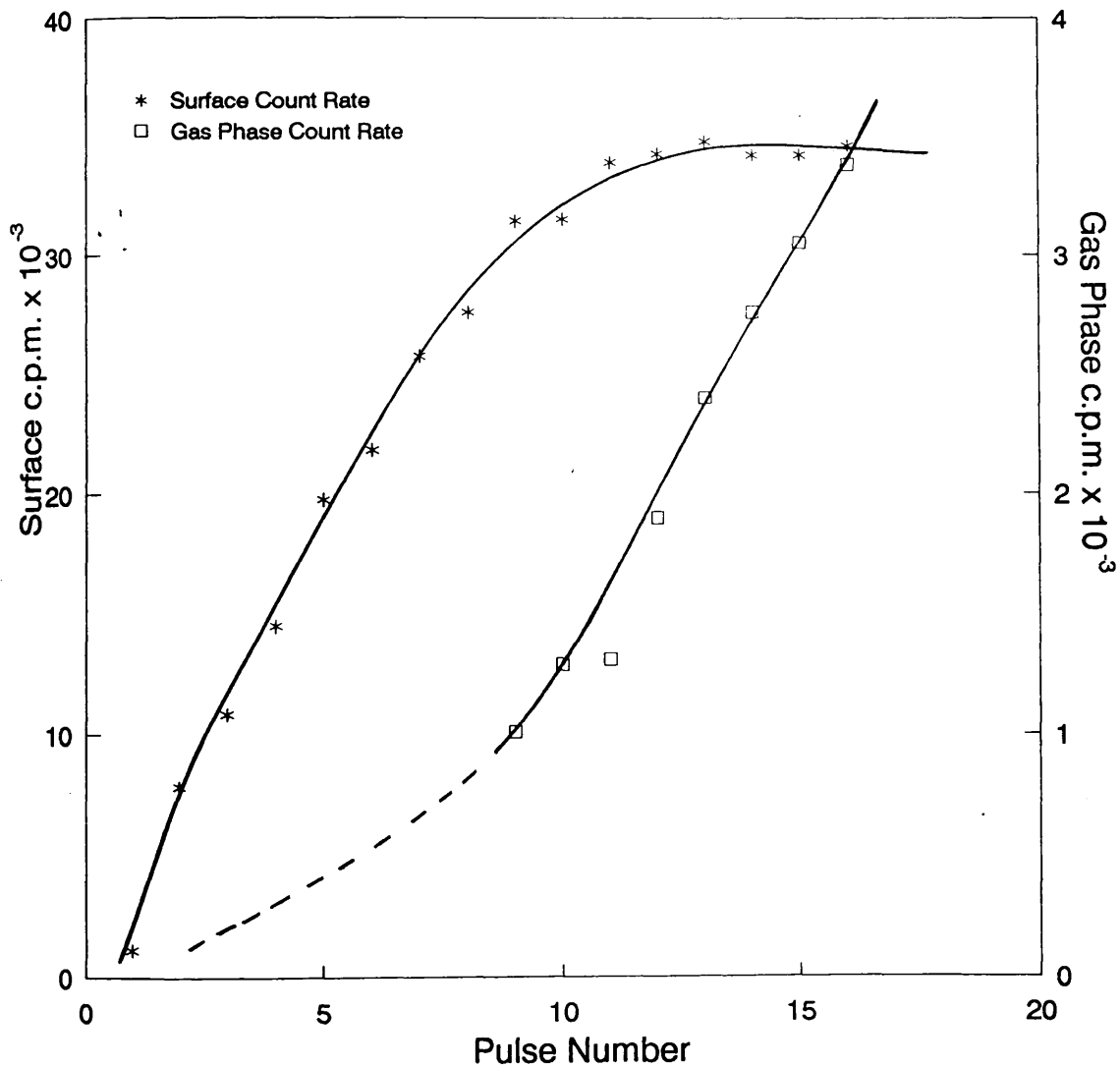


Table 6.1

The surface and gas phase count rate observed during the adsorption of $^{35}\text{S-H}_2\text{S}$ on $\text{Cu/Al}_2\text{O}_3$ surface

Pulse number	Net count rate c.p.m	
	Surface	Gas phase
1	1100	Bg*
3	10840	Bg
5	19778	Bg
7	25766	Bg
9	31436	1050
13	34717	1940
15	34274	3720

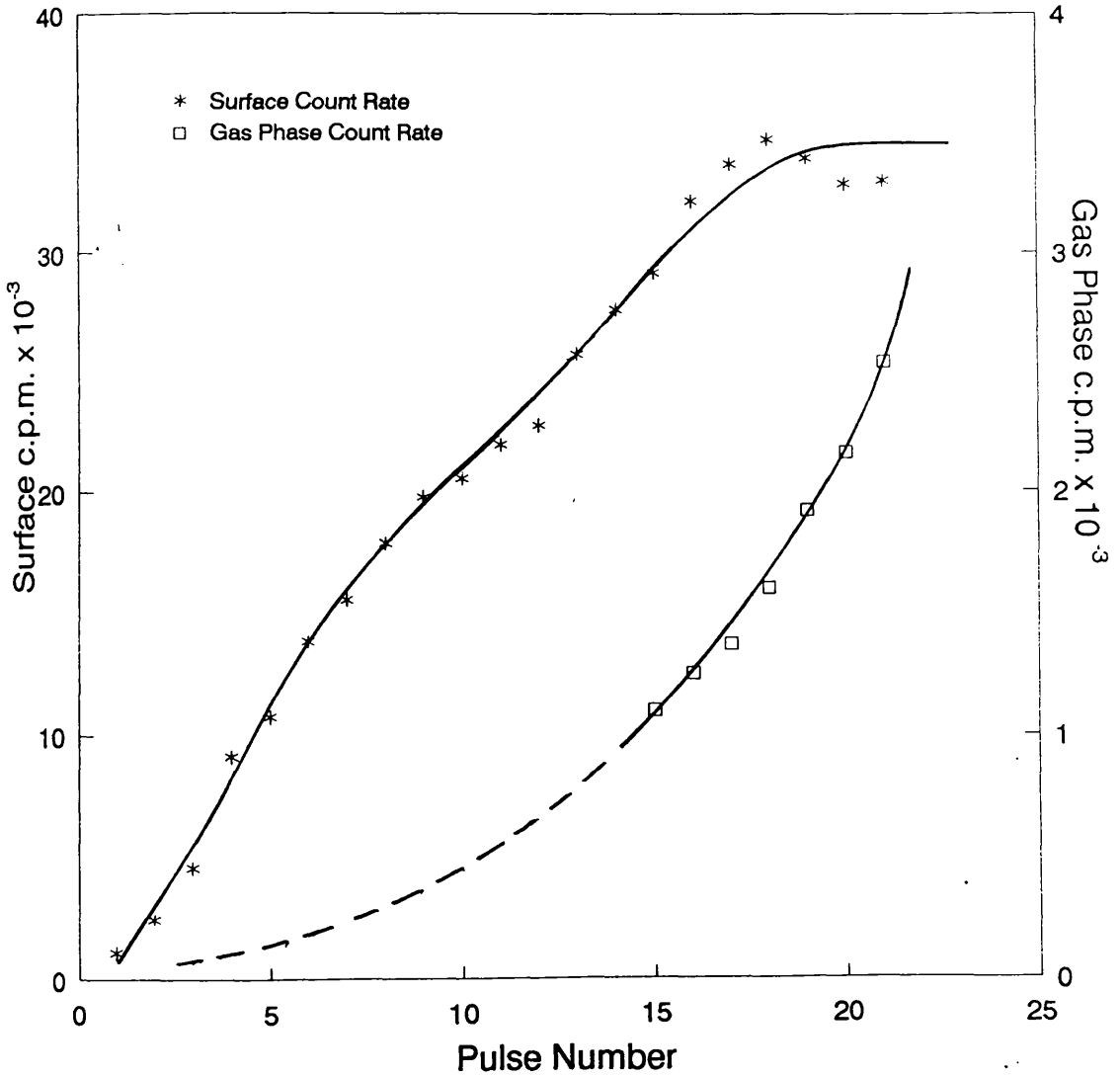
Bg* = GM background count

6.1.2 The Adsorption Isotherm of $^{35}\text{S-H}_2\text{S}$ on a $\text{Cu-ZnO/Al}_2\text{O}_3$

A similar isotherm was obtained for the adsorption of $^{35}\text{S-H}_2\text{S}$ on $\text{Cu-ZnO/Al}_2\text{O}_3$, figure [6.2], ie. a linear increase in the surface count rate with a corresponding absence of gas phase count over the first fifteen pulses of $^{35}\text{S-H}_2\text{S}$. At a surface sulphur coverage (θ_s) of about 0.15 the adsorption isotherm began to flatten, indicating the onset of surface saturation. The sulphur coverage (θ_s) value at maximum $^{35}\text{S-H}_2\text{S}$ uptake was found to be 0.2 corresponding to this plateau region. A linear increase

Fig: 6.2

³⁵Sulphur - Hydrogen Sulphide Adsorption on Copper - Zinc Oxide/
Alumina Reduced with 6% Hydrogen in Nitrogen at 250°C for 14 Hours
Adsorption at Room Temperature



in the gas phase count rate was then observed as the number of pulses was increased. As with Cu/Al₂O₃, flushing the catalyst sample of Cu-ZnO/Al₂O₃ with a 15 ml/min flow of helium at room temperature did not serve to remove any of the adsorbed H₂S species.

The variations in surface and gas phase count rate during the adsorption of ³⁵S-H₂S on Cu-ZnO/Al₂O₃ catalyst are presented in table 6.2.

Table 6.2

Surface and gas phase count rate of adsorbed ³⁵S-H₂S on
Cu-ZnO/Al₂O₃ catalyst

Pulse number	Net count rate c.p.m	
	Surface	Gas phase
1	1120	Bg [*]
3	5470	-
5	10742	-
7	15561	-
9	19780	-
13	25727	-
15	29122	-
17	32144	1250
19	33936	1965

Bg^{*} = GM background count

6.2 THE ADSORPTION OF $^{35}\text{S}-\text{H}_2\text{S}$ ON AN ALUMINA SURFACE

The alumina sample (0.15 g) was heated to 150°C under a helium flow (15 ml/min) for 2 hours before investigating the extent of $^{35}\text{S}-\text{H}_2\text{S}$ adsorption. The adsorption isotherm obtained after admitting successive pulses of $^{35}\text{S}-\text{H}_2\text{S}$ to the alumina surface at room temperature is shown in figure [6.3]. The isotherm is characterised by three steps (i) a rapid increase in both the surface and the gas phase count rate; (ii) a slow increase in both count rates as the number of $^{35}\text{S}-\text{H}_2\text{S}$ pulses is increased; (iii) a plateau region which shows no increase in sulphur uptake.

Following the adsorption of $^{35}\text{S}-\text{H}_2\text{S}$, the alumina sample was yellow but, after the desorption [figure 6.4] of most of the adsorbed sulphur the sample returned to its normal white colour. This finding suggests a weak adsorption of H_2S on the alumina surface. Furthermore, as depicted in figure [6.4] most of the adsorbed sulphur was removed after 20 minutes flushing in a helium stream (15 ml/min). In fact, a sharp increase in the gas phase count rate can be observed. Up to 57% of the total adsorbed sulphur was removed by this treatment.

Fig: 6.3

³⁵Sulphur - Hydrogen Sulphide adsorption on Alumina
Sample heated for 2 hours at 250°C under Helium
(flow rate 10ml/min.) Adsorption at Room Temperature

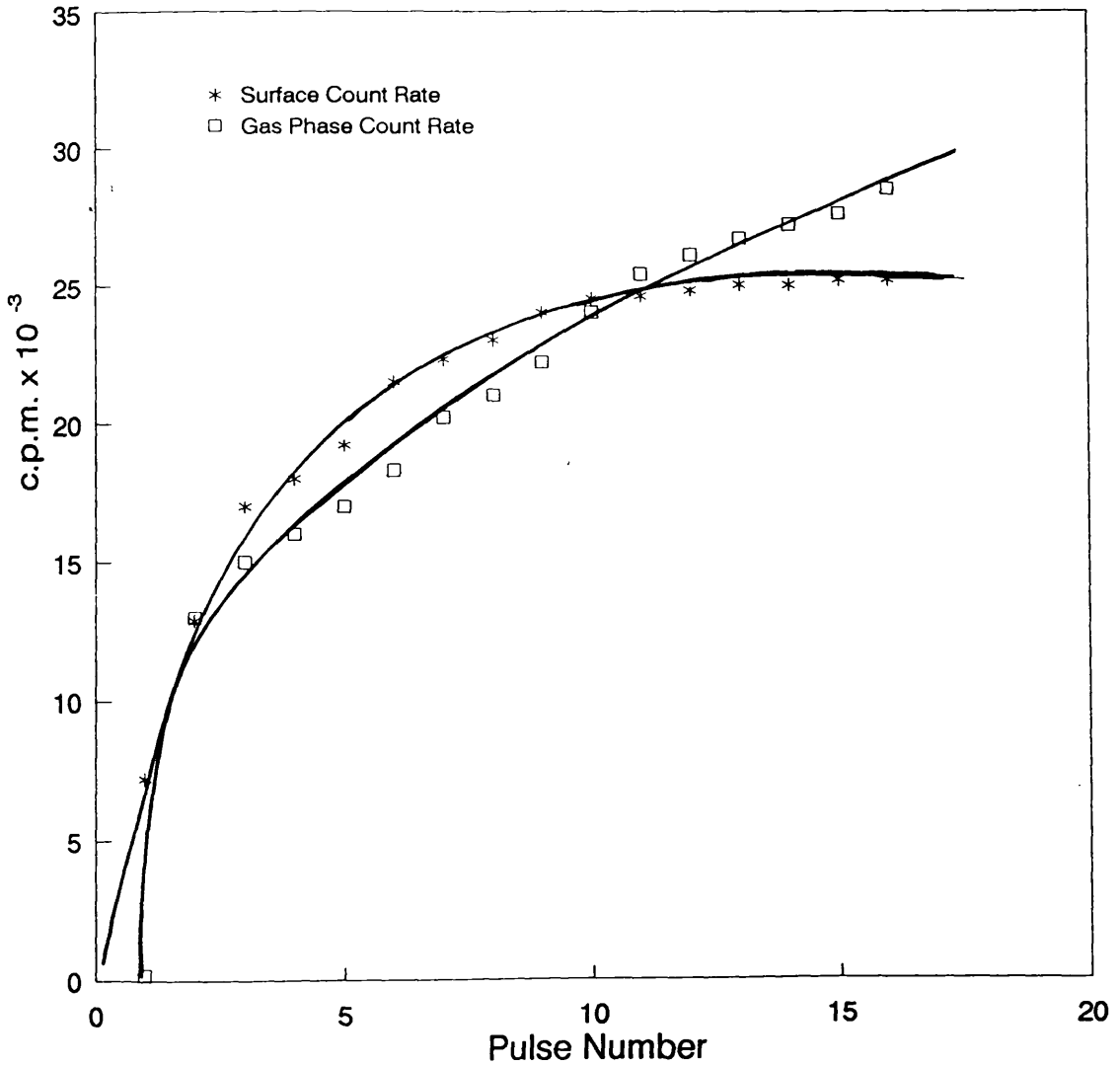
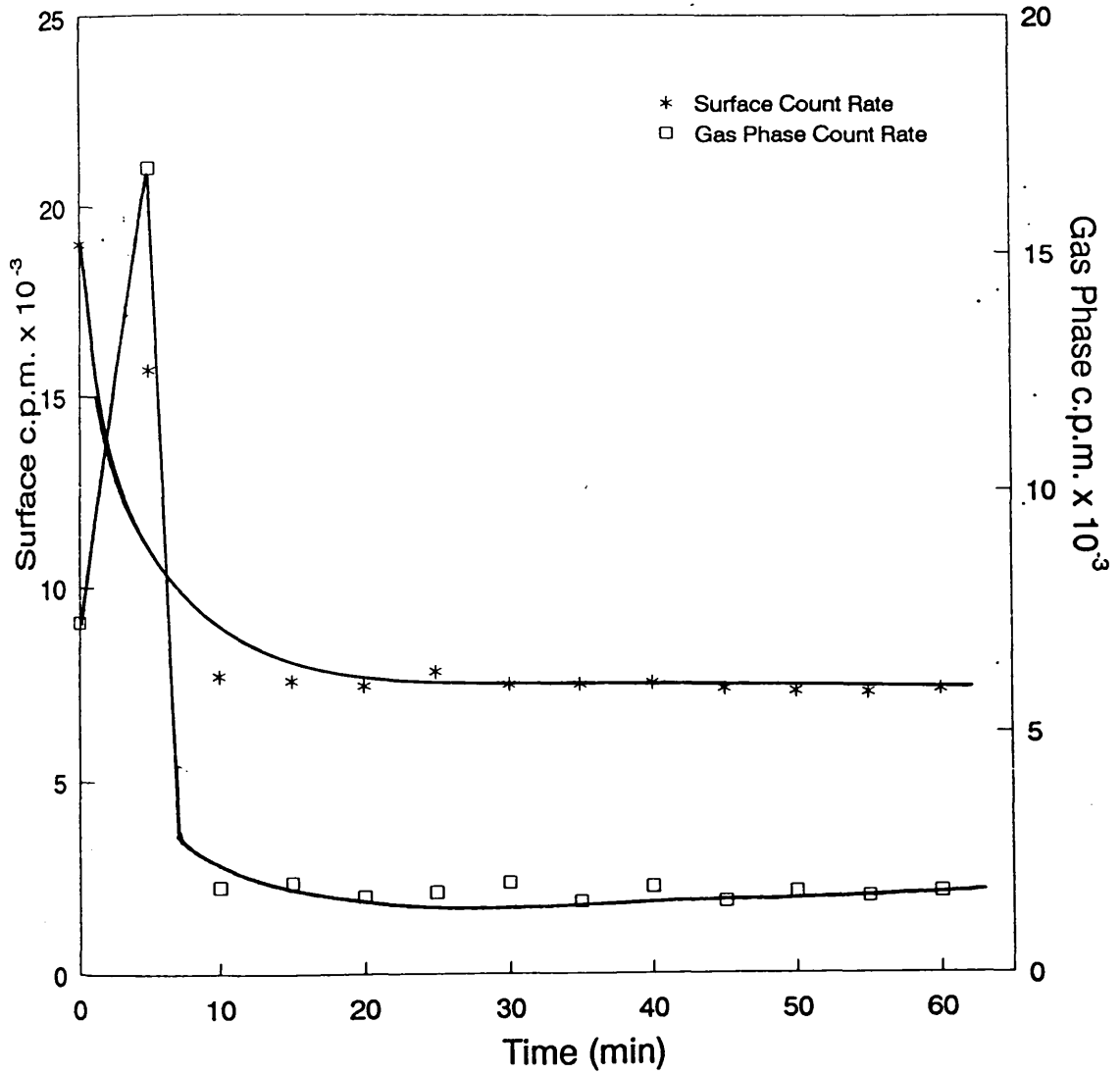


Fig: 6.4

³⁵Sulphur - Hydrogen Sulphide Desorption Following
Adsorption on Alumina Sample Heated for 2 Hours at 250°C
Desorption at Room Temperature



6.3 THE ADSORPTION OF $^{35}\text{S-H}_2\text{S}$ ON A ZnO SURFACE

The adsorption of $^{35}\text{S-H}_2\text{S}$ was studied on finely powdered ZnO sample (75-1) at room temperature in the same pulse flow system as in the above studies.

6.3.1 $^{35}\text{S-H}_2\text{S}$ Adsorption Isotherm on Untreated ZnO Surface

In this case, a powdered sample (0.36 g) of ZnO was left in a flow (ca. 15 ml/min) of helium for 2 hours at room temperature prior to the adsorption of $^{35}\text{S-H}_2\text{S}$.

The resultant room temperature isotherm is shown in figure [6.5]. It can be seen that the isotherm was of a similar shape to those obtained for the Cu/Al₂O₃ and Cu-ZnO/Al₂O₃ samples.

A rapid increase in the surface count rate was monitored by the GM tube. However, the gas phase activity did not increase significantly above the background count which indicates that all the sulphur had been adsorbed on the ZnO surface. After nine pulses of $^{35}\text{S-H}_2\text{S}$ had been introduced to the oxide surface, the surface count became constant, whereas the gas phase count did not exhibit any appreciable increase.

Flushing the saturated surface with helium (15 ml/min) resulted in a slow desorption of the strongly held sulphur species over a period of 11 hours, [figure 6.6]. In this interval, the surface count rate decreased by a

Fig: 6.5

³⁵Sulphur - Hydrogen Sulphide Adsorption on Zinc Oxide (0.356g)
Hydrogen Sulphide Press. 3 Torr

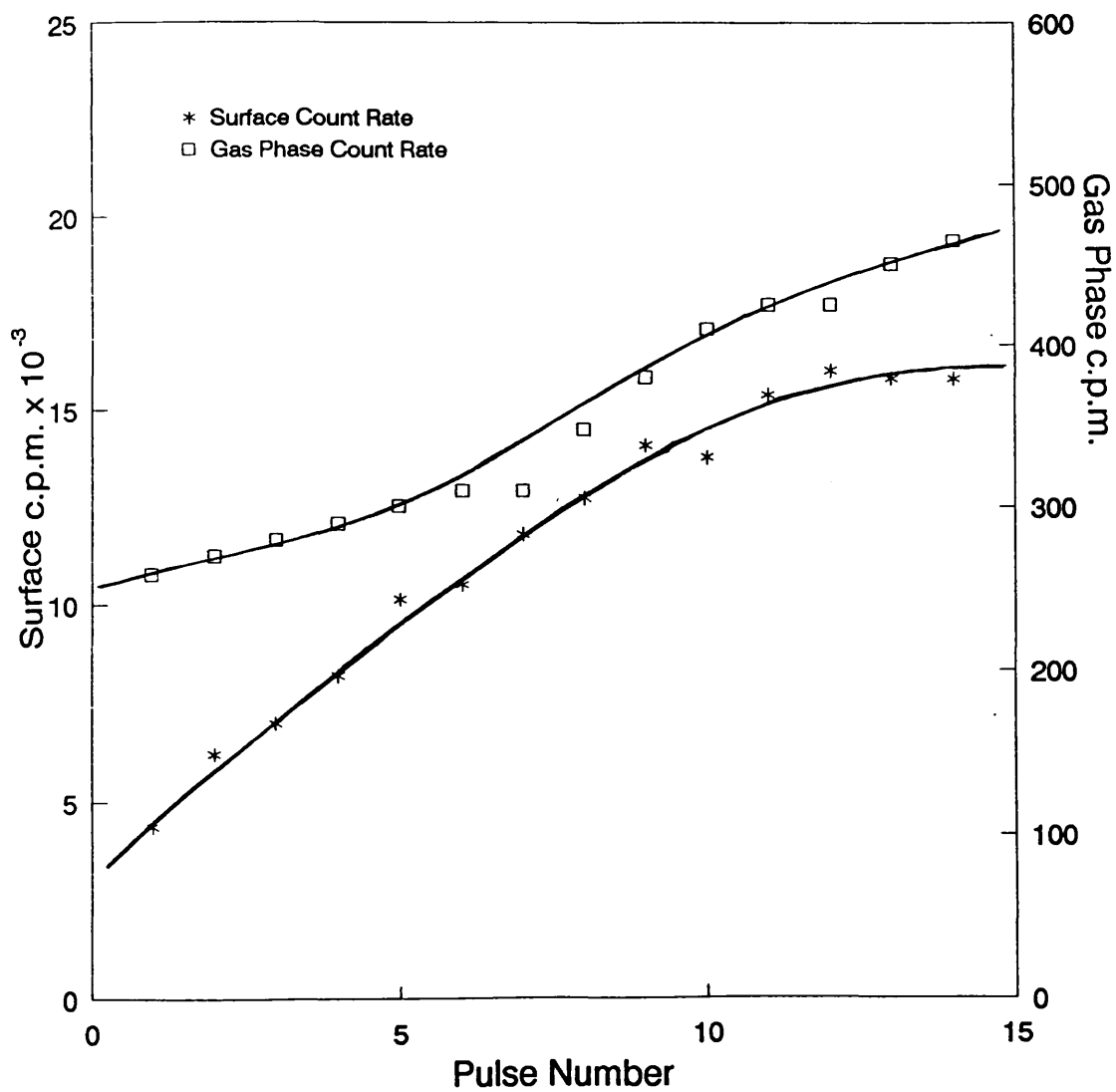
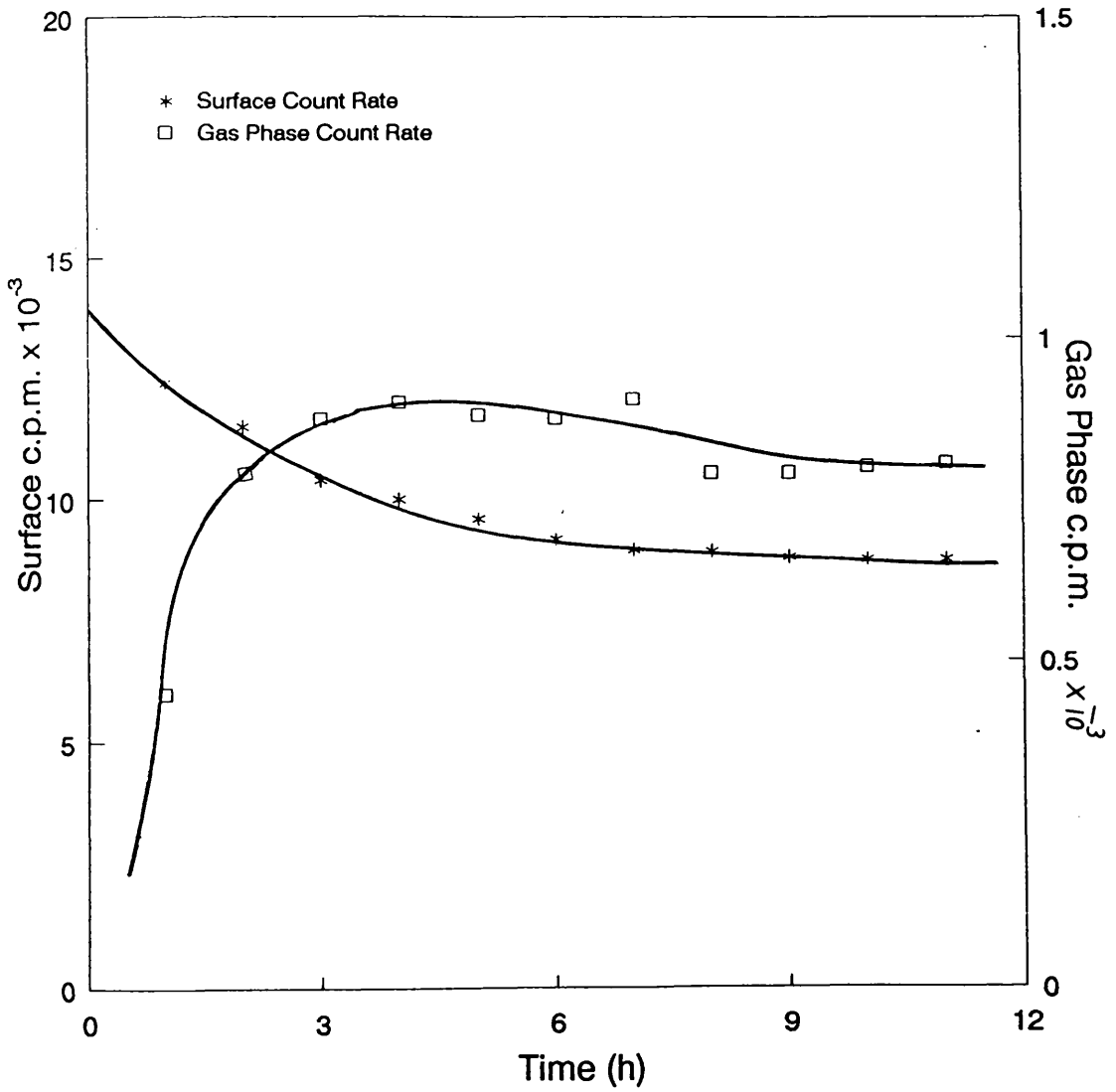


Fig: 6.6

³⁵Sulphur - Hydrogen Sulphide Desorption Following Adsorption on Zinc Oxide (0.356g) Sample



ca. 27% without a corresponding substantial increase in the gas phase counts. The variation in both count rates with time is given in table 6.3.

Table 6.3

The decrease in ZnO surface counts rate as a function of time under helium flow

Time (h)	Count rate c.p.m		% Decrease in surface count rate
	Surface	Gas phase	
1	11960	459	0
2	12052	526	0
3	10496	890	13
4	10088	913	16
5	9626	869	20
6	9175	865	24
7	8951	930	26
8	8797	782	27
9	8740	797	27
10	8797	811	27
11	8770	820	27

A further flushing of the catalyst in a 30 ml/min stream of helium for 48 hours resulted in a further drop in the surface count rate, comparing with table 6.3. The results are presented in figure [6.7] and table 6.4.

Fig: 6.7

³⁵Sulphur - Hydrogen Sulphide Desorption Following Adsorption on Zinc Oxide Sample (0.36g)
Catalyst left on 48 Hour

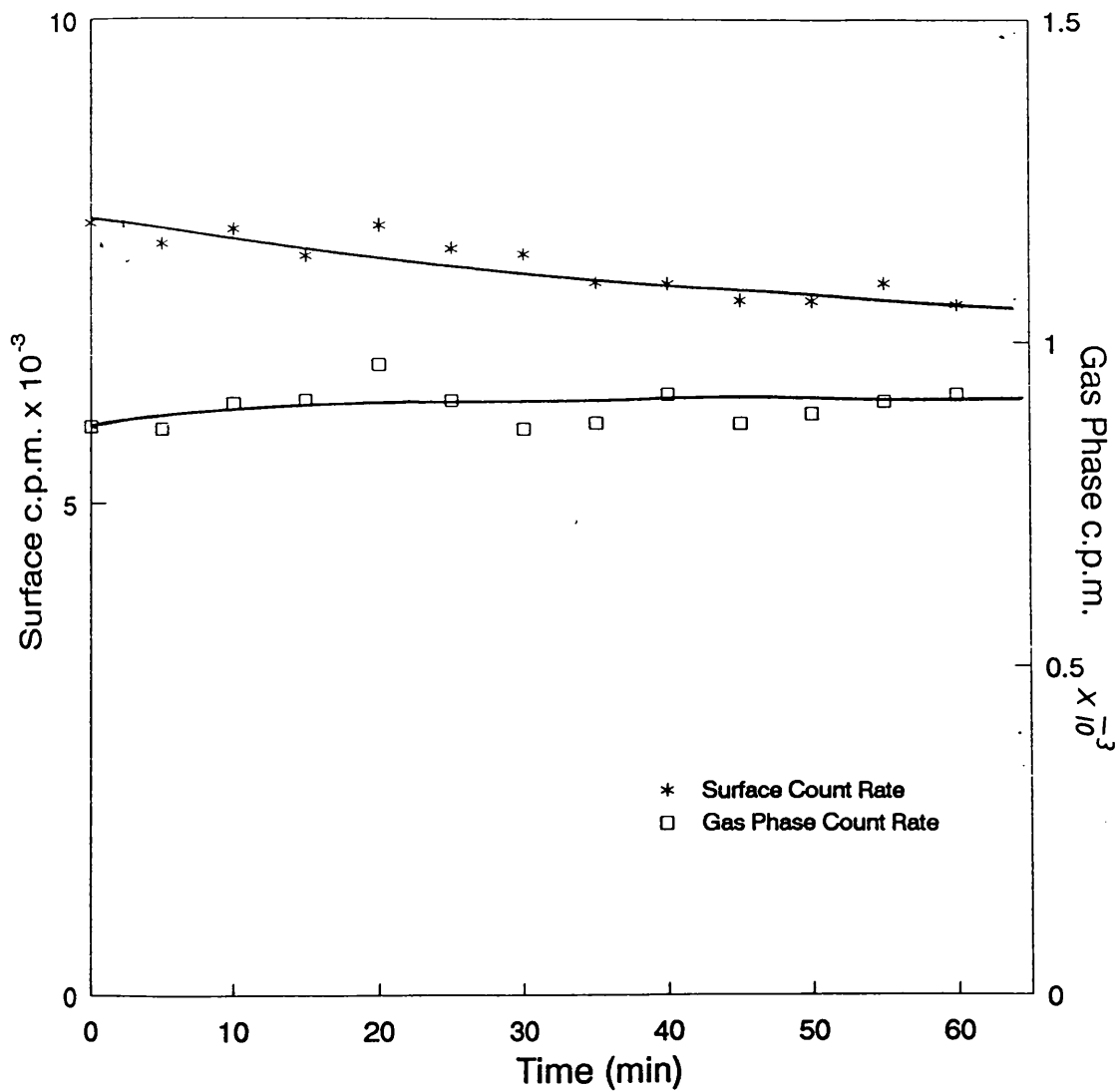


Fig: 6.8

³⁵Sulphur - Hydrogen Sulphide Desorption Following Adsorption at Room Temperature on Zinc Oxide (0.356g)
Sample left for 48 Hours under Helium

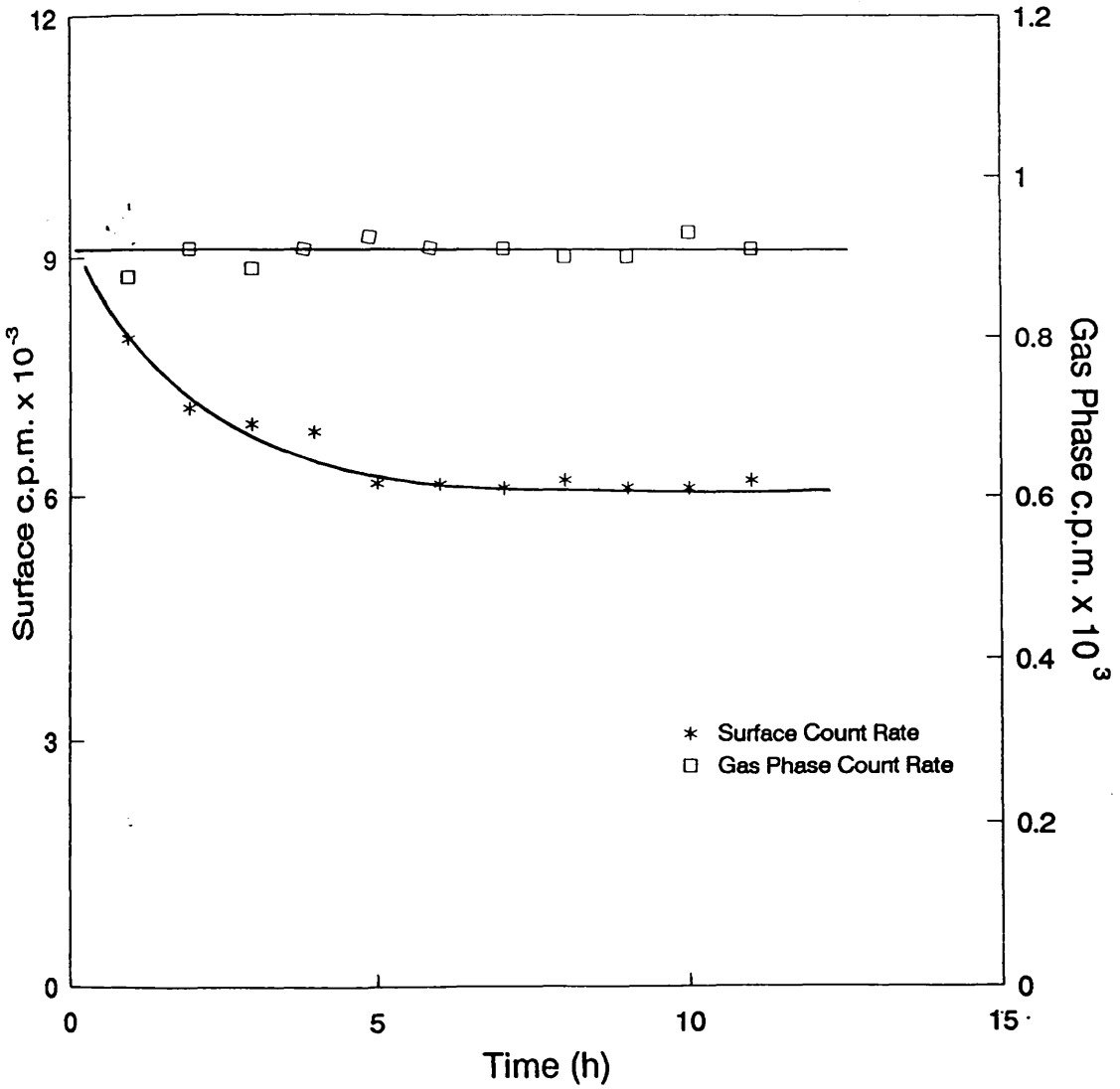


Table 6.4

The effect of 48 hours flushing in 30 ml/min of helium on
count rate

Time (h)	Count rate c.p.m		% Decrease in surface count rate
	Surface	Gas phase	
5	7685	868	27
15	7555	924	37
30	7577	878	37
35	7284	882	39
40	7101	876	41
50	7090	885	41
60	7068	919	41

It should be emphasised that although the surface phase count was lowered as a result of the helium purge, the gas phase count remained largely unaffected.

As a logical extension of this study a sample of ZnO (0.36 g) was treated in a flow of helium (15 ml/min) for 30 minutes prior to the saturation with H₂S, (ie. 14 pulses). Purging the surface in 15 ml/min stream of helium for 48 hours lowered the surface concentration of H₂S. As shown in figure [6.8], the surface count rate was measured at one hour periods for 11 hours. The initial measurement revealed 44% decrease in surface count, which decreased further over the next 5 hours, before a steady

count was attained. In this time period, the gas phase counts remained constant as is shown graphically in figure [6.8].

6.3.2 The Effect of Carbon Dioxide on the Adsorption Isotherm of $^{35}\text{S-H}_2\text{S}$ on ZnO

Carbon dioxide is believed to be adsorbed on ZnO forming a variety of species, e.g. carbonate and bicarbonate, which occupy sites thereby preventing the adsorption of other species.

To examine this phenomenon, the adsorption of $^{35}\text{S-H}_2\text{S}$ on a ZnO surface pretreated at room temperature with 20 torr of carbon dioxide was studied. As can be seen in figure [6.9], the preadsorption of carbon dioxide had a negligible effect on the $^{35}\text{S-H}_2\text{S}$ adsorption process.

Admitting more carbon dioxide to the catalyst surface during the adsorption isotherm measurement did not affect the surface capacity for $^{35}\text{S-H}_2\text{S}$. In effect, the surface was saturated with adsorbed $^{35}\text{S-H}_2\text{S}$ as though no other adsorbed species was present.

6.3.3 The Exchange of $^{35}\text{S-H}_2\text{S}$ with Unlabelled H_2S on ZnO Surface

To investigate the strength of adsorption of $^{35}\text{S-H}_2\text{S}$ on ZnO, a $^{35}\text{S-H}_2\text{S}$ saturated surface was exposed to successive pulses of unlabelled H_2S , whilst keeping the sample under a helium flow (10 ml/min). As shown in

Fig: 6.9

³⁵Sulphur - Hydrogen Sulphide Adsorption on Zinc Oxide Sample (0.356g) Effect of Carbon Dioxide on the ³⁵Sulphur - Hydrogen Sulphide Adsorption at Room Temperature

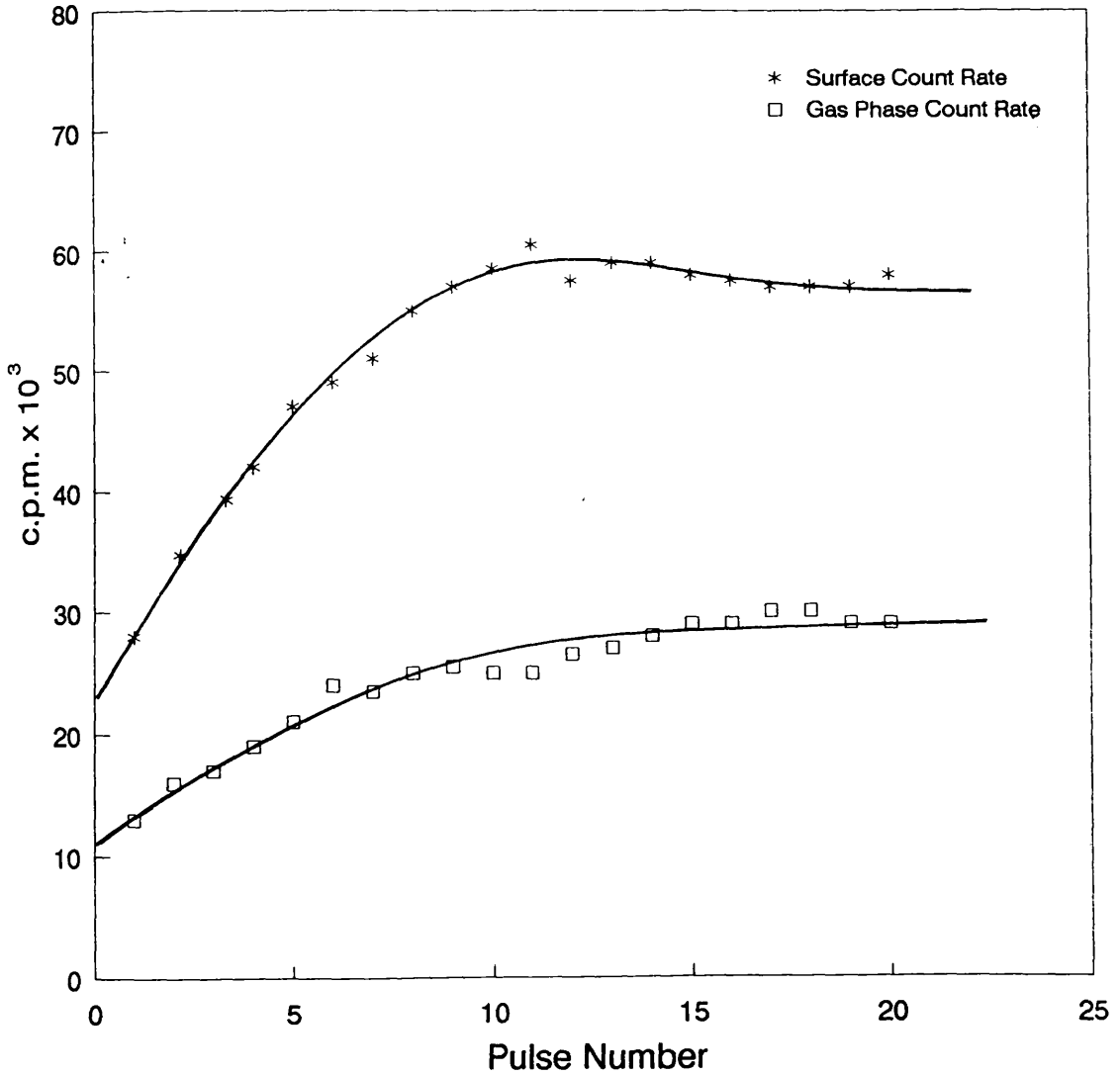


figure [6.10], there is no significant decrease in the surface count rate or a measurable increase in the gas phase count. The strength of $^{35}\text{S-H}_2\text{S}$ adsorption was further probed by admitting a 25 torr pulse of H_2S . The count rate was measured directly after exposure to unlabelled H_2S , in order to monitor any fast exchange after 6 such pulses, 10% decrease in the surface count rate was observed; there was no measurable increase in the gas phase count rate. These observations support the earlier desorption experiment which showed that only a small amount of adsorbed sulphur could be removed from the surface.

6.3.4 Effect of Water on $^{35}\text{S-H}_2\text{S}$ Adsorption Isotherm on ZnO Surface

To investigate the effect of water on the ability of ZnO to remove or adsorb H_2S in the presence of water, an experiment was conducted to examine the extent of $^{35}\text{S-H}_2\text{S}$ adsorption under such conditions. As shown in figure [6.11], the presence of water strongly influenced the extent of H_2S adsorption. Initially, the catalyst surface adsorbed $^{35}\text{S-H}_2\text{S}$ as normal, ie. a rapid increase in the surface count rate followed by a plateau region. At this point, a 5 torr water vapour pulse was introduced into the helium flow (20 ml/min) with the result that the surface count rate dropped by 38%. Further pulses of $^{35}\text{S-H}_2\text{S}$ resulted in an increase in the surface H_2S uptake. An

Fig: 6.10

³⁵Sulphur - Hydrogen Sulphide Adsorption on Zinc Oxide
Exchange with Hydrogen Sulphide

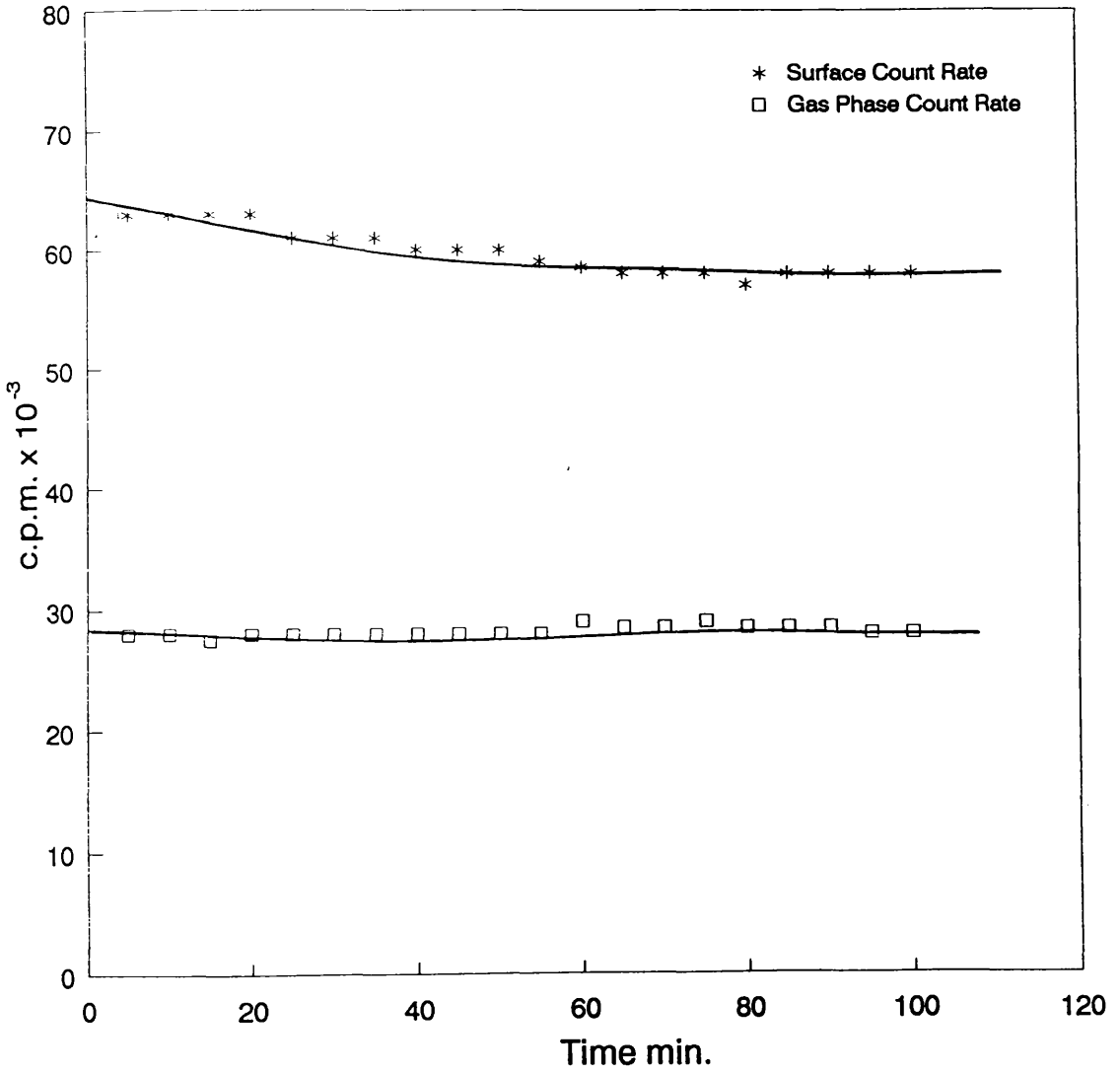
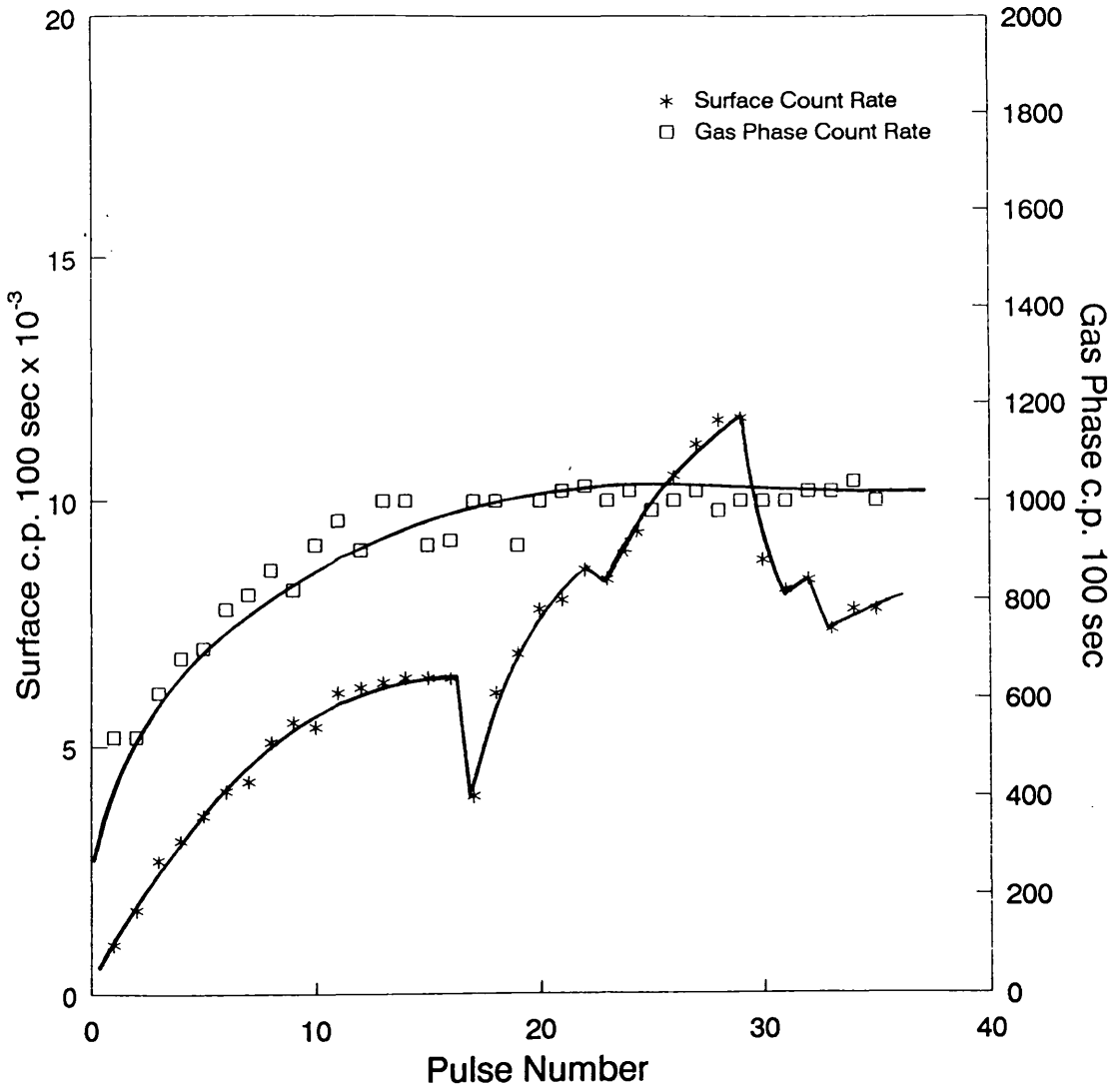


Fig: 6.11

Effect of Water on ^{35}S Sulphur - Hydrogen Sulphide
Adsorption on Zinc Oxide (0.356g) at
Room Temperature



additional 5 torr water pulse lowered the surface activity by ca. 2%; the surface count was again restored on admission of more $^{35}\text{S-H}_2\text{S}$ pulses. An increase in the gas phase count rate was only observed in the initial stage of adsorption. In fact, the surface count rate increased by 45% when compared with the plateau region obtained prior to admitting any water to the oxide surface.

Introducing more pulses of water (10 torr per pulse) into a helium flow of 30 ml/min resulted in even greater effect on the surface count rate, although no increase in the gas phase count rate was observed. However, little effect was observed if the catalyst was left for 24 hours under helium flow of 30 ml/min. These findings were summarised in table 6.5.

Table 6.5

The Effect of Both Water Adsorption and Flow Rate on the Uptake of $^{35}\text{S-H}_2\text{S}$ on ZnO

Pulse number	Water pressure (Torr.)	Count rate c.p.100 sec		% Decrease in surf. count	He flow rate ml/min
		Surface	Gas phase		
5	-	3587	733	-	10
10	-	5412	948	-	10
15	-	6446	955	-	10
17	5	4041	1091	38	20
18	-	6123	1027	-	10
22	-	8626	1008	-	10
23	5	8490	1080	2	20
28	-	11713	1078	-	10
30	10	8837	1082	25	30
33	-	7421	1196	16	30

A similar effect was observed when water was pulsed on to the H_2S saturated surface while the surface counts were being monitored. As shown in figure [6.12], a decrease in the surface count rate followed each pulse of water, generating a series of decreases in the surface count rate, although there was no observable increase in the gas phase count.

In a separate experiment, the introduction of 2 pulses of water to a sulphur saturated ZnO surface in helium flow of 30 ml/min resulted in a similar result to that shown in figure [6.13]. Interestingly, while the gas phase count was increased by 47%, the surface count rate only dropped by 29%.

Fig: 6.12

Effect of Water on ^{35}S Sulphur - Hydrogen Sulphide
Adsorption at Room Temperature on Zinc Oxide (0.356g)

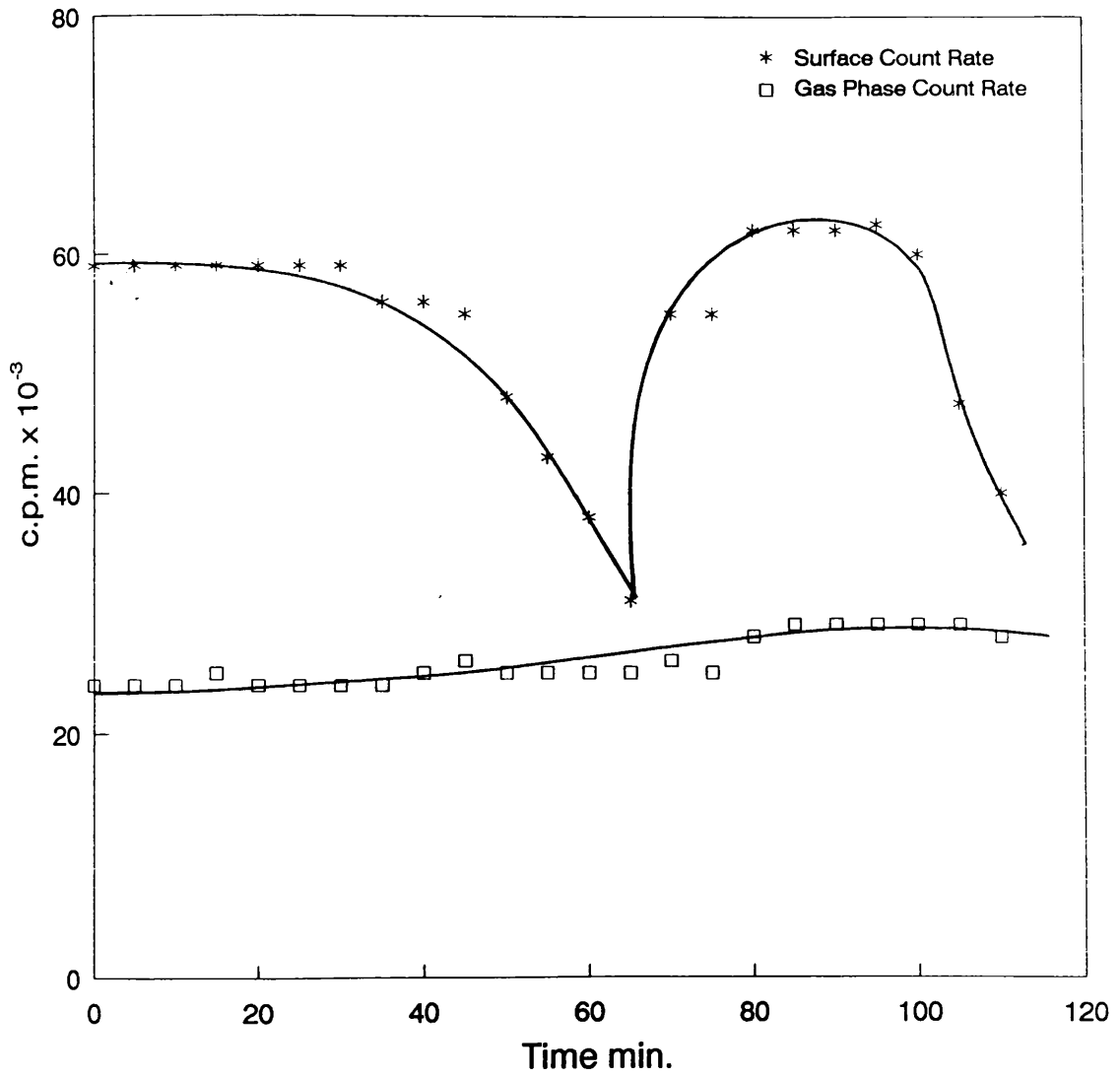


Fig: 6.13

Water Effect on ^{35}S Sulphur - Hydrogen Sulphide
Adsorption on Zinc Oxide (0.356g) at Room Temperature

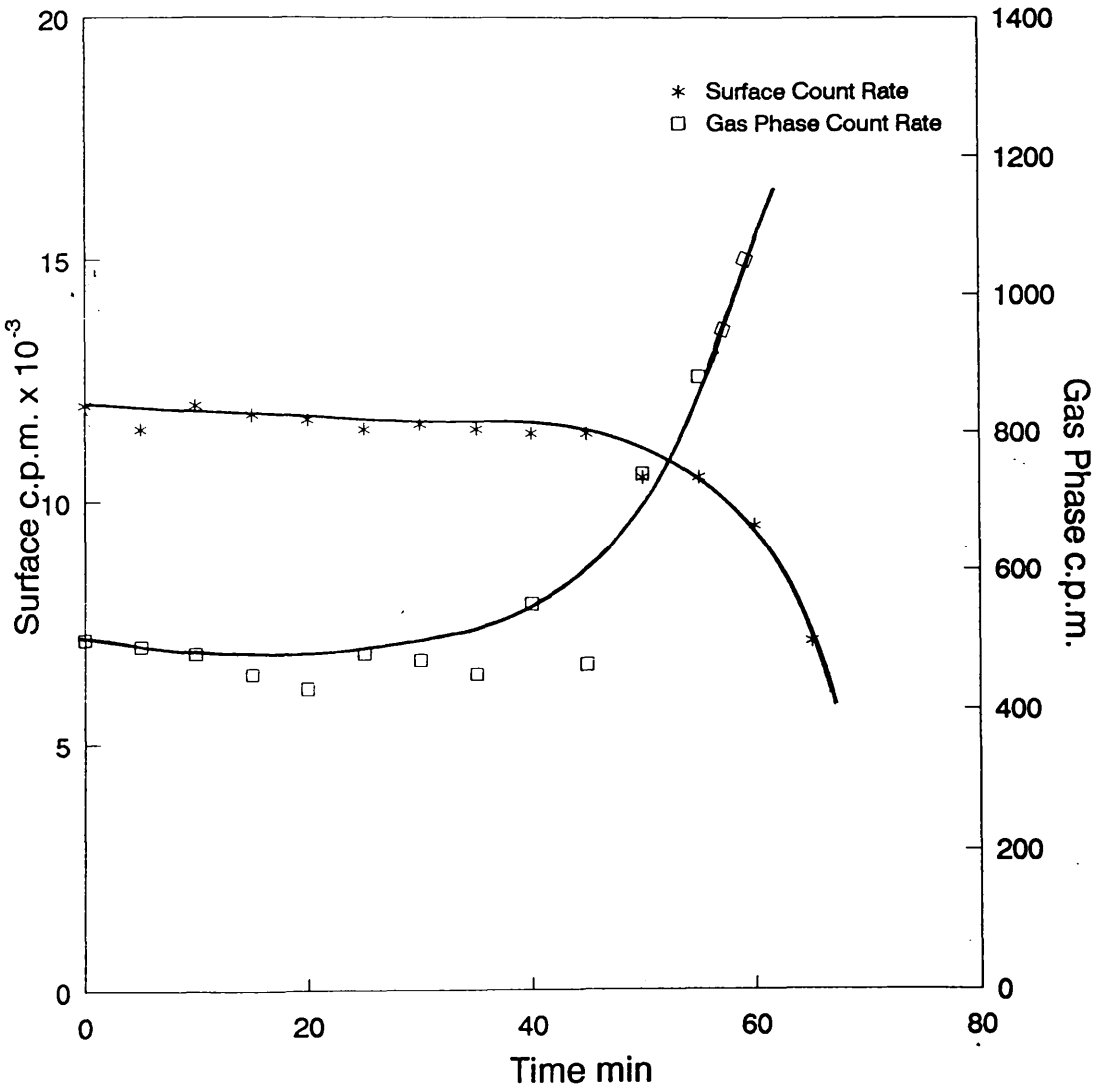
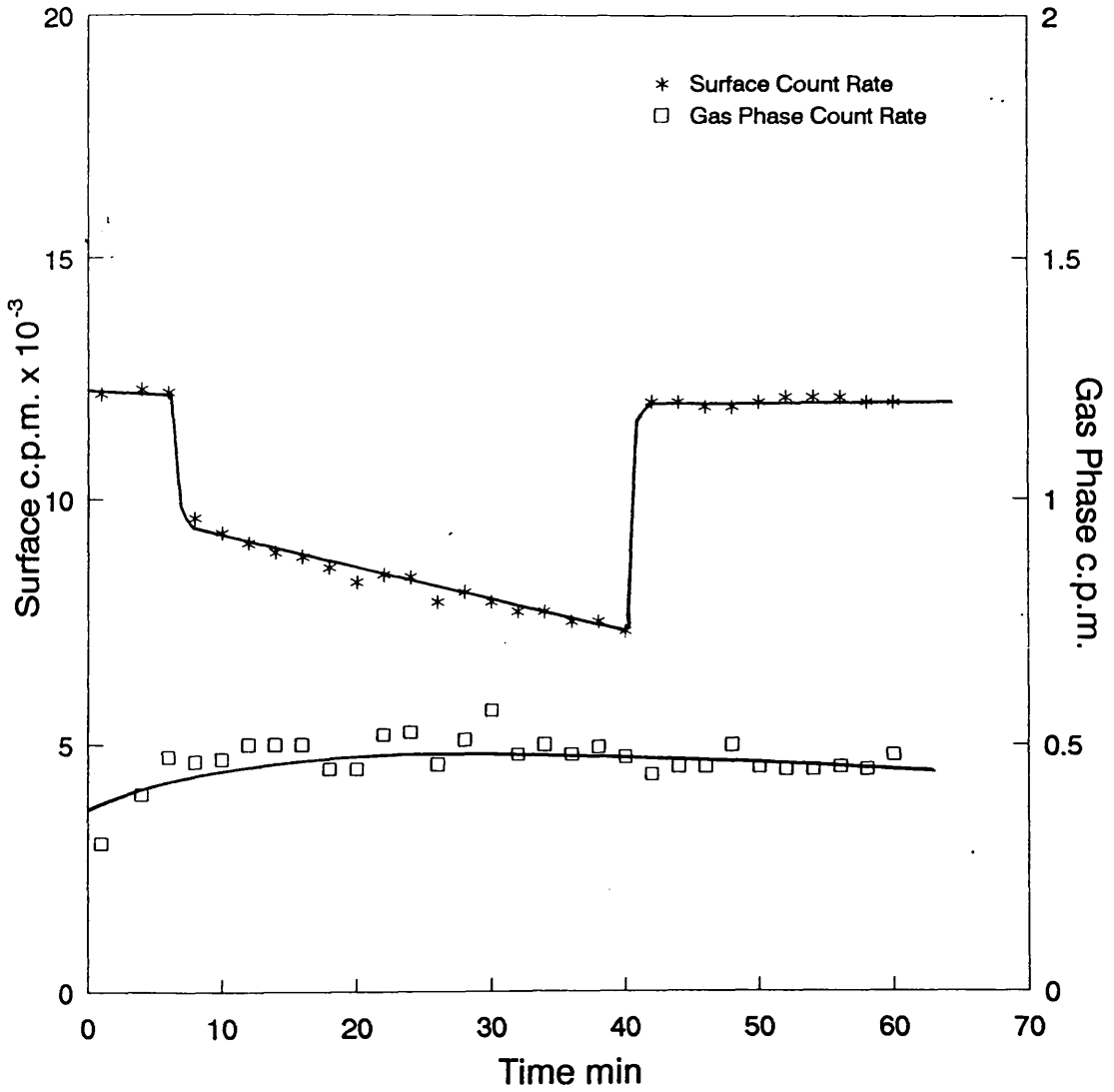


Figure [6.14] shows similar results obtained after the admission of 2 pulses of water to a sulphur saturated ZnO surface; a 40% drop in the surface counts was observed. The surface count could be restored if more $^{35}\text{S-H}_2\text{S}$ was introduced to the catalyst surface.

Fig: 6.14

Water Effect on ^{35}S Sulphur - Hydrogen Sulphide
Adsorption on Zinc Oxide (0.356g) at Room Temperature



CHAPTER SEVEN

THE SPECTROSCOPIC STUDY OF THE INTERACTION OF METHANOL AND CARBON MONOXIDE ON COPPER-BASED CATALYST SURFACES

7.1 The Interaction of Methanol with Copper-Based Catalysts

Catalyst samples were activated as described in section (2.2), and the spectra of the activated catalyst were then recorded and represent the reference spectra. Methanol was admitted to the IR flow cell by 10 μ l microsyringe injections into a helium flow of 25 ml/min⁻¹. The catalyst surface, after exposure to methanol, was left under a helium flow for 10-15 minutes before the first spectrum was recorded.

This was then followed by a range of procedures chosen to shed light on the roles of various experimental parameters (time, flow rate and temperature) in influencing the adsorption process.

7.1.1 FTIR Spectra of Methanol Adsorbed on Cu/Al₂O₃

Figure [7.1] shows a series of spectra recorded for the interaction of 10 μ l of methanol with Cu/Al₂O₃ at 200°C.

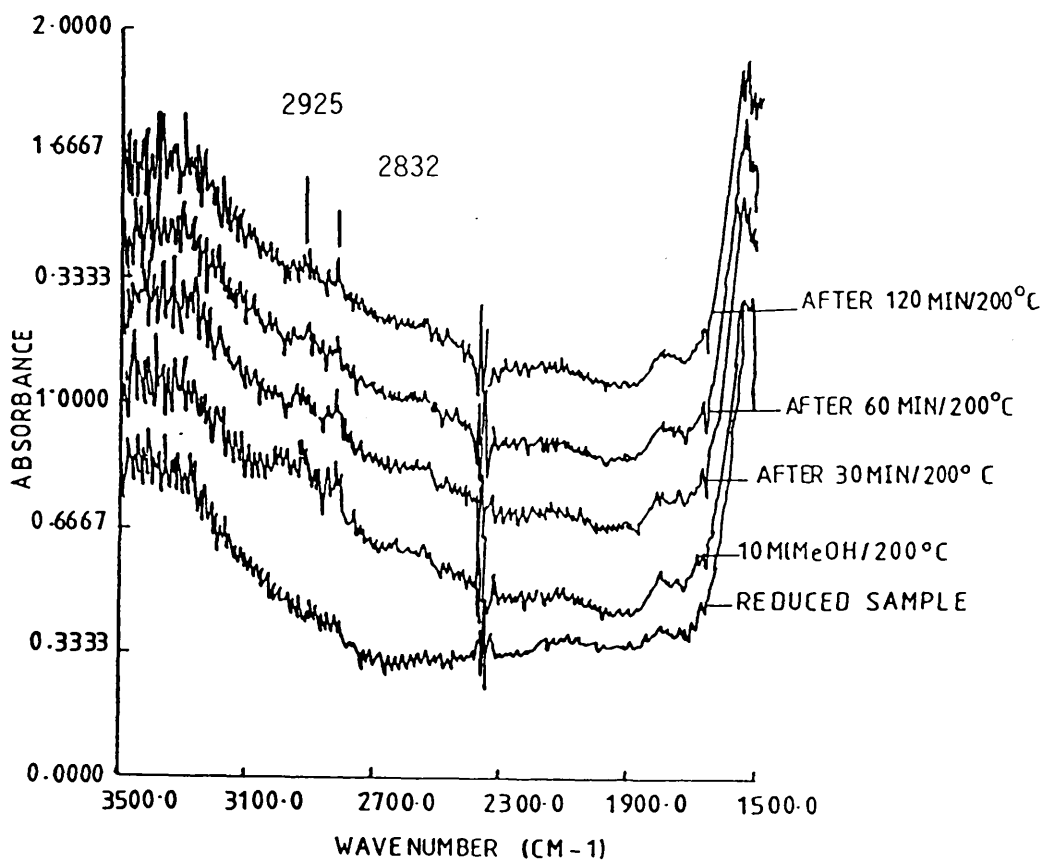


Fig. 7.1 The adsorption of Methanol (10 μ L) on copper/alumina at 200°C

Bands were observed at 2925 and 2832 cm^{-1} . These two bands are both assigned to the copper formate surface species (V CH vibration) ^[234]. When left under a helium flow rate of 25 ml/min these two bands decreased in intensity with time. However, this treatment had no effect on the positions of these bands which were very stable as shown in figure [7.1].

The interaction of methanol with $\text{Cu}/\text{Al}_2\text{O}_3$ at room temperature also resulted in spectra [figure 7.2] characterised by bands at 2925 and 2832 cm^{-1} . These were also assigned to a copper formate ^[234] species. As in the case of the higher temperature leaving the adsorbed species under a flow of helium was observed to have no effect on the positions of these bands, although the intensity of both bands was observed to decrease dramatically after one hour.

The effect of adsorption temperature was also investigated. Spectra were recorded following the admission of 10 μl of methanol under a helium flow of (25 ml/min) at a range of temperatures. As shown in figure [7.3], the adsorption temperature only affects the band (2925 and 2832 cm^{-1}); intensities; no shift was recorded in the band frequencies.

In addition, bands at 1060 and 990 cm^{-1} were initially observed, but disappeared after ca. 3 min. under the helium flow. These bands have been assigned to methoxy species

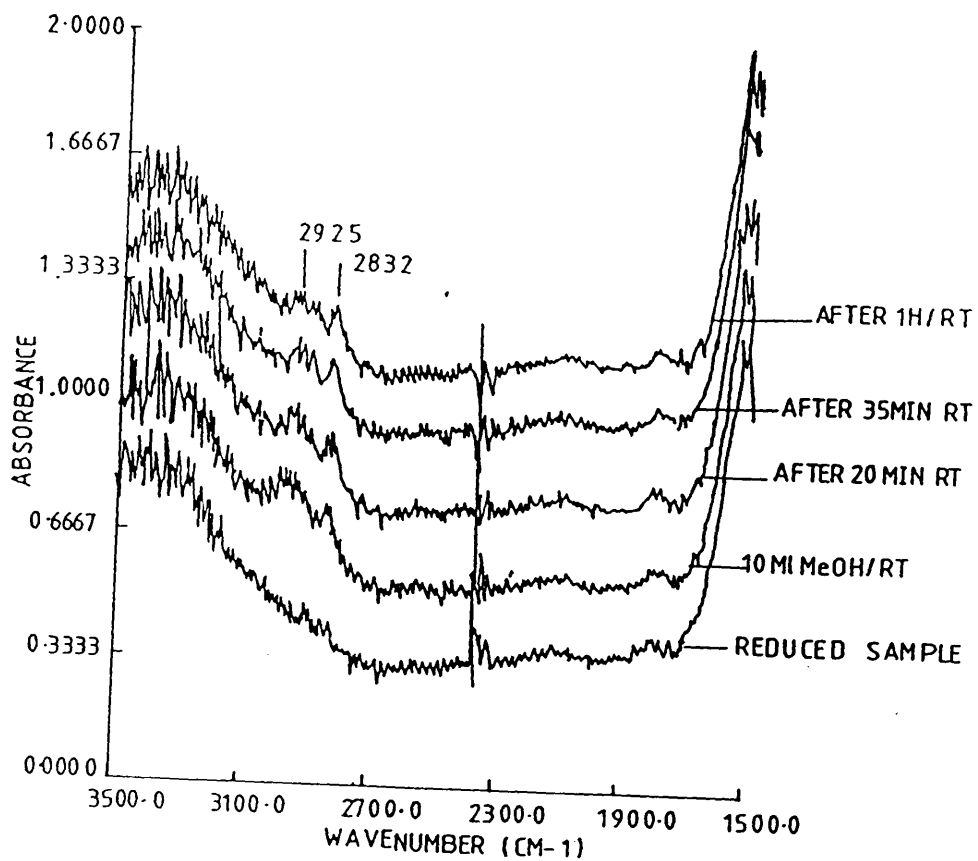


Fig. 7.2 The adsorption of Methanol (10 μ L) on copper/alumina at room temperature

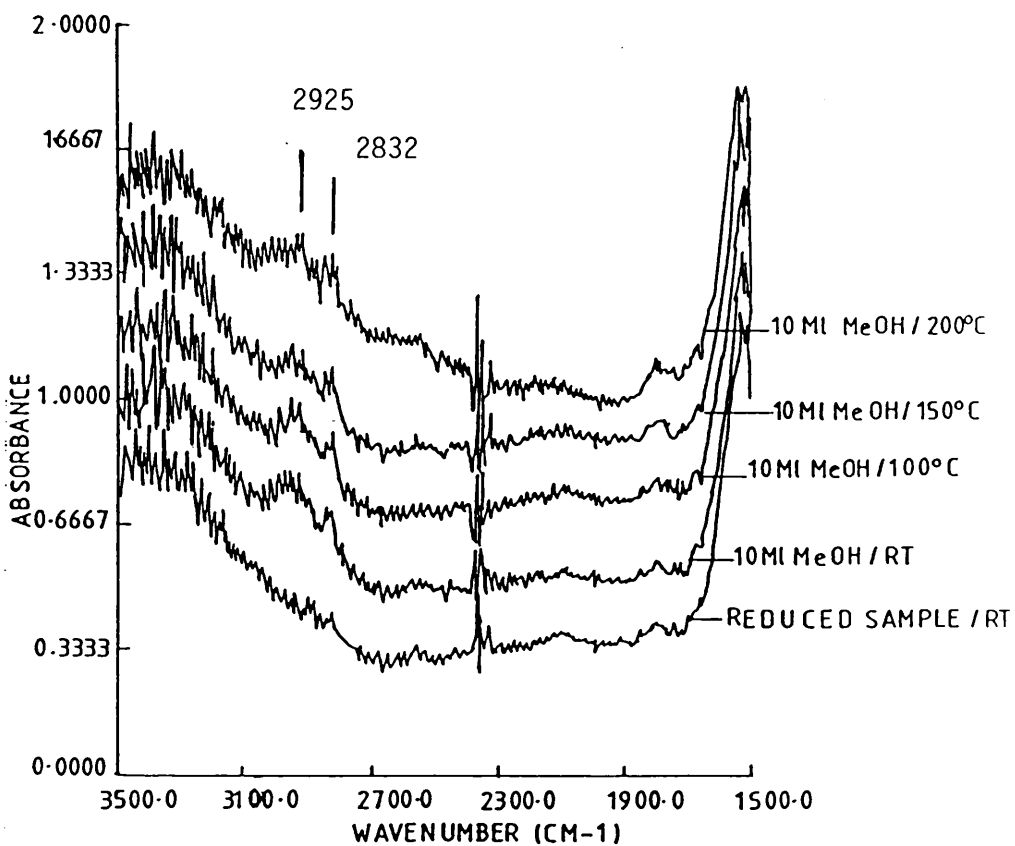


Fig. 7.3 The adsorption of Methanol (10 μ L) on copper/alumina at various temperatures

[235] (ν CO).

Under the present experimental conditions it was not possible to detect any bands characteristic of carbonate formation as residual carbonate species incorporated into the catalyst during preparation, gave rise to an intense band in the region $1510-1415\text{ cm}^{-1}$ which obscured any bands generated from methanol interactions.

7.1.2 The Interaction of Methanol with Cu-ZnO/Al₂O₃ Catalyst

Methanol adsorption on Cu/ZnO/Al₂O₃ also generated bands at 2925 and 2832 cm^{-1} . These are assigned to a formate species^[234]. Figure [7.4] shows the desorption of this formate species from Cu-ZnO/Al₂O₃ at 200°C. As a function of time under a helium flow of 25 ml/min a decrease in the intensity of these bands was observed, with no effect on the frequency.

Heating the catalyst to 200°C after exposure to 10 μl methanol at room temperature resulted only in the appearance of the same two bands, the intensity of which remained constant during treatment in helium flow of 25 ml/min for one hour, as shown in figure [7.5].

It can be seen from figure [7.6] that the adsorption of methanol decreased with increasing temperature, but some adsorbed species remain at 200°C.

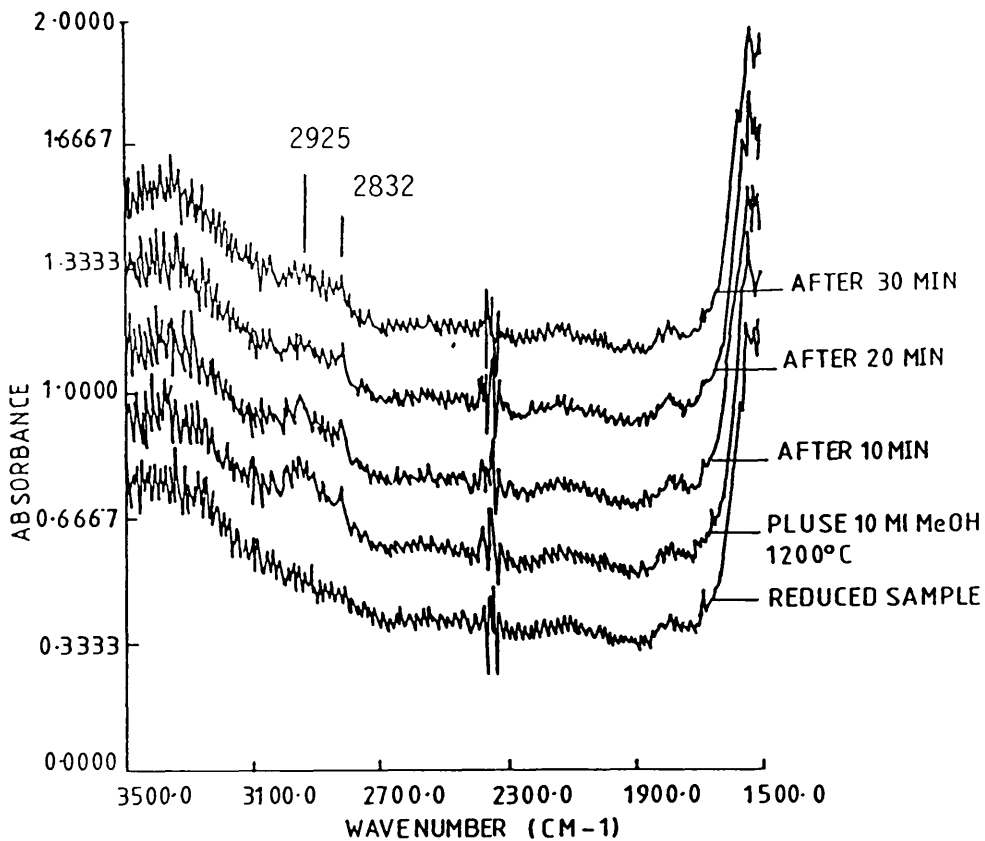


Fig 7.4 Methanol adsorption (10 μ L) on copper/zinc oxide/alumina at 200°C.

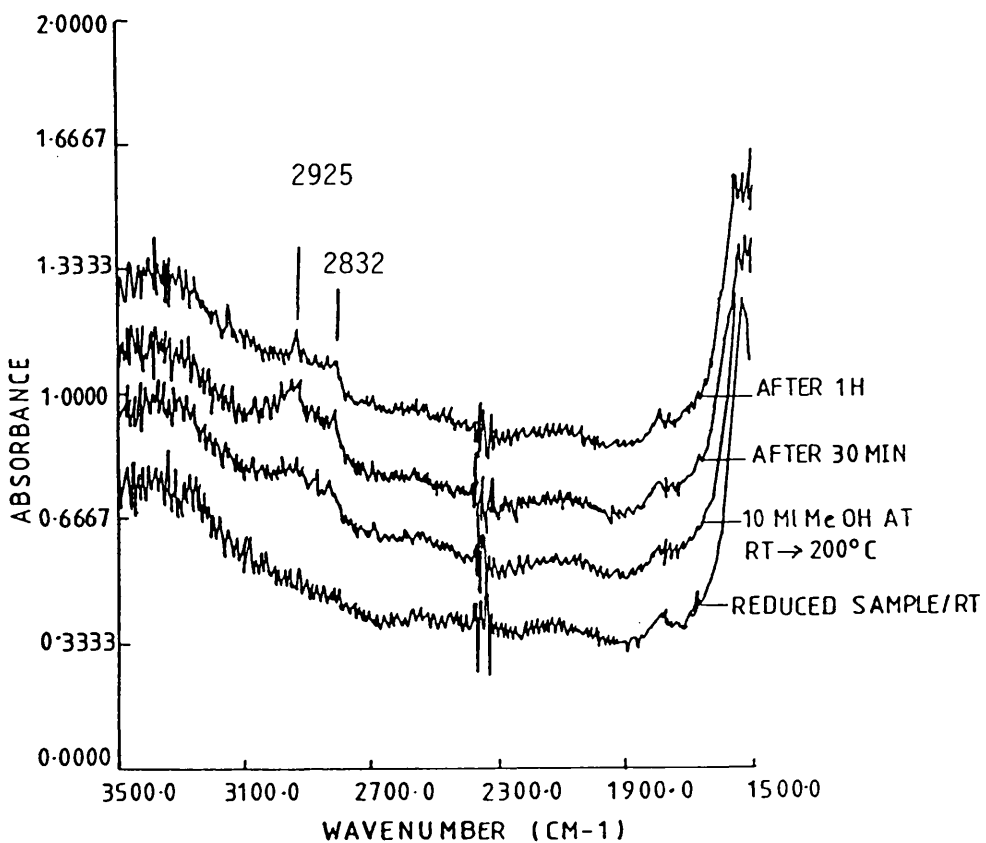


Fig 7.5 Methanol adsorption (10 μ L) on copper/zinc oxide/alumina at 200 $^{\circ}$ C. The effect of helium flow is presented

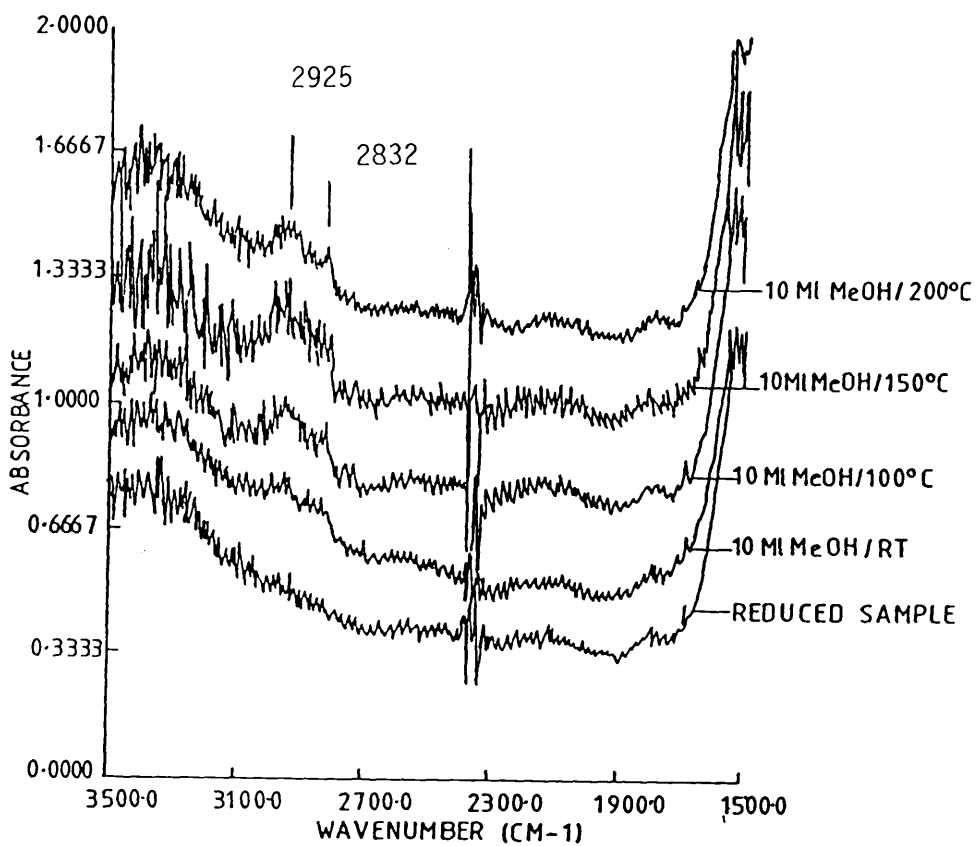


Fig 7.6 Methanol adsorption (10 μ L) on copper/zinc oxide/alumina at various temperatures

Due to the residual carbonate formed during catalyst preparation, it was again difficult to observe any carbonate band in the region $1510-1400\text{ cm}^{-1}$ arising from to the interaction of methanol with $\text{Cu-ZnO/Al}_2\text{O}_3$.

The small amount of information obtained from the interaction of methanol with both $\text{Cu/Al}_2\text{O}_3$ and $\text{Cu-ZnO/Al}_2\text{O}_3$ stems from the high loading of copper in the catalysts; 64 and 60%, respectively, which makes the catalyst colour very dark to be used in the FTIR investigation.

7.1.3 The Interaction of Methanol with a ZnO Catalyst

A zinc oxide (75-1) sample was reduced with 6% hydrogen in nitrogen at a flow rate of 25 ml/min at 350°C for 3 hours. The catalyst was then purged with a 25 ml/min flow of helium at 350°C for 30 minutes. The spectrum of the reduced sample was then recorded at the appropriate adsorption temperature.

The spectrum generated after the reduction of the zinc oxide sample is shown in figure [7.7] and is characterised by bands at 1788, 1700-1370 and 1081 cm^{-1} , which are assigned to a residual carbonate species. The large intensity band found between $1700-1370\text{ cm}^{-1}$ is again due to the carbonate compound added to catalyst during preparation. A small band also arose at 2332 cm^{-1} and can be assigned to gaseous carbon dioxide in the reaction

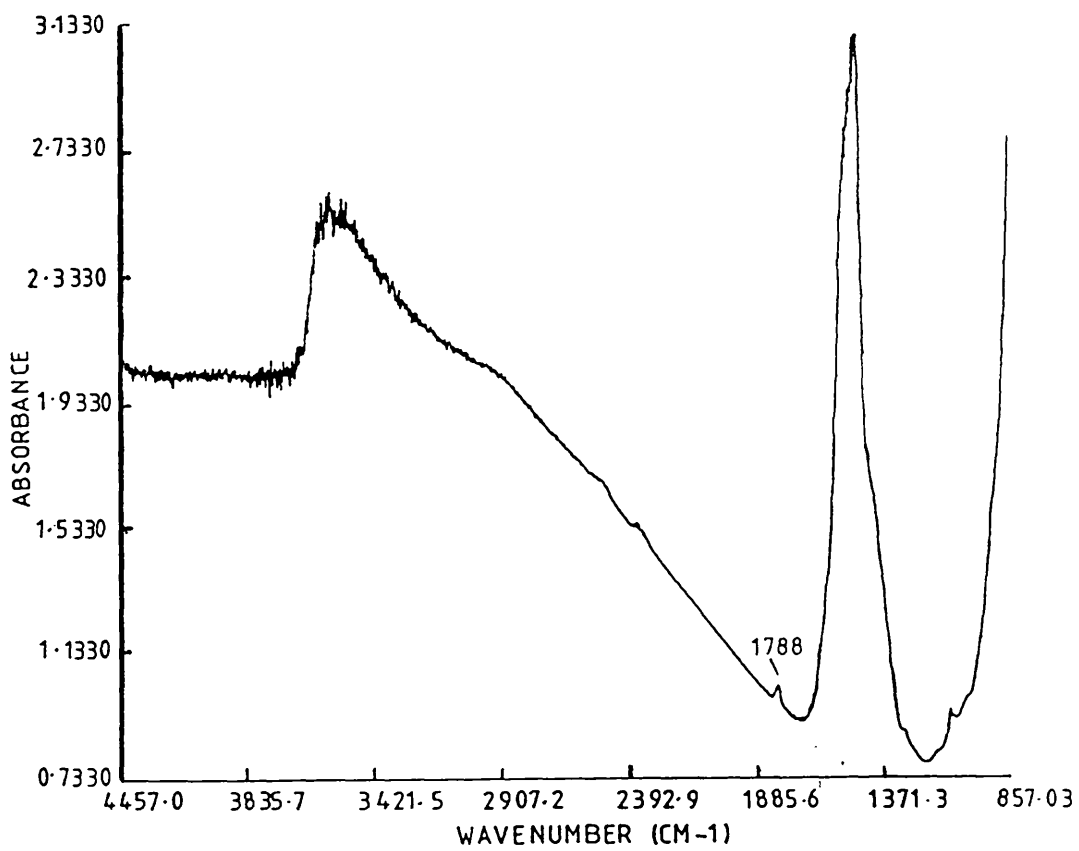


Fig 7.7 Reduced sample of zinc oxide with 6% hydrogen in nitrogen at 350°C for 3 hours.

vessel.

Exposing the catalyst surface to 5 μl of methanol at room temperature produced the spectrum shown in figure [7.8]. The bands at 2945 and 2828 cm^{-1} were respectively assigned to the CH_3 asymmetric and C-H stretching modes of surface methoxide ions^[236]. A band observed at 1416 cm^{-1} , assigned to a carbonate species, appeared as a shoulder of the residual carbonate in 1700-1370 cm^{-1} range. The band at 2076 cm^{-1} is assigned to carbon monoxide resulting from the interaction of methanol with the oxide surface. A strong band also occurred at 3500 cm^{-1} characteristic of hydrogen-bonded hydroxyl group, while the band found at 1046 cm^{-1} is assigned to a carbonyl stretching vibration of the methoxy group.

In order to examine the stability of the positions of the bands arising from exposure of the oxide surface to 5 μl of methanol at room temperature, another experiment was conducted. Methanol (10 μl) was introduced to the sample at room temperature followed by 15 minutes flow of helium (25 ml/min), then the spectrum was recorded. As presented in figure [7.9], no significant changes in the spectrum were observed apart from the appearance of a band at 2359 cm^{-1} due to carbon dioxide formation which was found to be stable under the experimental conditions.

Similar bands were observed for methanol adsorption at 100°C. Leaving the catalyst surface at this temperature under helium flow (25ml/min) for 15 minutes produced a

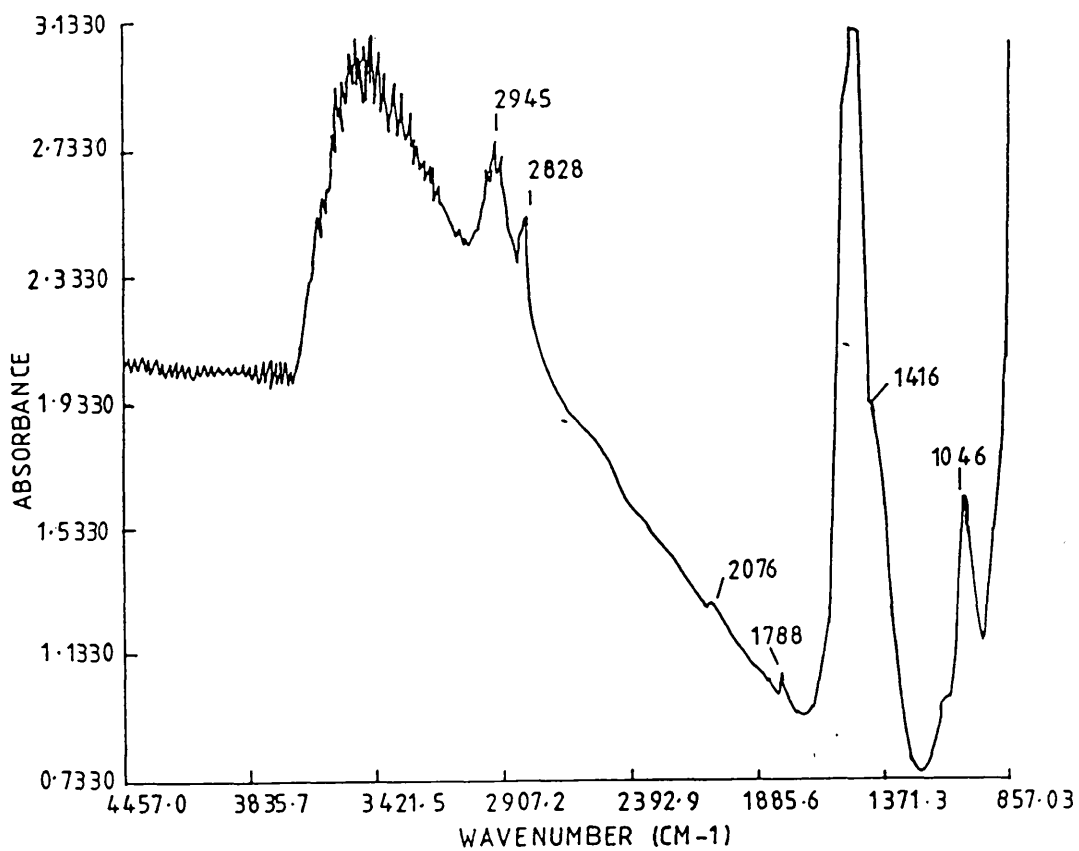


Fig 7.8 Methanol adsorption (5 μ L) on reduced zinc oxide sample at room temperature.

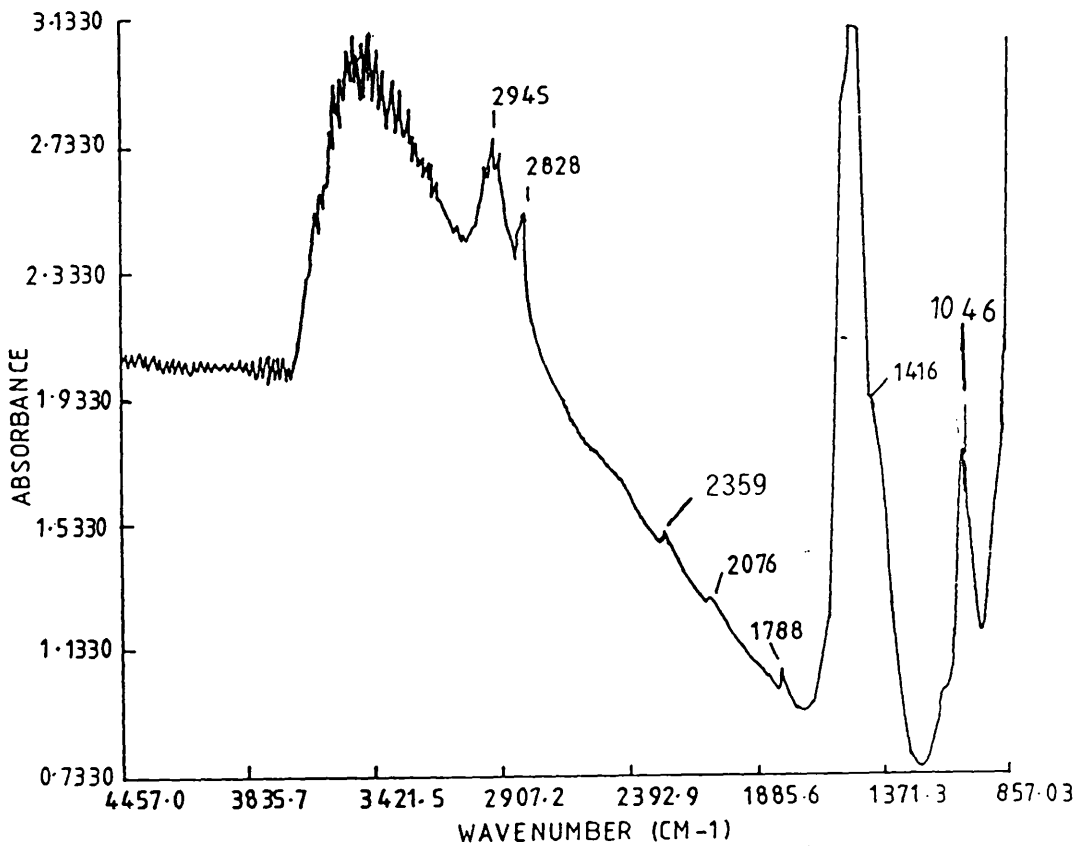


Fig 7.9 Methanol adsorption (10 μ L) on reduced zinc oxide sample at room temperature

spectrum [figure 7.10] with bands at 2872, 1573, 1381 cm^{-1} which were assigned to the C-H stretching, O-C-O anti-symmetric stretching and O-C-O symmetric stretching vibrations of surface formate ions ^[237]. However, the band which occurs at 1381 cm^{-1} can also be assigned to the C-H in-plane bending vibration of formate species ^[236]. Bands at 2352 and 2332 cm^{-1} are assigned to a transient formation of carbon dioxide gas. The 1142 cm^{-1} band was assigned to the C-H stretching of the formate ion.

Figure [7.11] illustrates the nature of methanol adsorption at 250°C after 30 minutes exposure.

The bands remaining at 2872, 1573, 1375 and 1142 cm^{-1} are assigned to similar stretching vibrations to those discussed above. The band at 2359 cm^{-1} is assigned to carbon dioxide gas, while that occurring at 2967 is assigned to asymmetric CH_3 stretching vibration of surface methoxy ions.

Heating the catalyst surface to 350°C produced a spectrum with bands at 2359 and 2332 cm^{-1} due to transient formation of carbon dioxide gas [figure 7.12]. This treatment led to the disappearance of the other bands which were observed in the previous experiments at low temperatures.

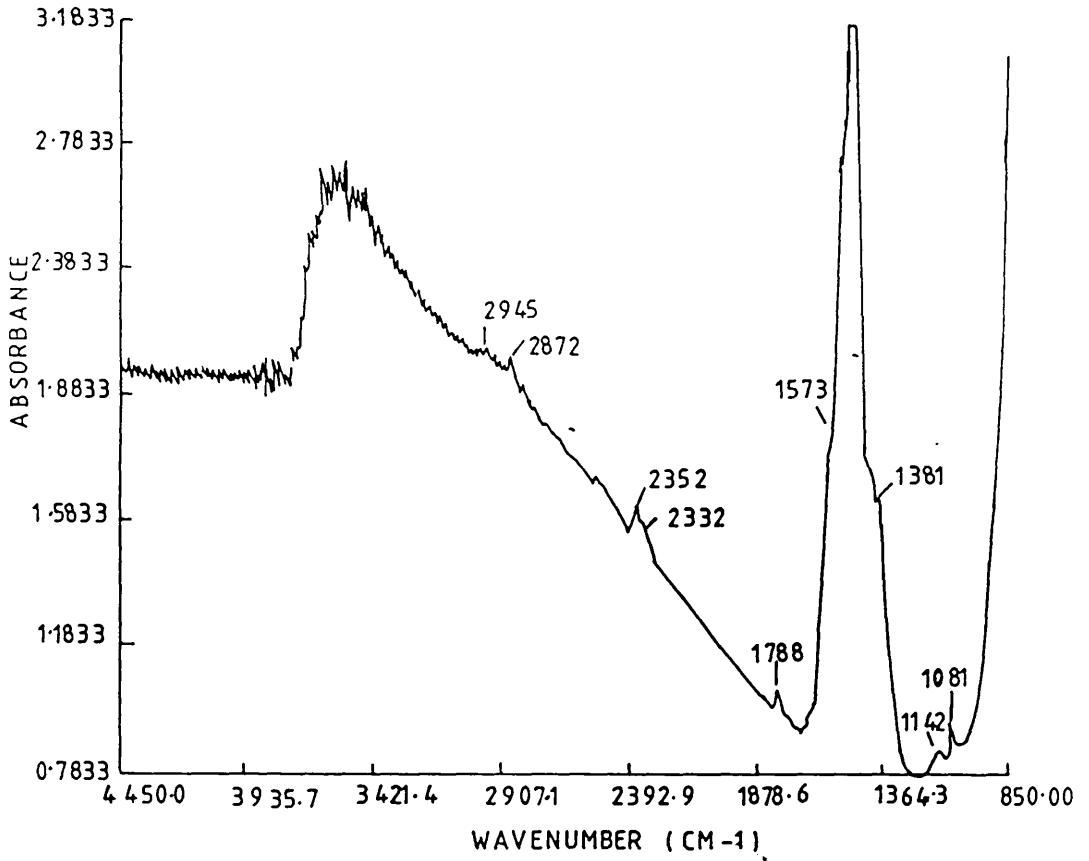


Fig 7.10 Methanol adsorption on reduced zinc oxide sample at 100°C. Spectra recorded after 15 minutes of methanol exposure.

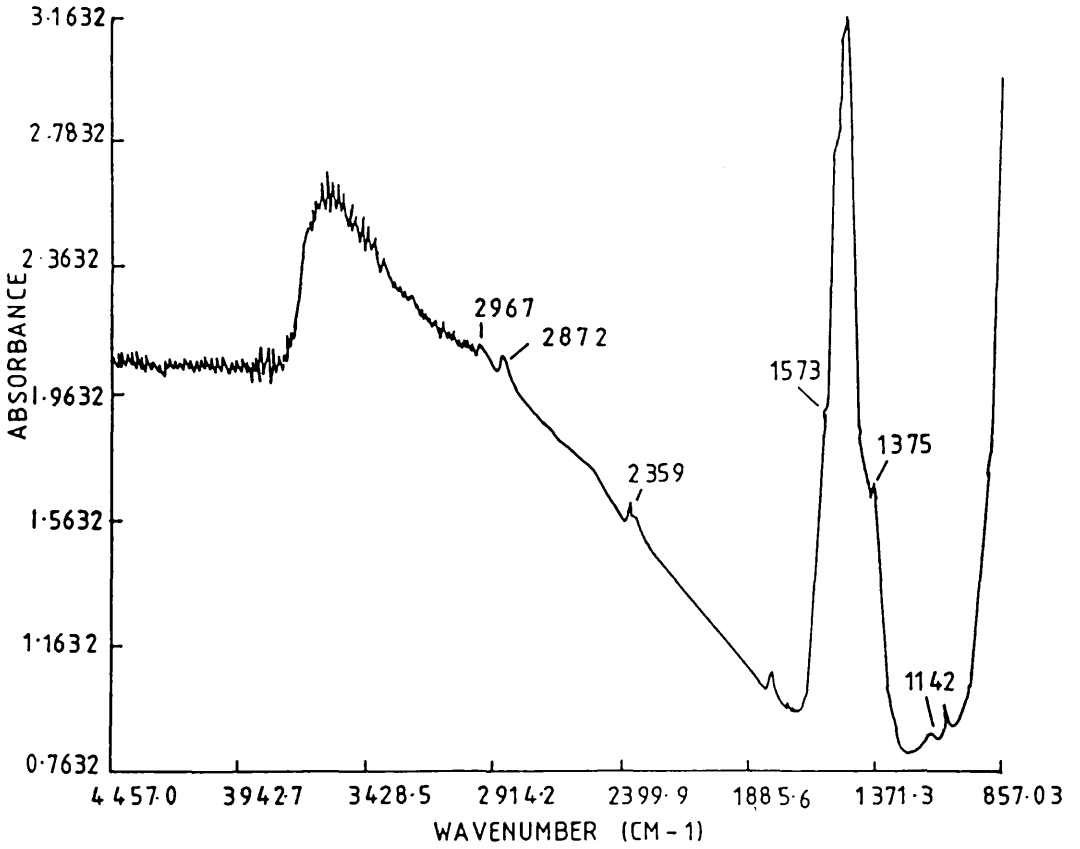


Fig 7.11 Methanol adsorption on reduced zinc oxide sample at 250 °C. Spectra recorded after 30 minutes of methanol exposure.

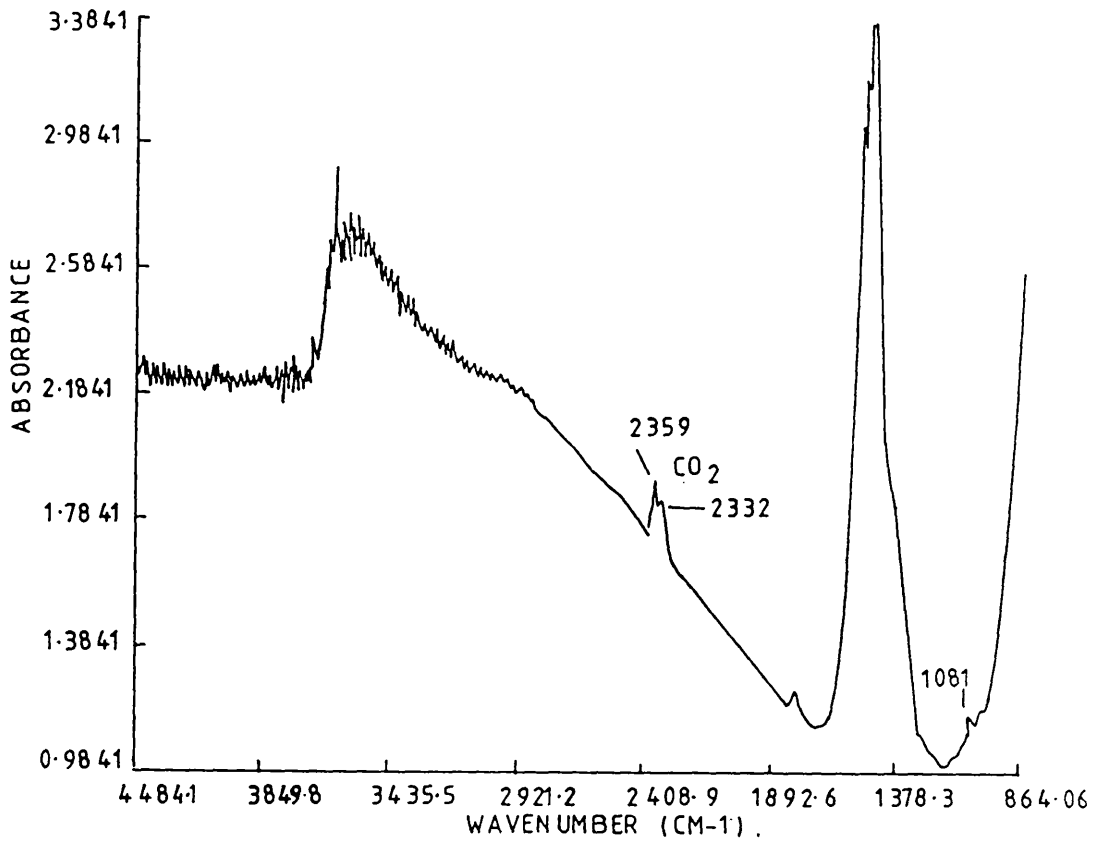


Fig 7.12 Methanol adsorption on reduced zinc oxide sample at 350°C.

7.1.4 Methanol Interaction with Alumina

Two activation procedures were used in the case of the alumina samples. In the first case, the sample was heated in a helium stream (25 ml/min) for 3 hours at 350°C; the spectrum was then recorded under similar conditions to those described in figure 7.13 [1]; the spectrum has residual carbonate bands in the region 1548-1381 cm^{-1} . The second activation method involved treating the alumina surface with 6% hydrogen in nitrogen (flow rate 25 ml/min) at 350°C for 3 hours, after which the sample spectrum was determined at the same temperature. The spectrum shown in figure 7.13 [2] also exhibits a band due to the residual carbonate species. Although both spectra were found to be similar, the second activation method was used for further experimental procedures.

Figure 7.14 [a] illustrates the nature of methanol adsorption at room temperature on activated alumina. The spectrum shows the presence of a large band due to hydroxyl groups on the surface of the alumina at 3500 cm^{-1} , while a complex set of bands occurs in the region 3100-2800 cm^{-1} and in the region 1700-1300 cm^{-1} .

The first set of bands, arising at 3006, 2982, 2973, 2943, 2923, 2866, 2843 and 2831 cm^{-1} {figure 7.14 [b]} are assigned to C-H stretching vibrations of CH_3 group(s) ^[238]. However, bands at 2943 and 2843 cm^{-1} are doublets and are due to C-H stretching vibrations. Bands in the second

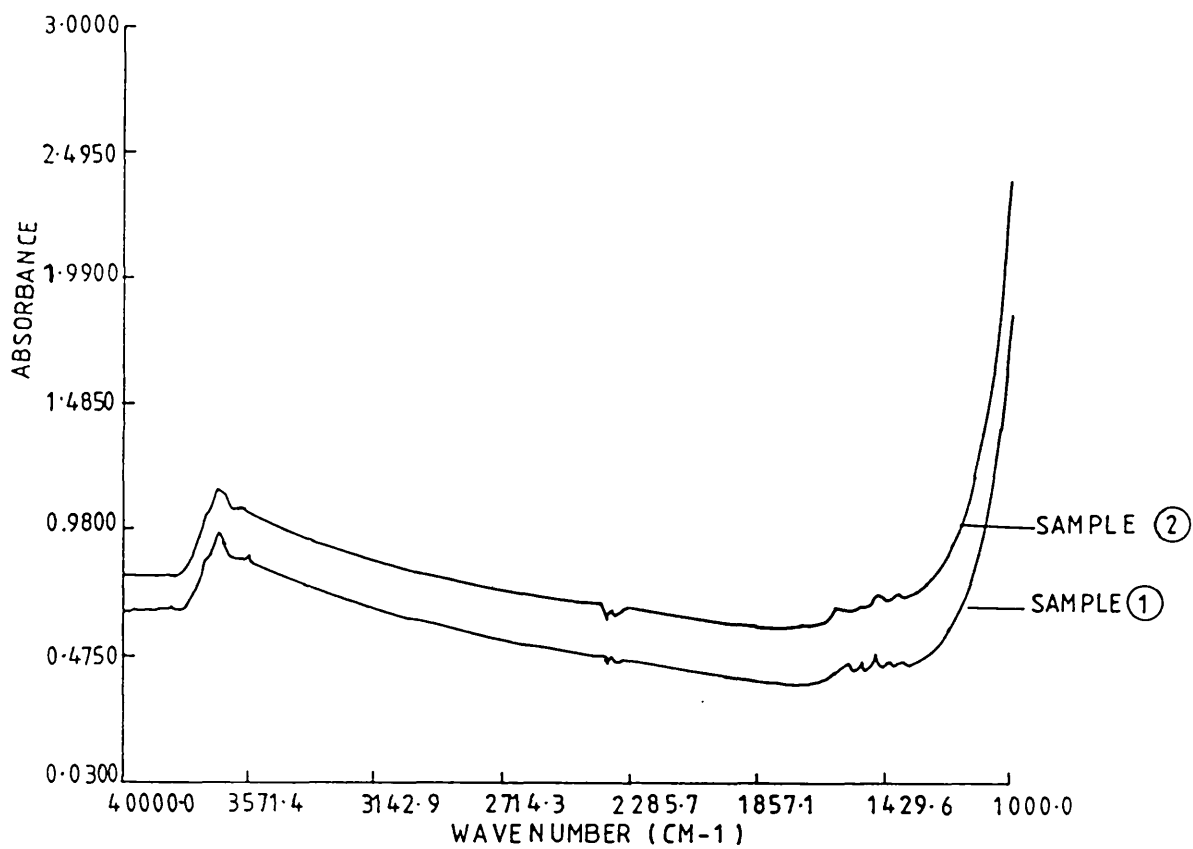


Fig 7.13 Reduced samples of alumina with 6% hydrogen in nitrogen at 350 °C. For 3 hours.

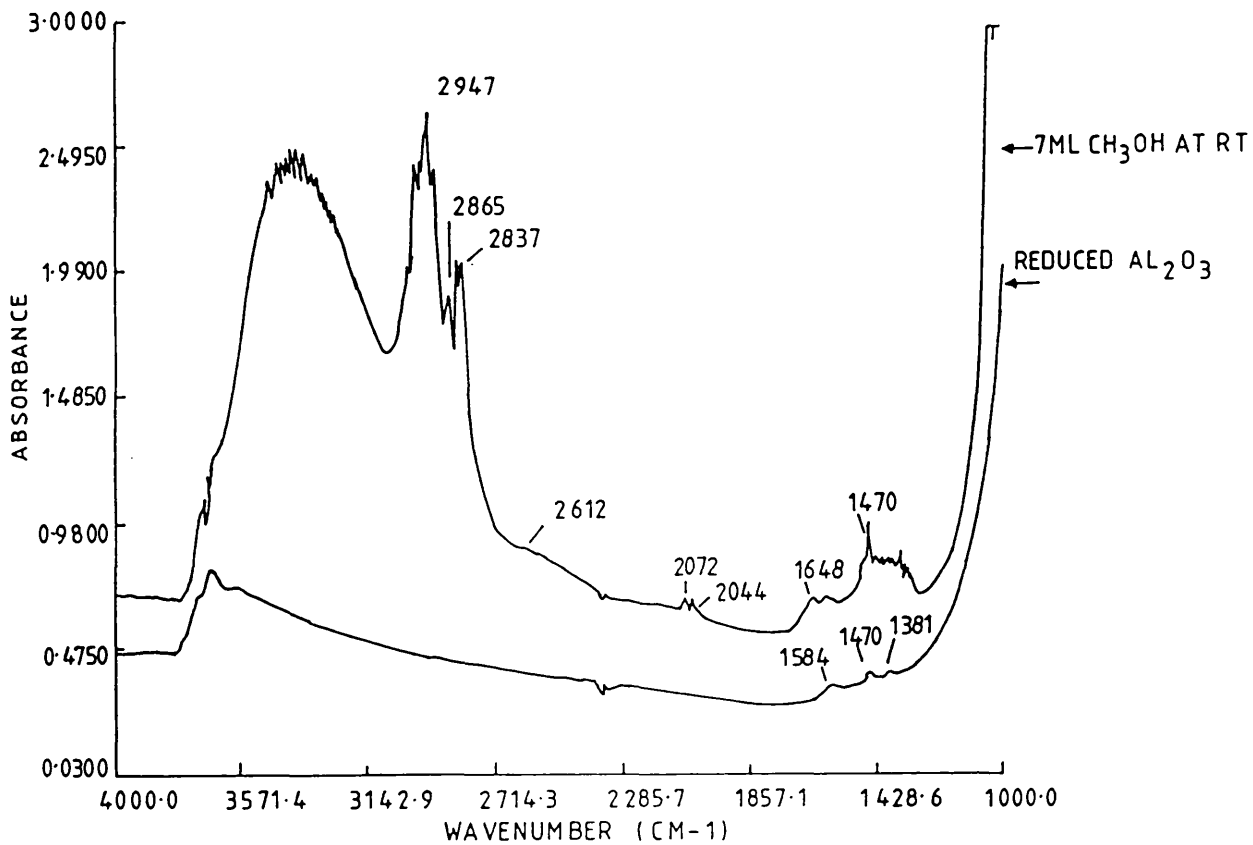


Fig 7.14a Methanol adsorption (7 μ L) on reduced alumina at room temperature.

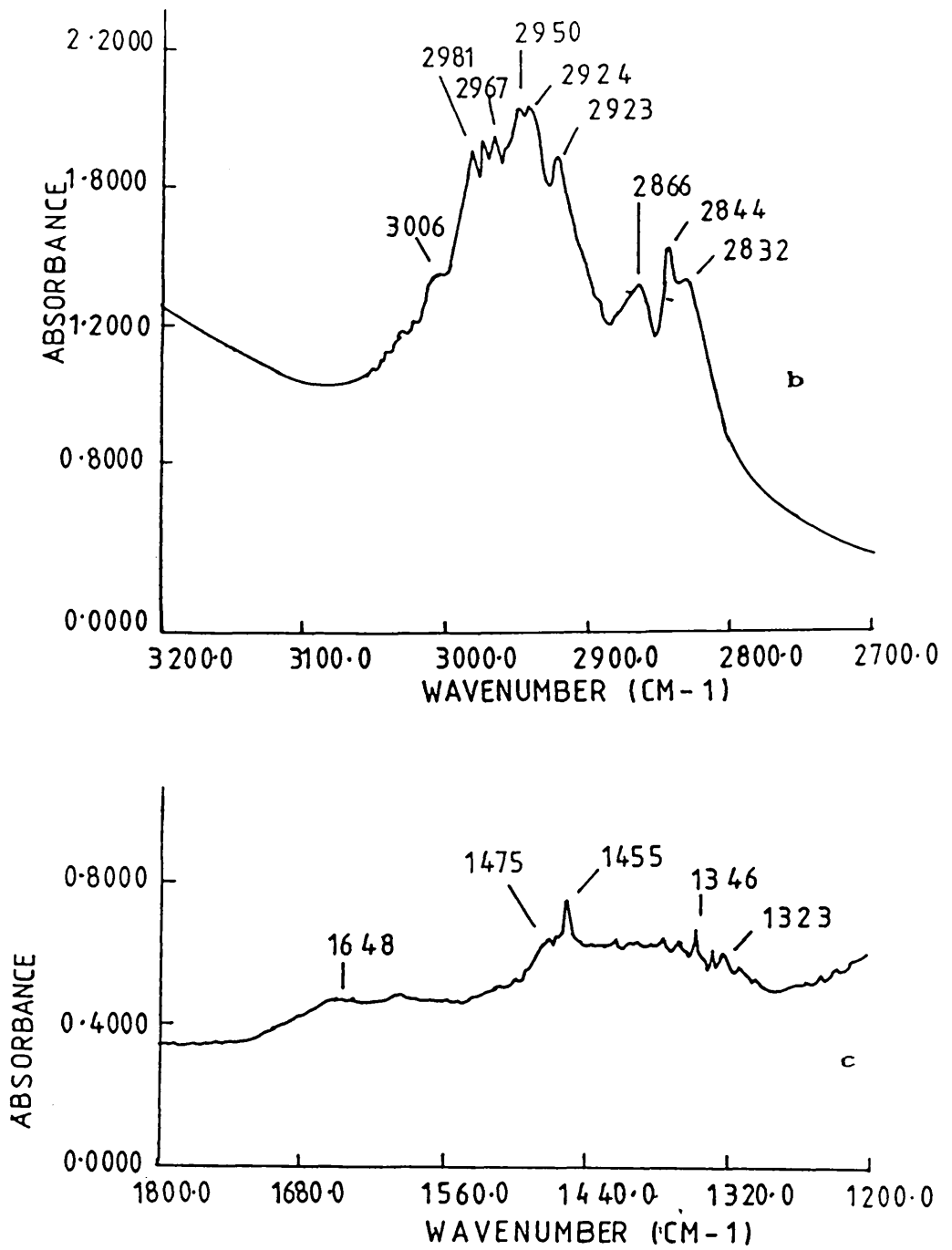


Fig 7.14b,c The vibrational spectrum of methoxy group (b) and carbonate (c) formed from the interaction of methanol with alumina surface at room temperature.

region {1700-1300 cm^{-1} , figure 7.14 [c]} are at 1648, 1475, 1455, 1346 and 1323 cm^{-1} . The bands at 1648 and 1475 cm^{-1} can be assigned, respectively, to the asymmetric and symmetric stretching vibrations of a surface formate ion, [238, 239] while the bands at 1455, 1346 and 1323 cm^{-1} are due to the CH_3 bending modes of the methoxy group and O-C-O symmetric stretching mode of the formate group respectively.

The presence of bands at 2072 and 2044 cm^{-1} must result from gas phase carbon monoxide produced from the reaction of methanol with the alumina surface.

Exposing activated alumina samples to 5 μl methanol and recording the spectrum directly after the exposure, produces the spectrum shown in figure 7.15 [a] (expanded regions in figures 7.15 [b] and 7.15 [c] respectively).

The bands shown in figure 7.15 [b] can be assigned as in figure 7.14 [b], while figure 7.15 [c] shows new bands at 1593 and 1393 cm^{-1} , which result from the asymmetric O-C-O stretching mode of formate group and from the C-H in-plane bending mode respectively [238, 239]. The band at 1375 cm^{-1} corresponds to the O-C-O symmetric stretching mode. These bands, as well as a band at 1070 cm^{-1} , which was assigned to alumina methoxy group, were observed [figure 7.16 a]. In addition, bands due to gas phase carbon monoxide was observed at 2070 and 2044 cm^{-1} . A new stable band at 1659 cm^{-1} on heating the surface to 120°C {figure 7.16 [c]} was observed. At this stage, it would be

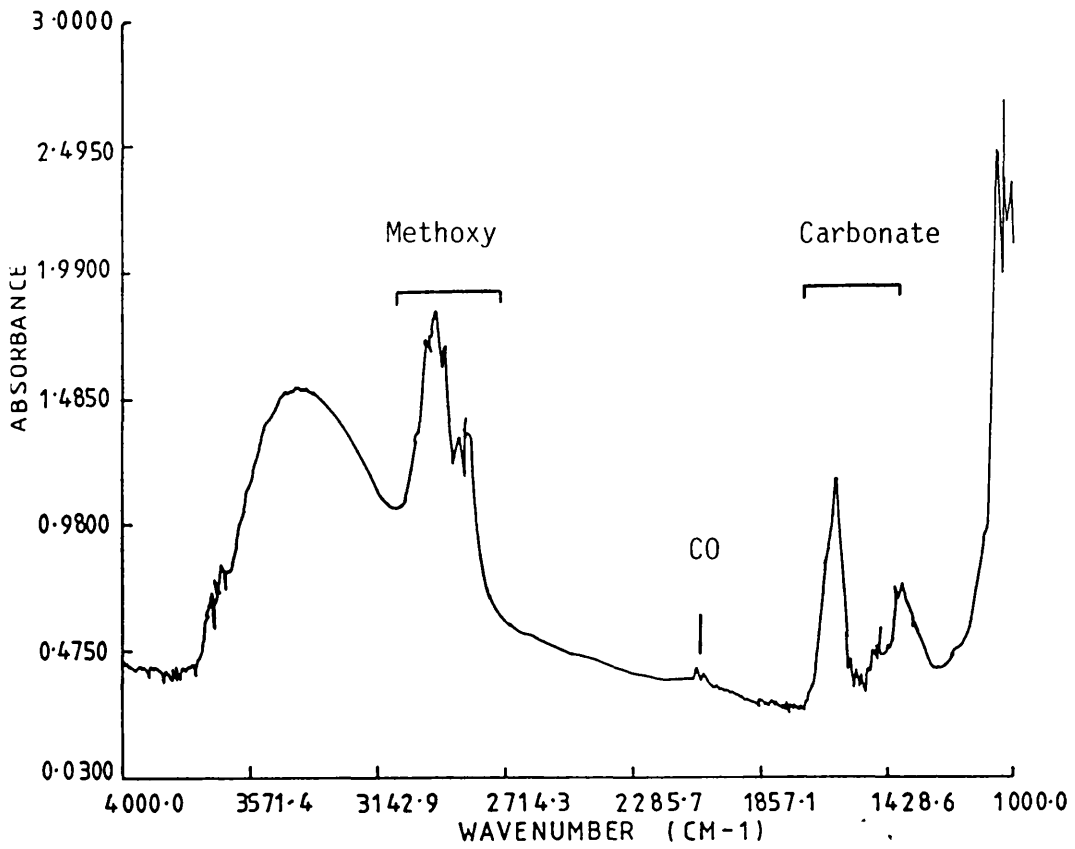


Fig 7.15a Spectrum of methanol (5 μ L) adsorbed on reduced alumina sample at room temperature.

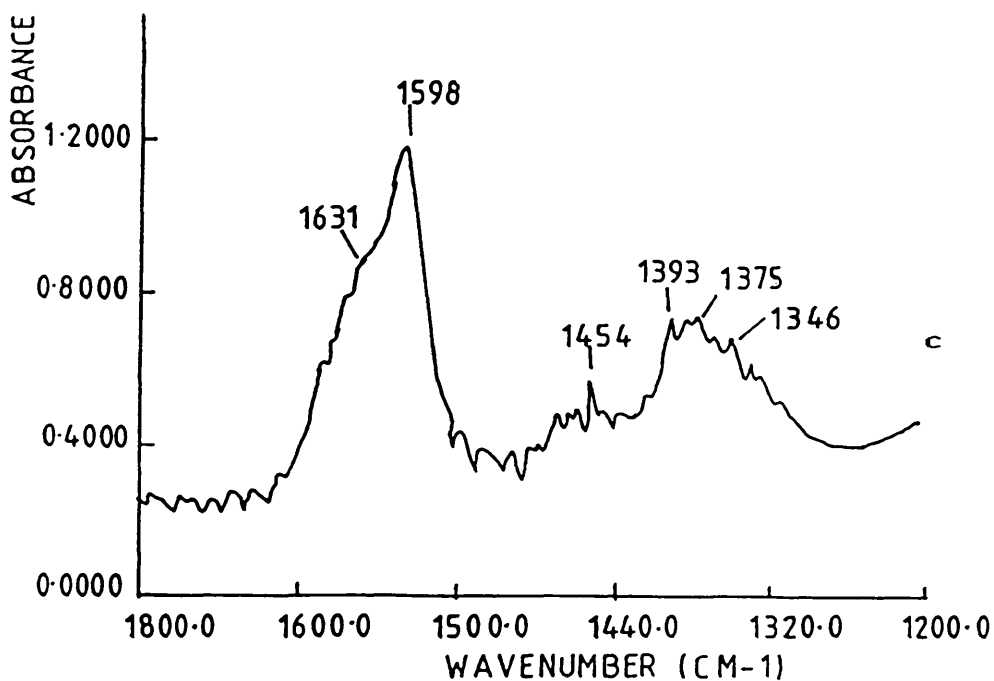
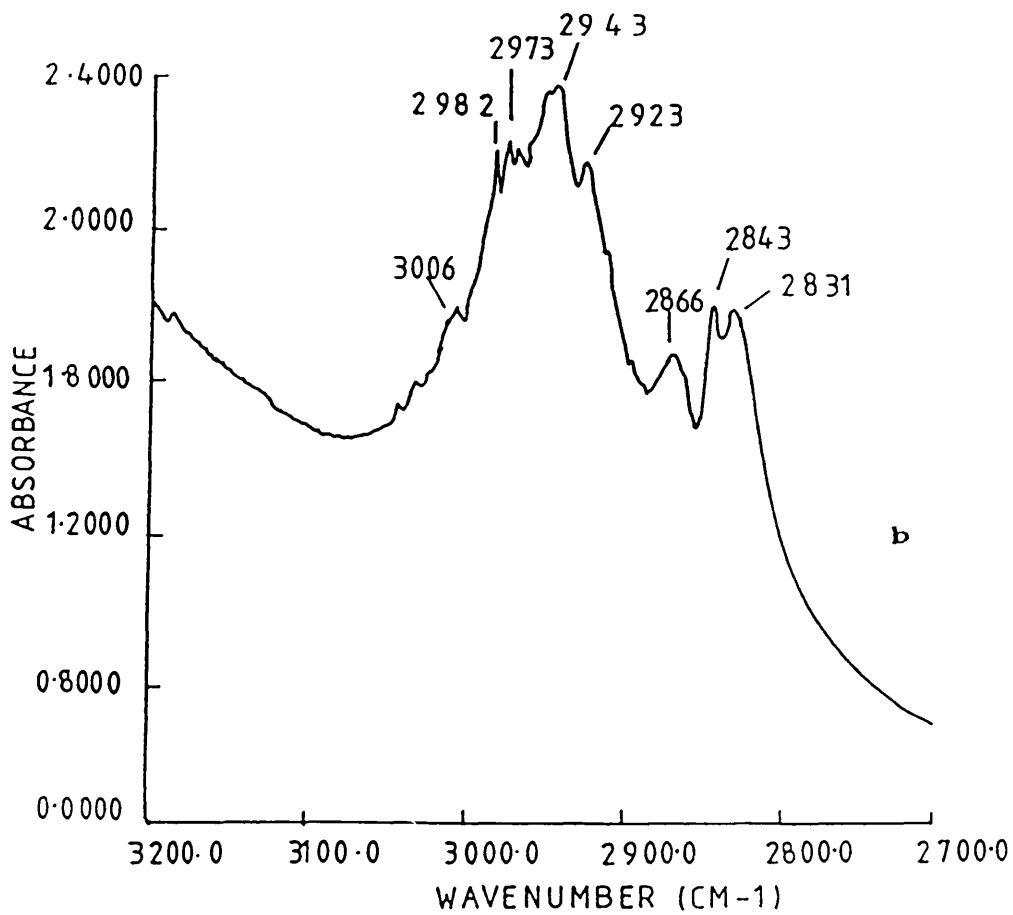


Fig 7.15b,c The vibrational spectrum of methoxy species (b) and carbonate group (c) following the interaction of (5 μ L) methanol with alumina surface.

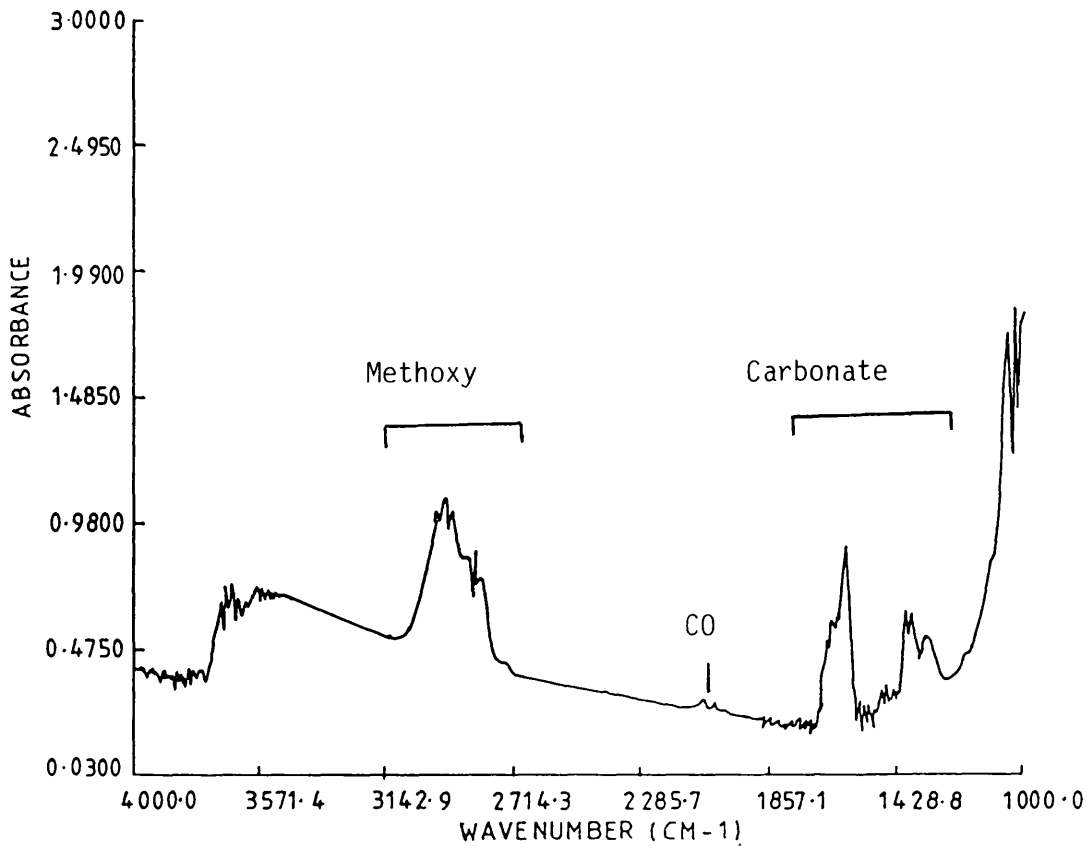


Fig 7.16a The interaction of (5 μ L) methanol with with alumina surface at 120°C.

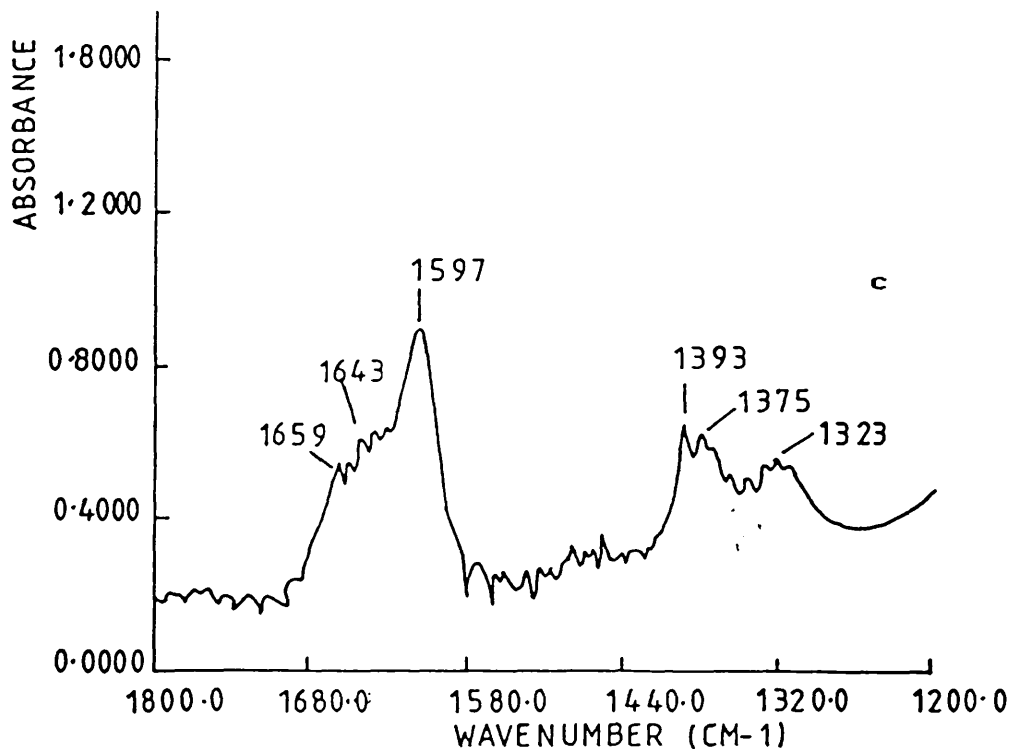
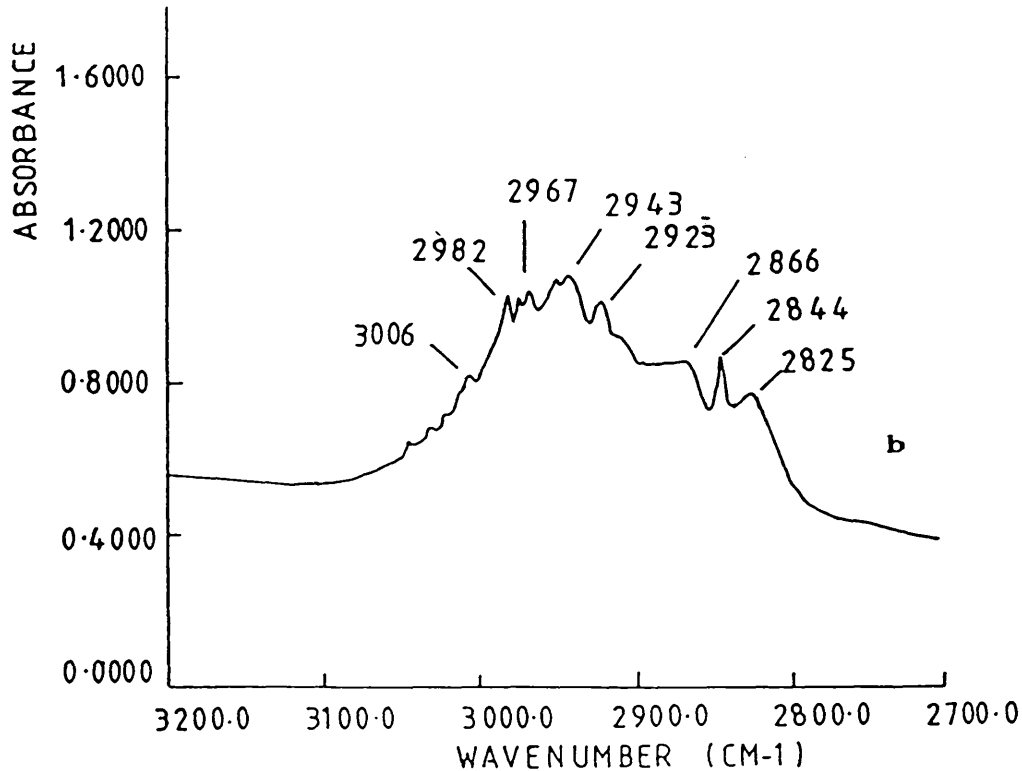


Fig 7.16b,c The bands appeared following (5 μ L) methanol interaction with alumina surface, (b) methoxy species, (c) carbonate species.

difficult to assign this band to any adsorbed species, but it could be due to adsorbed molecular water produced during methanol interaction on the alumina surface. Figure 7.16 [a] shows the carbonate bands. The band at 1659 cm^{-1} was also observed during the exposure of $5\text{ }\mu\text{l}$ of methanol at 220°C [figure 7.17 a] to an activated alumina sample, and shown in the expanded region in figure 7.17 [c]. In the case of figure 7.17 [d] the bands shown are probably due to atmospheric carbon dioxide as well as that produced from the interaction of methanol with alumina surface. To determine the position of the carbon dioxide band, the use of ^{13}C -labelled methanol represents an ideal way for further work to investigate the spectrum of adsorbed carbon dioxide.

Figure 7.17 [b] shows the methoxy bands formed during methanol interaction. The extent of the desorption of preadsorbed species as a function of temperature under helium flow (25 ml/min) was then investigated. As shown in figure [7.18], an increase in the desorption temperature results in a decrease in the intensities of the bands at 2947 and 2844 cm^{-1} (C-H stretching vibration of CH_3 group), With an increase in the intensities of the carbonate species bands ($1593\text{-}1375\text{ cm}^{-1}$). The bands at 1070 cm^{-1} (methoxy group) disappeared upon heating the surface from 160°C {figure 7.18 [b]} to 280°C {figure 7.18 [d]}. Most of these bands suffer a decrease in the intensity at temperature of 350°C after a 60 minutes helium flow {figure

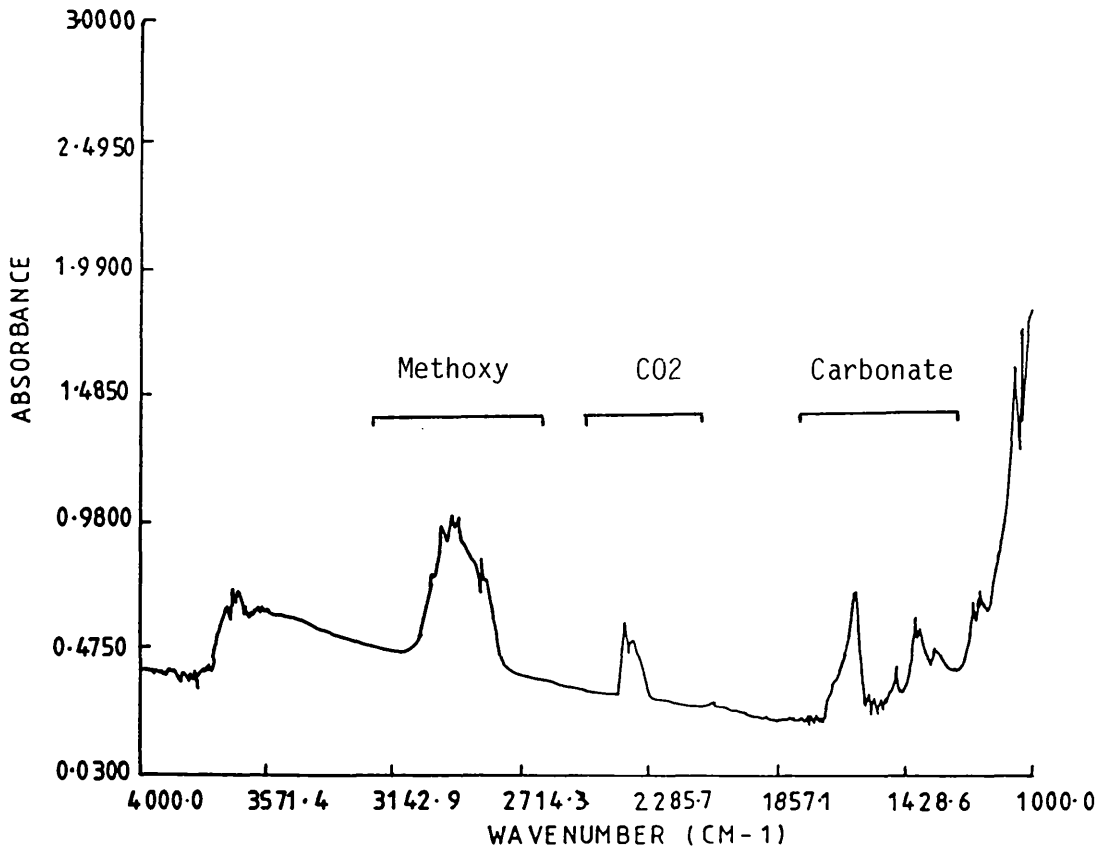


Fig. 7.17 a Methanol adsorption (5 μ l) on an alumina sample at 220 $^{\circ}$ C.

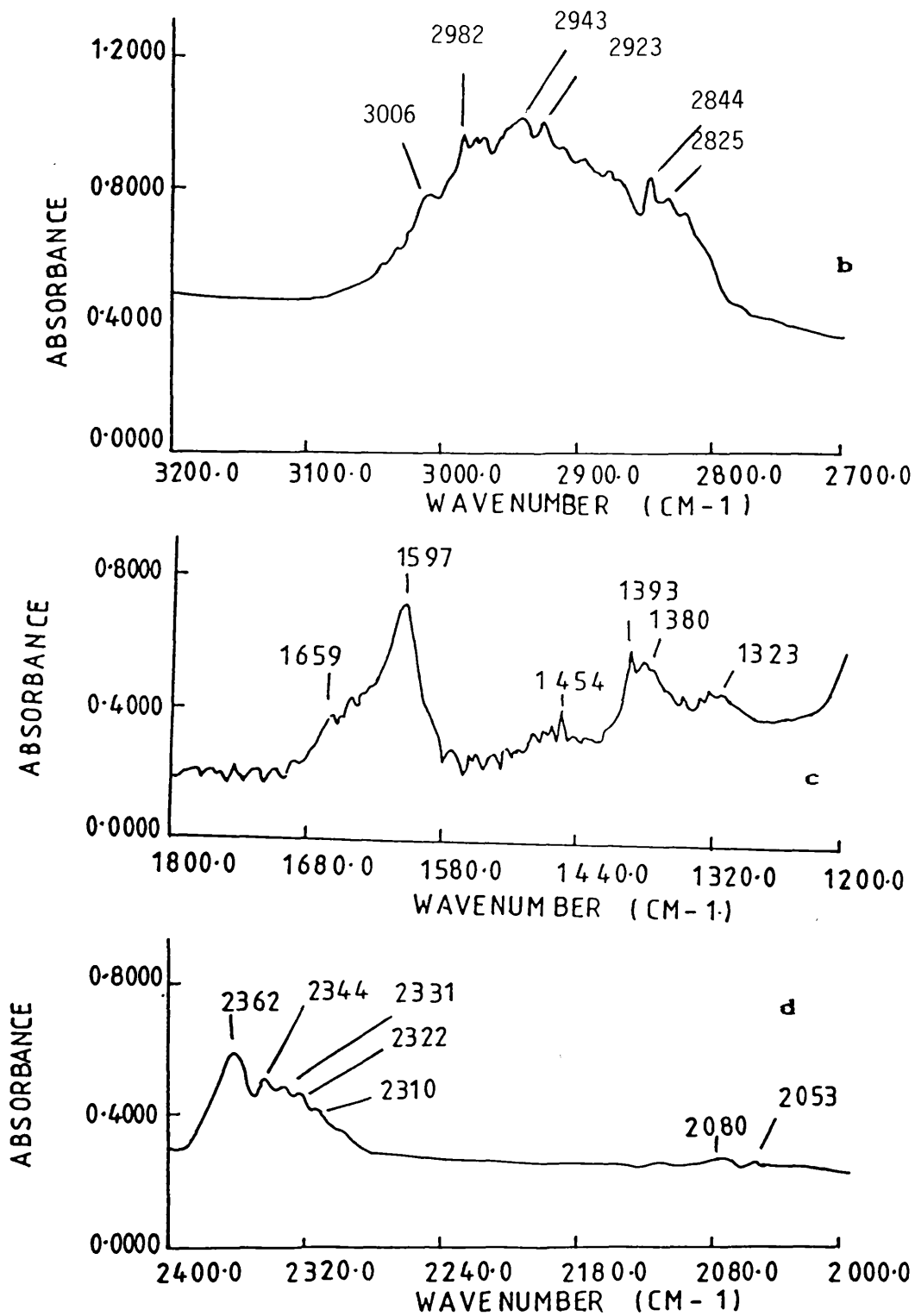


Fig 7.17 b, c, d The vibrational spectrum of (b) methoxy species, (c) carbonate species, and (d) carbon dioxide, obtained following the interaction of (5 μ l) methanol with an alumina surface at 220 $^{\circ}$ C.

7.18 [f]). The increase in the formate species upon heating the catalyst surface was reproducible even if the reverse action was taken (cooling the surface), as presented in figure 7.19 [a] spectra.

The spectral region of the formate ions was expanded and plotted in figure 7.19 [c], which clearly shows the increase in the intensity of the formate bands as well as the appearance of a band as a shoulder at 1640 cm^{-1} , which can be assigned to asymmetric stretching vibrations of formate ions. The methoxy bands at 1190 , 1070 , 1115 and 1053 cm^{-1} disappeared upon cooling the alumina surface under helium flow. In figure 7.19 [b] the vibration spectra of the C-H stretching of CH_3 group were plotted and show the disappearance of many bands under these conditions, while the bands at 3006 , 2954 , 2906 , 2893 and 2844 cm^{-1} were found to be stable under the experimental conditions. It can be clearly seen from a comparison of figures 7.19 [b] and [c] that, with each decrease in the C-H stretching band intensities, there is a corresponding increase in the intensities of the bands due to formate ions.

Figure 7.20 [a] illustrates the effect of the volume of methanol admitted on the resultant spectra. Bands due to methoxy groups associated with alumina appeared at higher methanol exposure ($10\text{ }\mu\text{l}$); these were observed at 1192 , 1178 , 1165 and 1115 cm^{-1} . In addition to these bands, a band due to a CO stretching mode (1053 cm^{-1}) of a methoxy

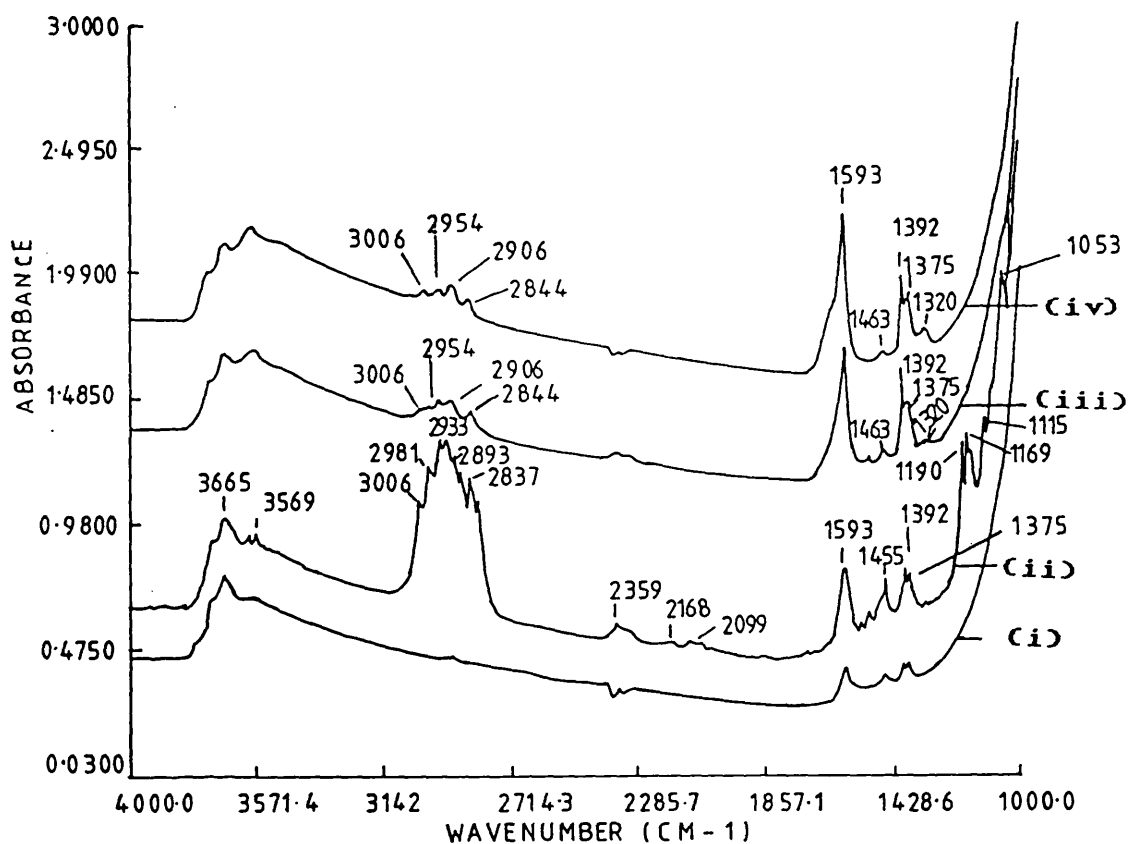


Fig 7.19 a The interaction of methanol with an alumina sample as a function of temperature; (i) reduced sample at 350°C, (ii) 10µl methanol at 350°C, (iii) sample cooled to 250°C, (iv) sample at 115°C.

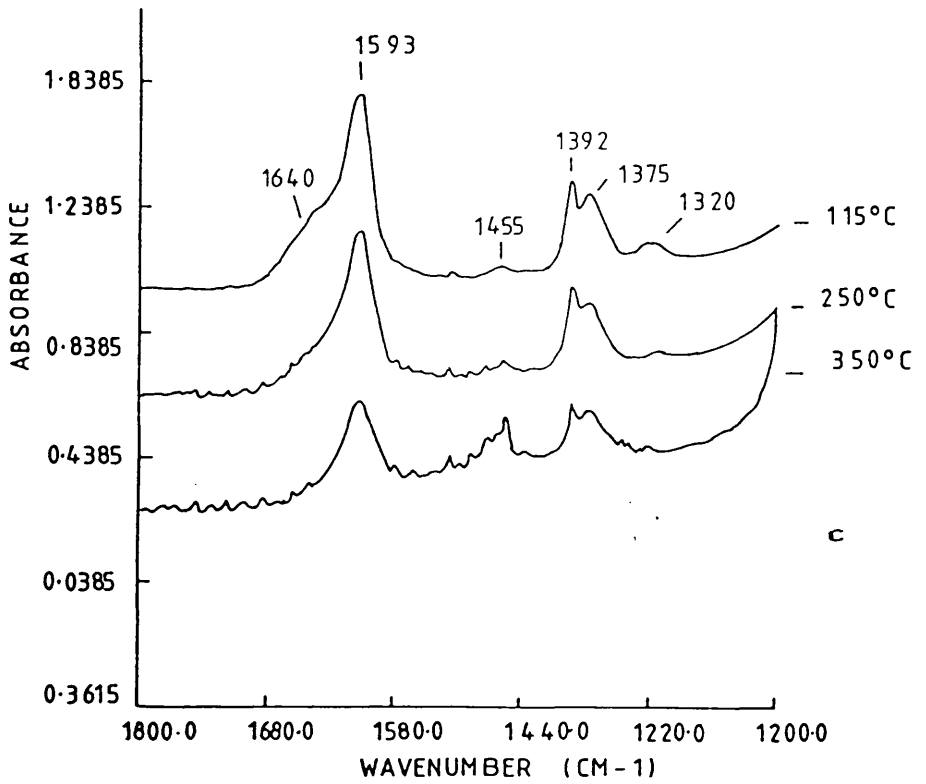
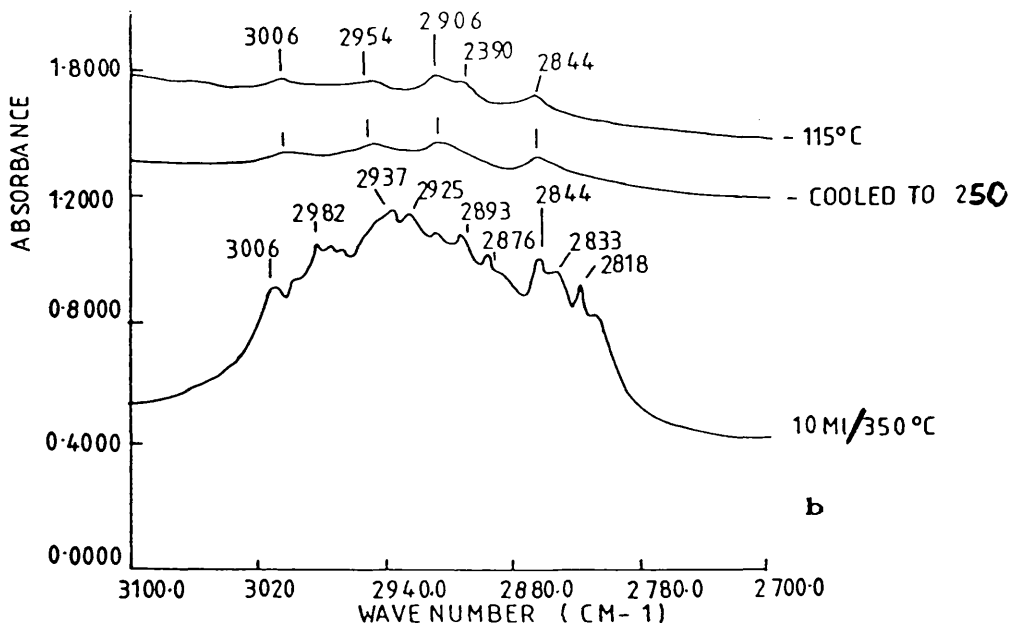


Fig 7.19b,c The decrease in the methoxy bands intensities, (b) as the carbonate bands (c) intensities increased.

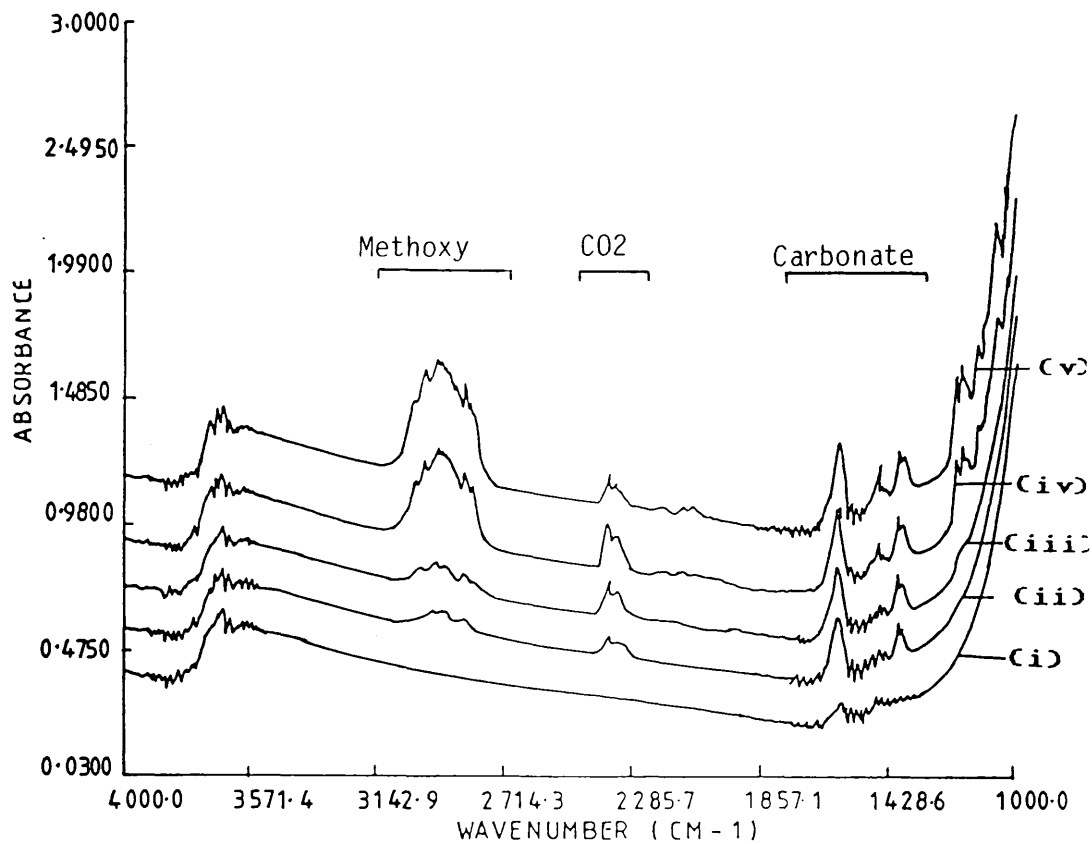


Fig.7.20 a Various amounts of methanol adsorbed on an alumina surface at 350°C, (i) reduced sample, (ii) 1 μ l, (iii) 2 μ l, (iv) 5 μ l, and (v) 10 μ l.

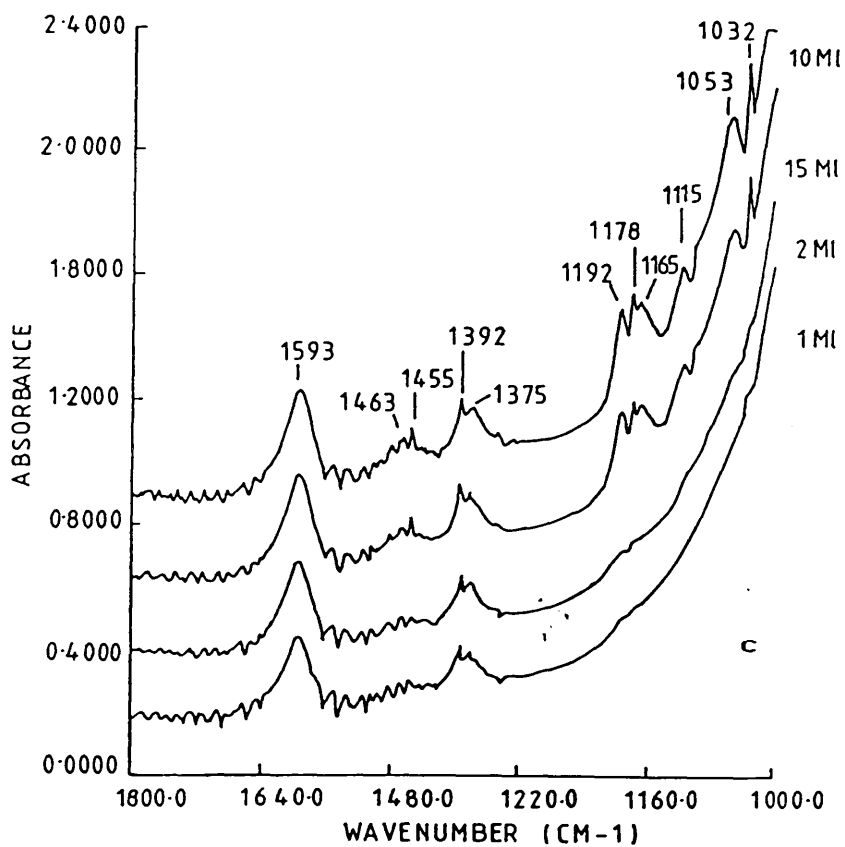
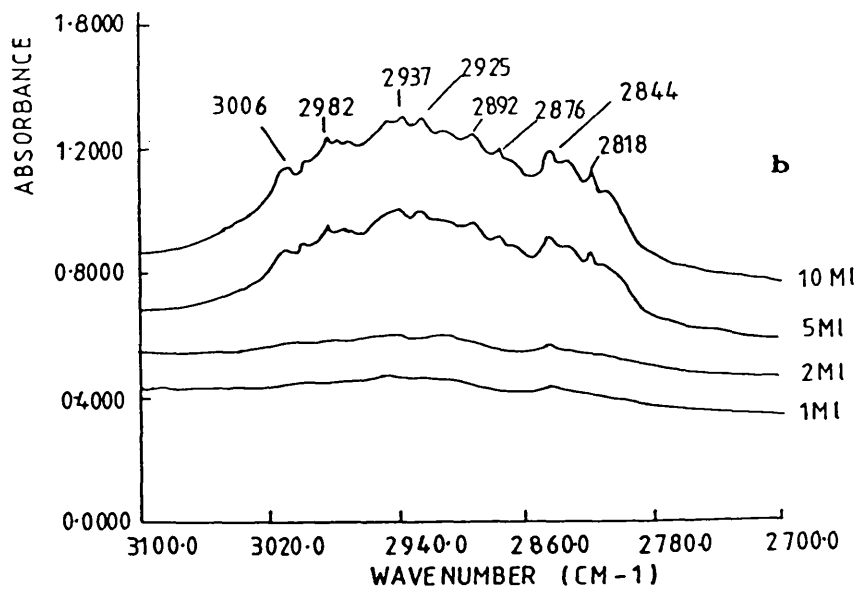


Fig 7.20b.c Intensity increase of methoxy species, (b) and carbonate species, (c) as a function of total methanol exposure at 350°C.

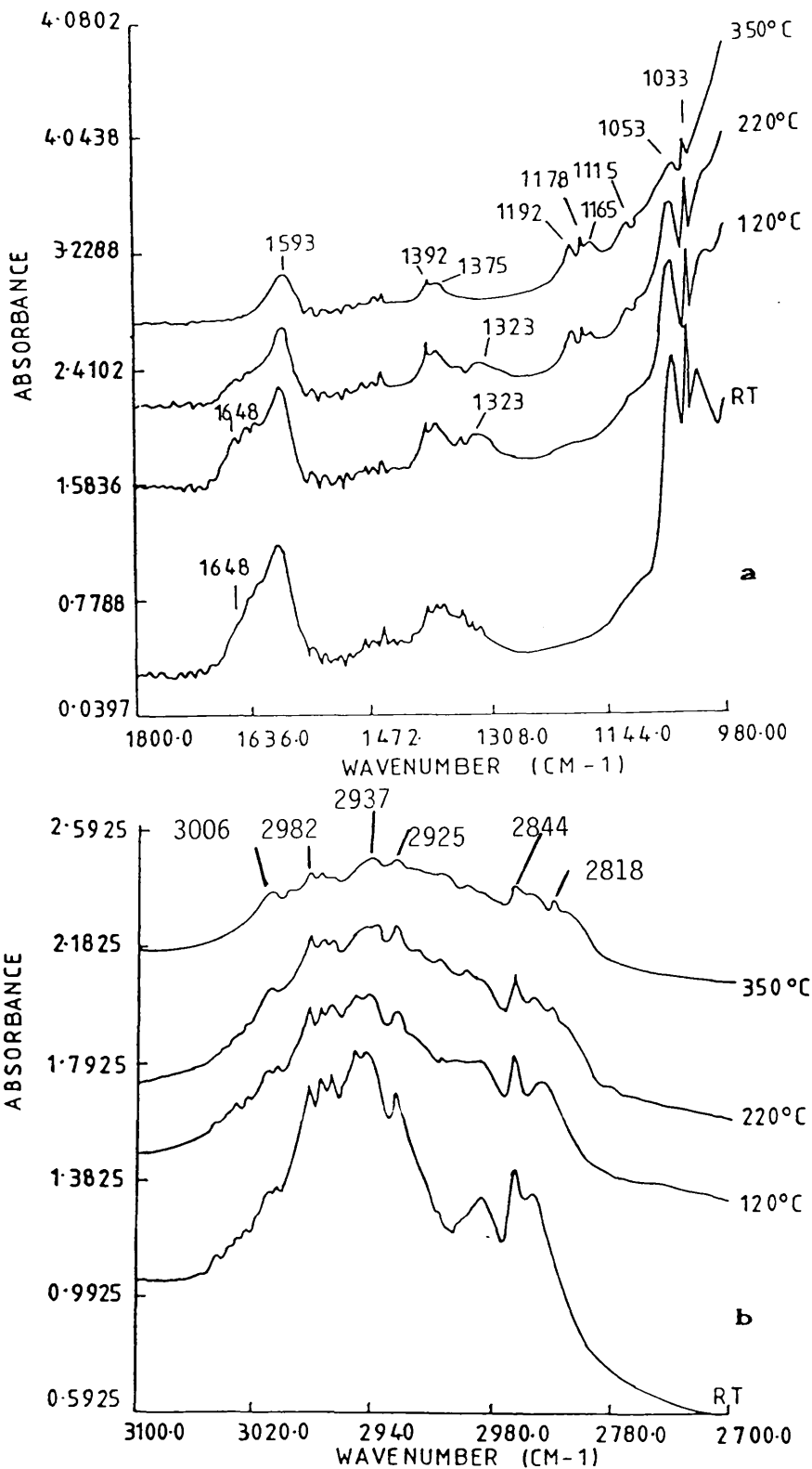


Fig.7.21 a,b The intermediate groups formed following methanol (5 μl) interaction with an alumina surface at various temperatures, (a) carbonate species, (b) methoxy species.

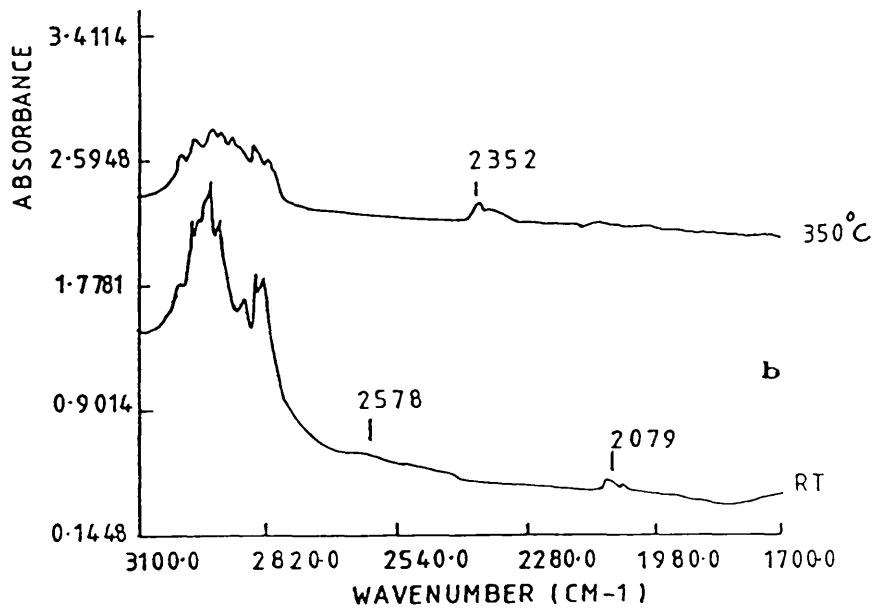
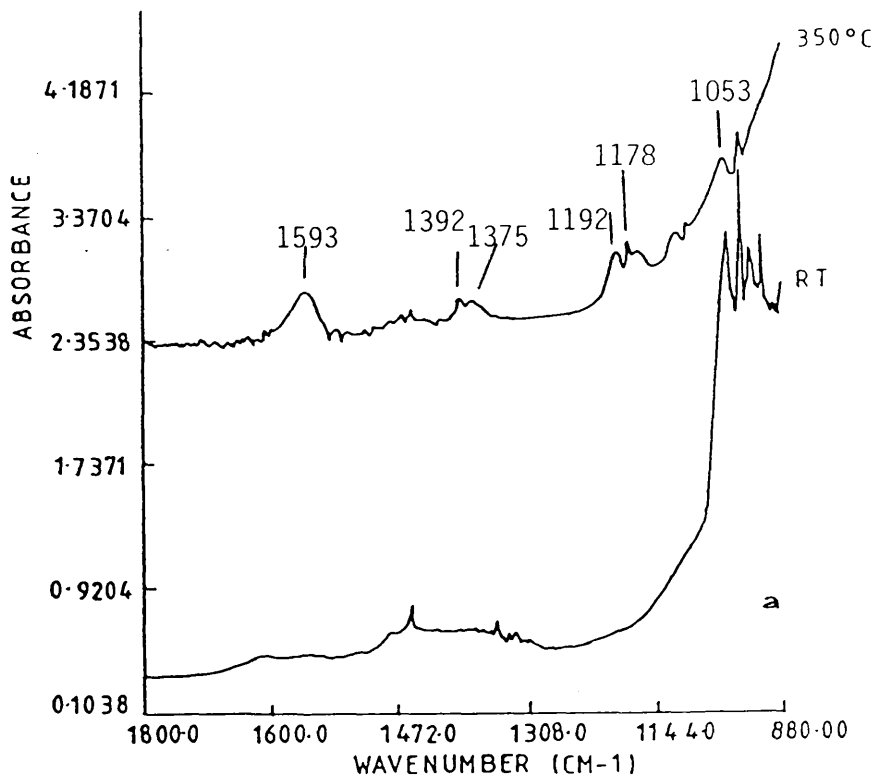


Fig.7.22 a,b The interaction of methanol (10 μ l) with an alumina surface, (a) carbonate species, (b) methoxy species.

group was also observed, while bands due to the stretching vibration of formate ions also appeared after high methanol exposure; bands at 1463 and 1455 cm^{-1} are clearly presented in figure 7.20 [c], while figure 7.20 [b] shows the C-H stretching vibration bands at both low and high exposure to methanol.

Most of the C-H stretching bands appeared at the higher methanol concentrations. Figure 7.21 [a] and [b] show the spectra obtained after exposing the alumina surface to 5 μl methanol at different temperatures. The decrease in the intensity of the methoxy bands is shown in figure 7.21 [b] at higher temperatures, as is the appearance of bands due to the alumina methoxide groups at 1192, 1178, 1165 and 1115 cm^{-1} {figure 7.21 [a]}. A decrease in the CO stretching of a methoxy group at 1053 and 1033 cm^{-1} was observed {7.21 [a]}. Also, a band at 1648 cm^{-1} , which may be assigned to molecular water, was observed at room temperature and at 120°C, while at 350°C there was no longer evidence for water or the C-H_n stretching band at 1323 cm^{-1} due to the formate ions. These differences between the spectra obtained at room and elevated temperatures are also presented in figure 7.22 [a] and [b], which show the spectra the alumina surface after exposure to 10 μl methanol at room temperature and at 350°C.

7.2 FTIR SPECTROSCOPIC STUDY OF THE INTERACTION OF CARBON MONOXIDE WITH COPPER-BASED CATALYST SURFACES

Catalyst samples were treated normally with 6% hydrogen in nitrogen and then used to investigate the adsorption of carbon monoxide at various temperatures.

7.2.1 Carbon Monoxide Adsorption on Cu/Al₂O₃

Figure [7.23] shows the spectra of carbon monoxide adsorbed on activated Cu/Al₂O₃, where spectrum (a) represents the activated catalyst sample. A stream of carbon monoxide was passed over the activated catalyst for 5-10 minutes at a flow rate of 25 ml/min, followed by a 10 minute flushing with helium at room temperature, at which point the spectrum of the adsorbed carbon monoxide was recorded (spectrum b). A single adsorption band was observed at 2106 cm⁻¹ which can be ascribed to carbon monoxide linearly bonded to Cu/Al₂O₃. Leaving the catalyst under a helium flow of 25 ml/min for 30 minutes results in a small shift in the band position to a lower wave number, 2099 cm⁻¹, as shown in spectrum (c). This treatment also resulted in a slow decay in the band intensity as illustrated in spectra (d), (e) and (f).

The adsorption of carbon monoxide on Cu/Al₂O₃ at 100°C was also investigated {see curves b-h in figure [7.24]}. At

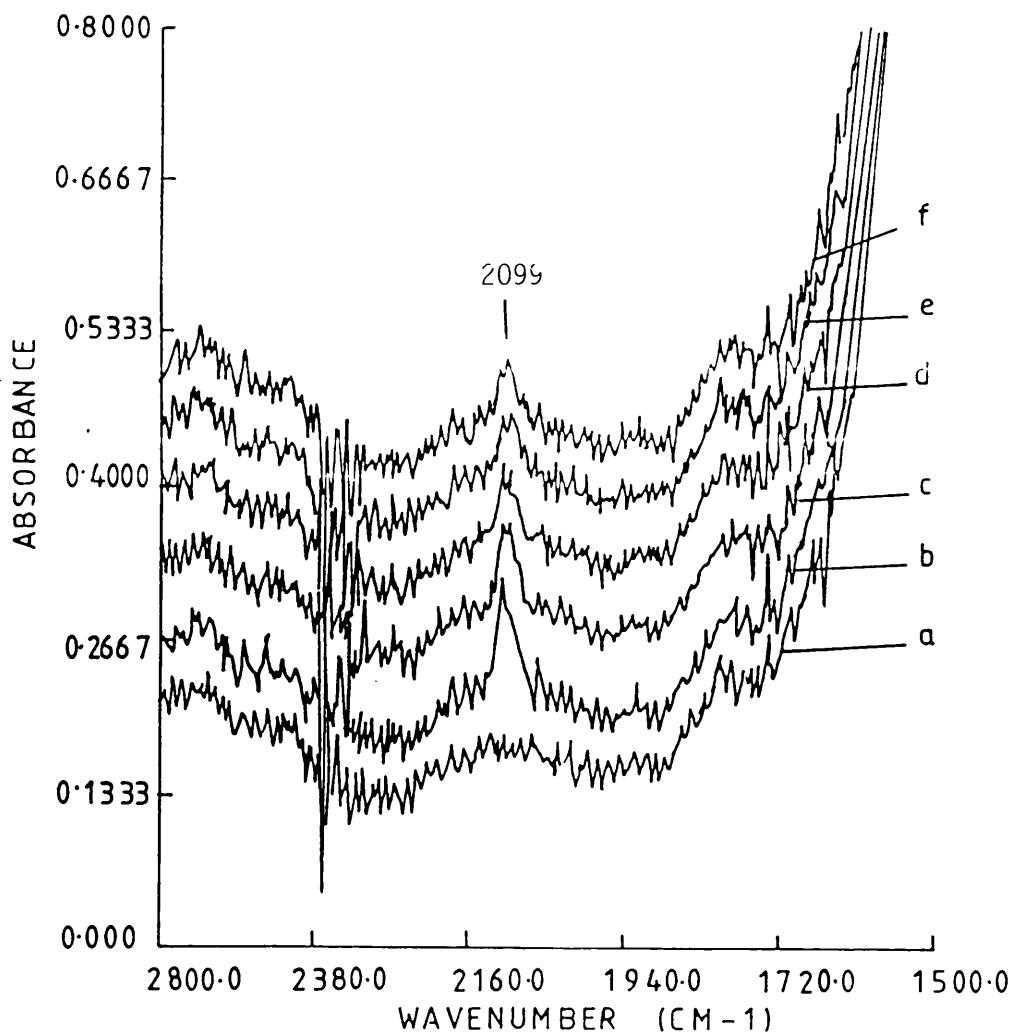


Fig.7.23 Carbon monoxide adsorption on a copper/alumina sample at RT, spectrum recorded as; (a) reduced sample, (b) sample after 5 min., (c) after 30 min., (d) after 60 min., (e) after 90 min., and (f) after 120 min.

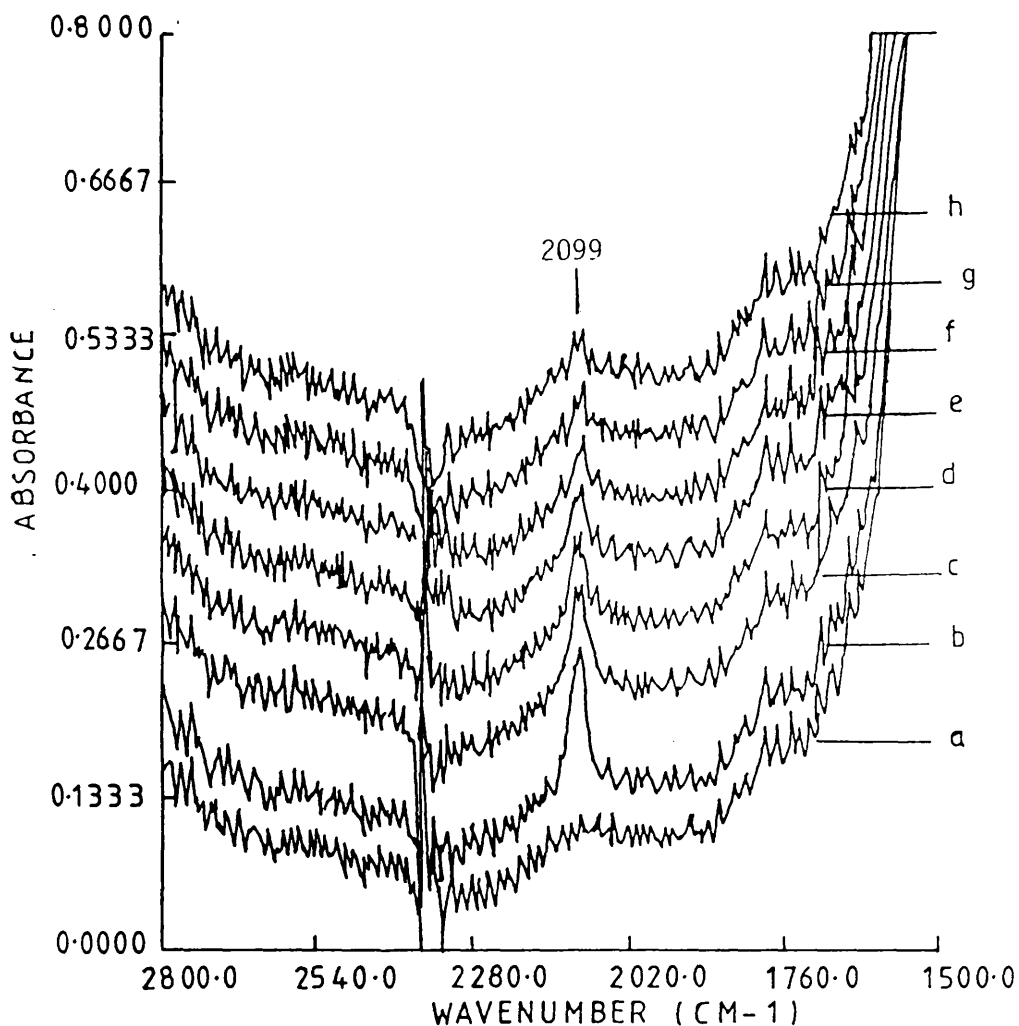


Fig.7.24 Carbon monoxide adsorption on a copper/alumina sample at 100°C, spectrum recorded as; (a) reduced sample, (b) sample after 5 min., (c) after 30 min., (d) after 60 min., (e) after 90 min.,(f) after 120 min., (g) after 150 min., and (h) after 180 min.

this temperature a band due to adsorbed carbon monoxide was observed at 2090 cm^{-1} . A slow decay was observed in the band intensity as a result of flowing helium at rate of 25 ml/min at 100°C , as shown by recording the spectrum at 30 minute intervals during this treatment. These findings are presented in spectra (c to h) in figure [7.24]. Figure [7.25] shows the same behaviour for the carbonyl band associated with $\text{Cu}/\text{Al}_2\text{O}_3$ at 150°C . A gradual decay in intensity with no shift in band position was observed. There was no carbonyl adsorption band in evidence when adsorption occurred at temperatures in excess of 200°C .

7.2.2 FTIR Study of the Interaction of Carbon Monoxide with $\text{Cu-ZnO}/\text{Al}_2\text{O}_3$

A sample of $\text{Cu-ZnO}/\text{Al}_2\text{O}_3$ was activated in similar way to that of $\text{Cu}/\text{Al}_2\text{O}_3$. The activated catalyst has an infrared spectrum similar to that described in section 7.1.2. After the activation procedure had been completed, a stream of carbon monoxide at a flow rate of 25 ml/min was passed over the catalyst at the appropriate temperature and spectra were recorded 10-15 minutes after the carbon monoxide treatment.

Figure [7.26] shows the spectra of carbon monoxide adsorbed on an activated sample of $\text{Cu-ZnO}/\text{Al}_2\text{O}_3$ at room temperature. An adsorption band due to chemisorbed carbon monoxide can be clearly observed at 2106 cm^{-1} and was found to be stable in helium for up to two hours {curves b to e

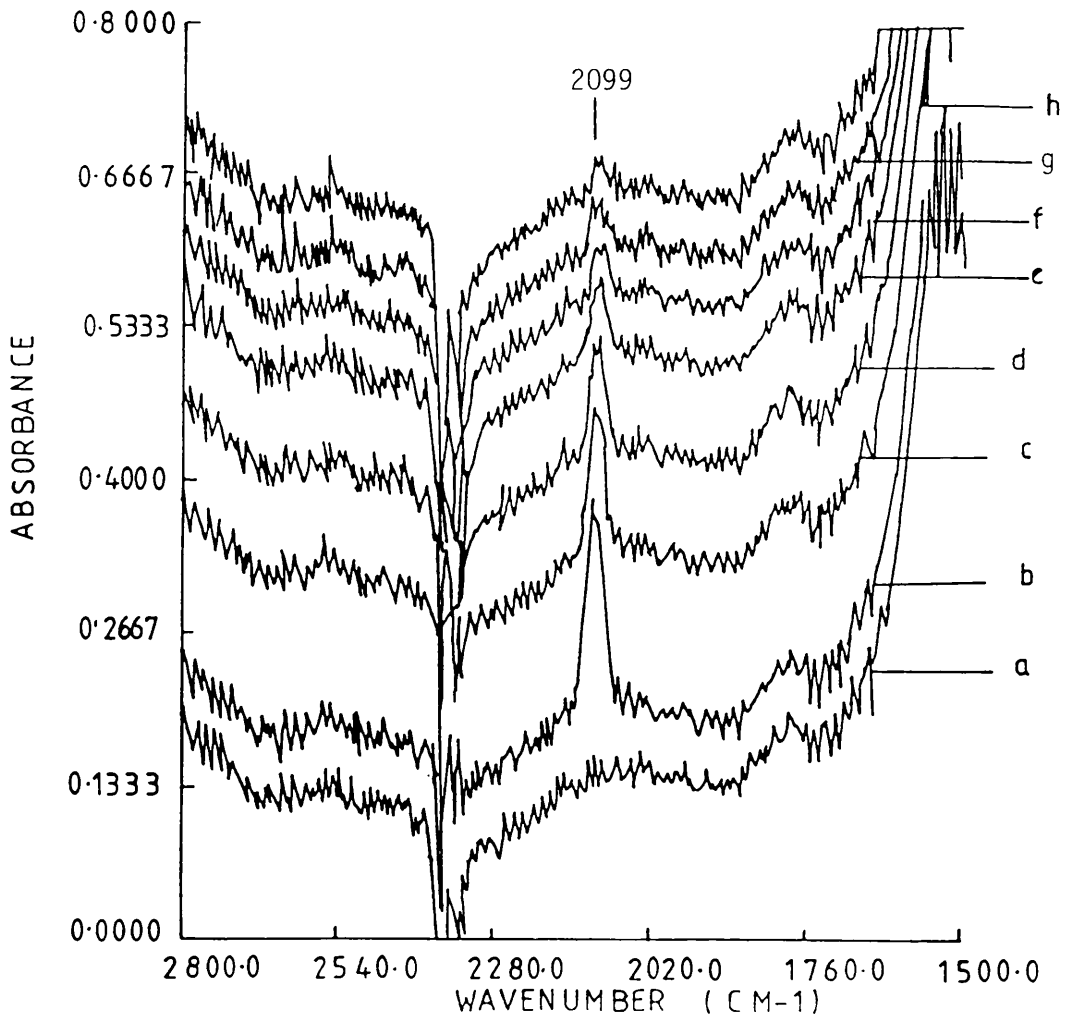


Fig.7.25 Carbon monoxide adsorption on a copper/alumina sample at 150°C, spectrum recorded as; (a) reduced sample, (b) sample after 5 min., (c) after 30 min., (d) after 60 min., (e) after 90 min., (f) after 120 min., (g) after 150 min., and (h) after 180 min.

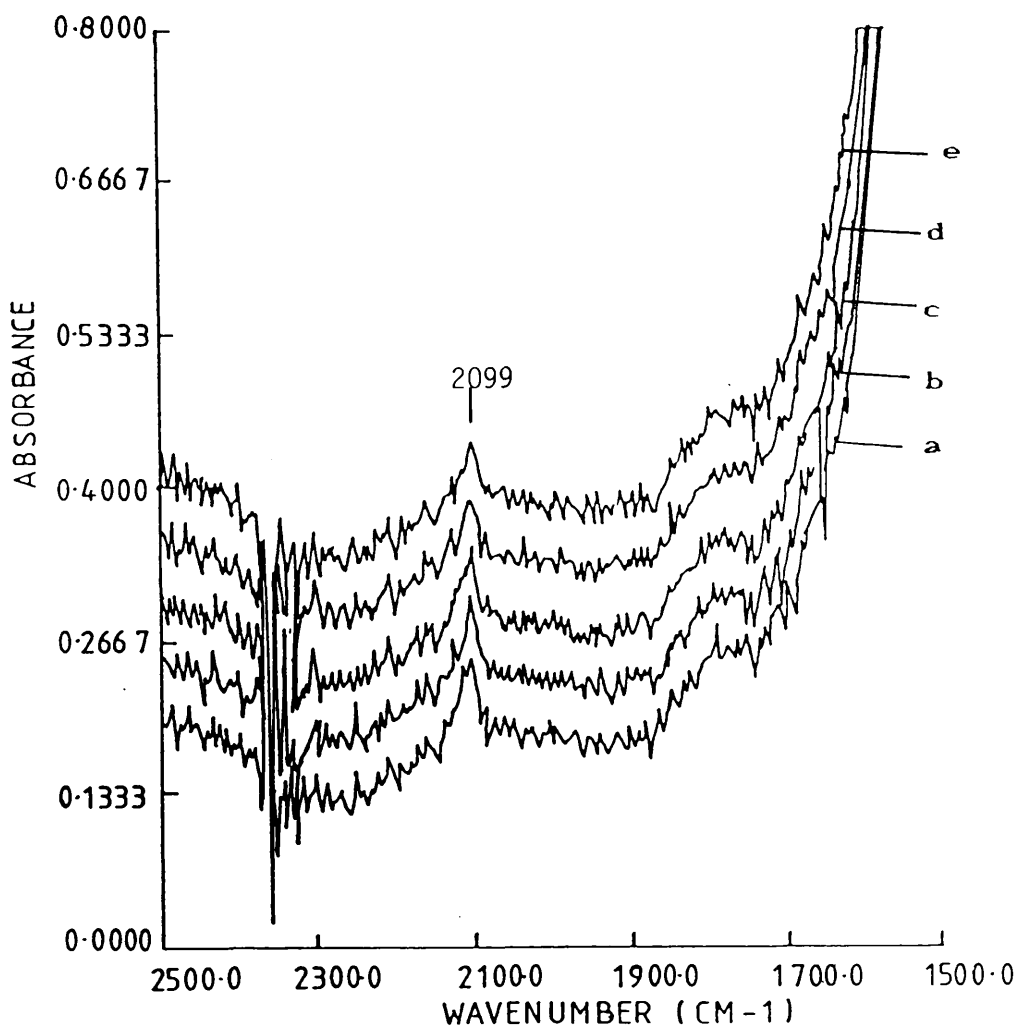


Fig.7.26 Carbon monoxide adsorption on a copper/zinc oxide/alumina sample at RT, spectrum recorded as; (a) sample after 5 min., (b) after 30 min., (c) after 60 min., (d) after 90 min., and (e) after 120 min.

in figure [7.26]).

Similar results were obtained with carbon monoxide adsorbed on the activated Cu-ZnO/Al₂O₃ sample at 100 or 150°C, as shown in figure [7.27].

The intensity of the band at 2106 cm⁻¹ decayed with time when carbon monoxide was adsorbed on Cu-ZnO/Al₂O₃ at 200°C [figure 7.28].

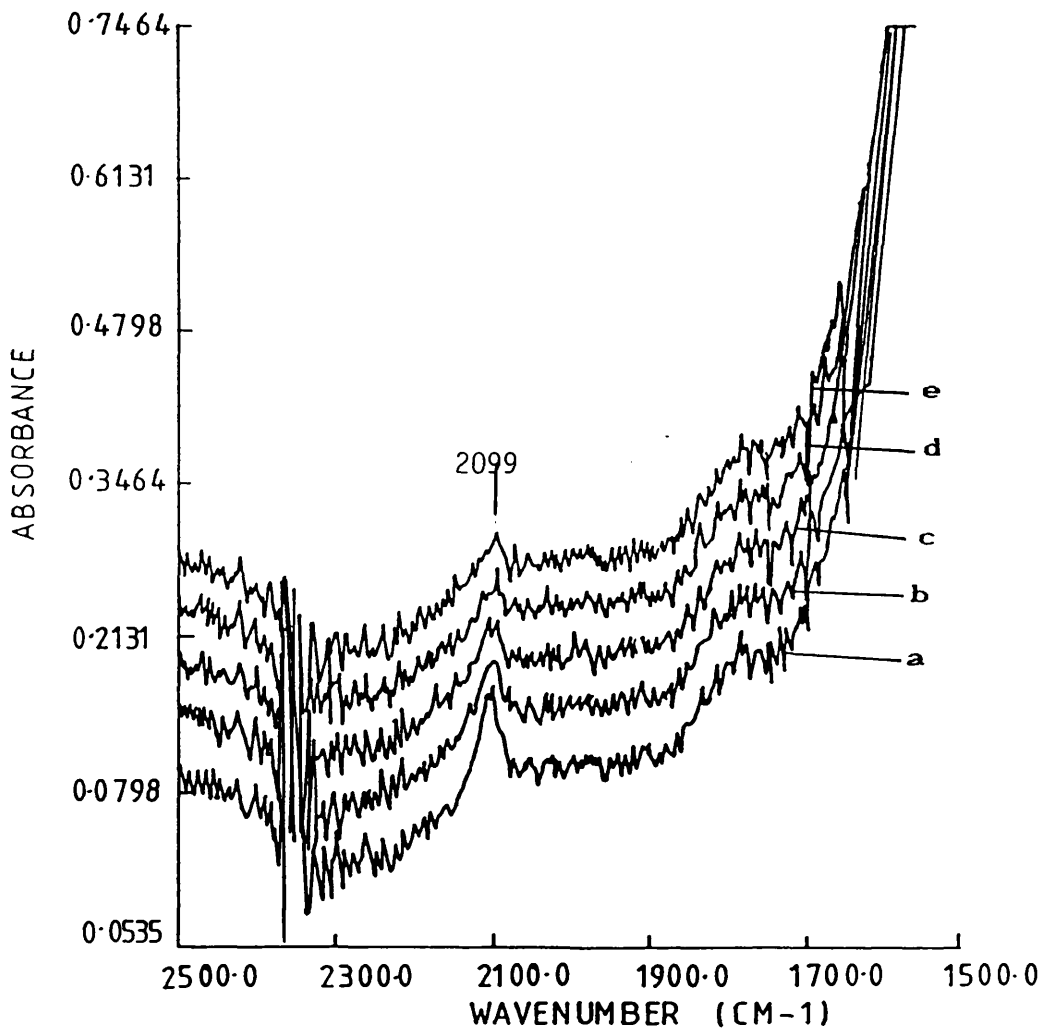


Fig.7.27 Carbon monoxide adsorption on a copper/zinc oxide/alumina sample at 100°C, spectrum recorded as; (a) sample after 5 min., (b) after 30 min., (c) after 60 min., (d) after 90 min., and (e) after 120 min.

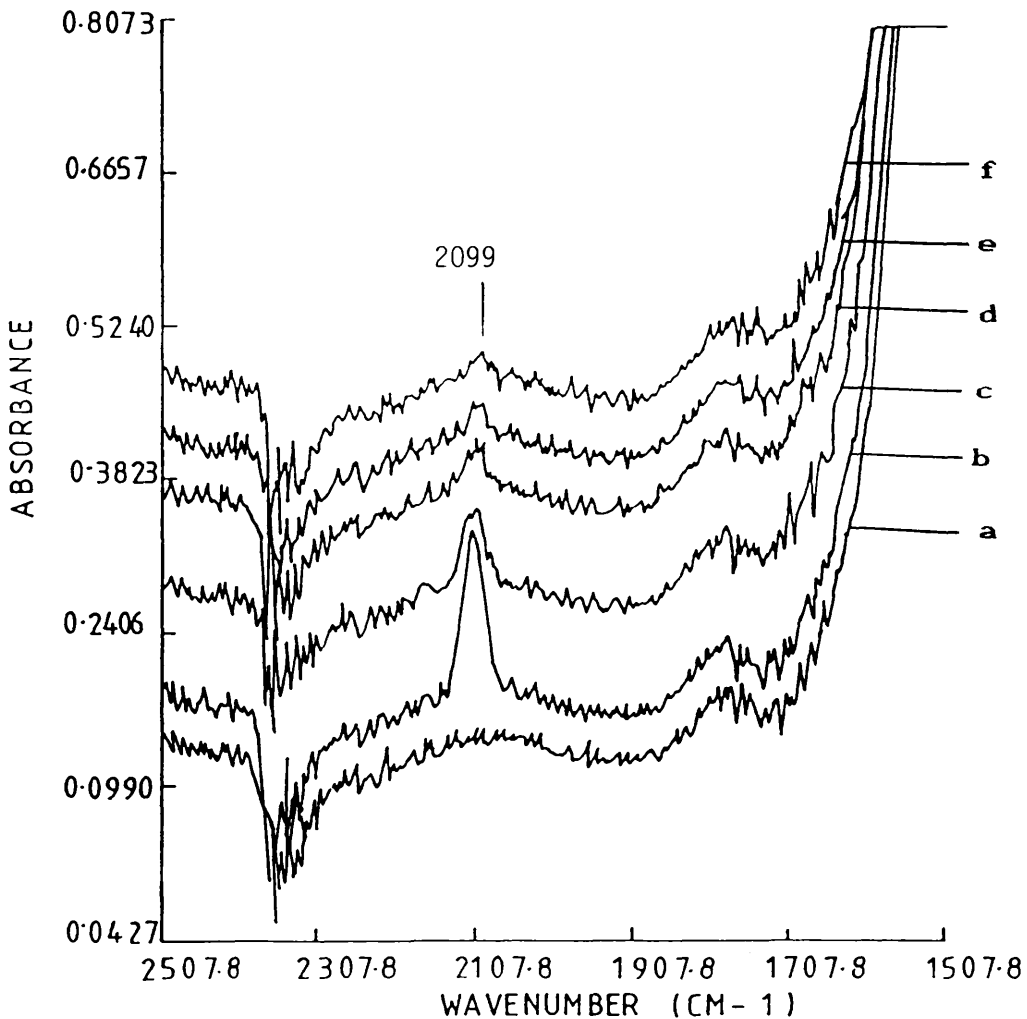


Fig.7.28 Carbon monoxide adsorption on a copper/zinc oxide/alumina sample at 200°C, spectrum recorded as; (a) reduced sample, (b) sample after 5 min., (c) after 30 min., (d) after 60 min., (e) after 90 min., and (f) after 120 min.

CHAPTER EIGHT

DISCUSSION

8.1 INTRODUCTION

The results presented in this thesis will be discussed in this chapter.

During the discussion, the effect of hydrogen sulphide poisoning will be presented within the relevant section in order to explain more clearly the poisoning effect on the adsorption and reaction of other molecules on copper-based catalyst surfaces.

The FTIR results will also be considered and are included as a part of the general discussion.

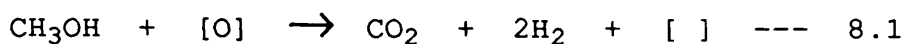
8.2 Methanol Decomposition on Cu/Al₂O₃ and Cu-ZnO/Al₂O₃ Catalysts

Reducing the Cu/Al₂O₃ catalyst with 6% hydrogen in nitrogen at 180°C prior to methanol adsorption, resulted in a liberation of hydrogen as a minor product as well as the carbon oxides (carbon monoxide and carbon dioxide), which were observed in the gas phase as a result of the decomposition reaction following the pulsing of methanol. The results displayed in figure [4.1] show that methanol was converted mainly to carbon dioxide, with a small amount

of carbon monoxide.

The yield of carbon dioxide is at its maximum at the beginning of the reaction, 89% of the products being carbon dioxide and only 11% being carbon monoxide. On increasing methanol pressure, the relative amounts of the carbon oxides were altered, such that the carbon monoxide concentration is higher than that of carbon dioxide.

Considering the results shown in figure [4.1] and taking in account the reduction procedure, it can be suggested that the high yields of carbon dioxide arise owing to the presence of surface oxygen according to the equation:



Where [O] represents the surface oxygen; and [] represents a surface site. The same behaviour was also observed when methanol was pulsed in a controlled manner over a Cu/Al₂O₃ sample reduced with 6% hydrogen in nitrogen at 250°C [figure 4.2]. When the distribution of reaction products was studied as a function of temperature, the results showed that at low temperature (the beginning of the experiment) the carbon dioxide concentration was very high (>80% of reaction product). The concentration of carbon dioxide was observed to decrease at first, then to increase again as the reaction temperature increased. At higher temperatures (>260°C) the carbon dioxide yield was

at its highest. The decrease in carbon dioxide production as a result of methanol interaction with $\text{Cu}/\text{Al}_2\text{O}_3$ must correspond to the complete reduction of the surface oxide (e.g. 8.1).

When carbon monoxide was used as a reducing agent following hydrogen reduction, the results show that although a decrease in the production of both carbon monoxide and carbon dioxide was observed, the concentration of carbon dioxide was still higher than that of carbon monoxide. Since the reduction with the carbon monoxide stream was only for short time (30 minutes), it would be difficult to state that the catalyst surface had been reduced completely. This conclusion was confirmed by results obtained from the reaction of methanol with a sample of $\text{Cu}/\text{Al}_2\text{O}_3$ which had been reduced in pure carbon monoxide at 250°C for 14 hours, following the normal reduction procedure with 6% hydrogen in nitrogen. In this experiment the concentration of carbon monoxide was higher than that of carbon dioxide, although carbon dioxide was still formed in small concentrations, which increased as the total amount of methanol introduced to the catalyst surface increased. The concentration of carbon monoxide increased linearly with pulse number and was noticeably higher than that of carbon dioxide.

A complete reduction of $\text{Cu}/\text{Al}_2\text{O}_3$ sample was obtained when the catalyst was reduced from the oxide form with

carbon monoxide for 14 hours at 250°C. This was confirmed by the formation of a higher concentration of carbon monoxide following the interaction of methanol with such sample [figure 4.8].

One has to note that at the beginning of each experiment a water peak was also detected for the first one or two reactions of methanol. The formation of water can be related to the reaction of hydrogen formed from the methanol decomposition with surface oxide, but the hydrogen peak was detected throughout the decomposition reaction, so the formation of water must be due to the consumption of the bulk hydrogen formed in the decomposition of methanol for the reduction of the surface:



Also, water could be formed by the water-gas shift reaction, which might contribute to the change in concentration of both carbon monoxide and carbon dioxide.

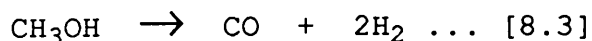
The concentration of carbon monoxide increased to a steady value while the rate of liberation of carbon dioxide fell with time until the surface reduction had been completed as a result of both reactions 8.1 and 8.2. A steady state was achieved in the system, such that carbon monoxide was the major product with a small concentration of carbon dioxide. The reason behind the formation of some carbon dioxide in all experiments will be discussed later

in this section.

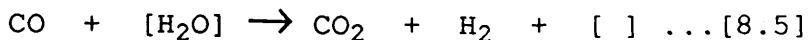
On the same basis, the reaction of methanol was studied on reduced Cu-ZnO/Al₂O₃ with 6% hydrogen in nitrogen at 180°C. The decomposition results show that carbon monoxide was the major product formed, and its yield increased as the total amount of methanol admitted to the catalyst was increased [figure 4.10].

Similar results to those obtained with Cu/Al₂O₃ were obtained on Cu-ZnO/Al₂O₃ [figure 4.11, 4.13], when the Cu-ZnO/Al₂O₃ was reduced with pure carbon monoxide at 250°C for 14 hours in that carbon monoxide and hydrogen were formed as the major products, together with trace amounts of carbon dioxide. However, in this experiment and during the investigation of the effects of reaction temperature using catalyst samples which had been reduced with pure carbon monoxide, the concentration of methanol decomposition products were lower than those produced from hydrogen treated catalyst sample.

To explain the reason for the formation of carbon dioxide, two hypotheses can be considered. On oxidised or partially reduced surfaces methanol interacts with the catalyst surface according to reaction [8.1]. However, on a fully reduced surface, carbon monoxide and hydrogen are formed:



From reaction [8.3] on well-reduced surfaces of Cu/Al₂O₃ or Cu-ZnO/Al₂O₃, carbon monoxide is the primary product; then the presence of carbon dioxide as a decomposition product can be explained by the reaction of carbon monoxide with surface oxygen and/or water:



Water could result from the interaction of hydrogen, formed during the decomposition reaction, with the oxygen present on the surface. In this case, carbon dioxide can be formed for the first few reactions. When reaction [8.5] is responsible for carbon dioxide formation, it would be reasonable to suggest that traces of water present in the methanol feedstock are responsible for the formation of carbon dioxide in the decomposition of methanol on catalyst sample which have been fully reduced with pure carbon monoxide at 250°C.

Figure [4.9] confirms that, according to the reduction procedure followed during this study using 6% hydrogen in nitrogen, reduction was not completed. Hence, the interaction of carbon monoxide with such a surface produced carbon dioxide.

On catalyst samples reduced with pure carbon monoxide, trace amounts of methane were detected in the gas phase in

amounts which remained stable throughout the experiment, but which were only observed at higher temperatures ($>280^{\circ}\text{C}$). The formation of methane appears to be associated with the appearance of reduced sites (probably by methanol), which are different in nature from sites reduced by carbon monoxide. Possibly, such sites are responsible for the formation of hydrocarbons during methanol synthesis.

Before we go any further in discussing the important effect of surface oxygen in the decomposition reaction of methanol with copper catalysts, or discussing the literature concerning this subject; it is important to consider the results obtained from the investigation by FTIR of the methanol interaction with copper-based catalysts. Although the loadings of copper in $\text{Cu}/\text{Al}_2\text{O}_3$ and $\text{Cu-ZnO}/\text{Al}_2\text{O}_3$ catalysts were very high, 64 and 60% respectively, the scale of information obtained from such investigations can only permit us to suggest the involvement of formate species in the decomposition reaction. This was supported by the appearance of two bands at 2925 and 2832 cm^{-1} on both $\text{Cu}/\text{Al}_2\text{O}_3$ and $\text{Cu-ZnO}/\text{Al}_2\text{O}_3$. However, this formate species was found to be stable under the experimental conditions at 200°C and helium flow rate of 25 ml/min.

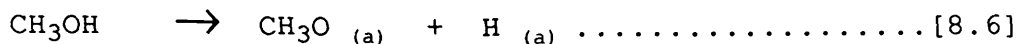
Formate was found to be the most stable intermediate [105] produced in the reaction of methanol on $\text{Cu}(110)$. This intermediate will decompose at temperature higher than

200°C to form adsorbed hydrogen and carbon dioxide. Edwards et.al. [165] observed a formate species and carbon dioxide in the gas phase, as a result of the decomposition of methoxy groups formed during the interaction of methanol with Cu-ZnO catalyst.

The formation of carbon dioxide was also explained by Russell et.al. [240] in terms of formate decomposition. The formate species may be formed by the interaction of (CH₂O) species with one or more surface oxygen atoms to form (HCOO⁻) species, and either (H) or (OH) species. However, in their investigations, Lawson and Thomson [169] stated that in the methanol decomposition, oxygen was removed from the surface of copper oxide forming carbon dioxide from carbon monoxide (reaction 8.4). The free electron derived from O²⁻ ions, would be transferred to Cu⁺ or Cu²⁺ ions, to build up the metallic phase.

Huang et.al. [241] concluded that carbon monoxide could be oxidised to carbon dioxide in partial oxidation of methanol on a copper catalyst, while Harno [174] suggests that the presence of water in methanol feedstock is responsible for the formation of carbon dioxide.

Based on the evidence obtained from the results presented in this thesis and on the cited literature in section 1.7 a mechanism for methanol decomposition on a well-reduced catalyst can be proposed;



As already pointed out, the presence of water in the methanol feedstock will also contribute to the formation of carbon dioxide through the water-gas shift reaction.

The catalyst surfaces were heated with hydrogen sulphide in order to study the poisoning effect of hydrogen sulphide on the catalytic activity of copper-based catalyst. As can be seen from figure [4.21], the catalytic activity of Cu/Al₂O₃ catalyst was lowered by the presence of hydrogen sulphide, however, no change in the selectivity was observed, although the product distribution which occurred were similar, but with different ratios. The carbon dioxide concentration was higher than that of carbon monoxide, and the carbon dioxide concentration decreased as the reaction number increased. It is clear that the yields of both carbon oxides were markedly suppressed compared with those on the clean surface.

The trace of water formed after the admission of hydrogen sulphide to the copper catalyst was due to the reaction between hydrogen produced from the dissociative

adsorption of hydrogen sulphide and surface oxygen. A comparison between figure [4.2] and figure [4.21] shows that a pretreatment of $\text{Cu}/\text{Al}_2\text{O}_3$ with hydrogen sulphide inhibits methanol decomposition, as was evident by the observation of undecomposed methanol on the poisoned sample. A greater fall in the catalytic activity of $\text{Cu}/\text{Al}_2\text{O}_3$ was observed as the amount of hydrogen sulphide increased [figure 4.22]. A linear decrease in the $\text{Cu}/\text{Al}_2\text{O}_3$ activity toward methanol decomposition was the result of hydrogen sulphide poisoning.

The $\text{Cu-ZnO}/\text{Al}_2\text{O}_3$ activity was also affected by adsorbed hydrogen sulphide [figure 4.23]. The amounts of both carbon oxides formed from the decomposition of methanol, were suppressed on the poisoned surface, but the product distributions showed similar behaviour to those on a clean $\text{Cu-ZnO}/\text{Al}_2\text{O}_3$ surface. Also, increasing amounts of hydrogen sulphide produced a linear decrease in $\text{Cu-ZnO}/\text{Al}_2\text{O}_3$ activity for methanol decomposition, but to a lesser extent from that of $\text{Cu}/\text{Al}_2\text{O}_3$. This was due to the presence of ZnO in the methanol synthesis catalyst, which serves as a guard for adsorbing the hydrogen sulphide impurity.

Table 8.1 illustrates the product distributions for methanol decomposition on clean and poisoned $\text{Cu}/\text{Al}_2\text{O}_3$ and $\text{Cu-ZnO}/\text{Al}_2\text{O}_3$.

Table 8.1

A comparison between products distribution of the methanol decomposition and the effect of H₂S on the catalyst activity of Cu/Al₂O₃ and Cu-ZnO/Al₂O₃.

Catalyst	CO ₂ :CO ratio	Activity decrease (Θ _S) 0.15
Clean Cu/Al ₂ O ₃	1:1.17	-
Poisoned Cu/Al ₂ O ₃	1:4.5	46
Clean Cu-ZnO/Al ₂ O ₃	1:0.2	-
Poisoned Cu-ZnO/Al ₂ O ₃	1:0.2	20

It is clearly resolved from the results obtained from the poisoned catalyst samples, that sulphur present on the catalyst surface acts to block the active sites for methanol adsorption and decomposition. It can also, be suggested that methanol decomposition occurs on single sites. This was confirmed by the absence of any change in the catalyst selectivity.

8.3 METHANOL DECOMPOSITION ON ZINC OXIDE

From the results presented in section 4.2.3, it is clearly shown that zinc oxide is not an active catalyst for methanol decomposition when reduced to a metallic state using carbon monoxide.

Both carbon monoxide and dioxide were formed from the decomposition of methanol on zinc oxide treated with 6% hydrogen in nitrogen, the ratio of CO/CO₂ changed as the reaction number increased. There was a decrease in carbon dioxide formation and a subsequent increase in carbon monoxide formation with the observation of the formation of metallic zinc, as indicated by the change in the colour of the zinc oxide sample. The change in the CO/CO₂ ratio is also a reflection of the reduction of the oxide surface. Thus the reduction of zinc oxide by methanol or its decomposition products must be associated with the formation of the high temperature products. This also suggests that methanol will be oxidised on the oxide surface to a formate-like species which then decomposes. It is not inconsistent with the involvement of formate-like species as intermediates later in the reaction.

The formation of carbon dioxide is believed to be either due to the reaction of the carbon monoxide with the oxide oxygen reducing the catalyst sample to a metallic zinc [33], or a formate species which decomposes to carbon dioxide. This formate species is formed during the interaction of methanol with zinc oxide surface [188], at higher temperatures.

For the formation of formate species from the interaction of methanol with the zinc oxide, the surface of the latter must be reduced [183]. This is reflected in the

decrease in the ratio of CO/CO₂ with increasing pulse number in a series of successive decomposition experiments.

The formation of methane at higher temperatures (>400°C) has been reported to be due to the reaction of methanol on prism surfaces of ZnO and then, only after exposing ZnO crystal to extreme reduction conditions [188]. The formation of methane has also been observed on such surfaces in a study by Kung's group [181, 182]. The formation of methane on the zinc oxide surface has been related to the role of O²⁻ vacancies during methanol decomposition [190]. However, methane was only observed at higher reaction temperatures and high methanol initial pressures. Thus it is likely that O²⁻ vacancies only play a significant role in the decomposition reaction at temperatures higher than 400°C.

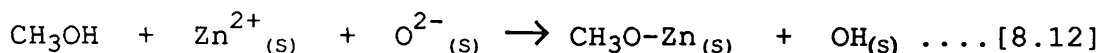
FTIR Spectra

The FTIR spectra presented in section 7.1.3 show clearly that methanol was adsorbed dissociatively on zinc oxide. The dissociative nature of methanol adsorption is confirmed by the frequencies of the asymmetric and symmetric C-H stretching modes of the adsorbed species (ca. 2945-2828 cm⁻¹).

It is also clear that the residual carbonate on the oxide surface strongly obscures the appearance of bands due to carbonate during the interaction of methanol with the

zinc oxide. Figure [7.8] shows that bands due to methoxy species (2945 and 2828 cm^{-1}) as well as a band due to carbon monoxide (2076 cm^{-1}) were also observed. A small shoulder at 1416 cm^{-1} can be assigned to a carbonate species. A carbonyl stretching vibration was observed at 1046 cm^{-1} appeared. On increasing methanol pressure, bands due to the carbon dioxide were observed at 2359 and 2332 cm^{-1} , while carbonate bands at 1573 and 1381 cm^{-1} . These clearly suggest the decomposition of a surface methoxy species. The adsorption of methanol also resulted in the observation of a strong hydroxyl group band at 3500 cm^{-1} .

It is possible to conclude that methanol adsorption produced a methoxy species bound to the surface Zn cation, with a proton being transferred to the surface O^{2-} anion.



The other clear result from the IR spectra [figure 7.11 and 7.12] is the fact that the $\text{HCOO}_{(a)}$ decomposition step at higher temperature ($>200^\circ\text{C}$) yields carbon dioxide. This permits us to conclude that methanol adsorbed on a Zn-O sites which gives rise to carbon dioxide. This implies that at these sites a neighbouring O^{2-} species is available that can be incorporated to form the formate intermediate which subsequently decomposes to carbon dioxide.

The extent of methanol adsorption and decomposition was greatly inhibited by the adsorption of hydrogen sulphide on

the zinc oxide sample. The effect of hydrogen sulphide on the decomposition reaction is clearly shown in figure [4.25]. A subsequent decrease in CO:CO₂ ratio was observed due to the overall catalytic activity decrease.

Although, the effect of hydrogen sulphide on the overall catalytic activity of the zinc oxide catalyst can be clearly seen, zinc oxide is believed to adsorb hydrogen sulphide strongly to form zinc sulphide and water (see section 8.11). The reaction between hydrogen sulphide and zinc oxide causes the removal of O⁻² from the surface and, in consequence, a decrease in the oxide activity towards methanol decomposition could be observed. In addition, whilst some of the active sites on zinc oxide are occupied by sulphur, other active sites may also be occupied by water formed from the reaction of hydrogen sulphide, or by the hydroxyl groups. Thus, adsorbed sulphur would not only eliminate the active sites, but also block others indirectly.

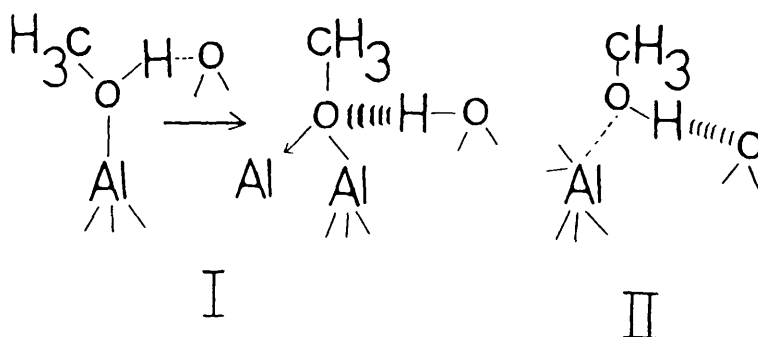
8.4 METHANOL DECOMPOSITION ON Al₂O₃

Methanol is adsorbed and decomposed at high temperature (>400°C) on 6% hydrogen in nitrogen treated alumina surfaces to carbon monoxide and methane, as major products, as well as carbon dioxide and water.

Carbon monoxide was a predominant product, and methane was significant, while traces of carbon dioxide and water

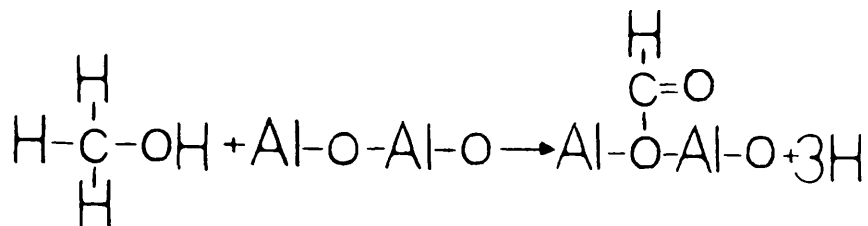
were formed throughout. Alumina surfaces seem to react with methanol in a different manner from those of copper catalysts. A thermal decomposition study [243] reported a decomposition to carbon monoxide, methane, water and carbon dioxide, which is in good agreement with our results, while another temperature programmed reaction spectroscopy study revealed [244] that at temperatures around -50°C , the initial reaction of methanol with alumina caused the formation of an oxidised surface and gaseous methane was evolved. These results were also obtained from XPS, TPRS and SIMS studies [244]. This study [244] showed that on clean alumina, methane and surface oxide were formed, and once a surface oxide was formed, methanol reacted to form methoxy species and surface hydroxide, through the abstraction of the methanol hydroxyl proton. The above proposed species formed during methanol decomposition can be compared with those revealed by an FTIR investigation as follows:

The $\nu(\text{C-H})$ stretching bands clearly show the formation of more than one type of adsorbed species. These species are characterised by pairs of bands at $2973, 2866\text{ cm}^{-1}$ and $2943, 2831\text{ cm}^{-1}$. These bands can be assigned to adsorbed species such as I and II respectively [239].

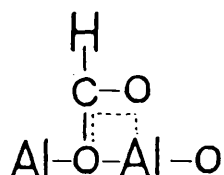


These species were found to be stable at high temperature under helium flow (see section 7.3).

Upon heating the alumina surface a formate species has been observed in the region 1700 to 1300 cm^{-1} in agreement with Grenler's study [239] of the adsorption of methanol on aluminium oxide surfaces. The formation of formate species on the alumina surface at higher temperature ($>100^\circ\text{C}$) suggests that methanol reaction takes place as follows:



It is possible to suggest that the formate could be present on the surface as a formate ion, in which case the bonding in the above structure will be different:



Since the species formed as a result of the interaction of methanol with the alumina surface, shows a spectrum consistent with a structure which has two oxygen atoms and one hydrogen atom attached to a carbon atom, it is reasonable to assume that one of the oxygen atoms is part of the alumina surface.

The hydrogen sulphide poisoning effect was also studied

on alumina surfaces. The hydrogen sulphide appeared to have an overwhelming effect on the reaction of methanol and its decomposition pathway. No carbon dioxide or water were detected, while methane was produced in higher concentration than carbon monoxide. A large decrease in the alumina activity was observed as a result of the presence of hydrogen sulphide on the surface. However, most of the catalytic activity could be restored in the catalyst by leaving it under helium flow at 450°C. This resulted in the removal of sulphur (see section 8.10).

8.5 THE ADSORPTION OF CARBON MONOXIDE ON COPPER-BASED CATALYSTS

The adsorption isotherm of ^{14}C -carbon monoxide on freshly reduced, unpoisoned samples of $\text{Cu}/\text{Al}_2\text{O}_3$ and $\text{Cu-ZnO}/\text{Al}_2\text{O}_3$ catalysts at 250°C showed a linear increase in surface count rate as the amount of carbon monoxide passed over the catalyst was increased, although the gas phase analysis showed the presence of only carbon dioxide in the first ten pulses indicating the presence of appreciable amounts of oxygen on the $\text{Cu}/\text{Al}_2\text{O}_3$ surface.

In the adsorption of carbon monoxide on freshly reduced $\text{Cu}/\text{Al}_2\text{O}_3$ and $\text{Cu-ZnO}/\text{Al}_2\text{O}_3$ at temperatures lower than 250°C, the two catalysts showed identical behaviour in which the main features were an initial increase in the surface adsorptive capacity at the beginning of the experiments

followed, at higher pulse number, by a slight positive gradient. These adsorption isotherms are similar to those observed by Pettigrew [225] using the same catalysts in a static system.

The positive gradient is related to the presence of traces of unreduced oxide which enhance the reaction between adsorbed carbon monoxide and surface oxide forming carbon dioxide.

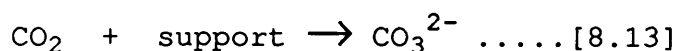
Most of the adsorbed carbon monoxide can be removed from the catalyst surface by heating under a helium flow of 30 ml/min to 500°C. The average amounts of adsorbed carbon monoxide retained on the surface following the heat treatment are given in table 8.2.

Table 8.2

% of adsorbed carbon monoxide species retained by the catalyst following heating after adsorption on "clean" surfaces.

Catalyst	% of CO retained
Cu/Al ₂ O ₃	20
Cu-ZnO/Al ₂ O ₃	11

The amounts of carbon monoxide retained on the surface following the high temperature treatment show that the adsorption of carbon monoxide on supported copper catalysts occurs in more than one state, the most weakly adsorbed species would be removed from the surface by the helium flow during the adsorption study; some of the more strongly adsorbed species are removed by treatment in helium at high temperature, whilst the very strongly adsorbed species are retained on the surface. The irreversible adsorption of carbon monoxide on the supported copper catalyst may be due to the interaction of the adsorbed carbon monoxide with surface oxygen forming carbon dioxide which itself is adsorbed on the catalyst. The adsorbed carbon dioxide then interacts further with the support forming a strongly held surface carbonate species:



or it may be due to the reaction of adsorbed carbon monoxide with hydroxyl groups, induced by the presence of copper, forming surface formate.

The present results are in a very good agreement with those obtained by Pettigrew, [225] Klier, [110] Kinnaird [114].

The desorption experiments [figure 5.3 and 5.6] show that, at least two adsorption states exist for carbon monoxide on the copper component of both Cu/Al₂O₃ and Cu-

ZnO/Al₂O₃ catalysts. However, if, as is generally accepted, the most weakly adsorbed carbon monoxide species are removed directly by the helium flow, it is suggested that the more strongly adsorbed carbon monoxide species with a calculated heat of adsorption in the range (56 kJ mol⁻¹ or 35.4) for the two respective catalysts, are easily removed at a relatively low temperature and these correspond to the first desorption peak in figure [5.3 and 5.6]. Our results thus suggest that metallic copper bonds carbon monoxide relatively strongly and reversibly [110].

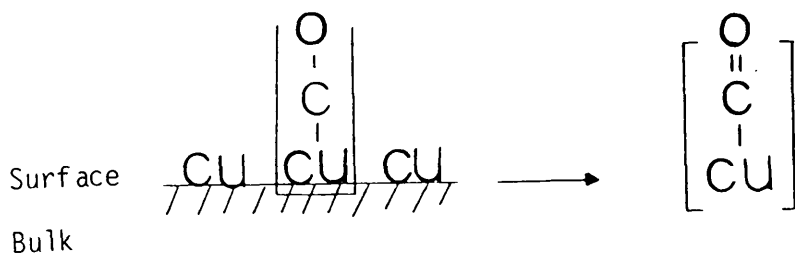
The high temperature desorption state (>250°C) corresponds to a very strongly bound species and this may be associated with the copper component itself [105]. It is evident from the desorption spectra [figure 5.3, 5.6] that desorption occurs from two distinct surface species. The discontinuity in the first desorption peak at about 250°C indicates the onset of the desorption of a second type of adsorbed species which is completely desorbed at 450°C. However, as we concluded earlier in the presence of oxygen, carbon monoxide interacts with the catalysts surfaces forming carbon dioxide. It is reasonable to suggest that the high temperature desorption peak is due to carbon dioxide. It might also be due to carbon dioxide resulting from the decomposition of carbonate species formed from the interaction of carbon monoxide with surface oxygen, as suggested earlier in the section.

The FTIR results (section 7.4) showed that carbon monoxide is only bound in a linear form in the temperature range from ambient to ca. 200°C. The FTIR spectra showed that the adsorbed carbon monoxide species on copper-containing catalysts at high temperature produces only the linear CuCO species, and since there is no evidence to suggest that adsorbed carbon monoxide is bound to a surface metal via the oxygen end, it is preferable

that CuCO is formed from a process such as that shown in figure [8.1].

Figure 8.1

possible surface process of carbon monoxide adsorption.



Despite the fact that all of the carbon monoxide desorption states described in figure [5.3] and [5.6] are assigned to different adsorption sites, in view of the FTIR results, the bonding mechanism of these states is probably the same. The 5σ electron pair of the carbon monoxide molecule forms a donor-acceptor bond with the vacant $4s$ orbital of copper cation or the partially filled $4s$ band of copper metal.

From the results discussed here, it is evident that the presence of oxygen enhances the production of the surface complex (CO_3^{2-}), which could be stabilised in the presence of excess oxygen. Thus some of the carbon monoxide species retained on the surface may be, in fact, surface carbonate type species, supporting the argument that hydrogen will only partially reduce the copper surface [114]. Carbon monoxide was also found to be adsorbed very weakly on the oxide surface of both alumina and zinc. Both surfaces were saturated rather quickly after the admission of carbon monoxide pulses; five and four pulses for zinc oxide and alumina respectively. The weak adsorption state of carbon monoxide is confirmed by the absence of a distinctive desorption peak when heating the oxide surface up to 500°C . This observation is in a good agreement with data obtained by Kinnaird [114].

The adsorption of carbon monoxide on hydrogen sulphide poisoned copper-containing catalysts is presented in the following paragraphs.

Although, the shape of the isotherms obtained on a poisoned sample are similar to those obtained on unpoisoned surfaces, the principal effect of adsorbed sulphur is to reduce the quantity of carbon monoxide adsorbed on the surface; a 25% decrease on $\text{Cu}/\text{Al}_2\text{O}_3$ and a 20% decrease on $\text{Cu-ZnO}/\text{Al}_2\text{O}_3$.

On the sulphur treated catalysts small shifts to lower temperature are observed in the carbon monoxide desorption

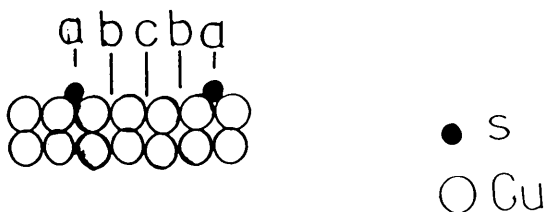
profiles. Such an observation is normally attributed to a reduction in the back-donation of electron from the metal into carbon monoxide $2\pi^*$ orbital. This has the effect of strengthening the carbon-oxygen bond, and weakening the metal-carbon bond.

Although, the shift to a lower desorption temperature has been observed, the site blocking effects of sulphur on the adsorption of carbon monoxide should not be ignored, although no linear decrease in the catalyst activity has been observed to support this mechanism.

The extent of sulphur poisoning effects on the adsorptive capacities of $\text{Cu}/\text{Al}_2\text{O}_3$ and $\text{Cu-ZnO}/\text{Al}_2\text{O}_3$ catalyst of carbon monoxide can be related to differences in the catalysts surface areas and to the presence of zinc oxide, which adsorbs sulphur more strongly than copper. However, both the site blocking and the electronic effects may be used to explain the increase in the quantity of carbon monoxide desorbed from the surface at the lower temperature. As shown in figure [8.2], there are sites which can be occupied by adsorbed sulphur and which prevent any further

Figure 8.2

Blocking and electronic effect of sulphur on the active sites.



adsorption of carbon monoxide (sites A), while weakly adsorbed carbon monoxide could be bound to neighbouring sites (sites B) subject to short-range electronic effects. Next neighbouring sites, affected by only long-range electronic effects would be able to adsorb carbon monoxide more strongly, and could be responsible for the second desorption peak (sites C).

8.6 THE ADSORPTION OF CARBON DIOXIDE ON COPPER-BASED CATALYSTS

The adsorption isotherms obtained for ^{14}C -carbon dioxide on $\text{Cu}/\text{Al}_2\text{O}_3$ catalyst showed that, at room or higher temperature, a rapid increase in the surface count rate was observed which represented a relatively rapid adsorption

process followed by a saturation level.

It was also noticed that the amount of carbon dioxide required for the copper surface to be saturated at room temperature was higher than that at higher temperature. The isotherms also showed two adsorption states for ^{14}C -carbon dioxide on $\text{Cu}/\text{Al}_2\text{O}_3$, a fast and a very slow adsorption, the second of which has been shown to achieve an equilibrium state. A slight positive gradient was observed and this may be assigned to the interaction of carbon dioxide with the oxide support forming carbonate species. This assignment is confirmed by the amount of ^{14}C -carbon dioxide retained on the surface following a desorption study (table 8.3).

A broad similarity in the shape of ^{14}C -carbon dioxide adsorption isotherms is shown by $\text{Cu-ZnO}/\text{Al}_2\text{O}_3$ sample. Here the positive gradient relates to the strongly held ^{14}C -carbon dioxide adsorbed on $\text{Cu-ZnO}/\text{Al}_2\text{O}_3$ surface which was retained on the surface as a carbonate species, following a heat treatment.

The desorption studies provide good support for the proposal that carbon dioxide strongly interacts with the catalyst surface (CO_3^{2-} formation). It shows a sharp desorption peak with a tail attributable to the presence of the strongly adsorbed species. Retention of ^{14}C -carbon dioxide on the surface (table 8.3) also occurs.

It has been shown ^[114] that an enhanced adsorption of carbon dioxide occurs on an oxidised $\text{Cu}/\text{Al}_2\text{O}_3$. This also supports the proposal of a strong interaction of carbon

dioxide with partially reduced copper samples in our study. In a similar manner Madix *et.al.* [105] concluded that the presence of surface oxygen influences the adsorption/desorption behaviour of carbon dioxide. The amount of adsorbed carbon dioxide was found to decrease as the total amount of pre-adsorbed oxygen was increased. However, on the oxygen free surface, greater than 99% of adsorbed carbon dioxide molecules dissociated to carbon monoxide and surface oxygen. This dissociation process has not been observed in the present study, probably as a consequence of the presence of both surface oxygen and the support.

The value for the heat of adsorption calculated from the adsorption of carbon dioxide at two different adsorption temperatures, 29.6 and 32.0 kJ mol⁻¹ for Cu/Al₂O₃ and Cu-ZnO/Al₂O₃ respectively, corresponds only to the strongly adsorbed species because in the flow system an equilibrium state cannot be achieved, as in the static systems.

The adsorption and interaction of carbon dioxide might result in the formation of a formate species (reaction 8.13) which is strongly bound to the catalyst surface. The apparent absence of an infrared band for carbonate species formed from interaction of carbon dioxide with surface oxygen (reaction 8.13) is probably due to the masking effect of the presence of a carbonate band remaining as a result of the catalyst preparation method, which obscures

the appearance of any new bands in the region 1700-1500 cm^{-1} .

The adsorption of ^{14}C -carbon dioxide was markedly affected by the presence of preadsorbed sulphur. Results obtained on the poisoned samples of $\text{Cu}/\text{Al}_2\text{O}_3$ and $\text{Cu-ZnO}/\text{Al}_2\text{O}_3$ showed that sulphur has an overwhelming effect on the adsorption capacities of copper-based catalysts.

On the $\text{Cu}/\text{Al}_2\text{O}_3$ sample poisoned with H_2S ($\theta_s = 0.13$), the results show that the poisoned catalyst surface becomes saturated with adsorbed carbon dioxide faster than the clean surface. This indicates that a site blocking mechanism is induced by adsorbed sulphur. A 45% decrease in the surface count rate was observed as an effect of adsorbed sulphur. The desorption of adsorbed carbon dioxide on $\text{Cu}/\text{Al}_2\text{O}_3$ showed no evidence of a tailing in the desorption peak, suggesting desorption of only the weakly adsorbed species.

Similar results obtained on a poisoned $\text{Cu-ZnO}/\text{Al}_2\text{O}_3$ sample showed that there was a 20% decrease in the surface count rate due to the effect of adsorbed sulphur. The desorption experiment showed two desorption peaks similar to those observed with the clean surface, but occurring in a low temperature range.

In the poisoning studies with both $\text{Cu}/\text{Al}_2\text{O}_3$ and $\text{Cu-ZnO}/\text{Al}_2\text{O}_3$ catalysts, the difference in the metal surface area has to be taken in to account as well as the presence

of zinc oxide. These two factors play a major role in determining the overall effect of hydrogen sulphide poisoning on these catalysts. The large surface area of Cu-ZnO/Al₂O₃ provides more active sites for the adsorption of those molecules despite the presence of adsorbed sulphur. However, sulphur adsorbs strongly on the zinc oxide component and this may reduce the amount of sulphur adsorbed on the active copper sites. These results are summarised in table 8.3.

Table 8.3

% of ¹⁴C- retained following ¹⁴C-carbon dioxide adsorption and subsequent thermal desorption

Catalyst	% C-material retained	% Decrease in uptake
Clean Cu/Al ₂ O ₃	10	-
Poisoned Cu/Al ₂ O ₃	6	45
Clean Cu-ZnO/Al ₂ O ₃	20	-
Poisoned Cu-ZnO/Al ₂ O ₃	8	20

8.7 THE ADSORPTION OF ^{14}C -CARBON DIOXIDE ON ZnO SURFACES

As explained in section 5.35 a negligible adsorption of ^{14}C -carbon dioxide has been observed on the (75-1) zinc oxide sample. This is probably due to the presence of a large quantity of carbonate material present in the oxide sample arising from the preparation method. The second zinc oxide sample (from basic zinc carbonate) exhibited a high adsorption capacity for ^{14}C -carbon dioxide at room temperature. The adsorption isotherm showed similar behaviour to that obtained for $\text{Cu}/\text{Al}_2\text{O}_3$ and $\text{Cu-ZnO}/\text{Al}_2\text{O}_3$, namely an increase in the surface count rate followed by a plateau region indicating surface saturation.

Heating the oxide surface generated a desorption peak (320-450°C) which was also identified by the Isoflo counter indicating the presence of labelled material in that desorbed. However, the second desorption peak (450-680°C) was not detected by the Isoflo counter and is, therefore, concluded as being due to the decomposition of the surface carbonate mentioned earlier.

The adsorption isotherm of ^{14}C -carbon dioxide on a hydrogen sulphide poisoned sample of zinc oxide, showed a similar initial increase in the surface count rate. However, the surface count rate was 16% less than that on unpoisoned the sample.

The interaction of carbon dioxide on zinc oxide can be

explained in a similar way to that for the adsorption on copper catalysts, in which carbon dioxide interacts with the surface oxygen forming carbonate species. This species is strongly adsorbed and retained on the surface during subsequent heating (table 8.4).

8.8 HEATS OF ADSORPTION OF CARBON MONOXIDE AND CARBON DIOXIDE ON COPPER-BASED CATALYSTS

When the Clausius-Clapeyron equation which describes the equilibrium between a condensed phase and a vapor, ie.

$$\frac{d(\ln P)}{dT} = \frac{-L}{RT^2},$$

is applied to the equilibrium between an adsorbed layer and a gas, the equation must be modified since the enthalpy change is not, in general, constant but depends on the surface coverage. The change in the enthalpy at a particular value of surface coverage is termed the isosteric enthalpy of adsorption ΔH_{st} . Assuming that ΔH_{st} is independent of temperature over a modest temperature range, the adsorption equation ;

$$\left(\frac{\partial (\ln P)}{\partial T} \right)_{\Theta} = \frac{\Delta H_{st}}{RT^2},$$

can be integrated to give

$$\ln \left(\frac{P_1}{P_2} \right)_{\Theta} = - \frac{\Delta H_{st}}{R} \left(\frac{1}{T_1} - \frac{1}{T_2} \right),$$

where $P_1, T_1 > P_2, T_2$ respectively.

The adsorption isotherms of carbon monoxide on both Cu/Al₂O₃ and Cu-ZnO/Al₂O₃ samples were studied at room temperature and 100°C. Varying the adsorption temperature had no effect on the basic shape of the isotherms.

It is very clear that at higher temperature the surface requires more carbon monoxide molecules to reach saturation as shown in figure [8.3] and [8.4], which show the isotherms for Cu/Al₂O₃ and Cu-ZnO/Al₂O₃ respectively at room temperature and 100°C.

During the determination of the adsorption isotherm at 100°C, gas phase analysis revealed only trace amounts of carbon dioxide. The heat of adsorption for carbon monoxide on Cu/Al₂O₃ was estimated to be ca. 56 kJ mol⁻¹, whilst a value of 35.4 kJ mol⁻¹ was obtained for the adsorption on the Cu-ZnO/Al₂O₃ sample.

The adsorption isotherms for carbon dioxide were also measured at two different temperatures, typical results are given in figures [8.5-8.7] which depict the isotherms obtained for the adsorption of carbon dioxide (unlabelled) on Cu/Al₂O₃, Cu-ZnO/Al₂O₃ and ZnO catalyst respectively. As

Fig. 8.3

Carbon Monoxide Adsorption on Copper/Alumina
at Room Temperature and 100°C

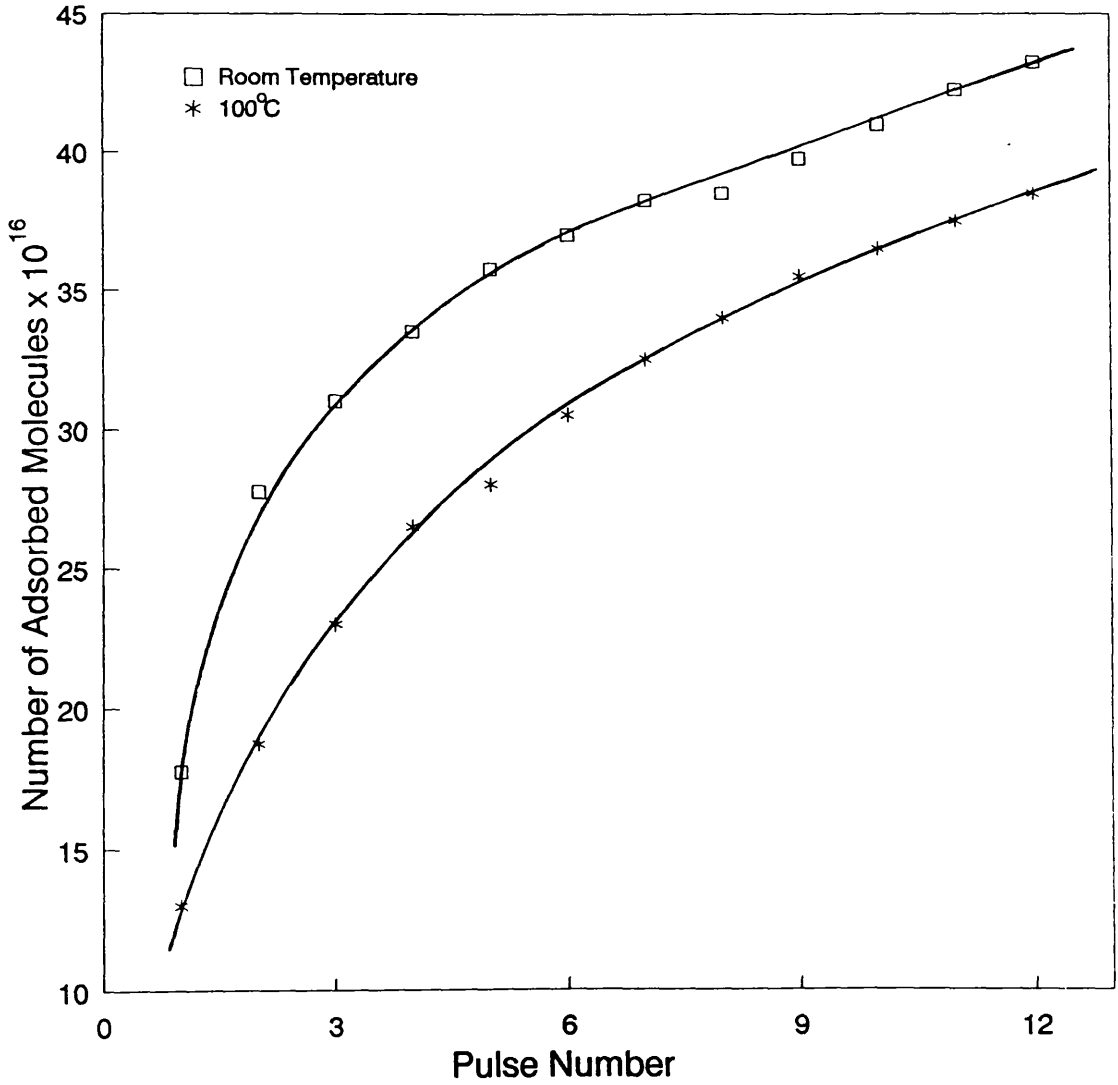


Fig. 8.4

Carbon Monoxide Adsorption at Room Temperature and at 100°C on Reduced Copper - Zinc Oxide/Alumina (0.156g) with 6% Hydrogen in Nitrogen at 250°C

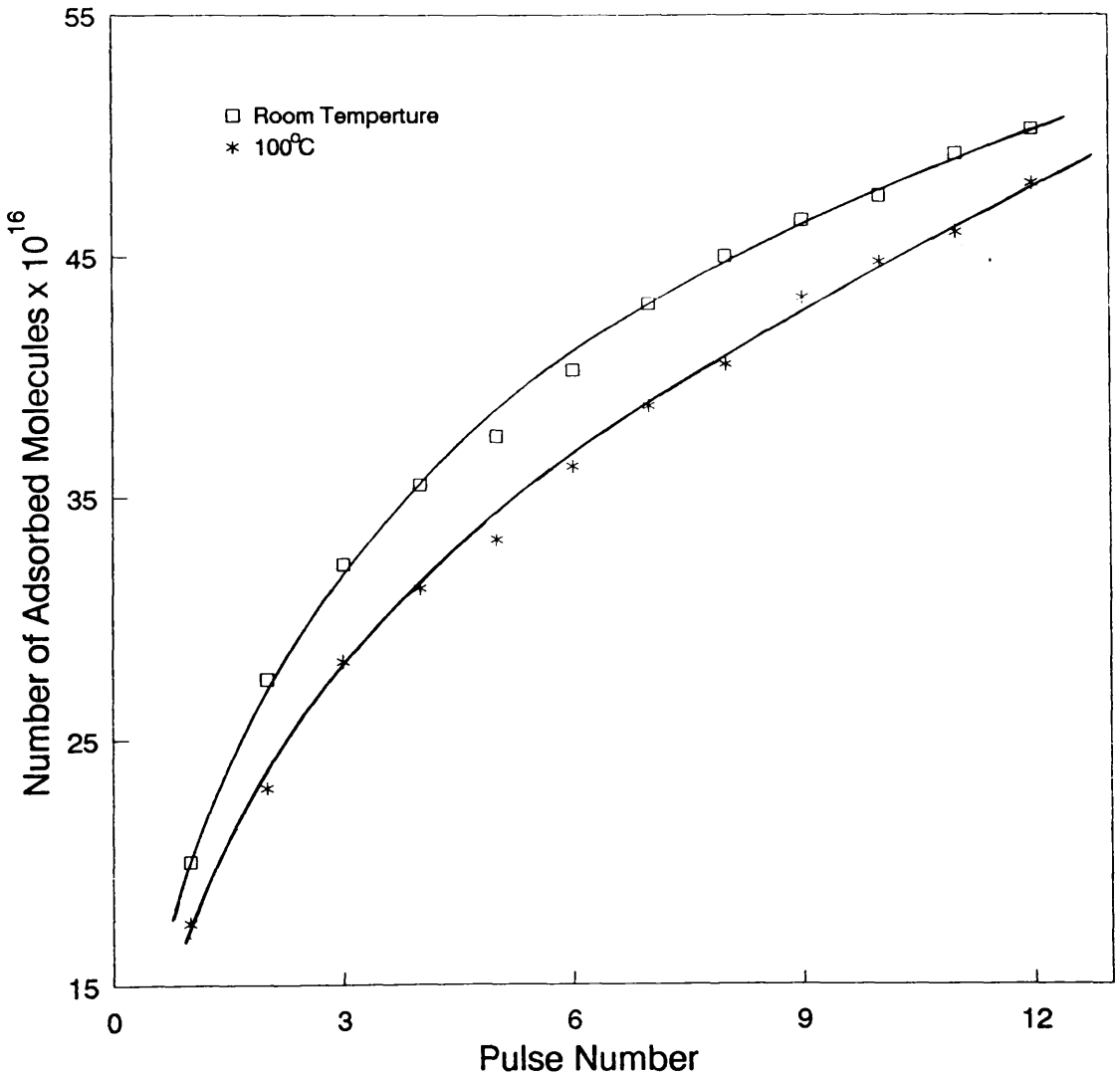


Fig. 8.5

Carbon Dioxide Adsorption on Copper/Alumina at 100°C and at Room Temperature on Sample Reduced with 6% Hydrogen in at 250°C

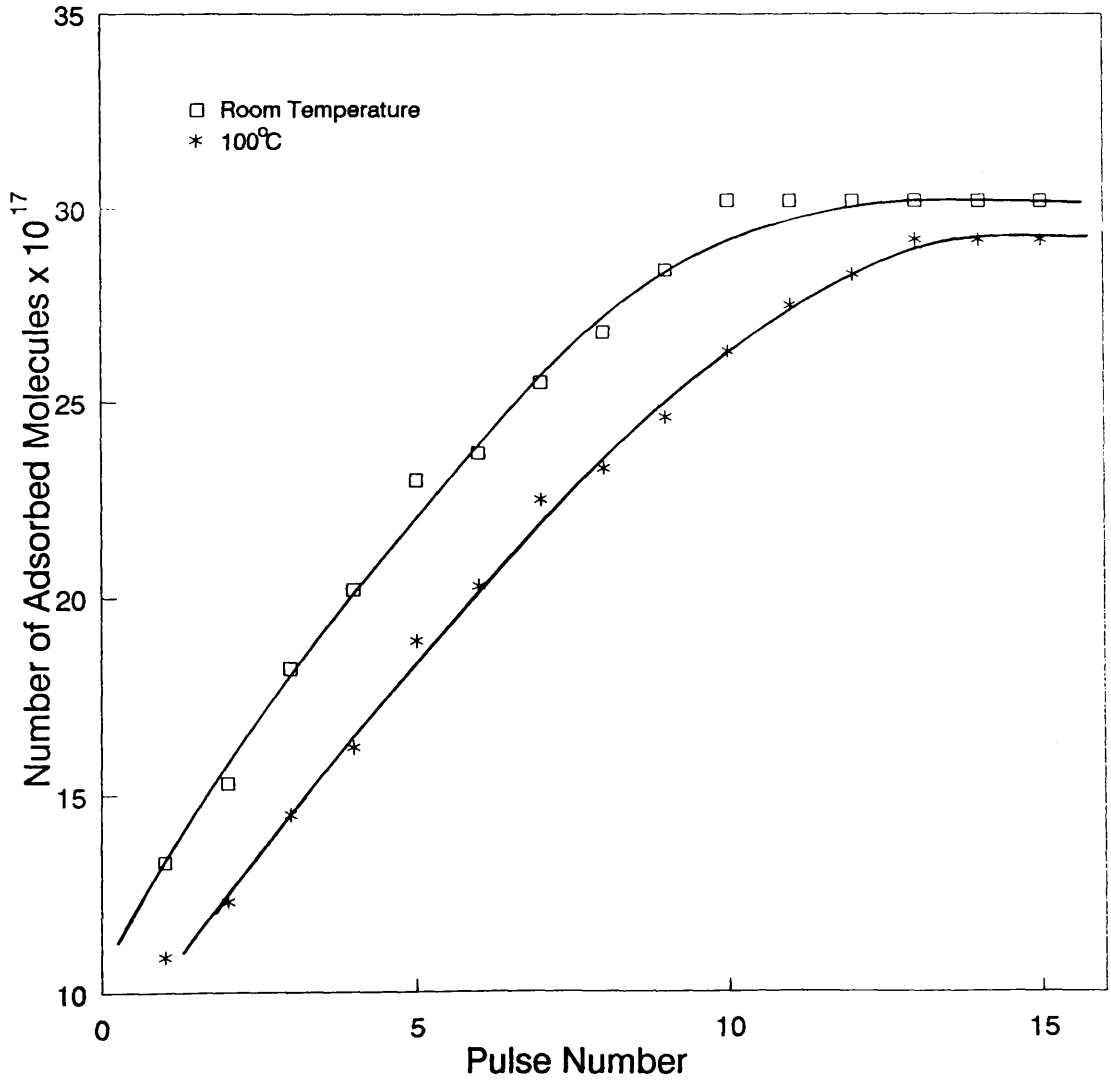


Fig. 8.6

Carbon Dioxide Adsorption on Copper - Zinc Oxide/Alumina
at 100°C and at Room Temperature on Sample Reduced with
6% Hydrogen in Nitrogen at 250°C

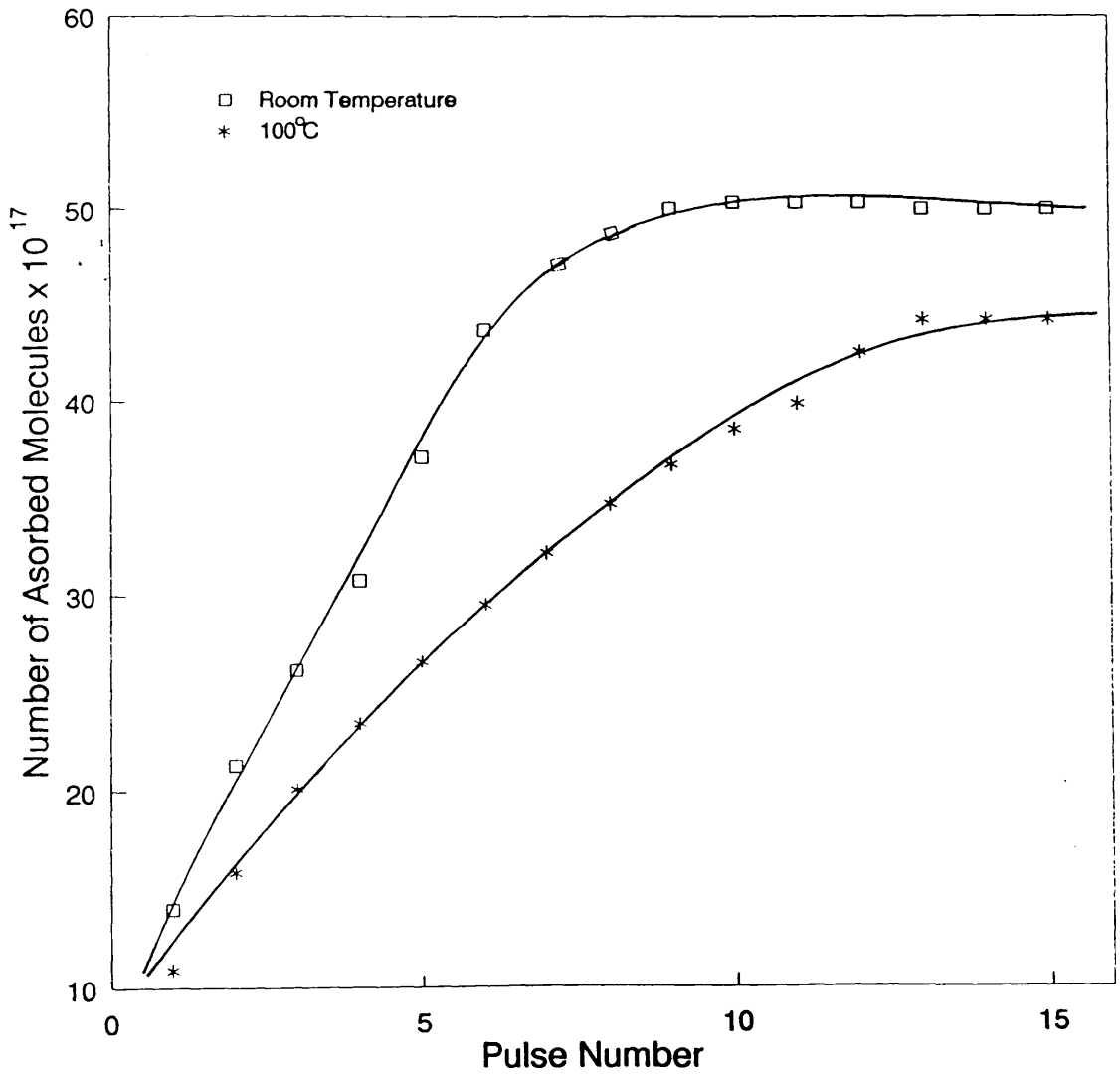
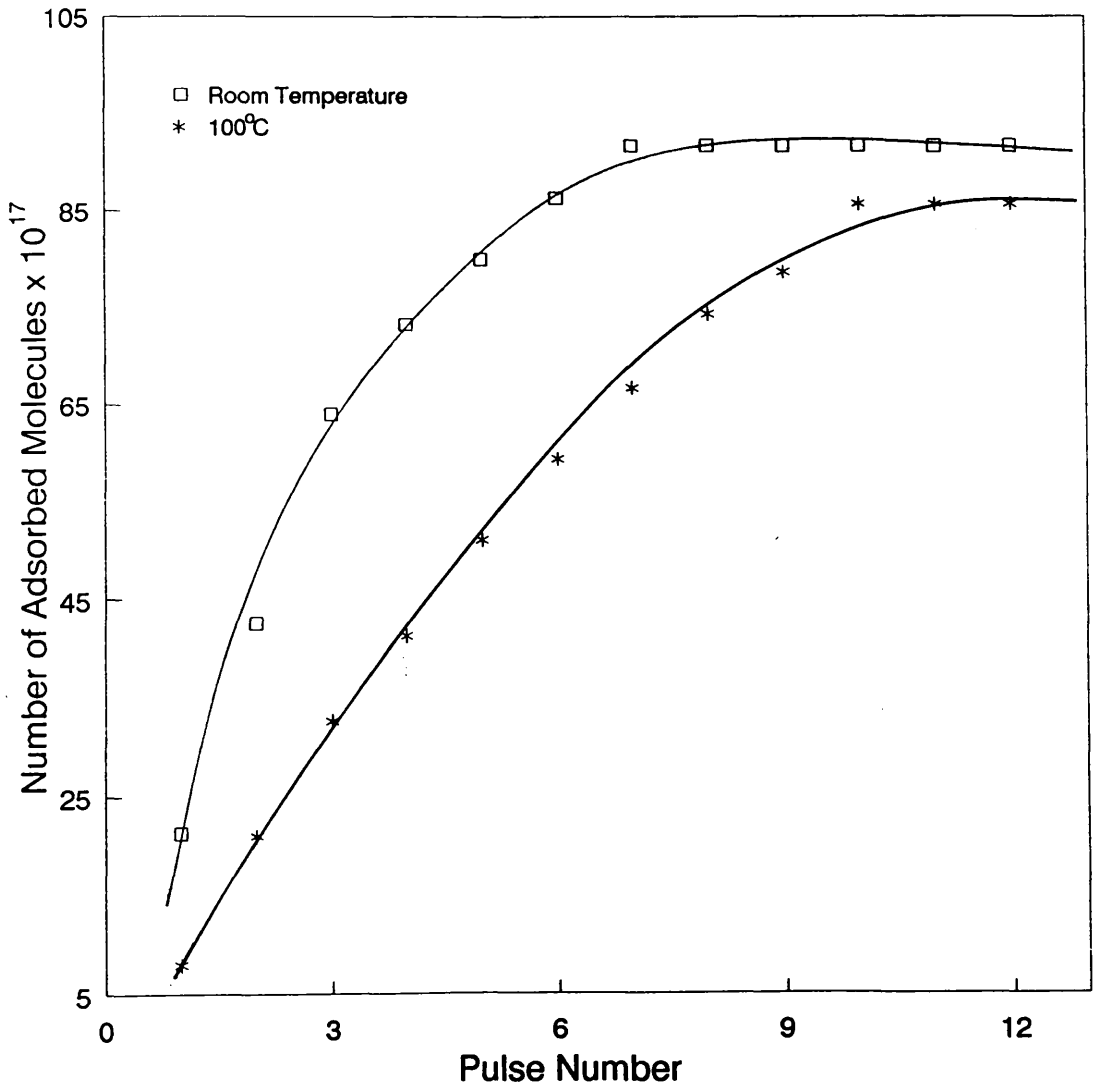


Fig. 8.7

Carbon Dioxide Adsorption on Zinc Oxide at Room Temperature and at 100°C Sample Reduced with 6% Hydrogen in N₂ , at 250°C



these figures show, the pressure required to produce a particular coverage, (the saturation coverage) is greater at higher temperatures. Curves such as those shown in figures [8.5-8.7] allow the heats of adsorption to be calculated as a function of coverage. In this case the saturation level was chosen, on the assumption that a proper equilibrium was established between the gaseous carbon dioxide and the adsorbed layer.

The estimated values of ΔH_{st} of adsorbed carbon dioxide on copper-based catalyst are given in table 8.4.

Table 8.4

The calculated heats of adsorption for carbon dioxide on Cu/Al₂O₃, Cu-ZnO/Al₂O₃ and ZnO catalysts systems

Catalysts	ΔH_{ads} kJ mol ⁻¹
Cu/Al ₂ O ₃	29.6
Cu-ZnO/Al ₂ O ₃	32.0
ZnO	37.7

8.9 THE ADSORPTION OF ^{14}C -CARBON DIOXIDE ON ALUMINA SURFACES

Small amounts of ^{14}C -carbon dioxide were found to be required for the saturation of an unpoisoned alumina sample. The adsorption isotherm shows that, although it was similar to that obtained on copper-based catalysts, the alumina surface showed saturation with much less of adsorbed carbon dioxide. This observation shows that the adsorptive capacity of alumina towards carbon dioxide is lower than that of either the copper-containing catalysts or zinc oxide. The desorption results indicate the presence of mainly weakly adsorbed carbon dioxide species, this adsorption state resulting in most of the adsorbed carbon dioxide (table 8.3) desorbing as a single peak at 180-380°C.

Hydrogen sulphide was found to have a great effect on the adsorptive capacity of an alumina surface. The adsorption isotherm obtained on a poisoned sample exhibited a 65% decrease in surface count rate compared with the unpoisoned surface, with an immediate attainment of a saturation level. The desorption of carbon dioxide from the poisoned alumina sample generated a similar peak to that from the unpoisoned sample, which occurred at 270°C; with only a small amount of carbon dioxide being retained on the surface (table 8.5). The retained species could be attributed to the removal of adsorbed sulphur by simple

helium flushing (see section 6.2), which regenerates vacant active sites available for the strong adsorption of carbon dioxide.

Table 8.5

^{14}C -material retained on "clean" and poisoned ZnO and alumina surfaces following ^{14}C -carbon dioxide adsorption, and subsequent thermal desorption

Catalysts	% Retained	% Decrease in surface count rate*
ZnO	51	-
Poisoned ZnO	10	16
Al_2O_3	8	-
Poisoned Al_2O_3	5	65

* The decrease was calculated relative to the surface count rate when the plateau region was reached.

8.10 The Adsorption of ^{35}S -Hydrogen Sulphide on Copper Catalysts

The data presented in section 6.1.1 and 6.1.2 indicate that hydrogen sulphide was adsorbed strongly on the copper component of the reduced sample of $\text{Cu}/\text{Al}_2\text{O}_3$ and Cu -

ZnO/Al₂O₃.

On Cu/Al₂O₃ the adsorption isotherm shows a linear increase in the surface count rate with pulse numbers, following the admission of ³⁵S-hydrogen sulphide, with no increase in the gas phase count rate. This suggests a rapid adsorption of ³⁵S-hydrogen sulphide on the catalyst surface. Only when the surface coverage (θ_s) of 0.22 was attained was an increase in the gas phase count rate observed. The catalyst surface reached the saturation level at surface coverage (θ_s) of 0.4.

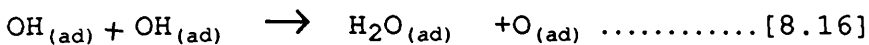
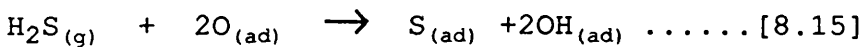
The strong adsorption of ³⁵S-hydrogen sulphide was indicated by the observation that helium flushing failed to remove any adsorbed sulphur from the surface, even at elevated temperatures.

The same behaviour was found for the adsorption of ³⁵S-hydrogen sulphide on Cu-ZnO/Al₂O₃ catalyst, but a residual gas phase count rate was observed at a surface coverage (θ_s) of 0.15, while surface saturation was attained at coverage (θ_s) of 0.2. This is surprising due to the presence of zinc oxide, which strongly adsorbs hydrogen sulphide.

Hydrogen sulphide is believed to be adsorbed in a dissociative manner to form an adsorbed sulphur and hydrogen [215, 227] according to the reaction:



However, the amount of dihydrogen evolved from the dissociative adsorption of hydrogen sulphide was found to be less than that expected for complete dissociative adsorption. This suggests the possibility of the formation of sulphhydryl species (SH) [217], which is believed to be the result of an irreversible dissociation of hydrogen sulphide at low surface coverage and low temperature. From the poisoning studies discussed in this chapter, and with the limitation of the pulse technique, it is very difficult to deduce the chemical identify of the adsorbed species arising from the adsorption of ^{35}S -hydrogen sulphide. However, it has been suggested earlier in this chapter that the catalyst surface was not fully reduced, and the poisoning studies revealed the formation of traces of water following the adsorption of hydrogen sulphide. Thus, the conclusion which might be drawn from this observation is that surface oxygen is involved in a hydrogen abstraction reaction to give surface hydroxyl species, this species then undergoes further dehydroxylation through the formation of molecular water which then desorbs:

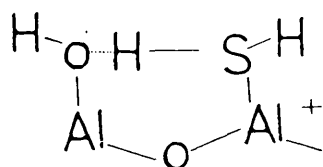


The reduction of copper in Cu-ZnO/Al₂O₃ has also been suggested to result from the reaction of hydrogen sulphide with the catalyst surface [216], with a subsequent increase in copper surface area.

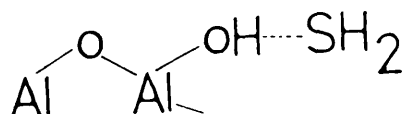
Although, the nature of the surface species arising from the interaction of hydrogen sulphide with copper catalysts is not fully understood, surface reconstruction has been observed. At high coverage adsorbed sulphur appears to form a two-dimensional surface sulphur layer [212]. Although, the amount of adsorbed sulphur, which was calculated using the adsorption isotherm for adsorbed hydrogen sulphide on copper catalyst only represents about half a monolayer of surface coverage ($\theta_s = 0.4$) surface reconstruction may occur at high exposure. It was also observed that even in the plateau region of the isotherm, additional hydrogen sulphide could also adsorb, only a small amount appearing in the gas phase. This might indicate either a surface reconstruction process in which sites have been regenerated for hydrogen sulphide adsorption, or a bulk sulphide formation process.

8.11 THE ADSORPTION OF ^{35}S -HYDROGEN SULPHIDE ON ALUMINA SURFACES

As shown in figures [6.3 and 6.4], the sulphur-alumina interaction is a weak interaction. The alumina colour was changed to yellow during the adsorption of ^{35}S -hydrogen sulphide, indicating formation of a surface alumina- H_2S compound. It is not clear whether hydrogen sulphide adsorbed through the sulphur atom to the surface as shown below [246]:



or through forming a hydrogen bond with a surface hydroxyl:



groups or water. The water molecules thus formed could be adsorbed on different sites and decompose to hydroxyl group and H^+ .

8.12 THE ADSORPTION OF ^{35}S -HYDROGEN SULPHIDE ON ZINC OXIDE SURFACES

The adsorption isotherm of ^{35}S -hydrogen sulphide on a sample of zinc oxide (75-1) shows a rapid increase in the surface count rate with no subsequent increase in the gas phase count rate. These results suggest that hydrogen sulphide reacts with zinc oxide surface forming zinc sulphide and water. Molecular water could be removed under helium flow. However, even when the plateau region of the adsorption isotherm has been reached the addition of more hydrogen sulphide had no effect on the gas phase concentration, which indicates the occurrence of further reaction between hydrogen sulphide and zinc oxide. This process might be due to the diffusion of sulphur through to the bulk of the oxide forming bulk zinc sulphide, with, at the same time, generation of further adsorption sites on the surface and, accordingly, an increase in the ability of the surface to react further with hydrogen sulphide [218]. It was also observed during the course of study that sulphur was adsorbed strongly on zinc oxide, as shown by the desorption experiments. Only a 27% decrease in the surface count rate was observed as an effect of the helium

flushing (tables 6.5. and 6.6). However, although a measurable decrease in the surface count rate was observed, there is no subsequent increase in the gas phase count rate. This observation supports the hypothesis of a sulphur diffusion in to the bulk of the oxide. Figure [6.8] also shows results obtained with a sample of oxide which had not been pretreated with hydrogen, but was otherwise subjected to the same treatment above. A 44% decrease in surface count rate was observed but again no increase in the gas phase count rate was observed.

Preadsorbed carbon dioxide was found to have a negligible effect on the adsorption capacity of zinc oxide for ^{35}S -hydrogen sulphide, a typical adsorption isotherm [figure 6.9] was obtained with a similar shape to that of a normal sample of zinc oxide, but with a slight increase in the gas phase count rate. This increase is due mainly to the high specific activity of ^{35}S -hydrogen sulphide, although, probably a displacement of sulphur by adsorbed carbon dioxide occurs. However, this hypothesis cannot be confirmed without further investigation of the adsorption behaviour of both molecules.

The displacement of ^{35}S -hydrogen sulphide with unlabelled hydrogen sulphide, was also investigated. The results [figure 6.10] showed that unlabelled hydrogen sulphide had no effect on the stability of ^{35}S -hydrogen sulphide on the zinc oxide surface. This suggests that both

labelled and unlabelled hydrogen sulphide react with zinc oxide in a similar manner forming both surface and bulk zinc sulphide.

The results discussed above show that dissociative adsorption of hydrogen sulphide on zinc oxide occurred, with conversion of zinc oxide to zinc sulphide. The extent of this conversion is not fully understood [218]. It has also been found [221] that the conversion of zinc oxide to zinc sulphide can be completed at higher temperatures (600-700°C), but, at temperature below 600°C the reaction between hydrogen sulphide and zinc oxide ceases well before total zinc oxide conversion has been obtained.

8.13 THE EFFECT OF WATER ON ³⁵S-HYDROGEN SULPHIDE ADSORPTION ON ZINC OXIDE

It has been observed (see section 6.3.4) that water has a great effect on the adsorption behaviour of ³⁵S-hydrogen sulphide on zinc oxide. The presence of water was found to cause a decrease in the surface count rate (table 6.9). Although this process has not been studied before, a general mechanism for the effect of water can be proposed in terms of both water adsorption on zinc oxide, and the diffusion of sulphur into the zinc oxide bulk, as mentioned earlier.

As shown schematically in figure [8.8], this mechanism may occur through a number of steps as detailed below:

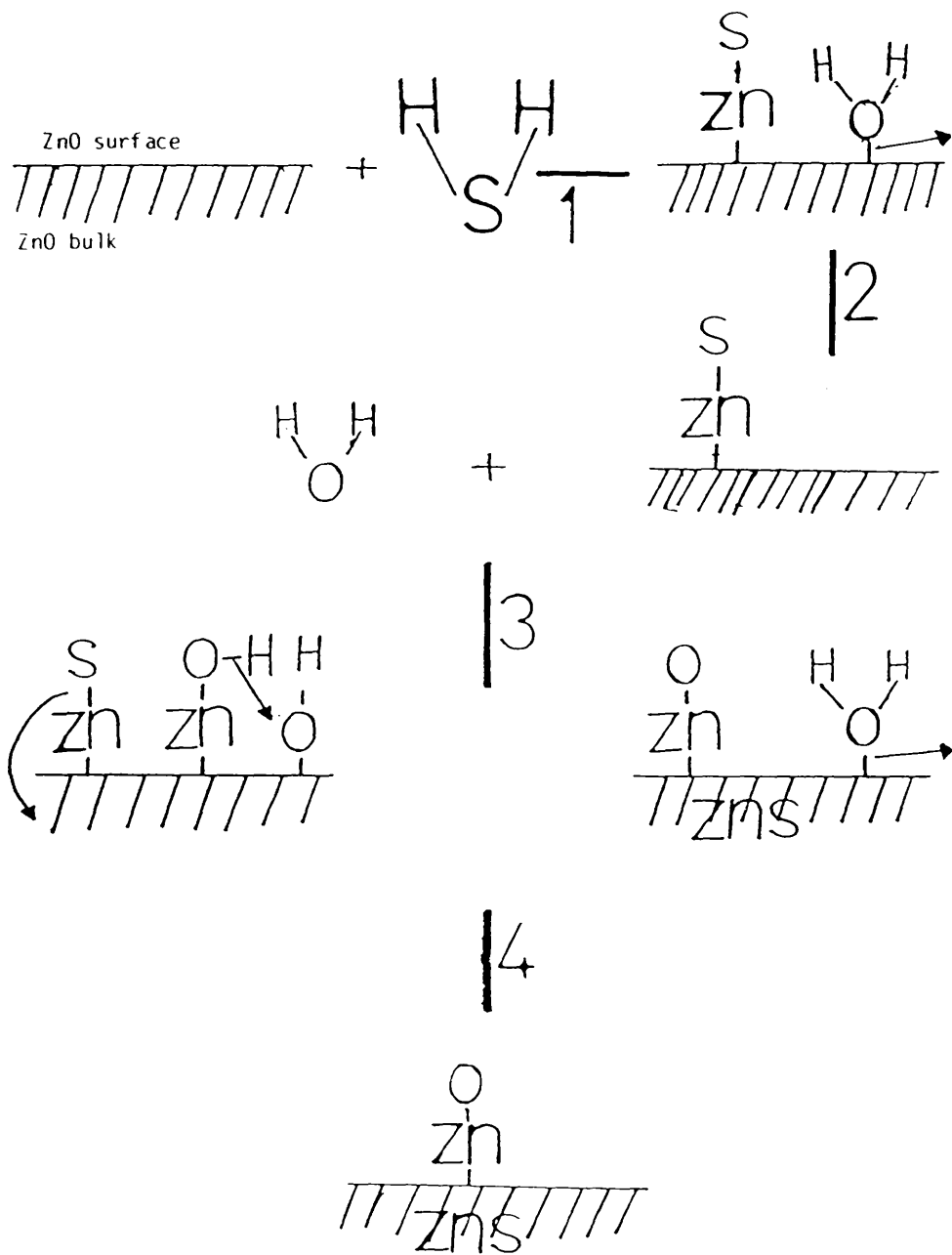
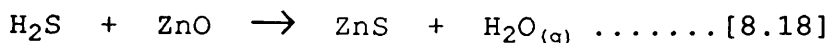


Fig. 8.8 The reaction between hydrogen sulphide and ZnO in the presence of water.

(1) Dissociative adsorption of hydrogen sulphide on zinc oxide forming surface zinc sulphide and adsorbed water. Step (I).



(2) The water molecule formed in [8.18] diffuses away leaving zinc sulphide on the surface. Step (II).

(3) On admitting water (III), dissociative adsorption of water occurs forming two hydroxyl groups. At the same time surface sulphur (from zinc sulphide) will diffuse to form bulk sulphide and, through hydrogen bonding, the hydrogen from the zinc hydroxyl group (Zn-OH) form a water molecule by reacting with the surface hydroxyl group. This process leaves an oxidised zinc atom (forming zinc oxide) which acts as a new site for the adsorption of hydrogen sulphide. Step (IV). This process explains the increase in the oxide capacity for the adsorption of hydrogen sulphide.

REFERENCES

1. H. S. Talyor, *Adv. Catal.*, **1**, 1 (1950).
2. R. P. H. Gasser, In "An Introduction to Chemisorption and Catalysis by Metal" Oxford University Press, 1985.
3. G. A. Somorjai, *Adv. Catal.*, **26**, 2 (1977).
4. J. M. Thomas and W. J. Thomas, In "Introduction to the Principle of Heterogeneous Catalysis" Academic Press, London, 1967. P299.
5. R. G. Herman, K. Klier, G. W. Simmons, B. P. Finn, J. B. Bulko, and T. P. Kobylinski, *J. Catal.*, **56**, 407 (1979).
6.
 - (a) J. M. Dominiquez, G. W. Simmons, and K. Kher, *J. Mol. Catal.*, **20**, 369 (1983).
 - (b) K. Klier, V. Chatikavani, and R. J. Herman and G. W. Simmons., *J. Catal.*, **74**, 343, (1982).
 - (c) J. B. Bulko, G. W. Simmons, K. Klier and R. J. Herman., *J. Phys. Chem.*, **83**, 3118 (1979).
7.
 - (a) Y. Okamoto, K. Fukino, T. Imanaka and S. Teranishi, *J. Phys. Chem.*, **87**, 3740 (1983).
 - (b) Y. Okamoto, K. Fukino, T. Imanaka and S. Teranishi, *J. Phys. Chem.*, **87**, 3747 (1983).
8. J. R. Monnier, M. J. Hanrahan and G. Apai., *J. Catal.*, **92**, 119 (1985).
9. G. Apai, J. R. Monnier and D. R. Preuss, *J. Catal.*, **98**,

- 563 (1986).
10. G. Sanker, S. Vasucleran and C. N. R. Rao, *Chem. Phys. Letts.*, **127**, 620 (1986).
 11. R. C. Baetzold, *J. Phys. Chem.*, **89**, 4150 (1985).
 12. J. W. Evans, *Appl. Catal.*, **7**, 369 (1983).
 13. J. B. friedrich, M. S. Wainwright and D. J. Young, *J. Catal.*, **80**, 1 (1983).
 14. T. H. Fleisch and R. L. Mievville, *J. Catal.*, **90**, 165 (1984).
 15. C. T. Campbell, K. A. Daube and J. M. White, *Surf. Sci.*, **182**, 458 (1987).
 16. H. Baussart, *Appl. Catal.*, **14**, 381 (1985).
 17. G. Vlaic, J. C. J. Bart, W. Cavigiolo and S. Mobilio, *Chem. Phys. Letts.*, **76**, 453 (1980).
 18. G. Vlaic, J. C. J. Bart, W. Cavigiolo, B. Pianzola and S. Mobilio, *J. Catal.*, **96**, 314 (1985).
 19. K. Shimomura, K. Ogawa, M. Oba and Y. Kotera, *J. Catal.*, **52**, 191 (1978).
 20. G. C. chinchin, K. C. Waugh and D. A. Whan, *Appl. Catal.*, **25**, 101 (1986).
 21. J. B. Bulko, R. G. Hermann, K. Klier and G. W. Simmons, *J. Phys. Chem.*, **83**, 3118 (1979).
 22. S. Mehta, G. W. Simmons, K. Klier and R. G. Hermann, *J. Catal.*, **57**, 339 (1979).
 23. J. C. frost, *Nature*, Vol. **334**, 577 (1988).
 24. G. henrici-Ollve and S. Ollve, *J. Mol. Catal.*, **17**, 89 (1982).

25. W. H. Rschwald, P. Bonasewicz, L. Ernst, M. Grade, D. H. Hofmann, S. Krebs, R. Littbarski, G. Neumann, M. Grunze, D. Kolb and H. Schultz, In "Current Topics in Materials Sciene" Vol. **7**, Ed. By E. Kaldis, Amsterdam, 1981, P143.
26. G. Heiland, E. Mollovo and F. Stockmann, Sol. State. Phys., **8**, 191 (1959).
27. In "Structural Inorganic Chemistry". Oxford University Press, fifth Ed. Ed: A. F. Wells, 1984.
28. S. Morrison, Adv. Catal., **7**, 259 (1955).
29. G. Parravano and M. Boudart, Adv. Catal., **7**, 47 (1955).
30. D. A. Wright, In "Semiconductors" Monographs in Physical Subject, Ed. By B. L. Worsnop, 1950.
31. L. E. Mollwo, Phys. Chem. Solids., **6**, 136 (1958).
32. P. Fuderer-Luetic and I. Sviben, J. Catal., **4**, 109 (1965).
33. A. J. Dandy, J. Chem. Soc., **5**, 5956 (1963).
34. J. M. Duck and R. Nelson , J. Chem. Soc., Faraday Trans., **70** (3), 436 (1974).
35. P. Miller and S. Morrison, J. Chem. Phys., **25**, 1064 (1956).
36. A. L. Dent and R. J. Kokes, J. Phys. Chem., **73**, 3781 (1969).
37. T. Morimoto and K. Moriskige, J. Phys. Chem., **79**, 1573 (1975).
38. D. A. Cadenhead and N. J. Wagner, J. Catal., **21**, 312 (1971).

39. C. S. Alexander and J. Pritchard, *J. Chem. Soc. Faraday Trans.*, **1**, **68**, 202, (1972).
40. M. Balooch, M. J. Cardillo, D. R. Miller and R. E. Stickney, *Surf. Sci.*, **46**, 358 (1974).
41. R. J. Mikovsky, M. Boudard and H. S. Taylor, *J. Am. Chem. Soc.*, **76**, 312 (1971).
42. L. S. Shield and W. W. Russell, *J. Phys. Chem.*, **64**, 1592 (1960).
43. T. Takeuchi, T. Takabatake, M. Sakaguchi and I. myoshi, *Bull. Chem. Soc. Jpn.*, **35**, 1390 (1962).
44. J. H. Sinfelt, W. F. Taylor and D. J. C. Yates, *J. Phys. Chem.*, **69**, 95 (1965).
45. L. H. Reyerson and L.E. Swearingen, *J. Phys. Chem.*, **31**, 88 (1927).
46. D. A. Cadenhead and N. J. Wagner, *J. Phys. Chem.*, **72**, 2775 (1968).
47. J. S. Campbell and P. H. Emmett, *J. Catal.*, **7**, 252 (1967).
48. R. P. Eischens, W. A. Pliskin and M. J. D. Low, *J. Catal.*, **1**, 180 (1962).
49. D. J. Thomas and J. J. Lander, *J. Chem. Phys.*, **25**, 1136 (1956).
50. Y. Kubakawa and O. Toyama, *J. Phys. Chem.*, **60**, 833 (1956).
51. T. S. Nagarjunan, M. V. C. Sastri and J. C. Kuriacose, *J. Catal.*, **2**, 223, (1963).

52. C. Ahraroni and F. C. Tompkins, *Trans. Faraday Soc.*, **66**, 434, (1970).
53. C. C. Chang, L. T. Dixon and R. J. Kokes, *J. Phys. Chem.*, **77**, 2634 (1973).
54. F. Boccuzzi, E. Borello, A. Zecchina, A. Bossi and M. Camia, *J. Catal.*, **51**, 150 (1978).
55. F. Boccuzzi, E. Borello, A. Zecchina, A. Bossi and M. Camia, *J. Catal.*, **51**, 160 (1978).
56. C. S. John, *Catalysis*, (London) Vol.3, 196, (1980).
57. H. Ibach and S. Lehwald, *Surf. Sci.*, **91**, 187 (1980).
58. B. A. Sexton, *Surf. Sci.*, **94**, 435 (1980).
59. E. M. Stuve, R. J. Madix and B. A. Sexton, *Surf. Sci.*, **111**, 11 (1981).
60. S. Andersson, C. Nyberg and G. C. Tengstal, *Chem. Phys. Letts.*, **104**, 305 (1984).
61. A. Spitzer and H. Luth, *Surf. Sci.*, **160**, 353 (1985).
62. C. Mariani and K. Horn, *Surf. Sci.*, **126**, 279 (1983).
63. P. S. Uy, J. Bardolle and M. Bujor, *Surf. Sci.*, **129**, 219 (1983).
64. A. Spitzer and H. Luth, *Surf. Sci.*, **120**, 376 (1982).
65. A. Spitzer, A. Ritz and H. Luth, *Surf. Sci.*, **152**, 543 (1985).
66. M. Nagao and T. Morimoto, *J. Phys. Chem.*, **73**, 3809 (1969).
67. W. C. Conner and R. J. Kokes, *J. Phys. Chem.*, **73**, 2436 (1969).

68. K. Atherton, G. Newbold and J. A. Hockey, *Disc. Faraday Soc.*, **52**, 33 (1971).
69. M. Bowker, H. Houghton and K. C. Waugh, J. A. Hockey, *Disc. Faraday Soc.*, **77** (1), 3023 (1981).
70. G. Zwicker and k. Jacobi, *Surf. Sci.*, **131**, 179 (1983).
71. R. R. Ford, *Adv. Catal.*, **21**, 51 (1970).
72. N. Sheppard and T. T. Nguyen, In "Advances in Infrared and Raman Spectroscopy" Eds. R. J. Clarke and R. E. Hester, Wiley, New York, Vol. **4**, 67 (1978).
73. R. P. Eischens, S. A. Francis and W. A. Pliskin, *J. Phys. Chem.*, **60**, 194 (1956).
74. R. P. Eischens and W. A. Pliskin, *Adv. Catal.*, **10**, 1 (1958).
75. C. W. Garland, R.C. Lord and P. F. Trdiano, *J. Phys. Chem.*, **69**, 1188 (1965).
76. J. F. Harrod, R. W. Roberts and E. F. Rissman, *J. Phys. Chem.*, **71**, 343 (1967).
77. J. Schwank, G. Parravano and H. L. Gruber, *J. Catal.*, **61**, 19 (1980).
78. A. C. Yang and C. W. Garland, *J. Phys. Chem.*, **61**, 1504 (1957).
79. D. M. Haaland, *Surf. Sci.*, **185**, 1 (1987).
80. K. Tanaka and J. M. White, *J. Catal.*, **79**, 81 (1983).
81. B. E. Hayden and A. M. Bradshaw, *Surf. Sci.*, **125**, 787 (1983).
82. G. Blyholder, *J. Chem. Phys.*, **36**, 2036 (1962).

83. H. L. Pickering and H. C. Eckstrom, *J. Phys. Chem.*, **63**, 512 (1959).
84. R. P. Eischens, In "The Surface Chemistry of Metals and Semi-Conductors" Ed. By H. C. Gatos, John Wiley and Sons., Inc., New York, P. 521 (1960).
85. J. T. Yates, JR, and C. W. Garland, *J. Phys. Chem.*, **65**, 617 (1961).
86. G. Blyholder, *J. Phys. Chem.*, **68**, 2772 (1964).
87. A. B. Anderson, *Surf. Sci.*, **62**, 119 (1977).
88. D. L. Roberts and G. L. Griffin, *Appl. Surf. sci.*, **19**, 298 (1984).
89. R. R. Gay, M. H. Nodine, V. F. Henrich, H. J. Zerger and E. Z. Solomon, *J. Am. Chem. Soc.*, **102**, 6752 (1980).
90. P. R. Norton and R. L. Tapping, *Chem. Phys. Letts.*, **38**, 207 (1976).
91. S. A. Isa, R. W. Joyner and M. W. Roberts, *J. Chem. Soc. Faraday Trans.*, **74** (1), 546 (1978).
92. J. Pritchard and P. Hollins, In "Vibrational Spectroscopies for Adsorbed Species", Eds. A. T. Bell and M. L. Hair, *ACS Symp. Series*, No. **137**, P. 51 ().
93. F. Boccuzzi, G. Ghiotto and A. Chiorino, *Surf. Sci.*, **156**, 933 (1985).
94. A. W. Smith and J. M. Quets, *J. Catal.*, **4**, 163 (1965).
95. J. Pritchard and M. L. Sims, *Trans. Faraday Soc.*, **66**, 427 (1970).
96. J. Pritchard, *Trans. Faraday. Soc.*, **59**, 437 (1963).
97. J. Pritchard, *Surf. Sci.*, **79**, 231 (1979).

98. P. Hollins and J. Pritchard., Surf. Sci., **134**, 91 (1983).
99. B. E. Hayden, K. Kretzschmar and A. M. Bradshaw, Surf. Sci., **155**, 553 (1985).
100. M. A. Chesters, S. F. Parker and R. Raval, Surf. Sci., **165**, 179 (1986).
101. G. Ghiotto, F. Boccuzzi and A. Chiorino, Surf. Sci., **178**, 553 (1986).
102. M. A. Kohler, N. M. Cant, M. S. Wainwright and D. L. Trimm, J. Catal., **117**, 188 (1989).
103. M. A. Chester, J. Pritchard and M. L. Sims, In "Adsorption-Desorption Phenomena" Ed. By F. Ricca, Academic Press. London, P. 277 (1972).
104. P. Hollins and J. Pritchard, Surf. Sci., **89**, 486 (1979).
105. I. Wachs and R. J. Madix, J. Catal., **53**, 208 (1978).
106. B. M. Trapnell, Proc. Roy. Soc., (London) A. **218**, 566 (1953).
107. R. M. Dell, F. S. Stone and P. E. Tiley, Trans. Faraday Soc., **49**, 195 (1953).
108. R. W. Joyner, C. S. McKee and M. W. Roberts, Surf. Sci., **26**, 303 (1971).
109. G. E. Parris and K. Klier, J. Catal., **97**, 374 (1986).
110. K. Klier, Adv. Catal., **31**, 243 (1982).
111. J. H. Taylor, Can. J. Chem., **39**, 531 (1961).
112. M. J. Sayers, M. R. McClellan, R. R. Gay, E. L. Solomon and F. R. McFeely, Chem. Phys. Letts., **75**, 575 (1980).

113. G. L. Griffin and J. T. Yates, Jr, *J. Chem. Phys.*, **77**, 3751, and 3744 (1982) .
- 114.
- (a) S. Kenniard, G. Webb and G. C. Chinchon, *J. Chem. Soc. Faraday Trans.*, **83**, 3399 (1987).
- (b) S. Kenniard, G. Webb and G. C. Chinchon, *J. Chem. Soc. Faraday Trans.*, **1**, **84**, 8416, 2135 (1988).
115. H.-J. Freund and R. P. Messmer, *Surf. Sci.*, **172**, 1 (1986).
116. A. B. Anderson, *Surf. Sci.*, **62**, or 76 119, or 207 (1977).
117. P. R. Norton and P. J. Richards, *Surf. Sci.*, **49**, 567 (1975) .
118. F. S. Stone and P. F. Tiley, *Faraday Soc.*, **8**, 246 (1950).
119. A. C. Collins and B. M. W. Trapnell, *Faraday Soc.*, **53**, 1476 (1957) .
120. F. H. P. M. Habraken, E. Kieffer and G. A. Bootsma, *Surf. Sci.*, **83**, 3 (1979) .
121. W. H. Weinberg, *Surf. Sci.*, **128**, L224 (1983) .
122. L. H. Bubojs and G. A. Somorjai, *Surf. Sci.*, **128**, L231 (1983) .
123. V. H. J. Grabke, B. Bunsenges, *J. Phys. Chem.*, **71**, 1067 (1967) .
124. H. Talyor and C. H. Anberg, *Can. J. Chem.*, **39**, 535 (1961) .
125. S. Matsushita and T. Nakata, *J. Chem. Phys.*, **36**, 665 (1962) .

126. S. Matsushita and T. Nakata, *J. Chem. Phys.*, **32**, 982 (1960).
127. T. Morimoto and K. Morishinge, *bull. Chem. Soc. Jpn.*, **47**, 92 (1974).
128. O. Levy and M. Steinberg, *J. Catal.*, **7**, 159 (1967).
129. P. M. G. Hart and F. Sebba, *Trans. Faraday Soc.*, **56**, 551 (1960).
130. T. Morimoto and K. Muraishi, *J. Phys. Chem.*, **80**, 1876 (1976).
131. P. Amigues and S. J. Teichner, *Discuss. Faraday Soc.*, **41**, 362 (1966).
132. W. Hota, W. Gopel and R. Haul, *Suf. Sci.*, **82**, 162 (1979).
133. G. W. Bridger and M. S. Spencer, In "Catalyst Handbook" 2nd Ed. Edited by M. V. Twigg, P. 441, (1989).
134. G. Nagta, In "Catalysis" Ed. P. H. Emmett, Reinhold, Vol. **3**, P. 349 (1955).
135. A. deluzarche, R. Kieffer and A. muth, *Tetrahedron Letts.*, **38**, 3357 (1977).
136. H. H. kung, *Catal, Rev. sci-Eng.*, **22**, 235 (1980).
137. J. F. Edwards and G. L. schrader, *J. Catal.*, **94**, 175 (1985).
138. T. Tagawa, G. Pleizier and Y. Amenomiya, *Appl. Catal.*, **18**, 285 (1985).
139. E. Rameroson, R. Kieffer and A. Kiennemann, *Appl. Catal.*, **4**, 281 (1982).
140. V. N. Ipatieff and G. S. Monroe, *J. Am. Chem. Soc.*, **67**, 2168 (1945).

141. G. C. chinchen, P. J. Denny, D. G. Parker, M. S. Spencer and D. A. Whan, *Appl. Catal.*, **30**, 333 (1987).
142. G. C. chinchen, P. J. Denny, J. R. Jennings, M. S. Spencer and K. C. Waugh, *Appl. Catal.*, **36**, 1 (1988).
143. G. Liu, D. Willcox, M. Garland and H. H. Kung, *J. Catal.*, **96**, 251 (1985).
144. Y. Amenomiya, *Appl. Catal.*, **30**, 57 (1987).
145. G. Liu, D. Willcox, M. Garland and H. H. Kung, *J. Catal.*, **90**, 139 (1984).
146. G. J. Schach, M. A. McNeil and R. G. Rinker, *Appl. Catal.*, **50**, 247 (1989).
147. Y. Okamoto, Y. Konishi, K. Fukino, T. Imanaka and S. Teranishi, *Proc. 8TH Int. Congr. Catal.*, **5**, V.159-V.170 (1984).
148. C. T. Campbell and K. A. Daube, *J. Catal.*, **104**, 109 (1987).
149. D. S. Newsome, *Catal. Rev. Sci-Eng.*, **21**, 275 (1980).
150. F. Garbassi and G. Petrini, *J. Catal.*, **90**, 106 (1984).
151. G. Petrini and F. Garbassi, *J. Catal.*, **90**, 113 (1984).
152. T. Van. Herwijnen and W. A. De Jong, *J. Catal.*, **63**, 83 (1980).
153. E. Fiolitakis and H. Hofmann, *J. Catal.*, **80**, 328 (1983).
154. H. Vchida, N. Isogal, M. Oba and T. Hasegawn, *Bull, Chem. Soc. Jpn.*, **41**, 479 (1968).
155. E. G. M. Knijpers, R. B. Tjepkema and W. J. J. Vanderwal, *Appl. Catal.*, **25**, 139 (1986).

156. D. C. Grenoble, M. M. Estadt and D. F. Ollis. *J. Catal.*, **67**, 90 (1981).
157. B. A. Sexton, *Surf. Sci.*, **88**, 299 (1979).
158. I. Kojima, H. Sugihara, E. Miyazaki and I. Yasunori, *J. Chem. Soc. Faraday Trans.*, **1**, 77, 1315 (1981).
159. J. Paul and F. M. Hoffmann, *Surf. Sci.*, **172**, 151 (1986).
160. R. Ryberg, *Chem. Phys. Letts.*, **83**, 423 (1981).
161. E. Miyazaki and I. Yasumori, *Bull. Chem. Soc. Jpn.*, **40**, 2012 (1967).
162. B. A. Sexton, A. E. Hughes and N. R. Avery, *Surf. Sci.*, **155**, 366 (1985).
163. E. V. Stuve, R. J. Madix and B. A. Sexton, *Surf. Sci.*, **119**, 279 (1982).
164. L. Chan and G. L. Griffin, *Surf. Sci.*, **173**, 160 (1986).
165. J. F. Edwards and G. L. Schrader, *J. Phys. Chem.*, **89**, 782 (1985).
166. J. B. Friedrich, D. J. Young and M. S. Wainwright, *J. Catal.*, **80**, 14 (1983).
167. J. B. Benziger, E. I. Ko and R. J. Madix, *J. Catal.*, **54**, 414 (1978).
168. M. Bowker and R. J. Madix, *Surf. sci.*, **95**, 190 (1980).
169. A. Lawson and S. J. Thomson, *J. Chem. soc.*, **2**, 1861 (1964).
170. M. Bowker and R. J. Madix, *Surf. sci.*, **102**, 542 (1981).
171. I. Wachs and R. J. Madix, *surf. Sci.*, **76**, 531 (1978).
172. E. Santacesaria and S. Carra, *Appl. Catal.*, **5**, 345 (1983).

173. R. J. Madix, *Catal. Rev. Sci-eng.*, **26**, 281 (1984).
174. K. Harno, *Chem. letts*, **12**, 1347 (1976).
175. L. A. Vytnova and A. Ya. Rozovskii, *Kintt. Katal.*, **25**, 302 (1984) English Trans.
176. K. Kawamoto, *Bull. Chem. Soc. Jpn.*, **34**, 795 (1961).
177. T. H. Fleish and G. J. Mains, *J. Appl. Surf. Sci.*, **10**, 51, (1982).
178. R. Ryberg, *J. Chem. Phys.*, **82**, 567 (1985).
179. A. Ueno, T. Onishi and K. Tamuru, *Trans. Faraday Soc.*, **67**, 3385 (1971).
180. M. Bowker, H. houghton, K. C. Waugh, T. Giddings and M. Green, *J. Catal.*, **84**, 252 (1983).
181. W. H. Cheng, S. Akhter and H. H. Kung, *J. Catal.*, **82**, 341 (1983).
182. S. Akhter, w. H. Cheng, K. Lui and H. H. Kung, *J. Catal.*, **85**, 437 (1984).
183. R. J. Kokes, A. L. Dent, C. C. Chang and L. T. Dixon, *J. Am. Chem. Soc.*, **94**, 4429 (1972).
184. G. L. Griffin and J. T. Yates, Jr, *J. Catal.*, **73**, 396 (1982).
185. W. Hirschwald and D. Hofmann, *Surf. sci.*, **140**, 415 (1984).
186. D. L. Roberts and G. L. Griffin, *J. Catal.*, **95**, 617 (1985).
187. L. Chan and G. L. Griffin, *Surf. sci.*, **155**, 400 (1985).
188. J. M. Vohs and M. Barteou, *Surf. sci.*, **94**, 303 (1980).

189. D. L. Roberts and G. L. Griffin, *J. Catal.*, **101**, 201 (1986).
190. J. Carrizosa, G. Manuera and S. Castanar, *Surf. Sci.*, **140**, 415, (1984).
191. C. Kemball, In "Catalysis Progress in Research", Eds. F. Basoto and R. L. Burwell, Jr, Plenum Publishing Comp.Ltd., P. 85, (1973).
192. C. H. Bartholomew, P. K. Agrawal and J. R. Katzer, *Adv. Catal.*, **31**, 135 (1982).
193. R. Hughes In "Deactivation of Catalysts" Academic Press, London, 1984.
194. J. G. McCarty and H. Wise, *J. Chem. Phys.*, **76**, 1162 (1982).
195. W. J. Kirpatrick, *Adv. Catal.*, **3**, 329 (1951).
196. R. A. Della Betta, A. G. Piken and M. Shelef, *J. catal.*, **40**, 173 (1975).
197. R. W. Joyner, C. S. McKee and M. W. Roberts, *Surf. sci.*, **27**, 179 (1971).
198. J. M. Moison and J. L. Domange, *Surf. sci.*, **67**, 336 (1977).
199. J. L. Domange and J. Oudar., *Surf. sci.*, **11**, 124 (1967).
200. P. Petrino, F. Moya and F. Cabane-Brouty, *J. Solid State Chem.*, **2**, 439 (1970).
201. J. Benard, *Catal. Rev. Sci-Eng.*, **3**, 93 (1969).
202. J. Oudar, *Catal. Rev. Sci-Eng.*, **22**, 171 (1980).
203. H. P. Bonzel and R. Ku, *J. Chem. Phys.*, **58**, 4617 (1973).

204. J. Benard, J. Oudar, N. Barbouth, E. Margot and Y. Berthier, *Surf. Sci.*, **88**, L35 (1979).
205. B. A. Sexton and G. L. Nyberg, *Surf. Sci.*, **165**, 251 (1986).
206. D. L. Seymour, S. Bao, C. F. McConville, M. D. Crapper, D. P. Woodruff and R. G. Jones, *Surf. Sci.*, **189**, 529 (1987).
207. E. B. Masted, *Adv. Catal.*, **3**, 129 (1951).
208. L. L. Hegedue and R. W. McCabe, *Catal. Rev. Sci-Eng.*, **23**, 377 (1981).
209. M. Shelef, K. Otto and N. C. Otto, *Adv. Catal.*, **27**, 311 (1978).
210. M. P. Kiskinova, *Surf. Sci., Reports*, **8**, 359 (1988).
211. Domasheveskay, *J. Electron. Spectrosc. and related Phenomena*, **9**, 261 (1976).
212. L. Moroney, S. Rassias and M. W. Roberts, *Surf. Sci.*, **10**, L249 (1981).
213. J. M. Saleh, *Trans. Faraday Soc.*, **68**, 1520 (1972).
214. Y. W. Chen and L. B. Lai, *J. Chin. Chem. Soc.*, **33**, 257 (1986) English Edition.
215. K. T. Leung, X. S. Zhang and D. A. Shirley, *J. Phys. Chem.*, **93**, 6164 (1989).
216. A. G. Baca, M. A. Schulz and D. H. Shirley, *J. Chem. Phys.*, **81**, 6304 (1984).
217. D. J. Koestner, M. Salmeron, E. B. Kolliu and J. L. Gland, *Chem. Phys. Letts.*, **125**, 134 (1986).

218. P. J. Carnell, In "Catalyst Handbook" 2nd Ed. Edited by M. V. Twigg, P. 209, and L. Lloyd, Ridler and M. V. Twigg, P. 311, (1989).
219. J. B. Gibson and D. P. Harrison, Ind. Eng. Chem. Process. Des. Dev., **19**, 231 (1980).
220. T. E. Fischer and S. R. Kelemen, J. Catal., **53**, 24 (1978).
221. C. H. Rochester and R. J. Terrell, J. Chem. Soc. Faraday Trans., **1**, 73, 609 (1977).
222. T. N. Rodin and C. F. Brucker, Solid State. Commun., **32**, 257 (1977).
223. M. Kiskinova and D. W. Goodman, Surf. Sci., **108**, 64 (1981).
224. R. J. Farrauto and B. Wedding, J. Catal., **33**, 249 (1973).
225. D. J. Pettigrew, Ph. D. Thesis, Glasgow University, 1990.
226. S. Johnson and R. J. Madix, Surf. Sci., **103**, 361 (1981).
227. R. J. Madix, In "The Chemical Physics of Solid Surfaces and Heterogeneous Catalysis, Chemical Engineering Series, Vol.4, 1982.
228. J. C. Ghosh and J. B. Bakshi, J. Ind. Chem. Soc., 1929.
229. N. ray, V. K. Rastogi, H. Mahapatra and S. P. sen, J. research Inst. Catal. Hokk. Univ., Vol.21, 187 (1973).
230. C. T. Campbell, B. E. Koel and K. A. Daube, Report, proc. 10th Intal. Vac. Congress, 6th Congr. on Solid Surfaces, 1986.
231. C. T. Campbell and B. E. Koel, surf. Sci., **183**, 100 (1987).

232. J. S. Campbell, *Ind. Eng. Chem. Process Des. Develop.*, **9**, 588 (1970).
233. P. W. Young and C. B. Clark, *Chem. Eng. Prog.*, **69**, 69 (1973).
234. J. Saussey and J. C. Lavalley, *J. Mol. Catal.*, **50**, 343 (1989).
235. C. Chauuin, J. Saussey, J. C. Lavalley, H. Idriss, J. P. Hindermann, A. Kiennemann, P. Chaumette and P. Courty, *J. Catal.*, **121**, 56 (1990).
236. M. Nagao and T. Morimoto, *J. Phys. Chem.*, **84**, 2054 (1980).
237. A. Ueno, T. Onishi and K. Tomaru, *J. Chem. Soc. Faraday Trans.*, **66**, 756 (1970).
238. G. Busca, P. F. Rossi and J. C. Lavalley, *J. Phys. Chem.*, **89**, 5433 (1985).
239. R. G. Greenler, *J. Chem. Phys.*, **37**, 2094 (1962).
240. J. N. Ressel, Jr, S. M. Gates and J. T. Gates, Jr, *Surf. Sci.*, **163**, 516, (1985).
241. T. J. Huang and S. W. Wang, *Appl. Catal.*, **24**, 287, (1985).
242. T. Matsushima and J. M. White, *J. catal.*, **44**, 183 (1976).
243. D. Al-Mawlawi and J. M. Saleh, *J. Chem. Soc. Faraday Trans.*, **1**, 77, 2965 (1981).
244. I. F. Tindall and J. C. Vickerman, *Surf. Sci.*, **149**, 577 (1985).
245. T. L. Slager and C. H. Amberg, *Can. J. Chem.*, **50**, 3416 (1972).